Improving the delivery and immunogenicity of an inhalable CpG-ODN DNA vaccine by bio-adhesive gemini nanoparticles in neonatal chickens

by

Daniella Calderon-nieva

A thesis

presented to the University of Waterloo

in fulfilment of the

thesis requirement for the degree of

Master of Science

in

Pharmacy

Waterloo, Ontario, Canada, 2017

Author’s declaration

I hereby declare that I am the sole author of this thesis. This is a true copy of the thesis, including any required final revisions, as accepted by my examiners.

I understand that my thesis may be made electronically available to the public.

Abstract

Cytosine-phosphodiester-guanine oligodeoxynucleotides (CpG-ODN) are nucleotide sequence motifs found in the bacterial genome that activate the mammalian innate immune response and have been found to boost humoral immunity when used as vaccine adjuvants in non-human primates and mice [1, 2]. Although species specific differences exist in the nature of the response, CpG-ODN can also activate chicken innate immune cells through the Toll-like receptor 21 (TLR 21) and has been found to protect against common bacterial infections in chickens such as *Escherichia coli* (E. coli) in neonatal broiler chicks after spray administration. The importance of CpG-ODN application is that the Canadian chicken industry voluntarily agreed to withdraw the prophylactic use of Category I antibiotics in poultry, which leaves chicks highly susceptible to infection and can result in high mortality rates and large economic losses.

Owing to the relatively low manufacturing cost, and ease of customization of oligonucleotides [3], CpG-ODN administration is a highly attractive strategy against *E. coli* infection in neonatal broiler chicks. Especially because the development of a non-species-specific *E. coli* vaccine is difficult due to the genetic variation of *E. coli*.

The objective of this thesis was to develop an inhalable nanoparticle CpG-ODN formulation that is superior to CpG-ODN on its own. Ultimately, the goal is to develop an inhalable nanoparticle carrier that can protect CpG-ODN, enhance innate immune stimulation, and prolong the protective effects in broiler chicks.

In practice, oligonucleotides are highly susceptible to degradation in biological environments. Moreover, in the lung, mucociliary clearance and enzymatic clearance play a role in preventing optimal immune stimulation and delivery of the vaccine to immune “hot spots”. In the human lung, bio-adhesive polymers have shown to improve DNA delivery by increasing residence time in mucosal membranes.

Gemini surfactant nanoparticles (NPs) are a novel nucleic acid delivery system that could deliver CpG-ODN to important innate immune activating cells for an optimal immune-protective effect. Bio adhesive polymers such as chitosan and polyvinylpyrolidone could also improve delivery of DNA to the lung. This work investigated how the physicochemical properties of nebulized bio adhesive polymer nanoparticle formulations influence delivery of the vaccine to

the avian lung and activation of the innate immune response in comparison to CpG-ODN on its own.

The dicationic gemini surfactants 12-3-12, 16-3-16, and 18-3-18 were used in combination with a phospholipid (DPPC), and different bio adhesive polymers to prepare various types of hybrid nanoparticles and assess their transfection efficiency in a chicken macrophage immortal cell line HD11. The transfection efficiency and toxicity of formulations was measured using flow cytometry. All formulations were also assessed in their capability to induce an innate immune response in HD11 cells by quantitating nitrite (nitric oxide) production using the Greiss assay. Size and zeta potential measurements were carried out using dynamic light scattering and fluorescence correlation spectroscopy to correlate physical parameters to transfection efficiency. Furthermore, confocal microscopy was used to evaluate cellular uptake after transfection. Finally, the biodistribution and ability to elicit a protective innate immune response in 1-day old chicks was tested for selected formulations.

Of the six formulation groups developed in this thesis, gemini surfactant nanoparticles (G-NP), gemini-lipid (GL-NP), biopolymer coated gemini-lipid (BGL-NP) formulations, and chitosan-gemini (CG-NP) formulations were the most reproducible and stable formulations that could increase uptake and retention of CpG-ODN in comparison to naked unformulated CpG-ODN. These formulations were also able to elicit chicken macrophage activation, and generate protective responses in one-day old broiler chicks when challenged with pathogenic *E. coli.*

Acknowledgements

I would like to take this opportunity to thank a handful of people who have been integral to the completion of this thesis. Above all, I would like to extend my deepest gratitude to Dr. Marianna Foldvari, who served as my Master's supervisor over the last two years. On a daily basis, I was reminded how passion and enthusiasm for learning are the hallmarks of scientific education. I am truly grateful for all the times that you offered detailed feedback on my work, encouraged me to take-on new challenges, and for your ability to convey important lessons. You always treated me with utmost respect and professionalism, and I would like to sincerely thank you for making my graduate studies a worthwhile and pleasurable experience. I would also like to extend my deepest gratitude to Dr. Susantha Gomis and his team in Saskatchewan: Kalhari Goonewardene, Betty Chow-Lockerbie, and Shelly Popowich for their outstanding support and collaboration. Your contribution to the in vivo protection studies and repeated handling of animals was integral to the completion of this thesis. As always, your patience and diligence are very much appreciated. Thank you, also, to Dr. Praveen Nekkar for your endless support and guidance. To my colleagues Roger Chen and Lokesh Narsineni, I would also like to thank you for your friendship and mentorship over the course of my thesis. I sincerely appreciate all of your help with method development, sample shipments and orders, as well as our many discussions over the last two years. Finally, to my family, without your relentless support and encouragement this thesis would not have been been possible. You offered me all the resources and love I needed to pursue this dream, and for that, I will be forever grateful.

Table of Contents

List of figures

List of tables

List of abbreviations

A-NP	Sodium alginate nanoparticle
BGL-NP	Bio adhesive gemini phospholipid nanoparticle
C-NP	Chitosan nanoparticle
CA-NP	Chitosan sodium alginate nanoparticle
CDC	Centers for Disease Control and Prevention
CG-NP	Chitosan gemini surfactant nanoparticle
CL-NP	Chitosan phospholipid nanoparticle
CLSM	Confocal Laser Scanning Microscopy
CMCNa	Sodium Carboxymethyl Cellulose
CpG-ODN	Cytosine phosphodiester guanosine oligodeoxynucleotide
DD	Degree of deacetylation
DNA	Deoxyribonucleic Acid
DPPC	1,2-Dipalmitoyl-*sn*-glycero-3-phosphocholine
E. coli	*Escherichia coli*
ERK2	Extracellular signal regulated kinases
FBS	Fetal Bovine Serum
FDA	Food and Drug Administration
FSC	Forward scatter
G-NP	Gemini surfactant nanoparticle
GL-NP	Gemini phospholipid nanoparticle
HA	Hyaluronic acid
HA-NP	Hyaluronic acid nanoparticle
HSP90α	Heat shock protein-90 alpha
I.M.	Intramuscular
i.n.	Intranasal
IFN-γ	Interferon gamma
IL-12	Interleukin 12
IL-6	Interleukin 6
kDa	Kilo dalton
LOD	Limit of detection
LOQ	Limit of quantification
MAP	Mitogen activated protein
mV	Millivolts
MW	Molecular weight

N/P	Nitrogen/Phosphorus
NaOH	Sodium hydroxide
NP	Nanoparticle
OD	Optical density
PBS	Phosphate buffered saline
PDI	Polydispersity Index
PEG 400	Polyethylene glycol 400
PG	Propylene glycol
pH	Potential of hydrogen
PI3K	Phosphoinositide 3-kinase
pKa	Acid dissociation constant
PVP 10,000	Polyvinylpyrrolidone molecular weight 10,000
PVP 40,000	Polyvinylpyrrolidone molecular weight 40,000
PVP Kollidon 25	Polyvinylpyrrolidone Kollidon 25
q.s.	Quantum satis
ROS	Reactive oxygen species
RPMI 1640	Roswell Park Memorial Institute Media 1640
S.C.	Sub-cutaneous
SSC	Side scatter
TE	Tris EDTA (Ethylenediaminetetraacetic acid)
TLR 15	Toll-like Receptor 15
TLR 21	Toll-like Receptor 21
TLR 9	Toll-like Receptor 9
WHO	World Health Organization
ζ	Zeta

Chapter 1: Introduction

Infectious diseases are normally treated with antibiotics. Given the global concern for antimicrobial resistance, the CDC, FDA, and WHO have announced the importance of regulating and controlling resistance [4]. In the past, the livestock industry has not only used antibiotics for treatment purposes, but also as preventative forms of therapy [5]. The problem is that their overuse in livestock has been linked to the emergence of antibiotic resistant strains of bacteria [6]. Because of this, in 2014, the Canadian poultry industry eliminated preventative use of category I antibiotics, those most vital to human health, in chickens. They are further working to eliminate category II and III antibiotics.

Given the elimination of these antibiotics, there is a major concern for *Escherichia coli (E. coli)* infection in broiler chicks. This is a common infection which plagues the modern broiler chick industry resulting in rapid loss of chicks and massive economic losses [7]. In order to prevent diseases in broilers that are primarily treated and controlled with antibiotics, alternative options must be implemented to promote the health and growth of the modern broiler chicken.

Vaccination is among the strongest infectious disease prevention strategies in humans. Similarly, broiler chickens and layer hens in the poultry industry are subject to intensive vaccination procedures that protect them against many infectious diseases [8]. In order to combat *E. coli* infection in chickens especially chicks, a promising alternative includes the implementation of large scale immunization with CpG-ODN DNA within poultry farms. Vaccination of neonatal broiler chicks with a DNA sequence adjuvant such as CpG-ODN has been shown to stimulate the avian immune response and protect against pathological events associated with bacterial infection [7].

By replacing drug therapies in food animals with vaccination, environmental build up and residue in food animal products can be reduced [9]. However, due to the large-scale nature of food producing facilities, cost effectiveness is also a major consideration. In chickens, pulmonary vaccination is attractive because of easy access, the high vascularity and permeability [10]. This could be of great importance in the livestock industry where administration of a large number of vaccinations could be limited by the availability of the number of trained personnel.

Additionally, needle-free vaccination is desirable in terms of safety due to both decreased risk of contamination from infected needles and potential irritation from injection [11, 12].

Pulmonary vaccine delivery has been widely studied in humans, and although there are major differences between the mammalian and avian respiratory systems, similar principles of pulmonary delivery apply. For example, the avian respiratory system also has high surface area in the gas exchange regions of the lung and the efficiency of respiration is higher than in humans. Due to the paucity of research investigating pulmonary vaccine delivery in chickens, the findings from mammalian systems will be applied to the present thesis.

Since most studies have found that mucosal delivery of the antigens alone especially DNA, using the pulmonary route is not efficient enough, nanoparticle (NP) technology has been applied to vaccine delivery and show potential in veterinary medicine as well [13-16]. NPs, defined as structures with at least one dimension in the range of 1-100 nm, recently gained wide interest in drug delivery [17]. NP vaccine systems are advantageous since they have the potential for limiting adverse effects, providing better stability, and stimulating the immune response enough so that adjuvants or repeated administration is not necessary [18]. Additionally, more sophisticated designs to incorporate selective targeting by ligand attachment or co-delivery of several antigenic components have been emerging. Research from small animal models and clinical trials have shown that NP carriers can enhance therapeutic and vaccine action in many routes of administration (subcutaneous, intravenous, inhalable, intramuscular) [19-22]. NP carriers are thought to protect the active substance from the physiological environment as well as aid the interaction between the active substance and its target [22, 23]. In fact, there are a variety of nano-pharmaceuticals already available on the market [24].

1.1 Motivation

1.1.1 Need for a prolonged immune response

The administration of a vaccine or therapeutic via inhalation has presented obstacles in the ability to produce a sufficiently high systemic immune response [25]. This has been attributed to the nebulization device, the anatomical, and the physiological features in the airways [25, 26].

For oligonucleotide vaccines, this effect is potentiated since oligonucleotides are highly susceptible to degradation in the lung environment. Although CpG-ODN has proven protective against *E. coli* challenge under experimental conditions, the main challenges include the large dosages necessary for an effective response and the rapid degradation and elimination from the circulation *in vivo* [27]. NPs have improved the immune response in comparison to free DNA, but research is still in the early stages and there are few links that correlate enhanced immunogenicity with protection. Since the immune response is a delicate balance between tolerance and protection, if a sufficient amount of immune stimulating oligonucleotide is not delivered and processed, immune tolerance rather than immunization occurs that leads to ineffective protection against the infectious agent [28].

By testing and comparing different types of NP formulations in this project, correlations between delivery system components and superior delivery can start to be elucidated.

1.1.2 Need for a reproducible, easy to manufacture, stable formulation, easy to deliver

While NP delivery systems show promise in improving delivery by increasing stability of its cargo within biological environments and have potential in lowering toxicity, cost and manufacturing conditions must also be considered. This is especially important in the poultry industry because cost-benefit ratios must be ideal so that administration can be implemented for a large number of animals [29]. Since NP formulations (especially with multifunctional purposes) introduce added complexity to safety regulations, synthesis, and purification [29, 30], an added motivation was to design NP formulations that could easily be manufactured in a short period of time without the need for high pressure homogenization.

Additionally, the mechanism of delivery was considered in order to avoid labor intensive processes of administering individual vaccines [29]. The pulmonary route is ideal since it can deliver agents both to the local mucosa and systemically. The formulation as such, could be easily applied throughout the chicken life span if necessary.

1.1.3 Correlating NP composition with delivery status

Preferred materials used for pulmonary NP delivery systems are lipids and polymers. At present, a variety of lipid and polymer based formulations have been synthesized by many

groups for effective pulmonary aerosol administration [31-38]. In addition, bio adhesive polymers are sometimes added to NP formulations to increase residence time in the lung and allow for increased cellular uptake, and therefore lasting gene expression/drug delivery [39]. NP formulations show improvement in comparison to naked plasmid or oligonucleotide delivery *in vitro* and *in vivo* in mice and various livestock animals [33, 39, 40]. However, comparisons between different types of formulations have not been explored to a great extent. This thesis, also aims to compare a novel cationic gemini surfactant gene delivery system to chitosan and phospholipids which have shown potential in lung gene delivery systems [23, 36, 38, 41-45]. Hybrid combinations of these NPs will also be compared drawing on the advantage of muco-adhesion from chitosan and the promotion of cell interaction from phospholipids to determine advantages of multifunctional particles.

1.2 Hypothesis

The hypothesis is that NPs will improve the transfection (uptake) of CpG-ODN by HD11 chicken macrophages and therefore will show increased bio distribution in the lungs after inhalation compared to free CpG-ODN and prevent mortality after *E. coli* challenge in neonatal chickens. Further, the composition of the NP (gemini, gemini-phospholipid, gemini-phospholipid-polymer, chitosan, gemini-chitosan, chitosan-phospholipid) will directly affect the uptake of CpG-ODN by HD11 macrophages, with mucoadhesive chitosan-gemini NPs improving the retention of CpG-ODN and increasing activation of the innate immune response in HD11 cells.

1.3 Thesis Objective

The main objective of the project was to evaluate and compare the delivery of CpG ODN 2007 into the lungs by bio-adhesive gemini surfactant-phospholipid NPs (BGL-NPs), chitosan NPs (C-NPs) and hybrid combinations of chitosan gemini NPs (CG-NPs), and chitosan phospholipid NPs (CL-NPs) after inhalation in neonatal chickens.

This thesis presents the design and development of different NP vaccine formulations using a combination of lipid, biopolymer, and gemini surfactants to encapsulate a phosphorothioate-modified CpG-ODN DNA sequence. By designing different kinds of hybrid NPs, an optimal formulation that effectively overcomes the lung environment and reaches the local lung and

systemic immune components will ultimately enter and activate immune stimulating chicken macrophages. This work aimed to develop a CpG-ODN vaccine formulation that has the potential to produce a longer lasting innate immunity to *E. coli* infection in chicks than CpG-ODN on its own. It also aimed to produce a reproducible and stable vaccine formulation that can be used out in the field.

With these goals in mind, several features of each of formulation were analyzed. The specific endpoints for characterization and evaluating effectiveness are outlined below:

A. NP preparation and characterization

(1) Preparation of several gemini, lipid, and polymer formulations by controlled manipulation of chemical and physicochemical features that affect gene delivery, including:

a. Bio adhesive polymer composition

b. Order of assembly of NPs

(2) Evaluation of size distribution and zeta potential of various formulations

a. In original (as prepared) form

b. In different biological buffers and media

(3) Characterization of NPs by fluorescence correlation spectroscopy

(4) Characterization of the effect of nebulization on particle properties

a. Size and zeta potential

b. CpG-ODN stability

B. Flow cytometry assessment of CpG-ODN uptake in HD11 macrophage cells

(1) Evaluation of the uptake of CpG-ODN solution versus CpG-ODN NP formulations in the HD11 cells by tracking Alexa Fluor 647 labeled CpG-ODN in cell populations

(2) Evaluation of the toxicity/viability of HD11 cells treated with CpG-ODN NPs

(3) Evaluation of innate immune activation in HD11 cells following CpG-ODN antigen presentation by measuring the extent of nitrite (nitric oxide) production by HD11 macrophages following treatment with different NP formulations

(4) Assessment of CpG-ODN localization by NPs in HD11 cells *in vitro:* trafficking of CpG-ODN NPs within HD11 cells using confocal microscopy

C. Confocal microscopic assessment of gene delivery and biodistribution of NP formulations in 1-day old chick lungs

Evaluation of the location and extent of deposition of optimized CpG-ODN NPs in the neonatal chicken respiratory tract after inhalation delivery using a nebulization chamber.

D. Evaluation of protection against *E. coli* infection in neonatal chicks after CpG-ODN NP formulations in collaboration with University of Saskatchewan

(1) Evaluation of the protective effect of immunization with CpG-ODN NPs on chick survival after challenge with pathogenic *E. coli.*

1.4 Thesis Organization

This thesis is divided into five chapters. Chapter 2 presents the necessary background to understand the current challenges and breakthroughs in pulmonary NP vaccine formulation in veterinary livestock. The application to the avian respiratory system is also discussed. NP design considerations for CpG-ODN delivery to the avian lung are discussed in more detail and materials applied to DNA-NP delivery systems to overcome the lung barriers are discussed.

Chapter 3 presents the experimental materials and methodology used to develop and evaluate the different components of NP formulations. The NP preparation methods are discussed as well as how size and zeta potential were evaluated. The design of the *in vitro* evaluation is also discussed as well as how the formulations were evaluated *in vivo*.

Chapter 4 presents the results on physical components affecting cellular uptake and lung delivery. Also, a look into manufacturing reproducibility and stability are discussed. Finally, uptake, immune activation, deposition, and protective effects for each formulation are compared.

Chapter 5 discusses the results and represents the conclusions obtained from this work. The limitations are discussed here. Lastly, future directions are proposed to further progress the NP formulation into a more commercially viable product.

Chapter 2: Background and Literature Review

This chapter provides an overview of the background together with a detailed discussion of the related work found in the literature to explain the specifics of the project. Initially, an overview of NP vaccine development targeted to the lung and nasal passageways in livestock animals is presented in a written review on the subject [40]. Next characteristics of CpG-ODN DNA as a vaccine in chickens is reviewed. Finally, an overview of NP materials used to overcome DNA delivery barriers in the human lung and avian respiratory tract are reviewed.

2.1 Application of nanotechnology in pulmonary veterinary vaccines

NP delivery systems applied to therapeutics and vaccines have been gaining momentum in human medicine, with a variety of nanopharmaceuticals already available in the market [24]. However, evidence of NP delivery systems in veterinary medicine is also emerging in the livestock industry. Specifically, applications of NP delivery systems for pulmonary delivery are promising for improving delivery at a large scale in a cost-effective manner.

In this section, a review of emerging applications for NP vaccine delivery via the respiratory route in a variety of livestock animals is presented next to give an overview of the progress in veterinary research. This section was recently published in the journal of Drug Delivery and Translational Research Veterinary vaccine nanotechnology: Pulmonary and nasal delivery in livestock, Calderon-nieva et al. [40].

Veterinary vaccine development has several similarities with human vaccine development to improve the overall health and well-being of species. However, veterinary goals lean more towards feasible large-scale administration methods and low cost- high benefit immunization. Since the respiratory mucosa is easily accessible and most infectious agents begin their infection cycle at the mucosa, immunization through the respiratory route has been a highly attractive vaccine delivery strategy against infectious diseases. Additionally, vaccines administered via the respiratory mucosa could lower costs by removing the need of trained medical personnel, and lowering doses yet achieving similar or increased immune stimulation. The respiratory route often brings challenges in antigen delivery efficiency with enough potency to induce immunity. Nanoparticle (NP) technology has been shown to enhance immune activation by producing higher antibody titers and protection. Although specific mechanisms

between NPs and biological membranes are still under investigation, physical parameters such as particle size and shape, as well as biological tissue distribution including muco-ciliary clearance influence the protection and delivery of antigens to the site of action and uptake by target cells. For respiratory delivery, various biomaterials such as muco-adhesive polymers, lipids and polysaccharides have shown enhanced antibody production or protection in comparison to antigen alone. This review presents promising NPs administered via the nasal or pulmonary routes for veterinary applications specifically focusing on livestock animals including poultry.

2.1.1 Veterinary vaccine nanotechnology: Pulmonary and nasal delivery in livestock animals [40]

Vaccination is a powerful tool for the prevention and control of infectious diseases [17]. In humans, vaccination has made the eradication of small pox possible, with polio soon to follow [17]. Despite these tremendous advances in human health intervention, several infectious diseases are still high burdens for the global economy and public health [46]. Zoonoses accounts for 60% of all infectious human pathogens that have a possibility to cause pandemics [47]. The farm/livestock industry is a major source of zoonotic potential where animals are in constant close proximity providing greater opportunity for viral mutation, or bacterial gene transfer which can be transferred directly to humans after consumption. Perhaps one of the most feared zoonotic infectious diseases is avian influenza, which could be prevented quickly and specifically, if a universal synthetic vaccine was available [18].

As such, not only does veterinary vaccination in livestock aim to prevent and control animal diseases, it also aims to prevent disease in food animals to avoid zoonosis or infection in human consumers and improve the efficiency of production of food animals [9]. For example, by replacing drug therapies in food animals with vaccination, environmental build up and residue in food animal products can be reduced [9]. However, due to the large-scale nature of food producing facilities, cost effectiveness is also a major consideration. Non-economical vaccines will not likely be widely adopted if cheaper alternative treatments are available [9]. While human vaccination also aims for cost-effective vaccines, individual health and well-being is a stronger consideration for compliance.

Current licensed vaccines in both livestock and humans are derived from live, modified, attenuated or killed vaccines [8, 48] . Unfortunately, attenuation is an expensive long process. Live vaccines also have the potential to revert to virulence and are not recommended for the immune-compromised [49]. Another drawback of vaccines is that they likely require an adjuvant and must be administered by needle, which requires trained personnel and proper disposal [21]. Some vaccinations even require multiple doses of vaccine to induce a sufficient immune response against the agent [18].

On the other hand, needle-free nasal vaccination and pulmonary vaccination is attractive because of easy access, the high vascularity and permeability, and limited metabolism in the nasal cavity [10]. This could be of great importance in the livestock industry where administration of a large number of vaccinations could be limited by the availability of the number of trained personnel. Additionally, needle-free vaccination is significant in terms of safety due to both decreased risk of contamination from infected needles and potential irritation from injection [11, 12]. In fact, the pulmonary route of vaccination has been around since the 1950's during the development of an aerosol New Castle Disease vaccine in chickens, which is now widely used [50, 51]. In ruminants, aside from averting first pass metabolism and the rumen, the respiratory mucosal surfaces of an organism not only have the potential to initiate immunity at the local site of administration, but also systemically due to the close proximity of the blood-lung barrier [13]. There is already evidence that immunization via the respiratory tract not only produces high local immune responses [11, 52] but also provides high systemic mucosal immunity in mice and non-human primates [11, 53]. This is especially important as many infectious diseases such as Influenza, *Escherichia coli* (*E. coli*) and *Mycobacterium tuberculosis (MTb)* are able to initiate their infectious process at mucosal surfaces [13].

In practice, both pulmonary and nasal delivery have highlighted biological challenges that can prevent the proper delivery of vaccine to the lung. In mammals, particles delivered via the nasal or pulmonary route can be lost to the oropharynx because of the turbulent air flow and continuous branching and narrowing of the airways [28, 54]. However, synchronic inhalation seems to improve loss by bypassing the esophagus [28]. Additionally, the mucociliary blanket in the upper airways and the nasal cavity is designed to constantly clear particles [10, 19, 28]. While there are some recognized anatomical differences between large livestock animals and a complete anatomical dissimilarity with the avian lung (poultry), the mucociliary blanket is

present in all of these species. The loss of particles delivered to the target site via inhalation in the air sacs of the avian system is also a concern despite their unidirectional air flow [55].

Even if particles are able to bypass mucociliary clearance barriers, the lower respiratory passageways are also not lacking in clearance mechanisms. Alveolar components and lysozymes can break down products near the blood-epithelial barrier in mammals [28]. Although the presence of immune cells in the lung is favorable to vaccine applications, the formation of tolerance or rapid clearance of a particle via innate immunity could hinder immune activation [28].

In order to improve vaccine potency and achieve needle-free delivery, nanotechnology has been incorporated into vaccine research [17]. More specifically, delivery of nanoparticle vaccines via the nasal or pulmonary (inhalable) route has become highly attractive. While most studies have found that mucosal delivery of the antigens alone using the pulmonary route is not efficient enough, Nanoparticle (NP) systems have been found to greatly improve delivery through the mucosa of the pulmonary system in humans and show potential in veterinary medicine as well [13-16]. NPs are defined as structures with at least one dimension in the range of 1-100 nm, that have been widely applied to drug delivery [17]. In vaccine delivery, "nano" platforms have mainly focused on developing delivery vehicles for vaccine antigens, but some materials such as the biopolymer chitosan have shown vaccine adjuvant properties [56, 57]. These systems are advantageous since they have the potential for limited adverse side effects, better stability, and may also stimulate the immune response enough so that adjuvants or repeated administration is not necessary [18]. Additionally, more sophisticated designs to incorporate selective targeting by ligand attachment or co-delivery of several antigenic components have been emerging.

The application of nanotechnology in veterinary vaccination is still in early stages. Some of the knowledge in this regard is available from small animal models used for human vaccine development. In fact, nanotechnology has been adapted to enhance the performance of the delivery of therapeutics in several areas like lung cancer and cystic fibrosis. Combined with nanotechnology, needle-free mucosal immunization can ease vaccination in the food production and livestock industry while ensuring sufficient protection against diseases which could cause serious economic losses on the farm. Several NP delivery vehicles have already been tested in

livestock veterinary vaccine development in order to achieve needle-free vaccination for mass immunization [8, 13, 14, 16, 58-60].

The advantages of vaccination via the pulmonary route as well as the feasibility of implementing such vaccination methods out in the field will be explored in this review. Additionally, the research and application of nanotechnology for inhalation or nasal vaccine developments in livestock, and especially poultry, will be discussed as an important aspect of protection for animals in the food chain and link to human safety.

2.1.1.1 Availability of devices for vaccine delivery via inhalation or nasal delivery and mass administration

Mucosal drug administration via the pulmonary route has been well established in humans for a long period of time for respiratory diseases such as asthma and chronic obstructive pulmonary disease (COPD) [61]. In fact, nebulizers and dry powder inhalers are standard aerosol devices designed to administer drugs via inhalation in humans [25]. Specific aerosol devices for drug delivery to the lung in veterinary species have not been described in livestock but metered dose inhalers for companion animals do exist including the AeroKat™ for cats, AeroDawg™ for dogs, and the AeroHippus™ for equine species (Trudell Medical International©). The delivery of aerosol therapeutics may be more difficult in animals as one cannot teach them to take controlled breaths when using inhalers or nebulizers [62]. On the other hand, nasal administration may be a better option for larger animals.

Inhaler or nasal devices specific to vaccine administration have not been developed. However, nasal or inhalable vaccines are attractive in humans for needle fearing individuals and children. Furthermore, inhalable or nasal vaccines are attractive strategies for mass immunization in livestock and humans. Depending on farm size, animal handling for vaccine administration could add to the already labour intensive nature of the food production industry [63].

Vaccine administration via intramuscular or subcutaneous injection is still the standard today even though an intranasal (i.n.) vaccine against bovine respiratory disease (PMH®IN) released by Merck in 2014 exists for cattle, and spray vaccination also exists in the poultry industry [8]. Especially, administration via a parenteral route ensures high bioavailability and drug absorption that can be accurately predicted, in contrast to nasal or inhalation administration

where absorption at the systemic level or amount lost at the oropharynx is not easily measured. As a result, veterinary syringes are designed to administer repeat-injections to aid farmers in administering multiple dosages of a vaccine without having to draw the vaccine formulation into the syringe each time prior to vaccination of the animal (Allflex©).

Among needle-free delivery devices for livestock, there are controlled release devices available for oral administration which are made of nylon or permeable materials [64] . The oral devices filled with drug can either have high density or expand upon entering the rumen to avoid regurgitation and ensure long term release of drug [64, 65]. Intravaginal devices similar to human intrauterine devices are also available mainly for hormonal, fertility, and anti-helminthic drugs, but not vaccine administration [64]. In the poultry sector, non-invasive approaches to vaccine administration seem to focus on oral or ophthalmic routes [65]. Drugs incorporated into skin tags and ear tags are also available [65]. Coarse spray vaccines in the poultry sector are designed for administration to the eye and upper respiratory tract and these can be easily administered through automation at the hatchery [66].

The complications involved in the design of inhalable controlled release devices or products results from the variation in physiology of animal species. For example, in food producing animals or livestock, there are two categories of species: the ruminants and the avian. Aside from the obvious differences that exist between the avian and mammalian respiratory system, interspecies differences also exist [63]. The result is differences in rates of biotransformation, differences in breathing pattern, and tissue distributions [63]. The consequence of the species differences is that each vaccine delivery system proposed must be specifically designed for a particular species [65].

Additionally, the administration approach is not only dependent on the type of animal but also on their housing facilities. For instance, in poultry, aerosol administration may be practical due to the close proximity and smaller housing facilities. Additionally, their smaller size and unidirectional airflow through their lung may favour deposition of aerosol vaccines in their respiratory tract. For example, an inactivated influenza vaccine has been shown to induce protection against lethal influenza challenge in chickens [67]. However, an influenza vaccine for example may not be desirable environmentally as an aerosol due to its zoonotic potential. In ruminants, due to their large body structure and nature of housing it may be more difficult to use

inhalable sprays that achieve proper dosing. However, if devices were designed specifically for inhalation or direct intranasal application for felines, dogs and horses, these might be incorporated into their upkeep. With all aspects considered, mucosal immunization could replace the hazardous potential of needle administration.

2.1.1.2 Current nano-pharmaceuticals in the market

Research from small animal models and clinical trials have shown that NP carriers can enhance therapeutic and vaccine action in many routes of administration (subcutaneous, intravenous, inhalable, intramuscular) [19-22]. NP carriers are thought to protect the active substance from the physiological environment as well as aid the interaction between the active substance and its target. In fact, there are a variety of nano-pharmaceuticals already available on the market [24]. The available nano-pharmaceuticals are mainly used to encapsulate cancer drugs. However, there is one nano-vaccine available in Switzerland for influenza. Other NP drugs carry anti-fungal and hormone replacement active ingredients. The approved NP pharmaceuticals are formulated from lipid, surfactant, polymer, metal materials, and even viral components with the ability to carry not only active molecules, but proteins as well [24]. This encompasses the variety of NPs that can be created and the versatility of applications and packages that they can hold.

Absent from this list, are any approved particles designed for pulmonary or nasal administration. Although the use of human aerosol devices has improved to deliver greater amounts of dose to the lung, achieving systemic delivery is still suboptimal [25]. Yet, in terms of vaccine application, dosing is critical to proper immune stimulation. A suboptimal dose may induce tolerance or no immune stimulation at all. On the other-hand over dose could result in detrimental immune stimulation. Regardless, the design of NPs for drug, gene, protein, and vaccine delivery via the airways is currently an exciting research field.

2.1.1.3 Physical and biological parameters involved in aerosol delivery

The fate of particles entering the airways is dependent on three aerodynamic properties: impaction, sedimentation, and diffusion. Whether or not a particle settles in the respiratory system by impaction, sedimentation or diffusion depends on the particle size distribution

generated by the delivery device and the type of breathing pattern during inhalation of the dose [25, 26]. Upon inhalation of a deep forceful breath, particles greater than 1 μm tend to impact as their higher density and momentum prevent it from changing direction if there is a change in airflow pattern. In the airways, these larger particles (3-6 μm) get trapped in the pharynx, mouth or the mucus of the trachea, which results in them being removed by swallowing [68, 69]. Upon slower air velocity or a slower breathing pattern, particles between 1-5 μm (NPs) in size tend to settle in the smaller airways and respiratory bronchioles by sedimentation (gravity), since their residence time within the lung increases [69]. Also, NPs have better chance of reaching the bronchioles and respiratory mucosa in the lower airways [26]. The smallest NPs less than 0.5 μm tend to deposit in the alveolar spaces resulting from Brownian motion [26, 69, 70]. Though, these smaller particles tend to get exhaled but if less than 34 nm in size, they enter the blood stream and are cleared via renal filtration [71]. Since systemic immune activation is critical to initiating cell mediated immune responses, targeting to the alveolar region at the interface of the blood-air boundary is highly desirable for a NP vaccine.

Since aerosols can be dry powders, liquid suspensions or liquid solutions, the type of formulation is also important in the development of aerosol vaccines. The final vaccine formulation must be compatible with the device chosen to administer the vaccine. For example, if a multi-dosing inhaler device is used, the interaction of the formulation with the holding chamber must be considered to ensure consistent dosing after every administration [25]. If a nebulizer is chosen, the NP formulation designed must be a liquid to allow the output to generate small droplets. Furthermore, different types of nebulizers are only compatible with certain types of formulations. For instance, ultrasonic nebulizers which generate aerosol droplets using high energy soundwaves are ineffective in nebulising more viscous solutions such as suspensions or liposomes [25]. But, vibrating mesh or plate nebulizers which physically break up the liquid into smaller droplets work very efficiently for suspensions or liposomes [25].

Unlike the aerosol delivery to the lung, the nasal cavity is a lot smaller and the aerodynamics does not play as large a role in deposition of particles. In nasal delivery, the goal of systemic vaccination is to reach the respiratory region. The respiratory region of the nasal cavity containing nasal turbinates have a high surface area and create turbulent air flow to allow better contact between the inhaled air and the mucosal surface. Nasal turbinates are in close

proximity to blood vessels. Additionally, the mucosal associated lymphoid tissue in the nose (nasal associated lymphoid tissue (NALT)) that is separated from the epithelial barrier containing the mucociliary blanket is the main target of mucosal vaccination in the nose.

The first physiological barrier in the nose is a mucociliary layer that clears entering particles which then go to the back of the throat and oesophagus to get cleared by the digestive system [54]. Furthermore, enzymatic activity within the nasal cavity mucus is a concern to drug delivery [19]. Perhaps the most important factor that affects particle delivery in the nasal mucosa, is actually membrane permeability. Large polar molecules do not pass through the epithelial cell membrane easily and must be accompanied by absorption enhancers such as bile salts and phospholipids to change the permeability of the epithelial cell layer [54].

2.1.1.4 Potential for enhanced pulmonary and nasal immune stimulation with various nanomaterials

In vaccine delivery, direct interaction between an adjuvant and an antigen presenting cell is critical to immune activation. Therefore, the interaction of NPs at the cellular level is very important to understanding mechanisms of NP adjuvanticity. Chitosan NP sizes around 400 - 1000 nm have been reported to elicit higher serum immunoglobulin A (IgA) levels than 3000 nm NPs [72, 73]. However, PLGA NPs around 1000 nm have also been found to induce stronger serum Immunoglobulin G (IgG) than 200 nm or 500 nm particles after i.n. immunization. At the cellular level NP size, surface charge, and surface morphology are known to influence the uptake and trafficking by pulmonary antigen presenting cells [74]. For example, it was found that 50 nm polystyrene particles are taken up by alveolar and non-alveolar macrophages, B-cells and dendritic cells in the lung, but only by dendritic cells in the lung-draining lymph nodes (inguinal, mesenteric and mediastinal) [75]. The surface charge of a particle can also influence type of cells recruited to the site of action. In fact, hydrogel rod shaped cationic particles have been found to associate with dendritic cell subtypes while alveolar macrophages were found to preferentially take up negatively charged particles [74, 75].

Contradictory theories between the correlation of size and immune activation are likely due to the different particles that have been directly characterized for NP-adjuvant-cellular interactions *in vitro*. Additionally, orientation of the antigen within or on the surface of the particle could influence the mechanism of antigen presentation [73, 76]. Theoretically,

nanoparticle drug therapies are thought to reduce dosing frequency due to the increased accumulation of drug per particle at specific sites [70]. Similarly, in vaccine delivery NPs can be made to carry several antigens at once. This is advantageous since it more closely mimics real pathogens which stimulate the immune system through recognition of various antigens.

Further emerging advantages of NP vaccines involve cell specific targeting by antibody or small molecule conjugation to the surface of the particle [70, 77-81]. Particle functionalization and targeting toward certain environments, tissues, cells, and even intracellular components could greatly enhance the stimulation of the immune response and reduce clinical signs of disease. The NP systems that have been applied to vaccinology and also tested in food producing veterinary species are discussed below.

2.1.1.5 Vaccine platforms against livestock and poultry diseases

While research on nasal or pulmonary vaccine delivery options for humans is quite extensive, for food animals and especially large animal livestock, delivery methods are much more limited. Inhalable vaccine delivery is preferred in the chicken industry, whereas nasal vaccine delivery is more applied to ruminants in livestock. The following sections are focused on veterinary species with developments in the ruminant and poultry industry separately mentioned.

2.1.1.6 The poultry industry

The poultry industry mostly consists of turkeys, broiler chickens and layer hens. Most studies of inhalable or nasal delivery focus on broiler chickens, although there are a few studies in turkeys and layer hens. As mentioned previously, broilers and layer hens are subject to intensive vaccination against many infectious diseases [8]. As a matter of fact, spray vaccination in poultry is standard against New Castle Disease virus (NDV) and Infectious Bronchitis Virus. However, spray vaccination in this regard refers to 100-200 μm liquid particles which do not specifically target inhalation but also seem to induce immunity through ocular, oral, and nasal mucosas. There is a grey area in the definition of spray vaccination in the literature to whether a spray drier is used versus a liquid spray generator or a nebulizer. However, the commonality of the three devices is that they all generate aerosols in which inhalation plays a role in the generation of immunity via the pulmonary or nasal mucosa. In this regard, this paper will state

whether a dry or liquid spray formulation was administered and if mentioned, whether nebulization was used to generate the vaccine formulation.

The two major pathogens targeted for NP immunization are NDV and influenza, although, vaccination against *E. coli* and Salmonella have also been investigated using NP carriers [7, 14, 27, 82, 83]. Studies of microparticle inhalable vaccines or nasal vaccines do exist in poultry, although there are few studies comparing the two delivery routes directly or the performance of the microparticle versus nanoparticle formulations. The preliminary studies will be described below.

Nasal vaccination using NPs in chickens has been tested against NDV and influenza using chitosan [83], liposome [84], and liposome-polymer particles [60]. Polymeric chitosan particles have been an attractive NP vaccine platform because of biocompatibility, mucoadhesive and permeating properties [28]. Additionally chitosan itself is thought to have adjuvant-like properties which could enhance immune stimulation [85]. In a study comparing chitosan and calcium phosphate particles, it was shown that both particles carrying inactivated NDV produced high antibody titers in blood and mucosa [83]. However, the chitosan particles performed better than calcium phosphate particles against NDV lethal challenge [83]. It is of note that the protection study involved three immunizations prior to challenge, and no physical characterization of the particles was stated.

Liposomal carriers are among the most characterized in the nanotechnology field. Conventional liposomes are lipid structures formed by one or more bilayers of amphiphilic lipids and they are thought to cross through epithelial barriers [19]. Liposomes are not immune-stimulatory themselves, however they have been found to induce higher IgA and IgG titers after immunization [19]. The charge of the liposome based on lipid composition has also been found to be important after i.n. immunization [19]. Both positively and negatively charged liposomes have been reported to be immune-stimulating [19]. The effect of liposome surface charge has been tested in chickens in efforts to improve the antigenicity of formalin-inactivated NDV after i.n. immunization [84]. Three differentially charged liposomes composed of phosphatidylcholine (PC), phosphatidylserine (PS), and stearylamine (SA) were tested for their ability to elicit mucosal and systemic humoral responses. Interestingly, the neutral liposome made with PC induced the highest secretory IgA and systemic humoral responses and protection against

challenge. The co-administration of LPS with the vaccine NP formulation further enhanced vaccine efficacy. The effectiveness of the PC liposome formulation was attributed to the fact that the transition temperature of the liposome is closer to the chicken body temperature than the others. Additionally, the head group was thought to play an important role in the recognition of APCs, but the mechanism is not known [84].

Since mucoadhesive polymers are thought to improve residence time in mucosal tissues, the addition of tremella or xanthan gum to liposome vaccine formulations containing inactivated influenza H5N3 were tested as i.n. vaccines [60]. The multilamillar mucoadhesive liposome vesicles induced higher immune response than the virus alone and liposome without the polymer. Additionally, the lower viscosity xanthan gum particle increased the efficiency of nasal vaccine delivery, which suggests that there may be a critical viscosity in which the formulation becomes too thick to effectively release the antigen to the nasal mucosal tissues despite the longer residence time in the nasal mucosa.

Aside from nasal NP vaccine delivery systems, a variety of studies have investigated nebulized or spray-dried vaccines in chickens. Both are inhalable formulations, but unlike nebulization that produces liquid inhalable particles, spray vaccines can involve transforming liquid to a dried inhalable powder. The final product is an inhalable dry spray. They are highly attractive for immunization via the lung because they are stable and tend to be delivered efficiently [28]. In humans, spray vaccines against influenza and tuberculosis have been tested [86-89]. In fact, an inhalable dry powder measles vaccine has undergone a phase 1 clinical trial and was proven to be safe and produced high levels of measles antibody [90]. In chickens, coarse spray vaccination has performed better in comparison to drinking water after challenge of *Salmonella enteritidis* strain and reduced colonization and shedding of bacteria [91]. Moreover, coarse spray administration of liposomes carrying inactivated avian pathogenic *E. coli* (APEC) showed protection against lethal *E. coli* challenge [92].

NP vaccine formulations have been most commonly tested against *E. coli* infection, particularly with synthetic CpG-ODN adjuvants. Nanoparticle formulations containing CpG-ODNs have been found to protect against several diseases in mice [93, 94], and *E. coli* and Salmonella in chickens [7, 14, 27, 42, 82, 95, 96]. However, these particle platforms are not delivered via the pulmonary route, yet they are effective against lethal *E. coli* challenge via *in*

ovo, intramuscular, and subcutaneous routes. Our group is investigating NPs for the pulmonary route of vaccination in broilers which present an easier vaccination method at the industrial scale [97-99].

Specific NP vaccination studies in chickens are sparse, however there is investigations of NP vaccines administered via the spray route [100, 101]. These studies have found that spray vaccines provide local and topical treatment in air sacs [102]. Some particle deposition studies can give clues about the characteristics of particle uptake to aid the design of optimal NP vaccine delivery systems. In order to establish local drug levels in the lung and air sacs, it has been found that particles less than 3 μm are able to bypass the mucociliary transport [103]. However, larger particles deposit in the upper airways, particularly the tracheal bifurcation [103, 104]. Particle deposition is also dependent on age and it was shown that in comparison to 2 and 4 week old broilers, 1-day old chicks contained more >3 μm particles in the nose and eyes and in the lower respiratory tract, while 1-3 μm particles deposited less compared to older chickens [104].

Interestingly, one study compared i.n. and spray administration against protection of infectious bronchitis virus using the commercial adjuvant Montanide [105]. Montanide can be used with a variety of veterinary antigens and it can come in NP, polymer, or oil-in-water formulations. In comparison to a non-adjuvanted commercial vaccine, it was found that both the NP and polymer technology of Montanide was better than the oil emulsion. However, i.n. immunization seemed to perform better than spray immunization and the polymer adjuvant performed best in spray form. Like the factors involved in nebulization of NPs and drugs in humans, the delivery of aerosol vaccines in chickens could be dependent on the device output and the interaction between the NP and the device itself. This is perhaps why the controlled administration of the i.n. formulation performed the best. However, there are no investigations of the interactions between vaccine formulations and coarse spray or nebulization devices for chickens.

2.1.1.7 Pulmonary and nasal vaccines in ruminants

From the literature, it can be concluded that nasal delivery of vaccines is preferred over aerosol delivery in the ruminants due to the lack of NP applications tested via inhalation. NP and in some cases microparticle delivery systems have been developed and tested in mainly the ovine

(sheep) and bovine (cattle) species. Initially, the sequence of vaccine development begins with testing small animal models, and testing parenteral administration prior to mucosal application in the target species. However, some studies have formulated NP vaccines and tested directly in the large animal model. Among these is one of the most commonly used vaccine viral vectors, adenovirus. Adenoviral vectors have been widely used in research for human vaccination against tuberculosis, HIV, and other respiratory diseases [106-111]. Since adenovirus is a species-specific virus that naturally infects the respiratory tract, it has been extensively studied for pulmonary and nasal administration. Additionally, they have the ability to infect both dividing and non-dividing cells, capacity to package large foreign genes, elicit strong antigen specific T cell responses, are relatively easy to produce recombinant virus, and they lack virulence [112]. Even concerns with integration and safety profile of viral vectors have faded [11, 52].

The Human Adenovirus 5 vector has been used to immunize cattle intranasally against Bovine Herpes Virus 1 (BHV-1) and was able to produce a specific antibody response stronger than the commercially available live attenuated vaccine. It also clinically protected cattle after challenge with high infectious dose of BHV-1 [113]. Due to safety concerns regarding zoonosis with using human viral vectors in domestic animals, bovine adenovirus 3 (BAdV-3) a natural non-pathogenic virus has been modified specifically for a vaccine delivery vehicle for cattle [112, 114]. Although primarily tested in cotton rats, BAdV-3 has been used to incorporate bovine specific viral antigens against BHV-1 or Bovine Respiratory Syncytial virus (BRSV) [112, 114]. After immunization, antibodies specific against both viral antigens were detected in the sera and nasal secretions of the rats [115]. Additionally, the co-expression of two viral antigens by BAdV-3 required less viral titer to induce the same quantity of antibody expression than BAdV-3 expressing either BHV-1 or BRSV antigens. It is suggested that the co-expression of two antigens may be more economically favorable than individual antigen expression [115]. The cotton rat is considered a suitable animal model for cattle. However, BAdV-3 has also been developed further as a BHV-1 vaccine expressing the cytokine Interleukin 6 (IL-6) to reduce viral shedding in cattle [116], which was not achieved with the sole expression of BHV-1 glycoprotein gD despite clinical protection in cattle after challenge [117]. The IL-6 did not improve protection or immune response in this investigation, but it was suggested that IL-6 may

not be enough to influence the mucosal immune response in calves and other potent adjuvants could be used to reduce viral shedding.

Immune Stimulating Complexes (ISCOMs) have also been developed to vaccinate against BHV-1 in calves [118]. Traditionally, ISCOMs are a 40 nm cage like structure held together by hydrophobic interactions between saponin and lipids [56]. However, for the BHV-1 vaccine, the ISCOM (30-35 nm) was made of glycoside Quil A, a plant adjuvant, which formed a honeycomb structure with BHV-1 viral membrane proteins. The ISCOM adjuvant NP vaccine produced higher antibody response and resulted in better protection than the available commercial attenuated vaccine. It is important to note that the ISCOM was administered through intramuscular injection and resulted in protection against viral challenge. Note, ISCOMs are known to be particularly strong mucosal adjuvants similar to parenteral and subcutaneous influenza vaccination and have resulted in higher IgA in serum, lung and nasal washings [119, 120]. It would be interesting to determine whether the BHV-1 ISCOM vaccine would perform better at lower dosing than intramuscular injection and compare it to the commercial attenuated vaccine.

Polymer particles are among the most popular vaccine formulations in ruminants. However, a variety of the polymer particle vaccines developed have not been NPs but are in the microparticle size range (>1 μm). Despite the main populations of particles in the 1-2 μm size range, BHV-1 vaccine loaded chitosan microparticles have been shown to be effectively taken up by bovine kidney cells, from both spray dried and gel chitosan microparticle formulations [58].

Chitosan microparticles are frequently used as i.n. vaccine delivery vehicles for cattle and sheep [58, 121]. However, they have mainly been studied for their ability to induce local and systemic humoral antibody responses, and not necessarily have been tested for inducing protection. In sheep, spray-dried chitosan microspheres containing a polymeric protein antigen (BLSOmp31) decorating the surface were able to induce local and systemic immune response after three i.n. immunizations over 40 days [121]. The microspheres produced a biphasic release of the antigen and were able to induce a nasal immune response despite the lower mucin adhesion with protein loaded particles versus blank chitosan particles. Although this was just a preliminary study, it would have been interesting to see if blank chitosan microparticles would also induce a slight immune response in sheep.

There is evidence of effectiveness using chitosan NP vaccines which have been prepared for immunization against Foot and Mouth Disease in livestock [122]. Unlike traditional chitosan, this group used fungal chitosan derived from a fungal cell wall since it can produce higher yields, has low molecular weight, and high degree of deacetylation [122]. The low molecular weight and high degree of acetylation is found to influence chitosan particle formation towards more stable complexes [123]. Since guinea pigs are a suitable animal model for cloven hoofed animals (pigs, cattle, sheep), the extent of the immune response was measured through antibody titer measurements from serum, intestinal tract and broncho-alveolar tissues after delivery of whole virus to the nasal tissue in guinea pigs [122]. All the particles compared ranged in size from 220-280 nm with low polydispersity index, unlike the commercial chitosan NPs which had the largest size. In comparison to vaccine delivery with just virus, all formulations (including commercially derived chitosan) produced higher IgG titers in sera over time. Even the systemic immune response produced by NPs was comparable to the traditional intraperitoneal alum-inactivated virus vaccine and nasal IgA produced from the NP vaccines was also higher in comparison to the injected vaccine. Effective mucosal IgA production was also seen in the intestinal mucosa, which was not produced from intraperitoneal injection with alum-FMD-v vaccine. It would also be interesting to compare the gel chitosan formulation [124] with the chitosan NP formulation to determine which would stimulate stronger immune responses.

Immunization with other mucoadhesive polymers like alginate have also been tested in the cattle species but only to determine whether alginate micro-particles can produce local immune responses [125]. The particles carried pig serum albumin as an antigen but were not geared to any specific disease. Since the alginate microparticle study aimed to compare the oral versus i.n. route of administration, the particles formed were mainly under 5 μm to optimize delivery. However, the study was only able to conclude that immunization with alginate microparticles may be plausible with both nasal and oral administration to provide specific immune responses against other antigens.

Other polymer particles that have been used to determine if they can enhance the immune response of vaccines in bovine and ovine species are poly(d, l-lactide-co-glycolide) (PLG) and polylactic-co-glycolic acid (PLGA). PLG particles were carrying SAG1 surface antigen from a *Toxoplasma gondii* tachyzoite [126]. These particles were under 2 μm and polydisperse, but with

more than 60% of the population being NPs. Antigen was present both inside the particle and adsorbed to the surface upon particle formation. After three i.n. immunizations over 2 weeks, there was evidence of consistent local IgA in comparison to the soluble antigen, however, the formulation failed to protect against oocyst challenge. Addition of cholera toxin to the PLG-SAG1 particle also didn't seem to improve the immune response significantly. In this particular study, even IgG production in the nasal mucosa and serum was very low, which is in contrast to previous studies in mice [126].

Perhaps a more insightful report compares the immune response created by a commercial vaccine against the Bovine parainfluenza 3 virus respiratory pathogen in dairy calves to the same vaccine formulated in PLGA NPs (225 nm, -22.7 mV) [16]. Unlike the commercial vaccine, the PLGA vaccine elicited greater IgA response in the mucus which persisted over the whole study period. The serum IgG response was also similar to the commercial vaccine but appeared to be more of a sustained release of antigen due to transient antibody production. It would be interesting to see in the future how the release profile of the antigen correlates with protection against respiratory disease in comparison to the commercial vaccine, as this platform also produced IgG to a comparable level of that of the commercial vaccine.

2.1.1.8 Conclusions and future directions

The pulmonary route of vaccination is promising for eliciting effective immune responses. Although many researchers are investigating pulmonary vaccines of human disease it is important to remember that vaccinating livestock and food producing animals is also important to prevent animal and zoonotic pathogens. The development of veterinary vaccines is highly dependent on cost-benefit ratio. However, this should not limit the major aim of veterinary vaccines of ensuring the health of animals and herd immunity. While the nasal and pulmonary route of vaccine administration has not quite made it to the market in humans, the use of NP delivery systems can help enhance vaccine effectiveness and help to ensure better delivery through devices that are specifically tailored for each species. In fact, materials that overcome delivery barriers determined from human findings have been translated into investigations of vehicles in livestock and poultry vaccines. Studies of nasal immunization with NP systems are common in both ruminants and chickens, however, data involving spray or nebulization of

vaccines is lacking. It is expected that both research and translation of pulmonary vaccine delivery using NPs in livestock and poultry will be rapidly expanding.

Table 1 Nasal and pulmonary nanoparticle and microparticle vaccines in development for livestock and poultry

Nanoparticle Type	Composition	Antigen	Species	Delivery Route	Efficacy	Ref
Polymeric	Poly(d, l-lactide-co-glycolide) (PLG) polyvinyl alcohol microparticle and 60% nanoparticle mix	*Toxoplasma gondii* Tachyzoite protein extract: SAG1 Cholera Toxin (CT)	Ovine (sheep)	i.n.	Systemic and local immune response. Consistent and higher IgA in nasal secretions and serum than soluble antigen. Not clear whether CT improved immune response in comparison to PLG-SAG1 alone.	[126]
Polymeric	Poly lactic-co-glycolic acid (PLGA)	Bovine parainfluenza 3 virus (BPI3V) proteins	Dairy calves (bovine)	i.n.	Enhanced and sustained mucosal IgA response compared to i.n. modified live virus commercial vaccine.	[16]
Liposome-mucoadhesive polymer	Phosphatidylcholine (PC) (zwittterionic) and tremella or xanthan gum	Inactivated influenza H5N3	SPF Leghorn chicken	i.n.	Mucoadhesive liposome vesicles induced higher immune response than the virus alone and liposome without the polymer. Viscosity affects vaccine efficacy.	[60]
Polymeric	Chitosan	Inactivated NDV	Broiler chicken, layer hens	i.n.	Increased IgA humoral response in layers, not broilers.	[83]
Liposome	Phosphatidylcholine (PC) (zwittterionic); Phosphatidylserine (PS) (-ve) or Stearylamine (SA) (+ve)	Formalin inactivated NDV	SPF Leghorn chicken	i.n.	PC induced the highest secretory IgA and systemic humoral responses. LPS co-administration increased vaccine efficacy.	[84]
Liposome	Hydrogenated soybean phospholipids	Inactivated APEC strain KAI-2, O-78	SPF Chicken	Coarse Spray Eye drop	Reduction in the number of challenged bacteria and clinical signs, was observed in chickens after a challenge with APEC.	[92]

Nanoparticle Type	Composition	Antigen	Species	Delivery Route	Efficacy	Ref
Montanide™ IMS adjuvant NP	Unknown	Live IBV	SPF Chicken (also commercially used in all farm animals)	i.n. Coarse Spray	Better than non-adjuvanted vaccine and montanide oil-in-water emulsion. i.n. administration performed better than coarse spray.	[105]
Adenovirus	BAdV-3	Bovine specific viral antigens: BHV-1 glycoprotein gD, BRSV IL-6	Bovine (cattle)	i.n.	Induces antigen specific immune responses. Co-expression of different vaccine antigens seems to produces similar response with lower viral titer.	[112, 114] [115]
ISCOMs	Glycoside Quil A	BHV-1 viral membrane proteins	Bovine (calves)	i.m.	Better protection than commercial attenuated vaccine and higher antibody response produced.	[118]
Polymeric	Chitosan spray-dried microparticle with recombinant polymeric protein antigen (BLSOmp31)	Brucellosis	Ovine (sheep)	i.n.	Induced local and systemic immune response in sheep, biphasic release of antigen from microsphere.	[121]
Polymeric	Fungal chitosan	Foot and Mouth disease whole virus	Guinea pig	i.n.	Higher IgG production in comparison to vaccination with virus alone. Systemic immune response comparable to traditional intra peritoneal alum-inactivated virus vaccine, IgA production resulting from NP vaccine was higher than alum inactivated viral vaccine.	[122]

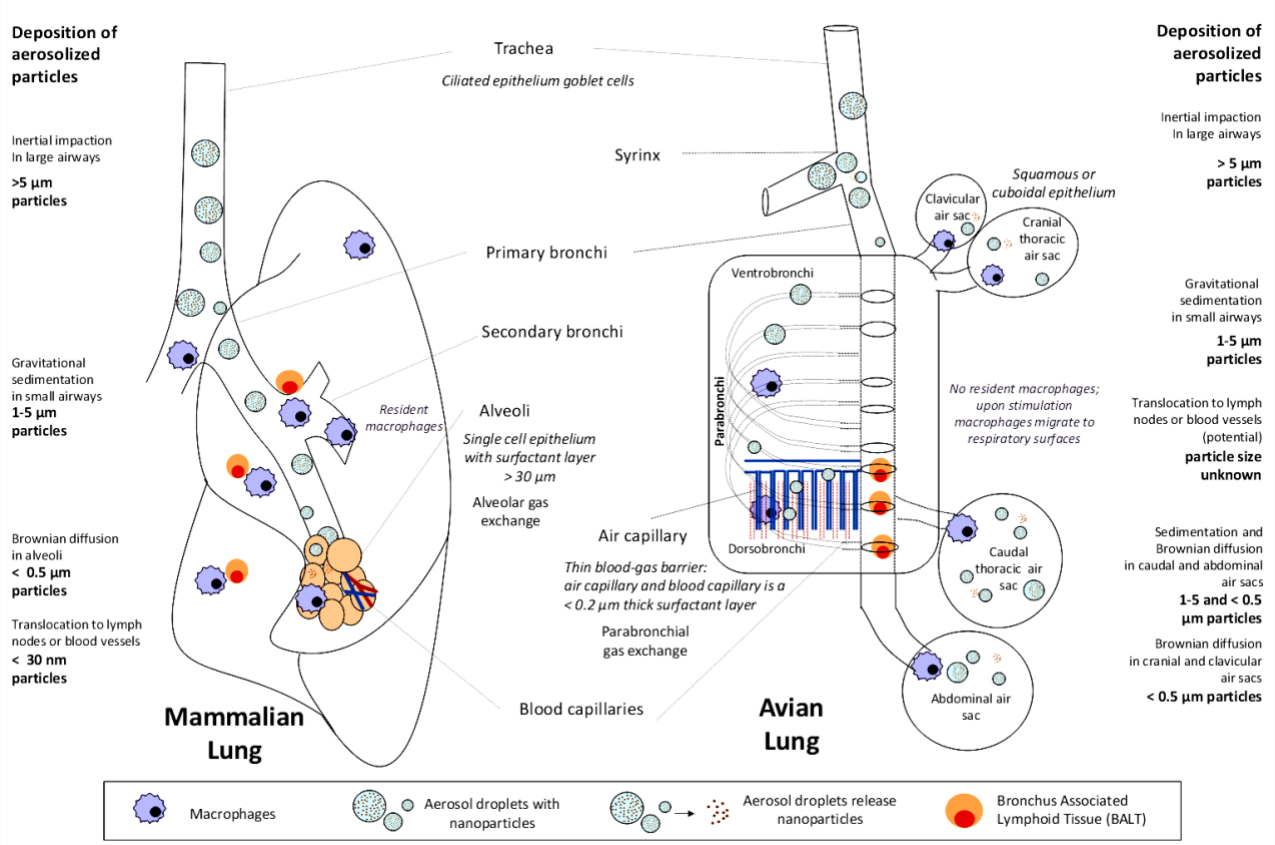

Figure 1 Comparative schematic diagram of the anatomical and immunological features of mammalian and avian respiratory system with respect to vaccine administration. Also shown is the size-dependent deposition pattern of aerosol droplets and the relevance of novel vaccine design involving nanoparticle carriers for antigens and adjuvants within aerosol droplets.

Inhalation of particles >5 µm results in inertial impaction in the large airways and are mainly cleared by mucociliary mechanisms in the trachea of both species which are swallowed. The main trend of deposition in both species is that smaller 1-5 µm particles have the ability to penetrate deeper into the lungs, either the alveoli or air capillary, i.e. the blood-air interface. In birds aerosol particles of <1 µm have been shown to deposit in the cranial thoracic air sacs, and even smaller <0.1 µm particles can deposit in the caudal thoracic air sacs of birds although the fate of these particles is not well known. [103, 127-131]

Unlike the mammalian lung, the avian lung lacks the constant surveillance of foreign particles by resident macrophages but they are rapidly recruited upon stimulation. The presence of BALT at the junctions of the primary and caudal secondary bronchi in the avian lung may aid in immune stimulation and lymphocyte recruitment. In the mammalian lung BALT forms after activation of the immune system and the possibility of inducing tolerance over immune activation is a consequence of constant surveillance by lung macrophages present in the tissue and in the alveoli.

Nanoparticles can be released from aerosol droplets in the alveoli and translocate to the lymph nodes and/or blood vessels. This was shown in mammalian (mouse) models. [102] Since in avian species the blood-air interface epithelium is 60% thinner than the mammalian epithelium, it is anticipated that the delivery of nanoparticle vaccines to the systemic circulation is also possible.

2.2 Pulmonary delivery of CpG-ODN in broiler chickens

CpG-ODN is a DNA sequence that can be used as a vaccine to prevent infectious diseases. In general, DNA vaccination involves introducing nucleic acid to host cells where it can produce short-term expression of a target antigen so that immune cells (antigen presenting cells) can initiate an immune response [132]. Ultimately, a nucleic acid vaccine aims to produce long-term immune memory by initiating antigen presentation to eventually produce long term-cellular immunity. DNA vaccines have the ability to provide targeted immune responses and deliver prophylactic and therapeutic vaccines [133, 134]. However, synthetic and DNA vaccines have generally not produced strong enough immune responses in clinical trials [1, 17, 20, 21, 49]. DNA vaccines such as CpG-ODN in broiler chickens have become an attractive approach because they are easy to design, manipulate, manufacture, cheaper, and fairly stable at room temperature [3]. They have also proven to be generally safe in human patients and some are approved in veterinary species such as horses and dogs [3].

2.2.1 Mechanism of CpG-ODN innate immune stimulation

Unlike conventional DNA vaccines, CpG-ODN does not require expression of a target antigen prior to initiating an immune response. CpG-ODN are unmethylated DNA sequence motifs already present in bacterial DNA that are automatically recognized by pattern recognition receptors in the mammalian and avian innate immune systems [135]. As such, CpG-ODN is an antigen that activates the innate immune system. Three types of CpG-ODN classes exist, and can activate murine and human immune cells (Table 2).

Table 2 Classes of CpG-ODN identified to activate the human immune system

CpG-ODN Type	Sequence Example	Structure	Immunostimulatory Activity
Class A (D-type)	5'-ggGGGACGA:TCGTCgggggg-3' (ODN 2216)	Phosphorothioate/phosphodiester mix Single CpG motif CpG motif flanked by palindromic sequence (underlined) 3' poly-G tail	Plasmatoid dendritic cells
Class B (K-type)	5'-tcgt**cg**ttttgt**cg**ttttgt**cg**tt-3' (ODN 2006)	Phosphorothioate backbone Multiple CpG motifs (bold)	Plasmatoid dendritic cells and B cells
Class C	5'-tcgtcgttttcggcgc:gcgccg-3' (ODN 2395)	Phosphorothioate backbone Palindromic CpG motifs (underlined)	B cells

Mechanisms of innate immune stimulation by CpG-ODN has been more widely studied in mammalian cells lines because it can be used as a vaccine adjuvant and is currently being tested as an adjuvant in hundreds of clinical trials, with no major concerns for safety issues [1]. In mammals, CpG-ODN is known to activate Toll-like Receptor 9 (TLR 9), which chickens (avian) do not express.

However, CpG-ODN can still stimulate avian macrophages, dendritic cells and B cells in neonatal chicks [136, 137]. Mechanistically, CpG-ODN in chickens stimulates TLR 21, the functional homolog of TLR 9 [138-140], but has also been found to stimulate TLR 15 depending on CpG class [141, 142]. As with human TLR 9, TLR 21 is located intracellularly in the endoplasmic reticulum [139, 140, 143]. The expression of TLR 21 in chickens has also been identified in the Bursa of fabricus, spleen, non-lymphoid tissues including mucosal areas like lung and small intestine as well as skin, kidneys, brain, and liver [140].

Although specific mechanisms of CpG-ODN innate immune activation have not been fully identified, certain cytokines are characteristic upon TLR 21 stimulation by CpG-ODN. It has been found that stimulation of both the chicken cell line HD11 and peripheral blood mononuclear cells with CpG-ODN results in the generation of nitric oxide and IL-1β [144-146]. Additionally, studies have found that activation of chicken immune cells also produce IL-6, IL-

12, and IFN-γ, which induce a predominant T-helper 1 (Th1) immune response [137, 145, 147]. Further characterization of the signal transduction events still must be elucidated. Nonetheless, there is evidence that immune activation by CpG-ODN is dependent on clathrin endocytosis and the binding to heat shock protein 90 subtype α (HSP-90α) (involved in activating ERK2 and PI3K signaling pathways) for full activation [136]. Mechanisms that have been identified so far in CpG-ODN activation are shown in Figure 2.

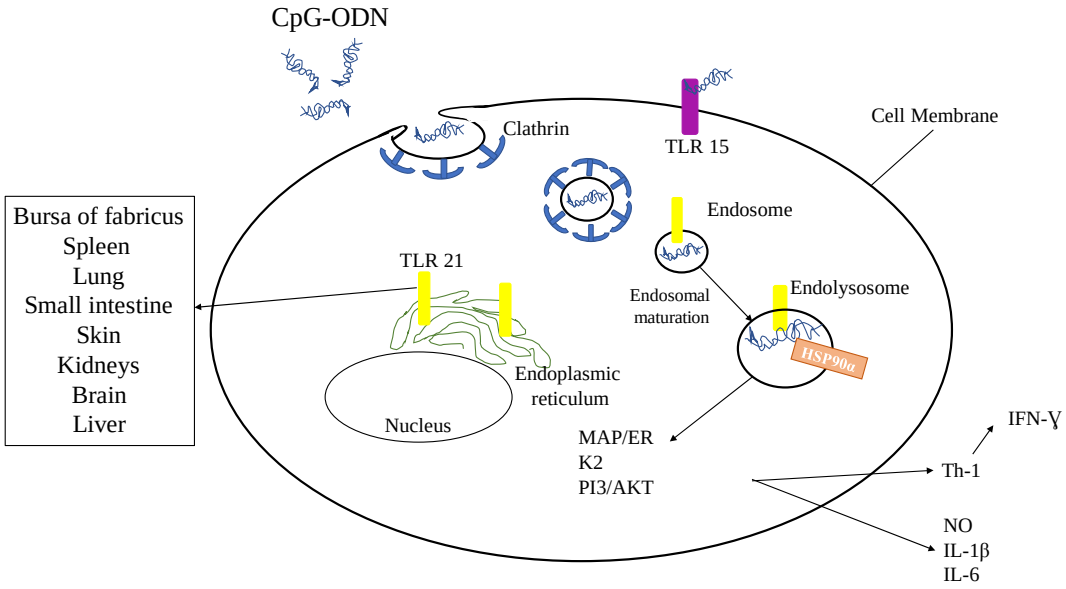

Figure 2 Mechanisms of CpG-ODN immune activation in the avian immune system

Of the three types CpG-ODN classes that exist, not all are able to stimulate chicken macrophages and the specific motif exhibits differences in the strength of activation and cytokine expression in the chicken immune system [144, 147]. Additionally, the modification of the phosphodiester bond in the DNA backbone to phosphorothioate by replacing the non-bridging oxygen with a sulfur atom also seems to increase stimulation [144, 147] (Figure 3).

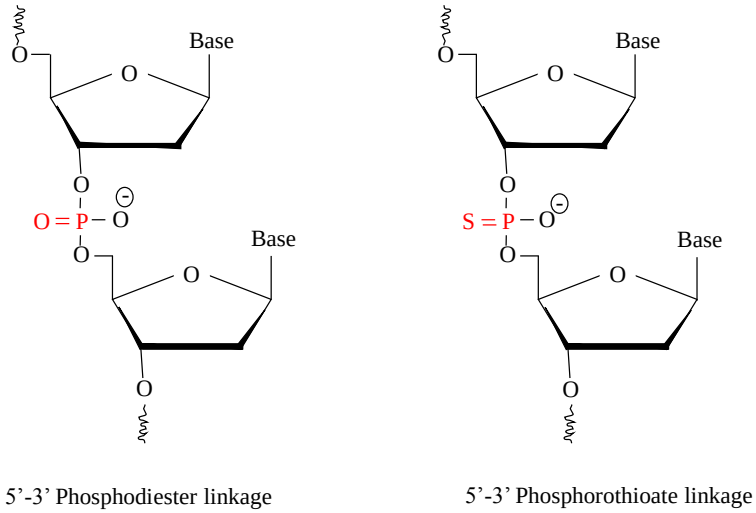

Figure 3 Depiction of phosphorothioate modification in DNA sequences
Phosphorothioate modification of DNA phosphodiester linkage (left) to phosphorothioate linkage (right).

Of the three classes of CpG-ODN, Type B 2006 which activates human macrophages also stimulates HD11 cells and PBMCs [136, 137, 146]. Additionally, CpG 2007 type B which is active in porcine and bovine immune cells has also activated HD11 cells (Figure 4) [136, 137]. The sequence GTC GTT has been shown to increase activation in human cells as well as the avian HD11 cell line [147].

CpG-ODN 2006 –Class B Human

5’ – tcg tcg ttt tgt cgt ttt gtc gtt -3’

CpG-ODN 2007 – Class B Bovine/porcine

5’ – tcg tcg ttg tcg tt -3’

Figure 4 CpG-ODN sequences known to stimulate avian species.

2.2.2 Evidence of protective effect against bacterial infection in chickens

Due to the innate immune stimulating abilities of CpG-ODN in chicken macrophages and peripheral blood mononuclear cell (PBMCs), its administration prior to detrimental bacterial infection by *Salmonella* and *E. coli* has been tested for antimicrobial and protective capabilities in chickens. Since the production of nitric oxide in macrophages is an innate immune mechanism that has bactericidal activity, the intracellular killing of *Salmonella enteriditis* (SE) was tested after stimulation with CpG-ODN [146]. Ultimately, nitric oxide generation in HD11 cells led to reduced bacterial counts in cells, which is important for the health of humans, who are susceptible to SE infection.

Further study has proven that CpG-ODN is able to prevent septicemia by *S. typhimurium,* which causes high mortality in neonatal chickens after *in ovo* and intramuscular (I.M.) administration [82]. Additionally, the immune response generated after administration of synthetic CpG-ODN 2007 adjuvant alone, has also protected neonatal chicks against infectious bronchitis virus and *E. coli* infection [7, 27, 82, 96, 148]. Moreover, the protection from *E. coli* infection has been established via various routes of administration: subcutaneous, I.M. and *in ovo* (chicken egg embryo) [7, 27, 82, 96, 148]. Of these studies, doses from 1-50 µg per bird have been examined and dosing has been given over different days of the chicken lifespan to test the length of immunity [7, 82, 96]. A dose of 50 µg per bird was able to protect birds against pathology and lower bacterial cell counts after *in ovo* and I.M. administration, with 50 µg per bird showing similar protection to 10 µg per bird I.M. against *E. coli* infection, but not salmonella septicemia in neonatal chicks [7, 82]. The 50 µg per bird dose has also protected adult birds at 22 days of age after administering the dose 3-6 days before challenge [96]. In each of these studies, it was concluded that the response to CpG-ODN treatment can last 3-6 days.

The proof of concept for using CpG-ODN as a vaccine to prevent common bacterial (*E. coli)* infection during the first week of life has been established from these studies, and phosphorothioated CpG-ODN 2007 is the main sequence being used *in vivo*. However, the question of long term immunity is still being defined in order to expand use of CpG-ODN throughout the bird lifespan without too many repeated immunizations while avoiding detrimental developmental effects. The use of a common veterinary antigen Emulsigen® has

been tested to determine improvement of CpG-ODN stimulation in terms of protection, but there was not a significant difference in protection [7]. To improve on this, the idea of NP technology to enhance long-term immunity, or develop slow release systems is beginning to emerge.

2.2.3 Role of delivery systems in improving protection of neonatal chicks

The development of new adjuvants and vaccine formulations to increase immunogenicity of subunit and protein vaccines has been an area of research that involves the development of particulate antigens such as liposomes and emulsions. The advantages of these delivery systems including enhanced innate immune stimulation has been tested in the chicken *E. coli* infection model.

The first test of this was using Emulsigen® as previously mentioned. However, further investigation compared several types of particulate delivery systems including polyphosphazenes, liposomes, cationic lipid, and Emulsigen® for their ability to enhance protection and prolong innate immunity generated against *E. coli* challenge after *in ovo* administration [14]. Interestingly, the polyphosphazene PCPP was the only formulation to improve survival, lower bacterial count, and lower the clinical score in comparison to unformulated (naked CpG-ODN). However, it was not able to prolong the duration of protection of neonatal chicks against *E. coli*.

A more recent study incorporates two different formulations of CpG-ODN DNA which take into consideration advances in gene therapy and delivery. In this study, four formulations categorized into single walled carbon nanotubes and lipid surfactant formulations were administered *in ovo* to compare whether they improved survival of chicks in comparison to unformulated CpG-ODN [27]. Once again, the formulations improved the survival of chicks and lowered the bacterial counts in comparison to naked CpG-ODN. However, there were differences in the formulations. The lipid-gemini surfactant formulation seemed to perform better than the gemini surfactant only formulation. However, direct comparison is not possible as different derivatives of cationic surfactants were used in each formulation. It was concluded that the delivery system was important to achieve protection of neonatal chicks but further

characterization and optimization of the formulations and understanding the mechanism of CpG-ODN immune stimulation is still required.

2.3 Mucosal vaccination via inhalation

The delivery of therapeutics to local respiratory tissues *via* aerosols has been well established and is a standard non-invasive therapy for the treatment of local respiratory diseases such as asthma and chronic obstructive pulmonary disease in humans [149]. For vaccine delivery, this route is attractive because it is non-invasive and suitable for mass administration. Additionally, the respiratory mucosal surfaces of an organism not only have the potential to initiate immunity at the local site of administration, but also systemically due to the close proximity and large surface areas of the blood-lung barrier [13]. There is already evidence that immunization via the respiratory tract not only produces high local immune responses [11, 52] but also provides high systemic mucosal immunity in mice and non-human primates [11, 53]. Another advantage is that since infectious diseases including *E. coli* in poultry can initiate their infectious process at mucosal surfaces, more delivery of the DNA vaccine at the site of infection could produce a stronger immune response, and initiate immune memory [13, 150].

2.3.1 Challenges involved in therapeutic and DNA delivery to the lung

The focus of aerosol delivery has been on new technologies to improve formulation characteristics and the delivery devices to produce more efficient delivery and deposition deeper in the lung [149]. In humans, the mechanisms of particle deposition in the lung have been extensively studied and inhalable drugs used today have achieved further drug delivery to the deeper airways [151]. There is paucity of studies of avian particle deposition in the airways, but there is some data available related to airway dynamics.

2.3.1.1 Delivery Devices

A variety of devices exist to deliver inhalable drugs to the respiratory system in humans. These include metered dose inhalers (pressurized and breath actuated), dry powder inhalers, and nebulizers [152]. Each type aerosol device delivers drug to the respiratory system differently and contains specific factors that affect drug deposition within the lung. Since the delivery of CpG-

ODN to chicks uses a nebulization device in this project, the main focus will be on compression nebulizers.

Nebulizers generate aerosols by generating small droplets from a liquid solution or suspension by jet nebulization or ultrasonic sound waves [152]. Jet nebulizers particularly break up liquid into a fine mist by using compressed gas flow. The large droplets are impinged upon baffles which are positioned in the path of the aerosol in order to further reduce the particle size of the exiting aerosol and deliver fine mist [152, 153] (Figure 5). Each nebulizer performs differently due to design, flow, pressure, tubing, and whether compressed gas or an electrical compressor is used [152].

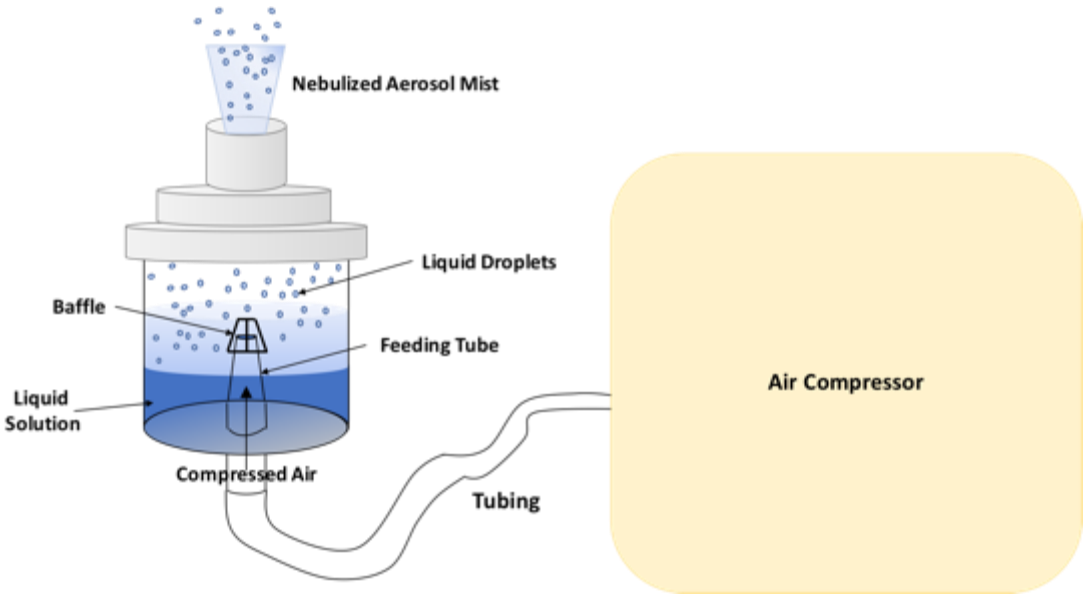

Figure 5 Mechanism of liquid to aerosol formation by a compressor jet nebulizer

Aerosol devices directly influence the size of particles delivered to the respiratory system and produce a heterogeneous population of aerosol droplets [151]. Due to the large variation of drug deposition from nebulizers and the relatively low drug delivery compared to other devices [152], many have studied formulation characteristics and device configurations to improve delivery to the lung [154-156]. The type of excipients used in a formulation can affect size

output of aerosol particles generated, which directly affects what area the particle gets delivered in the respiratory tract [157, 158]. If a nebulizer is chosen, the NP formulation designed must have low viscosity to allow the output to generate small droplets. Furthermore, different types of nebulizers are only compatible with certain types of formulations. For instance, ultrasonic nebulizers which generate aerosol droplets using high energy soundwaves are ineffective in nebulizing more viscous solutions such as suspensions or liposomes [25]. But, vibrating mesh or plate nebulizers which physically break up the liquid into smaller droplets work very efficiently for suspensions or liposomes [25].

As mentioned previously, broiler chickens and layer hens are subject to intensive vaccination against many infectious diseases [8]. In fact, spray vaccination in poultry (chicken, turkey) is standard against New Castle Disease virus (NDV) and Infectious Bronchitis Virus. However, spray vaccination in this regard refers to 100-200 μm liquid particles which do not specifically target inhalation but also seem to induce immunity through ocular, oral, and nasal mucosas. The definition of spray vaccination is not specifically defined in literature in terms of whether a spray drier is used versus a liquid spray generator or a nebulizer. However, the interconnection of the three devices is that they generate inhalable aerosols that play a role in the generation of immunity via the pulmonary mucosa.

What has not been collectively studied, are effects of nebulization on the stability of DNA formulations.

2.3.1.2 Airway mechanics

The localization of particles in the human lung has been widely studied. After inhalation of aerosol particles, their aerodynamic properties guide the mode of deposition in the lung: impaction, sedimentation, and diffusion. The particle size distribution, delivery device, and the type of breathing pattern during inhalation of the dose influence whether the particle deposits in the respiratory system by impaction, sedimentation or diffusion [25, 26]. Upon inhalation of a deep forceful breath, particles greater than 1 μm tend to impact as their higher density and momentum prevent it from changing direction if there is a change in airflow pattern. In the airways, these larger particles (3-6 μm) get trapped in the pharynx, mouth or the mucus of the trachea, which results in them being removed by swallowing [68, 69]. Upon slower air velocity

or a slower breathing pattern, particles between 1-5 μm tend to settle in the smaller airways and respiratory bronchioles by sedimentation (gravity), since their residence time within the lung increases [69]. Also, similar particles have better chance of reaching the bronchioles and respiratory mucosa in the lower airways [26]. The smallest particles less than 0.5 μm tend to deposit in the alveolar spaces resulting from Brownian motion [26, 69, 70]. Though, these smaller particles tend to get exhaled but if less than 34 nm in size, they enter the blood stream and are cleared via renal filtration [71]. Since systemic immune activation is critical to initiating cell mediated immune responses, targeting to the alveolar region at the interface of the blood-air boundary is highly desirable for a vaccine.

Although the theory of aerodynamics can be applied to chickens, the specific particle sizes and deposition cannot be extrapolated since the avian respiratory system is significantly different than the mammalian system in terms of lung structure and air flow.

In chickens, the upper respiratory tract consists of the very long trachea which splits at the syrinx into two extra-pulmonary primary bronchi each going to a lung and its associated air sacs [159] (see Figure 6). Unlike the mammalian lung, the avian lung has a very rigid structure due to the constant unidirectional flow of air driven by the air sacs [159]. During inspiration air flows from the trachea into the primary bronchi and into the caudal air sacs (Figure 6A). Expiration drives air from the caudal air sacs through the lung (Figure 6B) into the cranial air sacs (Figure 6C) which then gets expired out through the trachea [160].

The parabronchi provide a large area for gas exchange and is surrounded by blood and air capillaries [161]. In comparison to the anatomy of the mammalian respiratory system, the avian respiratory system is more efficient with larger surface area as the blood comes in contact with air capillaries [161]. The air-blood capillary interface is approximately 60% thinner than the mammalian interface, which means it is highly efficient but may predispose birds to environmental irritants and pathogens [159]. This could be advantageous when delivering a vaccine through inhalation.

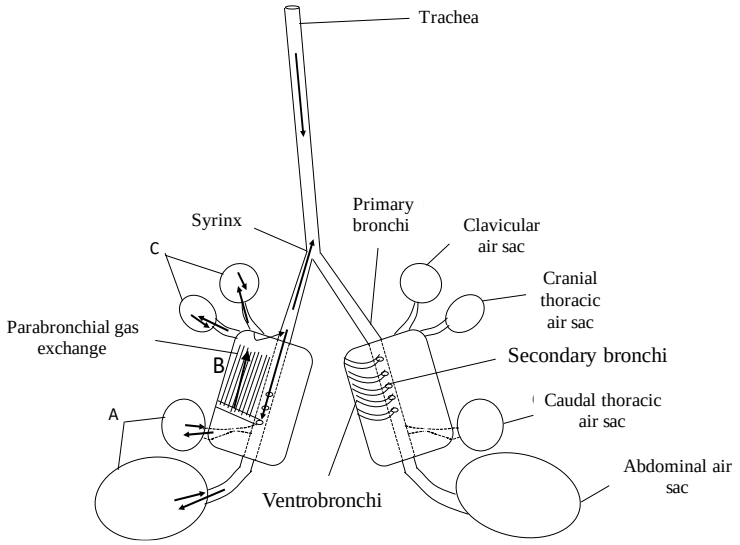

Figure 6 Structure and direction of air flow in the avian respiratory system

Components of the avian respiratory system are outlined. Arrows indicate direction of air flow through inspiration and expiration. Air is inhaled and passes through the trachea and primary bronchi to the abdominal and caudal air sacs (A). Air sacs push air through the lung upwards through the parabronchi (B) toward the trachea and into the clavicular and cranial air sacs (C). Air sacs push air back out through the trachea during expiration. [131, 160-162]

Most studies of aerosol delivery focus on broiler chickens, although there are a few studies in turkeys and layer hens. In order to establish local drug levels in the lung and air sacs, it has been found that particles less than 3 µm are able to bypass the mucociliary transport [103]. However, larger particles deposit in the upper airways, particularly the tracheal bifurcation [103, 104]. The advantage of NP formulation, is that the aerosol droplet particles can contain large amounts of individual NPs which can bypass the upper airways and get to the lung and closer to the circulation while depositing a greater amount of the therapeutic. Particle deposition is also dependent on age and it was shown that in comparison to 2 and 4 week old broilers, 1-day old chicks contained more >3 µm particles in the nose and eyes and in the lower respiratory tract, 1-3 µm deposited less than older chickens [104]. For smaller sized or NPs, aerosol particles of <1 µm have been shown to deposit in the cranial thoracic air sacs, which in a sense is advantageous because it means the particles passed through the lung. Even smaller <0.1 µm particles can deposit in the caudal thoracic air sacs of birds although the fate of these particles is not well known [103, 127-131].

Biological Parameters

In both the avian and mammalian respiratory system, a major barrier to particle and DNA entry is the ciliated epithelium and mucus producing goblet cells lining the upper respiratory tract [149, 159]. In combination, these two factors are termed as muco-ciliary clearance. Muco-ciliary clearance traps and moves particles up to the esophagus to be swallowed, or exhaled out. It also prevents diffusion through the mucosal barrier and can decrease particle residence time in the lung and lower the delivery of DNA/nucleic acid into the deeper airways [163]. In humans mucocilliary clearance lines the trachea until the secondary bronchi and in avians, it is also found in the primary bronchi and roots of the secondary bronchi [159]. In a way, it is the primary barrier which pulmonary DNA and drug delivery must overcome in order to effectively transport them to the deeper airways, retain genes to the underlying epithelial layer and maximize retention in the lung.

In humans, localization of gene delivery to the deep lungs and alveoli is required to achieve effective immunization because it allows access to immune cells. Covering the epithelial cells of the peripheral deep lungs is the pulmonary surfactant also called alveolar lining fluid [164]. Pulmonary surfactant may also have an effect on the stability of the vaccine formulation and the delivery of the DNA to the lung. However, the surfactant layer also contains components involved in the immune response such as Surfactant Protein A (SP-A) and alveolar macrophages which can quickly clear foreign particulates [165, 166]. The active phagocytic nature of macrophages however is advantageous in vaccine applications for eliciting immune activation.

In the avian respiratory system, mechanisms of immunity within the lung parenchyma are still under investigation. However, phagocytosis is a major mechanism in reaction to foreign particulates. A major difference between mammals and avians is that resident macrophages are not found in the avian respiratory system. Instead, macrophages quickly migrate into respiratory organs upon immune stimulation [159, 162]. This means that in the case of an inhalable NP formulation, the NP must stay in the lung environment long enough to recruit macrophages and other professional antigen presenting cells. Proteins and the environment of the lower respiratory system in the chicken respiratory tract would also play a role in vaccine formulation

compatibility, release, and degradation, however mechanisms of antigen uptake, processing and presentation are not completely elucidated [167].

Development of an inhalable vaccine requires an optimal delivery system to maximize antigen delivery to target cells in the body. In order to develop a delivery system suitable for CpG-ODN delivery to the avian lung, the size and characteristics of the particle must be taken into account. Since the target for innate immune activation is the avian macrophage, particles targeted to the lung are necessary to promote a protective immune response. Meanwhile, the immune system is a delicate balance between immune activation and tolerance, a sufficient delivery of antigen must be achieved to elicit an immune response that also initiates immune memory. Cellular uptake by macrophages and other antigen presenting cells may not be a hurdle for DNA vaccination, but the lack of retention of the antigen may prevent the ability for antigen presenting cells to process and stimulate long lasting immunity, Due to the differences between the avian and mammalian systems aerodynamics, particle sizes and cellular interactions that improve delivery in the mammalian system do not necessarily apply to the avian system and therefore must be optimized for effective pulmonary vaccine delivery.

2.3.2 Non-viral nanoparticles to improve gene delivery to the lung

In efforts to improve nucleic acid delivery to the lung, NP delivery vectors have been modified to pass the mucosal barrier, overcome clearance mechanisms, and reach the deeper lungs. Although gene delivery using viral vectors has resulted in increased success, safety concerns have pushed for research using non-viral vectors including biocompatible lipids, polymers, and surfactants. DNA delivery using a non-viral vector involves forming DNA complexes by the electrostatic interaction of cationic lipids, surfactants or polymers and the negatively charged phosphate groups in DNA (Figure 7) [23, 44].

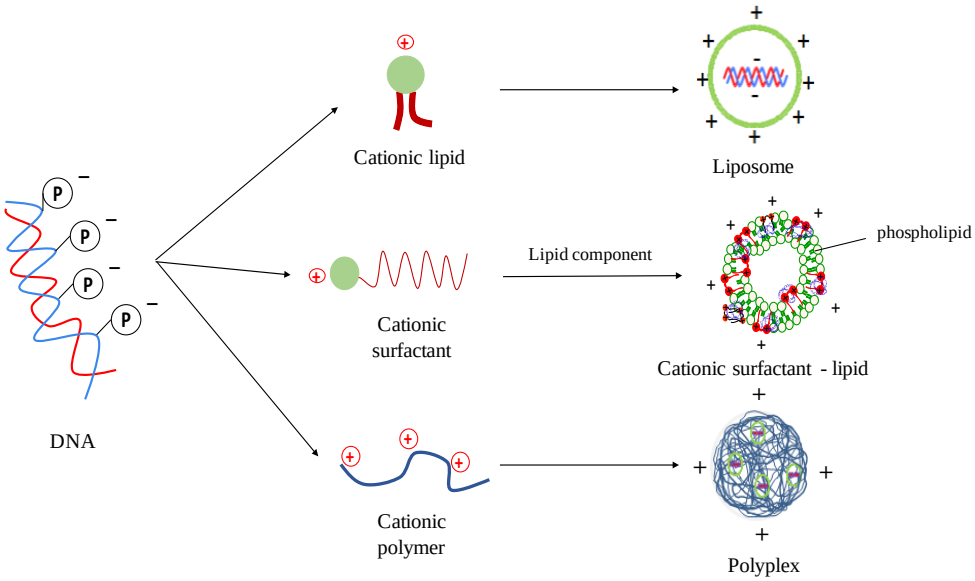

Figure 7 Representation of nanoparticle formation with DNA and cationic non-viral gene delivery vectors

Examples of DNA nanoparticles formed by complexation with cationic lipids, surfactants and polymers

The main advantage is that they are able to protect nucleic acids from degradation by nucleases in the physiological environment, which could increase delivery at the site of action [23]. But now, NPs have been tailored to their application by varying composition, size, shape, and surface properties [134]. The result is improved uptake by target cells by increasing binding affinity with target cells, increased deposition to the target site, reduced off target accumulation, extended delivery, and increased drug/therapeutic stability [168, 169]. Although most investigations have been conducted mainly in mammalian models, similar strategies can be adopted for optimizing delivery vehicles for CpG-ODN delivery in chickens.

Despite low efficiency with single component NPs, strategies including using muco-adhesive or bio-adhesive materials such as polyethylene glycol (PEG), carboxymethylcellulose, polyacrylic acid, and chitosan have been used for mucoadhesive formulation development [170]. Because of the "interfacial molecular attractive forces amongst the surfaces of the biological substrate and the natural or synthetic polymers" [170], the mucoadhesive polymers increase residence time of the particulate delivery system and enhance uptake of the biodegradable particulate vaccine at the mucosal surface [170, 171]

A variety of bio adhesive polymers exist, and some have been applied to pulmonary delivery of nucleic acids. Some groups have synthesized PLGA and chitosan based particles to

improve mucoadhesion in attempts to avoid clearance by mucociliary transport, improve transit time, and promote gene localisation to the lung epithelial cells [172, 173]. Furthermore, improvement of gene delivery to the lungs has been achieved using viscoelastic gels like carboxymethylcellulose to improve residence time in the airways and reduce mucociliary clearance. When 0.5% carboxymethylcellulose was complexed with lipid GL67A (gold standard for human pulmonary delivery) there was an increase in gene expression compared to GL67A alone to the nasal epithelium of mice [174]. Based on theories behind mucoadhesion and investigations in mammals, bio adhesive polymers could also be applied to the delivery system for and inhalable CpG-ODN vaccine in broilers.

Recent studies have adopted localization of gene delivery to the lower airways including the alveolar macrophages, alveolar type II cells, and lung smooth muscle cells [175-177]. Commonly used delivery systems are polymers, including chitosan, PEI, and PLGA based NPs. Indeed, polymer systems seem most promising for targeting the lower airways and promoting gene delivery. For example, PEI based polymers have been complexed with plasmid DNA and applied nasally in mice to test a mucosal vaccine priming strategy [178]. This study compared deacetylated PEI (dPEI) to lipid based carrier DOPE/DOTAP/Squalene (DDS), dPEI was found to be less toxic, produce a stronger antigen specific humoral response (Cd4+T cell response), and protect against influenza challenge [178]. More current studies involve using several different types of components like lipids and polymers or different types of polymer combinations to create NPs with improved delivery, safety, and uptake. For example, PLGA polymer containing PEI moieties on its surface for DNA complexation was tested *in vivo* for a prime boost with *Mycobacterium tuberculosis* vaccine [179]. After comparing endotracheal aerosol to intramuscular immunization, aerosol administration produced a higher proliferative response in splenocytes and T cells, and IFNγ production after re-stimulation of cells with MTb hypoxic lysate. This result confirmed that the non-invasive aerosol administration improved localized pulmonary delivery compared to intramuscular injection [179].

2.4 Gemini surfactants gene delivery systems

Efforts to drive gene therapy to the clinic has resulted in the synthesis of a large number of cationic materials to improve transfection efficiency and optimize targeting to specific cell types [180]. A variety of rate limiting steps are involved in the gene delivery process including the

interaction between particle and cell surface, internalization of the particle, and the release of the nucleic acid from the delivery vehicle to allow for cell processing [180]. Among the variety of cationic molecules synthesized for gene delivery, gemini surfactants are a relatively new class of amphiphilic molecules which have been typically shown to be useful transfection agents [181].

Gemini surfactants contain two hydrophobic tails and two hydrophilic head groups linked by a spacer group [182]. Gemini compounds can be tailored as a delivery platform by varying hydrophobic chain length, hydrophilic head groups and spacer groups, which could improve the transfection efficiency of the nucleic acid to the cell [183]. An example of one structure is gemini 12-3-12 that is made up of a positively charged quaternary ammonium linked to a 12-carbon chain. This is in turn linked to an identical molecule by a 3-carbon spacer (Figure 8). Names of quaternary ammonium gemini surfactants are designated as *m-s-m* corresponding to tail 1 length – spacer length - tail 2 length. These surfactants can self-assemble into a range of structures including micellar to inverted micellar or bilayer structures depending on molecular modifications [184]. The molecular structure of gemini surfactants also influences the physiochemical properties. The advantages of gemini surfactant physiochemical properties include lower critical micellar concentration (CMC), better ability to reduce surface tension and higher solubilisation power [185]. Due to their ability to be easily modified, having lower CMC values, and solubilisation power, benefits include minimizing *in vivo* concentration which could reduce toxicity risks and costs [185].

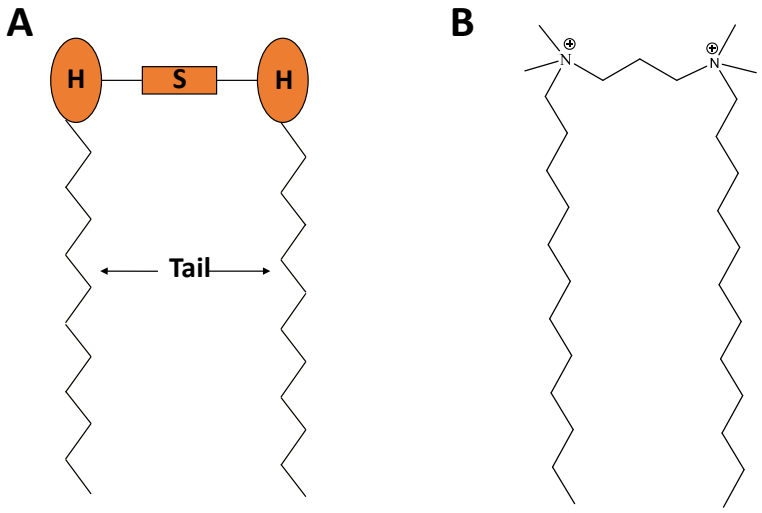

Figure 8 General structure of a gemini surfactant (A) and the 12-3-12 gemini surfactant (B)

The general structure of gemini surfactants (A) are composed of two amphiphilic molecules connected by a spacer group (s). Each amphiphilic molecule contains a polar head group (H) and two hydrophobic tail groups. This work used gemini surfactants consisting of quaternary ammonium groups as the polar head group, with a carbon tail (m), and carbon chain spacer (s). A representative example of gemini 12-3-12 (B) composed of a 12-carbon tail length and 3-carbon spacer is also shown (m=12, s=3).

Aside from NP systems physically delivering DNA to the target site, formulation uniformity, morphology, compaction and release are also important indicators of NP formulation effectiveness. A formulation must compact and package DNA effectively to create complexes with certain sizes and morphology, protect from degradation and undergo phase changes to efficiently release contents at the target site [184]. Gemini surfactant complexes have been shown to be advantageous to meet these requirements and with further modifications can be tailored to specific delivery sites [184].

Our group has used gemini delivery systems to improve gene delivery in culture and animal models for topical administration in dermal and ocular applications [182, 186, 187]. Applications of gemini delivery systems could also be expanded to mucosal gene delivery. In fact, recently amino-acid substituted gemini delivery systems have been created for vaginal mucosal gene delivery [45]. Therefore, gemini delivery systems also show potential for delivering DNA to the respiratory mucosa and surpassing clearance mechanisms to be able to reach the lung in order to activate the innate immune system for optimal immune-protective vaccines.

2.5 Chitosan gene delivery systems

Chitosan polymer is another cationic molecule that has been used to form NPs for a wide variety of applications including lung and nasal delivery owing to its mucoadhesive properties and biocompatibility [188]. Recently, use of chitosan has expanded to several gene delivery applications. The molecular structure of chitosan is made up of repeating D-glucosamine and N-acetyl-D-glucosamine units linked via (1-4) glycosidic bonds (Figure 9). Every deacetylated unit of chitosan contains a primary amine group with a pKa around 6.5 that becomes positively charged in acidic media such as acetic acid [41]. Chitosan is a weak base, rendering it insoluble in neutral and alkaline pH media [41]. In fact, its low solubility limits using simple chitosan-DNA NPs for gene delivery.

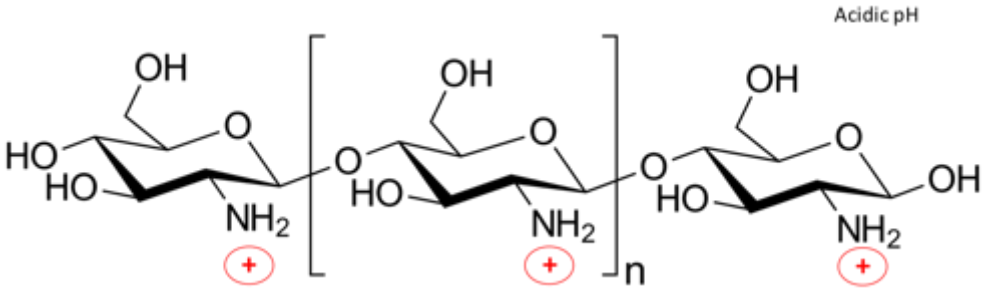

Figure 9 Chitosan Polymer structure (in acidic pH)

Chitosan polymer made up of repeating monomers of D-glucosamine and N-acetyl-D-glucosamine units linked via (1-4) glycosidic bonds (n). Dissolving in acidic media results in protonation (red) of amine groups.

Despite limitations, several factors are involved in chitosan NP complexation and its effectiveness in the gene delivery process has been widely studied. First, the MW of chitosan influences the size of NP complexes formed. On one hand the NP size decreased upon decreasing chitosan MW from 213 kDa to 48 kDa, but further decrease to 17 kDa and 10 kDa resulted in an increase in particle size [189]. The correlation between size and transfection efficiency has also been explored, although it is influenced by the particular cell line [190]. Generally, smaller chitosan NP sizes made from 20 kDa to 200 kDa chitosan resulted in greater transfection efficiency compared to 480 kDa chitosan NPs. However, there is a delicate balance

between MW and stability of the NP: higher MW chitosans improve NP stability while lower MW weight chitosans don't form as stable complexes. The result is slower or delayed expression by larger MW chitosan NPs and faster or premature release of DNA prior to entering the cell using low MW chitosan NPs [41, 188, 190, 191].

A second factor that influences gene delivery is the degree of deacetylation (DD) of chitosan. The DD is a measure of the percentage of deacetylated primary amine groups along the polymer chain. In other words, it determines the positive charge density when chitosan is dissolved in acidic conditions [41]. The DD determines how well the polymer can form stable complexes with DNA and higher DD results in more stable complexes with smaller NP size that can transfect target cells [191]. Whereas a DD >65% is sufficient for plasmid DNA complexation, a DD >80% may be more important for shorter siRNA oligonucleotide binding and stability [192].

A final major important factor involves the N/P ratio, which is also an important factor for all cationic gene delivery systems. The N/P ratio is measure of the number of positive charges per DNA phosphate. This is known to influence the outer charge of the particle (zeta potential) that impacts the stability of the particle. A higher N/P ratio indicates higher concentration of chitosan that could assist release of the DNA out of the endosome. Yet, if too low, the transfection efficiency may decrease [190, 191]. The N/P ratio also affects the size of the NP and structural shape. In fact, N/P ratios ranging from 5-10 have been effective for cell transfection of plasmid DNA, and ratios as high as 150 reported to be superior for siRNA [193-196].

Chapter 3: Materials and methods

3.1 CpG-ODN Characterization and Labeling

3.1.1 CpG-ODN stability: Ultra Performance Liquid Chromatography (UPLC)

CpG-ODN phosphorothioated double stranded DNA oligonucleotide was provided by Dr. Susantha Gomis (University of Saskatchewan) obtained from Merial Canada Inc. (now part of Boehringer Ingelheim); eurofins mwg/operon 7596610 CpG 2007; melting temperature 60.8℃ mw: 7056.5; 547 OD; desalted; dry; 12/18/12. 5'-TCGTCGTTGTCGTT-3'.

UPLC separation of CpG-ODN was performed with reverse phase liquid chromatography (H-class Bio ACQUITY, Waters). Mobile phases consisted of hexafluoroisopropanol (HFIP) >99% (Sigma-Aldrich Canada Co., Oakville, Ontario, Canada), and triethylamine (TEA) HPLC grade (Millipore Sigma, Billerica, Massachusetts, United States). CpG-ODN was dissolved in biotechnology grade water and 2 μL of the sample was injected into the column (XBridge™ OST C18, Waters) at a flow rate of 0.2 mL/min. Gradient separation from 45% to 90% of mobile phase A (50% Methanol in 400mM HFIP/16mM TEA) in mobile phase B (400mM HFIP, 16mM TEA) was completed in 10 minutes. The CpG-ODN was detected at a retention time of 3.4 minutes using the PDA detector at 260 nm.

Preparation method of mobile phases can be seen in the table below.

Table 3 Preparation of TEA/HFIP mobile phase for separation by UPLC

Mobile Phase A: 16 mM TEA plus 400 mM HFIP aqueous buffer final pH ~7.9

Ingredient	Molecular Weight	Concentration in Buffer	Density	Amount per 1L	Amount per 500 mL
HFIP	168.04 g/mol	400 mM	1.596 g/mL	42.1 mL	21.5 mL
TEA	101.19 g/mol	16 mM	0.726 g/mL	2.2 mL*	1.1 mL* (26 drops)
MilliQ Water				955.7 mL	477.4 mL

*Note: 22-26 drops of glass Pasteur Pipet = 1 mL, i.e. 24 drops=1 mL

To prepare mobile phase A: HFIP was added to milliQ water while mixing for at least 5 minutes with magnetic stir bar at speed 4 until well mixed. TEA was slowly added dropwise one at a time via glass pipet while mixing for 5 minutes until contents were completely solubilized and no immiscible bubbles were visible. Mobile Phase B consisted of 50% methanol and 50% 16 mM TEA 400 mM HFIP solvent. TEA/HFIP solvent was divided into two halves. To one half, 50% methanol was added in parts while mixing for 5 minutes.

3.1.2 Labeling CpG-ODN Oligonucleotide with Alexa Fluor A647

The nucleotide was labeled using the Ulysis™ Alexa Fluor™ 647 Nucleic Acid Labeling Kit (Life Technologies, Burlington, Ontario, Canada) according to manufacturer's instructions at a labeling ratio of 100 μg per labeling reaction. Briefly, CpG-ODN DNA was reconstituted in sterile biotechnology grade water (Fisher Bioreagents, Fair Lawn, New Jersey, USA) and was incubated with labeling reagent in an 80°C water bath for 15 minutes. The reaction was stopped by plunging reaction tube into an ice bath. DNA mixture was purified by spin column centrifugation at 14000 g using Amicon ultracentrifuge filters (3kD cut-off) from Millipore Corporation (Billerica, MA, USA).

3.1.2.1 Labeling Efficiency Calculation

Labeling efficiency was determined by determining the ratio of base to dye using the equation:

$$Base{:}Dye = \frac{(A_{nucleic\ acid} \times \varepsilon_{Alexa\ Fluor\ 467})}{(A_{Alexa\ Fluor\ 647} \times \varepsilon_{nucleic\ acid})}$$

Where $A_{\text{nucleic acid}}$ and $A_{\text{Alexa Fluor 647}}$ are the absorbance measured at 260 nm and 650 nm respectively. The extinction coefficients for nucleic acid and Cy5 dye were previously determined to the values $\varepsilon_{\text{Alexa Fluor 647}}$ = 239000; $\varepsilon_{\text{nucleic acid}}$= 6600.

3.2 Nanoparticle Preparation and Characterization

Several types of NP formulations were prepared: gemini only (G-NPs), gemini-phospholipid (GL-NP), gemini-phospholipid-biopolymer (BGL-NP), phospholipid-chitosan (CL-NP), chitosan-gemini (CG-NP), chitosan (C-NP), hyaluronic acid (HA-NP), and chitosan-sodium alginate (CA-NP). The G_{12}L-NP (no biopolymer) and PVP 10,000 BG_{12}L-NP (PVP 10,000 polymer coating) were the starting point previously designed and tested in our group.

The following excipients and materials were used in formulation development. Solvents used included autoclaved MilliQ water (prepared in house) and biotech grade water (Fisher Bioreagents) used to dissolve polymers and CpG-ODN, respectively. The selected polymers included polyvinylpyrrolidone (PVP), MW 10,000, PVP 10,000; Kollidon® 25); PVP, MW 40,000, PVP 40,000 (Sigma Aldrich, St. Louis, Missouri, USA)); Avicel RC-591 sodium carboxymethylcellulose (CMCNa) (FMC Biopolymer, Philadelphia, Pennsylvania, USA); chitosan low MW 50-190 kDa, 75-85% deacetylated (Sigma Aldrich); chitosan 2.5 kDa, Creative PEGWorks (Chapel Hill, North Carolina, USA); PROTANAL® CR 8133 (sodium alginate), (FMC Biopolymer); hyaluronic acid (Creative PEGWorks); mPEG-DSPE (Creative PEGWorks); propylene glycol USP, (PG) (Spectrum Laboratory Products Inc., Gardena, California, USA); polyethylene glycol 400 N.F. (PEG 400) (Spectrum Laboratory Products Inc.)

Lipids used included 1,2-Dipalmitoyl-sn-glycero-3-phosphocholine (DPPC) (Sigma Aldrich); Phospholipon 100H, Nattermann, Batch # 92000300, Identification # 13052; NBD-PC (Avanti® Polar Lipids, Inc., Alabaster, Alabama, USA);

Gemini surfactants included three first generation compounds (without modification): Gemini 12-3-12 (manufactured in house Lot #:120804-3); Gemini 16-3-16 (manufactured in house Lot #:280404); Gemini 18-3-18 (manufactured in house Lot #:070606-3)

Other excipients used were acetic acid (Sigma Aldrich); sodium hydroxide (Sigma Aldrich); phosphate buffered saline, pH 7.4 (prepared in house); Tris-EDTA, TE buffer (Thermo Fisher Scientific, Rockford, Illinois, USA)

Table 4 Gemini-phospholipid NP formulations (G_{12}L-NPs, BG_{12}L-NPs)

Formulation code	Formulation components	Concentration in final formulation
G_{12}L-NP (PEG 400)	DPPC Gemini surfactant 12-3-12 PEG400 Water CpG Solution	10 mg/mL 2.2 mg/mL 10 mg/mL 4.87 mg/mL 1 mg/mL
PVP 10,000 BG_{12}L-NP (PEG 400)	DPPC Gemini surfactant 12-3-12 PEG400 PVP 10,000 CpG Solution	10 mg/mL 2.2 mg/mL 10 mg/mL 4.87 mg/mL 1 mg/mL
PVP Kollidon 25 BG_{12}L-NP (PEG 400)	DPPC Gemini surfactant 12-3-12 PEG400 PVP Kollidon 25 CpG Solution	10 mg/mL 2.2 mg/mL 10 mg/mL 4.87 mg/mL 1 mg/mL
PVP 40,000 BG_{12}L-NP (PEG 400)	DPPC Gemini surfactant 12-3-12 PEG400 PVP 40,000 CpG Solution	10 mg/mL 2.2 mg/mL 10 mg/mL 4.87 mg/mL 1 mg/mL
CMCNa BG_{12}L-NP (PEG 400)	DPPC Gemini surfactant 12-3-12 PEG400 CMCNa CpG Solution	10 mg/mL 2.2 mg/mL 10 mg/mL 4.87 mg/mL 1 mg/mL
G_{12}L-NP (PG)	DPPC Gemini surfactant 12-3-12 Propylene glycol Water CpG Solution	10 mg/mL 2.2 mg/mL 10 mg/mL 4.87 mg/mL 1 mg/mL
PVP 10,000 BG_{12}L-NP (PG)	DPPC Gemini surfactant 12-3-12 Propylene glycol PVP 10,000 CpG Solution	10 mg/mL 2.2 mg/mL 10 mg/mL 4.87 mg/mL 1 mg/mL
PVP Kollidon 25 BG_{12}L-NP (PG)	DPPC Gemini surfactant 12-3-12 Propylene glycol PVP Kollidon 25 CpG Solution	10 mg/mL 2.2 mg/mL 10 mg/mL 4.87 mg/mL 1 mg/mL

Formulation code	Formulation components	Concentration in final formulation
PVP 40,000 BG_{12}L-NP (PG)	DPPC Gemini surfactant 12-3-12 Propylene glycol PVP 40,000 CpG Solution	10 mg/mL 2.2 mg/mL 10 mg/mL 4.87 mg/mL 1 mg/mL
CMCNa BG_{12}L-NP (PG)	DPPC Gemini surfactant 12-3-12 Propylene glycol CMCNa CpG Solution	10 mg/mL 2.2 mg/mL 10 mg/mL 4.87 mg/mL 1 mg/mL

*CpG-ODN was dissolved in biotech grade water with a final concentration of 4 mg/mL

Table 5 Lipid-gemini PEG hybrid NP formulations

Formulation code	Formulation components	Concentration in final formulation
7a	DPPC mPEG-DSPE Gemini 12-3-12 CpG-ODN Sterile water	10 mg/mL 1mg/mL 2.2 mg/mL 1 mg/mL q.s. to 1mL

Table 6 Chitosan Lipid NP formulations (CL-NPs)

Formulation code	Formulation components	Concentration in final formulation
CL-NP (T5)	Phospholipon 100H Propylene Glycol Chitosan CpG-ODN 4M NaOH Sterile Water	25 mg/mL 25 mg/mL 2.2 mg/mL 1 mg/mL q.s. to pH 5.2 q.s. to 1 mL

*Low MW Chitosan (50-190 kDa) was dissolved in acetic acid prior to use in formulations (0.1% chitosan solution in 1% acetic acid, pH 3.4)

Table 7 Gemini CpG-ODN NP Complexes (G-NPs)

Formulation code	Formulation components	Concentration in final formulation
G_{12}-NP (11, 11R)	Gemini 12-3-12 CpG-ODN	1.65 mg/mL 1 mg/mL
G_{16}-NP (14)	Gemini 16-3-16 CpG-ODN	1.65 mg/mL 1 mg/mL
G_{18}-NP (15)	Gemini 18-3-18 CpG-ODN	1.65 mg/mL 1 mg/mL

*Gemini powder was dissolved in sterile molecular grade water. Starting concentration of gemini solutions were 2.2 mg/mL, CpG-ODN starting concentration was 4 mg/mL

Table 8 Chitosan Nanoparticles (C-NPs)

Formulation code	Formulation components	Concentration in final formulation
0.1% Low MW C-NP (10, 10d)	CpG-ODN 0.1% Chitosan 50KDa stock solution in 1% acetic acid	1 mg/mL 7.22 mg/mL
1% ultra-low MW C-NP (16)	CpG-ODN 1% Chitosan 2.5k MW stock solution in 1% acetic acid	1mg/mL 7.5 mg/mL
1% ultra-low MW C-NP (1f)	CpG-ODN 1.5% Chitosan 2.5K stock solution in 1% acetic acid	1 mg/mL 10 mg/mL

*CpG-ODN was dissolved in biotech grade water at 4 mg/mL prior, final formulations had a pH range of 3.5-4.2

Table 9 Second generation chitosan NP formulations (CG-NPs)

Formulation code	Formulation components	Concentration in final formulation
0.1% CG_{12}-NP (11b-12)	Gemini 12-3-12 CpG-ODN 0.1% Chitosan stock solution	0.44 mg/mL 1 mg/mL 0.55 mg/mL
0.1% CG_{12}-NP TE (11b-TE)	Gemini 12-3-12 CpG-ODN in TE buffer 0.1% Chitosan stock solution	0.44 mg/mL 1 mg/mL 0.55 mg/mL
0.1% CG_{16}-NP (11b-16)	Gemini 16-3-16 CpG-ODN 0.1% Chitosan stock solution	0.44 mg/mL 1 mg/mL 0.55 mg/mL
0.1% CG_{18}-NP (11b-18)	Gemini 18-3-18 CpG-ODN 0.1% Chitosan stock solution	0.44 mg/mL 1 mg/mL 0.55 mg/mL
1% CG_{12}-NP (11d-12)	Gemini 12-3-12 CpG-ODN 1% Chitosan in 1% acetic acid pH 4.0	0.44 mg/mL 1 mg/mL 5.5 mg/mL
1% CG_{16}-NP (11d-16)	Gemini 16-3-16 CpG-ODN 1% Chitosan stock solution	0.44 mg/mL 1 mg/mL 5.5 mg/mL
1% CG_{18}-NP (11d-18)	Gemini 18-3-18 CpG-ODN 1% Chitosan stock solution	0.44 mg/mL 1 mg/mL 5.5 mg/mL
2% CG_{12}-NP (11f-12)	Gemini 12-3-12 CpG-ODN 2% Chitosan stock solution	0.44 mg/mL 1 mg/mL 11 mg/mL
2% CG_{16}-NP (11f-16)	Gemini 16-3-16 CpG-ODN 2% Chitosan stock solution	0.44 mg/mL 1 mg/mL 11 mg/mL
2% CG_{18}-NP (11f-18)	Gemini 18-3-18 CpG-ODN 2% Chitosan stock solution	0.44 mg/mL 1 mg/mL 11 mg/mL
0.1% CG_{12}-NP PBS (11e-12)	Gemini 12-3-12 CpG-ODN 0.1% Chitosan stock solution Phosphate buffered Saline	0.44 mg/mL 1 mg/mL 0.4 mg/mL 150 µL/mL
0.1% CG_{16}-NP PBS (11e-16)	Gemini 16-3-16 CpG-ODN 0.1% Chitosan stock solution Phosphate buffered Saline	0.44 mg/mL 1 mg/mL 0.4 mg/mL 150 µL/mL

Formulation code	Formulation components	Concentration in final formulation
0.1% CG_{18}-NP PBS (11e-18)	Gemini 18-3-18 CpG-ODN 0.1% Chitosan stock solution Phosphate buffered Saline	0.44 mg/mL 1 mg/mL 0.4 mg/mL 150 µL/mL

*gemini was dissolved in sterile MilliQ water at 2.2 mg/mL, CpG-ODN was dissolved in biotech grade water at 4 mg/mL. Chitosan was dissolved in 1% v/v acetic acid (stock solution). 0.1% chitosan solution pH: 3.15, 1% chitosan solution pH: 4.0, 2% chitosan solution pH: 4.48.

Table 10 Sodium Alginate NP formulations

Formulation code	Formulation components	Concentration in final formulation
AC-NP (3-1b)	Sodium Alginate CpG-ODN 1.5% Chitosan 2.5k stock solution	0.044 mg/mL 1 mg/mL 10 mg/mL
A-NP (13a)	CpG-ODN Sodium alginate	1mg/mL 3.3 mg/mL
AG_{12}-NP (13b-12)	Gemini 12-3-12 CpG-ODN Sodium Alginate	0.44 mg/mL 1 mg/mL 2.42 mg/mL
AG_{16}-NP (13b-16)	Gemini 16-3-16 CpG-ODN Sodium Alginate	0.44 mg/mL 1 mg/mL 2.42 mg/mL
AG_{18}-NP (13b-18)	Gemini 18-3-18 CpG-ODN Sodium Alginate	0.44 mg/mL 1 mg/mL 2.42 mg/mL

*Chitosan was dissolved in 1% v/v acetic acid (stock solution). Sodium alginate was dissolved in sterile milliQ water at 4.4mg/mL. Gemini was dissolved in sterile MilliQ water at 2.2 mg/mL. CpG-ODN was dissolved in biotech grade water at 4 mg/mL

Table 11 Hyaluronic Acid NP formulations

Formulation code	Formulation components	Concentration in final formulation
1c	0.01% Hyaluronic Acid CpG-ODN 1.5% Chitosan 2.5k solution	0.01 mg/mL 1 mg/mL 10 mg/mL
12	CpG-ODN 0.01% Hyaluronic acid	1mg/mL 0.5mg/mL
12a	CpG-ODN 0.01% Hyaluronic Acid 0.1% Chitosan solution	1 mg/mL 0.025 mg/mL 0.5 mg/mL
12aTE	CpG-ODN in TE 0.01% Hyaluronic Acid 0.1% Chitosan solution	1 mg/mL 0.025 mg/mL 0.5 mg/mL

* Hyaluronic acid was dissolved in sterile milliQ water (m/v). 0.1% Chitosan stock solution (m/v) consists of low MW chitosan dissolved in 1% acetic acid (v/v) pH 3.15. 1.5% Chitosan stock solution (m/v) consists of ultra-low MW chitosan dissolved in 1% acetic acid (v/v).

Formulations were prepared with non-labeled CpG-ODN for characterization purposes and with Alexa Fluor 647 labeled CpG-ODN for further *in vitro* and *in vivo* experiments. For blank particles formulations, CpG-ODN solution was replaced with sterile water.

3.2.1 Gemini Phospholipid Nanoparticle Preparation (G_{12}L-NPs)

DPPC and the appropriate gemini surfactant, were weighed in a glass scintillation vial. The excipient (PEG400 or PG) was weighed and added to the lipid and surfactant. The contents were heated in a 75°C water bath and vortex mixed intermittently with heating until all ingredients were uniformly mixed (lipid phase) (Table 4).

3.2.1.1 Variation of biopolymer

Polymer solutions were dissolved in sterile MilliQ water. Each biopolymer was diluted as a stock solution of 100 mg in 15 mL water. The polymer solution (or water for non-biopolymer formulation) was heated to 40°C and added to the lipid phase and vortex mixed and heated intermittently in a 75°C water bath until the mixture was homogeneous and uniform until there

were no visible particles. The solution was cooled to 40°C and CpG-ODN was added to the vesicles and vortex mixed and warmed intermittently until formulation was translucent, uniform and there were no visible particles. Final formulation was bath sonicated for 5 minutes to evenly distribute particles.

3.2.2 Gemini CpG-ODN NP complexes (G-NPs)

Gemini 12-3-12, 16-3-16, 18-3-18 solutions were also prepared in MilliQ water at room temperature, with the exception of gemini 16-3-16 and 18-3-18 which were heated briefly to 60°C in order to uniformly dissolve.

CpG-ODN lyophilized powder was reconstituted using sterile biotech grade water to make a stock solution of 4 mg/mL. Appropriate volumes of the stock solution were used for the formulations. The final CpG-ODN concentration in the NP formulations was 1 mg/mL, unless otherwise noted.

Gemini complexes with CpG-ODN were formed at room temperature by the addition of CpG-ODN solution to gemini solution while stirring with magnetic stir bar at 900 rpm. NP complexes were sonicated for 10 minutes or until the formulation was translucent (Table 7).

3.2.3 Chitosan NP Preparation

3.2.3.1 Stock solution preparation

Different chitosan polymer quantities were dissolved in 1% v/v acetic acid in order to produce Chitosan NPs. Three different chitosan concentrations were tested. 0.1%, 1%, 2% m/v. All NP preparation was performed at room temperature.

Gemini 12-3-12, 16-3-16, 18-3-18 solutions were also prepared in MilliQ water at room temperature, with the exception of gemini 16-3-16 and 18-3-18 which were heated at 60°C in order to uniformly dissolve.

CpG-ODN stock solution was made at 4 mg/mL so that the final CpG-ODN concentration in the NP formulation was 1 mg/mL.

3.2.3.2 Chitosan only NPs (C-NPs)

Two different MW chitosan polymers were used to make C-NPs. A low MW chitosan 50-90 kDa based on viscosity and an ultra-low MW chitosan of 2.5k. For formulation of CpG-ODN with low MW chitosan, the CpG-ODN solution was first added to a scintillation vial while stirring with a magnetic stir bar. The chitosan solution was added dropwise to CpG-ODN solution while stirring at 900 rpm for 10 minutes. NPs were bath sonicated for 2 minutes and returned to stirring overnight (~20 hours) until uniform translucent uniform slightly turbid solution was observed.

A higher 1% w/v chitosan solution was also used to develop chitosan-CpG-ODN NPs, however uniform NP dispersion was not achieved due to clumping within the solution.

The ultra-low MW chitosan was formulated in the same manner, without the overnight stir (Table 8).

3.2.3.3 Chitosan – gemini NPs (CG-NPs)

Stock solutions of 50-90 KDa chitosan (low MW, Sigma) were prepared in 1% acetic acid. The stock solution of CpG-ODN (4 mg/mL in sterile water) was added to the gemini solution, swirled to mix and vortexed intermittently at room temperature. The complex was then bath sonicated 25 minutes at room temperature. The corresponding chitosan solution was added as the final component, dropwise to the CpG-ODN- gemini complex while mixing with a magnetic stir bar at 1000 rpm. The mixing was continued for 15 minutes until a uniform milky solution was formed. The NPs were further bath sonicated at room temperature for 10 minutes to ensure uniform NP formation. For formulations with PBS, the PBS was added after complex formation (Table 9).

3.2.4 Sodium alginate, hyaluronic acid NP preparation

Stock solutions of sodium alginate and hyaluronic acid were prepared in sterile MilliQ water.

3.2.4.1 Sodium alginate particles

Sodium alginate solution was added to CpG-ODN solution and vortexed to mix evenly (A-NPs). For chitosan-sodium alginate formulation (AC-NPs), ultra-low MW (2.5k) chitosan solution was added at once and vortexed to mix until a uniform solution was observed (Table 10).

3.2.4.2 Sodium alginate- gemini particles (AG-NPs)

Gemini – CpG-ODN complexes were first formed by adding CpG-ODN solution to gemini 12-3-12, 16-3-16, or 18-3-18 solutions. Mixture was vortexed until a translucent uniform solution was observed. Appropriate volume of sodium alginate solution was added to the gemini – CpG-ODN complexes and vortexed to mix until a uniform mixture was observed (Table 10).

3.2.4.3 Hyaluronic acid-chitosan particles (HAC-NPs)

Appropriate volume of hyaluronic acid solution was added to CpG-ODN solution and the clear solution was vortexed to mix. The corresponding volume of low MW 50-90 kDa chitosan solution was added dropwise with intermittent vortexing. The solution was bath sonicated at 40°C for 10 minutes until a translucent uniform solution was produced (Table 11).

3.2.5 Assessment of particle size, polydispersity and zeta potential

Size (hydrodynamic diameter), polydispersity index and zeta (ς) potential measurements were carried out on all particle formulations. Aliquots of 100 μL and 1000 μL of each formulation were prepared for size and zeta potential measurements, respectively. Measurements were performed using the Nano ZS Zetasizer (Malvern Instruments, Worcestershire, UK) which measures the hydrodynamic diameter of particles using dynamic light scattering (DLS). Measurements were carried out in triplicates for each condition. Z-average values as expression of mean particle size are considered valid for samples with a PDI index < 0.5 (according to manufacturer's protocol).

3.2.6 Assessment of DNA packing into particle (Fluorescence Correlation Spectroscopy)

FCS measurements were performed on a Zeiss LSM 710 confocal laser scanning microscope (CLSM) with Confocor 3 system (Zeiss, Jenna, DE). NPs were prepared with Alexa Fluor 647 labeled CpG-ODN DNA. Alexa Fluor 647 was excited by a 633 nm He-Ne laser at approximately 50 μW and reflected by a dichroic beam splitter (488/633) and focused 200 nm into the sample through a 40x Zeiss Apochromat NA 1.2 water-immersion objective lens. Emission spectra were collected through a 580 nm long-pass filter and recorded by an avalanche photodiode detector (APD). A 45 μM (1 Au) pinhole blocked out-of-focus emission. The lateral radius of the focal volume for the 633nm laser was determined by a calibration dye (Cy5-NHS-ester) to be 590 nm. FCS measurements were carried out in 150 μL volumes of diluted GL-NPs and BGL-NPs in a 4 well CELLview coverslips (Grenier-Bio One, Frickenhausen, DE). NP samples were prepared in triplicate for FCS and measurements were taken for 3 s, forty times for each sample. Calibration of the system was performed with a 1.25 nM Cy5 solution.

3.2.6.1 FCS data analysis

The count rate gathered from the avalanche photo detector was used to determine the autocorrelation function (ACF) as described previously [197]. A three-dimensional Gaussian excitation intensity distribution was assumed and the free diffusion of a single species was calculated using the formula below:

Where N is the mean number of molecules in the excitation volume, S is the ratio between the equatorial and axial radii of the focal volume, and τ_d is defined as the characteristic diffusion time of the particle. Diffusion coefficients (D) were determined using the Stokes-Einstein equation below.

$$D = \frac{\omega_{\mathcal{R}^2}}{4\tau_d}$$

where ω_R is the lateral radius of focal volume experimentally determined by measuring the diffusion time of calibration (τ_{dCy5}) with the known diffusion coefficient of Cy5-NHS ester (3.2×10^{-6} cm^2/s. τ_d for the sample is obtained from the fitted autocorrelation function.

3.3 Testing the nanoparticle delivery vehicle in a chicken macrophage cell model

3.3.1 CpG-ODN uptake assay in the HD11 cell line

As avian macrophages are thought to be a major player in CpG-ODN immune stimulation and have been found to be recruited to the avian lung during infection with avian pathogenic *E. coli* (APEC), they were used for an *in vitro* screening model of nanoparticle formulations prepared. HD11 chicken macrophages are derived from chicken hematopoietic cell line transformed by avian myelocytomatosis virus strain MC29 (replication defective leukemia virus). It is a heterogeneous non-adherent cell population containing mainly round hybridoma like cells (HD11) and a small population of long fibroblast cells [198, 199]. The HD11 cell line has been widely used for studying chicken immune mechanisms.

3.3.1.1 Cell culture and dose application

HD11 cell culture: Chicken macrophages HD11 (kindly provided by Dr. S. Gomis) were grown in suspension culture. HD11 cells were cultured in T75 flasks with RPMI 1640 media with L-glutamine (basic media) (HyClone™, GE Healthcare Life Sciences, Logan, Utah) supplemented with 10% FBS and 1:1000 gentamicin (complete media). Cells were grown to confluency $5x10^5$ cells /ml and passaged every 2 days.

Cell dosing:

HD11 cells (P7-20) were removed from flask and placed in a 50mL conical tube. Cells were centrifuged using the Sorvall Legent RT centrifuge (ThermoFisher) at 200g for 5 minutes, the supernatant was discarded and the cells were re-suspended in RPMI 1640 media with L-glutamine (basic media). Cells were counted using a hemocytometer with light microscopy (VistaVision inverted light microscope, VWR international, model#: 82026-630) with Trypan blue stain (Life Technologies) and seeded into a non-treated 96-well U-bottom plate at 30,000 cells per well and suspended in 250 µL basic media.

Cells were transfected in triplicate using a dose of 1 µg CpG-ODN per well (1 µL of formulation) and incubated at 37°C for 2 hours in basic media. After transfection, plates were centrifuged at 400g for 10 minutes and the supernatants were discarded. Cells were re-suspended

in 300 µL complete media and placed back in the incubator for 12 hours. After 12-hour incubation, cells were centrifuged at 400g for 10 minutes and 150 µL of supernatants were transferred to a 96-well clear bottom plate pre-filled with 130 µL sterile water for the Greiss assay. The rest of the supernatants were discarded. Three hundred µL of complete media was added to each well, the cells were re-suspended, and incubated further for 12 hours.

At the end of the second 12-hour incubation (total = 24 hours) cells were centrifuged at 400g for 10 minutes and 150 µL of supernatant from each well was collected and transferred to a clear bottom glass 96-well plate with each well pre-filled with 130 µL sterile water for the Greiss assay.

The remaining cell supernatants were discarded and cells were re-suspended in 250 µL of PBS mixed with either MitoTracker™ Green FM (Life Technologies), or Calcein AM (Life Technologies) cell viability stain for flow cytometry.

3.3.1.2 Fluorescence set up of flow cytometry

The CpG-ODN NP uptake and toxicity of various prepared NPs were assessed using the Attune® Acoustic Focusing Flow Cytometer (Applied Biosystems, Life Technologies, Carlsbad, California, USA). Assessment of CpG-ODN uptake was recorded by measuring fluorescence associated with the Alexa Fluor 647 label following stimulation. The viability was assessed after measuring the fluorescence associated with a viability dye (shown below). The CpG-ODN uptake was calculated based on the percentage of viable cells that exhibited a fluorescence signal above the threshold signal. The threshold value was determined based on the background fluorescence of untreated cells.

Statistical Analysis of CpG-ODN uptake

Statistical analysis was performed using the GraphPad Prism software (GraphPad Software, La Jolla, CA, USA). Two-way ANOVA in conjunction with Tukey post hoc tests were used to analyze CpG-uptake for multi-variable analysis. A p-value of less than 0.05 was considered as statistically significant.

3.3.2 Assessment of NP's toxicity in HD11 cells

Cell viability after stimulation with different CpG-ODN NP formulations was assessed by measuring viability fluorescence following treatment with MitoTracker™ Green FM. Viability stain was carried out as per manufacturer's protocol. Briefly, cells were treated with PBS containing MitoTracker™ Green FM at a concentration of 100 nM per well. Cells were incubated at 37°C for 15 minutes prior to reading fluorescent output using flow cytometry.

For certain formulations, cell viability was also assessed with Calcein AM cell permeant viability dye from the LIVE/DEAD® viability/cytotoxicity kit (Life Technologies). Briefly, calcein AM stock solution was diluted 80-fold in high quality anhydrous dimethyl sulfoxide (DMSO) (Fluka, Honeywell) and added to PBS warmed at 37°C so that 2 µL of diluted calcein AM was added per well. The cells were incubated under dark conditions for 20 minutes at room temperature prior to reading fluorescence output by flow cytometry.

3.3.3 Assessment of immune activation in HD11 cells: Greiss Assay

Immune activation of macrophages was assessed at 12 and 24 hours after HD11 stimulation with CpG-ODN for 2 hours. Nitrite concentration produced by cells treated with the various NP formulations was measured in triplicate using the standard Greiss Assay Kit (Life Technologies). The assay was carried out as per manufacturer's protocol. Briefly, after 12 hours post stimulation, cells were centrifuged at 400g for 10 minutes and 150 µL of supernatant from each well was collected in a separate glass bottom microplate. A 130 µL aliquot of MilliQ water was added to each sample. Greiss assay reagents for cell supernatants were prepared at a 1:1 ratio of kit component A to B. Twenty µL of Greiss reagent (components A+B) was added to each well and the plate was incubated for 30 minutes at room temperature, in the biosafety cabinet under dark conditions. Absorbance at 548 nm was read using a microplate reader and nitrite concentration was assessed using a nitrite standard curve (1-100 µM).

3.3.3.1 Statistical Analysis of immune stimulation

Statistical analysis was performed using the GraphPad Prism software (GraphPad Software, La Jolla, CA, USA). Two-way ANOVA in conjunction with Tukey post hoc tests were

used to analyze nitrite production for multi-variable analysis. A p-value of less than 0.05 was considered as statistically significant.

3.3.4 Localization of CpG-ODN during immune stimulation: Confocal imaging

Based on findings from *in vitro* experiments and formulation development, selected formulations were chosen for further study including confocal imaging and testing formulation stability after nebulization.

To determine localization of DNA upon transfection of HD11 macrophages at the cellular level, fluorescence imaging of Alexa Fluor 647 CpG-ODN was performed using the Zeiss 710 CLSM (Carl Zeiss, Oberkochen, Germany). HD11 cells were transfected as mentioned above and uptake of CpG-ODN NPs were imaged after 2 and 24 hours post stimulation containing labeled CpG-ODN with Alexa Fluor 647 only. Thirty µL of PBS was aliquoted into a 96-well glass bottom cell culture treated microplate. Twenty µL of suspension cell culture was transferred to the 96-well glass bottom cell culture plate and stained with 1 µL Vybrant^{TM} CM-Dil cell membrane stain (Life Technologies). Cells were incubated for 20 minutes at 37ºC prior to viewing in the microscope.

3.3.5 Nebulization model for testing formulation stability and functionality

Selected NP formulations were nebulized using the Med-Pro Compressor Nebulizer (AMG Medical Inc., Montreal, Quebec, Canada). One mL of NP formulations was placed in the chamber and a 4mL glass scintillation vial was placed upside down into the nebulizer holder. The formulation was nebulized for 2 minutes. The nebulizer was turned off and the nebulized formulation was collected from the glass vial and the medication holder (Figure 10). Analysis of nebulized formulations was performed using DLS for measuring size and ζ potential.

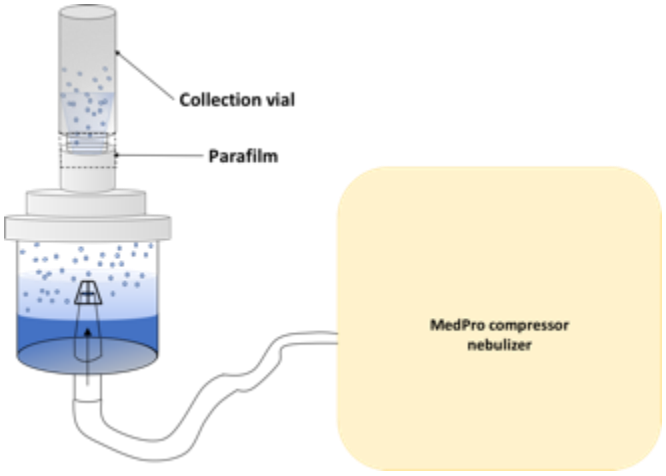

Figure 10 Experimental setup for nebulized NP collection for physicochemical characterization and *in vitro* testing

3.4 Assessing delivery and effectiveness of CpG-ODN nanoparticles in a live chick model

This experiment was completed in collaboration with Dr. S. Gomis and his group, at the University of Saskatchewan. The purpose of this experiment was to investigate biodistribution patterns and the improvement in protection of CpG-ODN against *E. coli* challenge resulting from NP formulations in 1-day old chicks.

3.4.1 Animals and *in vivo* experimental design

Neonatal 1-day old broiler chicks were randomly assigned to different experimental groups: I) saline negative control (2 chicks), II) chicks nebulized with naked CpG-ODN (5 animals for biodistribution assessment, 40 birds for *E. coli* challenge protection), III) chicks nebulized with selected CpG-ODN formulations (5 animals for biodistribution assessment, 40 birds for *E. coli* challenge protection).

3.4.2 CpG-ODN NPs preparation for biodistribution and protection assessment

Selected formulations for protection assessment were prepared as previously mentioned. For formulations for assessing biodistribution, CpG-ODN containing 12.5% of CpG-ODN labeled with Alexa Fluor 647 was used as a tag to identify distribution within the respiratory tract. Additionally, the particles themselves were also labeled with 5% fluorescent lipid: Oregon Green™ 488 1,2-dihexadecanoyl-sn-Glycero-3-phosphoethanolamine (DHPE) Lipid (Life

Technologies) or 1-palmitoyl-2-{6-[(7-nitro-2-1,3-benzoxadiazol-4-yl)amino]hexanoyl}-sn-glycero-3-phosphocholine (NBD-PC) lipid (Avanti Polar Lipids Inc.) for gemini- phospholipid formulations. For formulations containing chitosan, 2% of fluorescent Fluorescein isothiocyanate (FITC)-chitosan (synthesized in house, see section 3.5.2.1) was used as a tag. The formulations were prepared so that chicks were nebulized with a dose of 100 µL of formulation containing 100 µg CpG-ODN per chick.

3.4.2.1 Chitosan-FITC Synthesis

A labeling method modified from Huang et. al, 2004 was used to prepare FITC conjugated chitosan polymer [200]. Stock solutions of FITC (Sigma Aldrich) in methanol (2 mg/mL) and 1% w/v low MW 50-190 kDa chitosan in 0.1 M acetic acid were prepared. Ten mL of dehydrated methanol (HPLC-grade, Fisher), 5mL of FITC in methanol, and 10 mL of the 1% chitosan in acetic acid was mixed and incubate at room temperature in the dark for 3 hours. After incubation, 10mL of 0.2M NaOH was added to precipitate the polymer and the mixture was inverted to mix. The chitosan mixture was centrifuged at 20000g for 30 minutes and the supernatant was removed. 10mL of 70:30 v/v of methanol:water was used to wash the chitosan and the solution was subsequently centrifuged at 20,000g for 10 minutes. The chitosan was washed until there was no yellow color in the supernatant. After washing, the chitosan was dissolved in 0.1 M acetic acid and all traces of free FITC label were removed by dialysis in MilliQ water. The FITC-chitosan was lyophilized in a glass scintillation vial overnight.

3.4.3 Experimental design for *in vivo* pulmonary delivery of NP formulations

On the day of hatch, formulation doses were administered by nebulization (Med-Pro Compressor Nebulizer) to commercial 1-day old broiler chicks in a nebulization chamber (Figure 11).

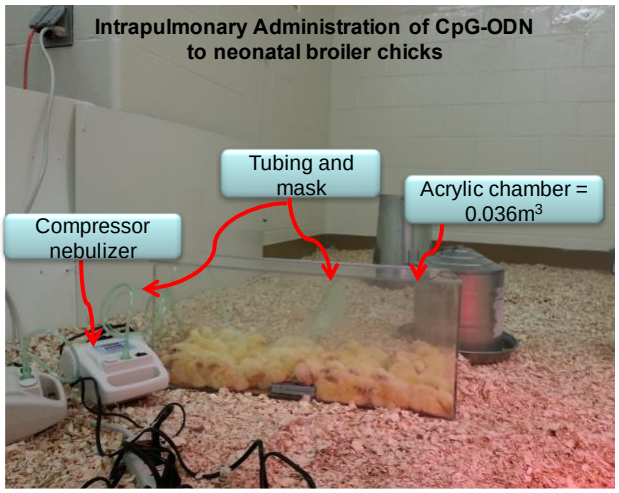

Figure 11 Experimental set-up for the administration of CpG-ODN NP formulations via nebulization in 1-day old chicks

Groups of 1-day old commercial broiler chicks were nebulized in an acrylic chamber for 15 minutes with a dose of 100µg/100 µL per chick. Chicks nebulized with fluorescent formulations were sacrificed at 2 and 24 hours post nebulization (Table 12).

For the biodistribution assessment, chicks were euthanized at 2 hours (n=5) and 24 hours (n=5) post nebulization. The respiratory organs were harvested at each time point for each formulation. The trachea, syrinx, and lung respiratory organs were isolated and snap frozen in optimal cutting temperature (OCT) compound (Thermo scientific, Waltham, MA, USA), ensuring right orientation for longitudinal lung sections after harvesting (Figure 12). Tissues were stored at -80ºC until they were sectioned. 80 µm tissue sections were sectioned with a cryo-stat and observed by CLSM at appropriate excitation and emission wavelengths for Alexa Fluor 647, NBD-PC, Oregon Green 488 and FITC to determine localization of NP and CpG-ODN within the chick respiratory tract.

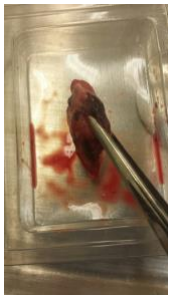

Figure 12 Lung tissue orientation in cryo-mold for biodistribution assessment
Lung tissue of chicks was placed in cryo-mold for sequential longitudinal sections throughout the lung tissue.

Table 12 Experimental design of *in vivo* biodistribution experiment

	Treatment/ Number of animals	Tissue collection (post nebulization)	Analysis
Experiment 1	**Code:** 3F **G_{12}L-NP** n=10	15 min. n= 5 2h n=5	confocal microscopy
	Code: 4F **PVP 10,000 BG_{12}L-NP** n=10	15 min. n= 5 2h n=5	confocal microscopy
Experiment 2	**Code:** F-CpG **Naked CpG-ODN** n=10	2h n= 5 24h n=5	confocal microscopy
	Code: 11 **G_{12}-NP** n=10	2h n= 5 24h n=5	confocal microscopy
	Code: 11d-12 **1%CG_{12}-NP** n=10	2h n= 5 24h n=5	confocal microscopy
	Code: 11d-16 **1%CG_{16}-NP** n=10	2h n= 5 24h n=5	confocal microscopy
Experiment 3	**Code:** 3F **G_{12}L-NP** n=10	2h n= 5 24h n=5	confocal microscopy
	Code: 4F **PVP 10,000 BG_{12}L-NP** n=10	2h n= 5 24h n=5	confocal microscopy
	Code: T5 **CL-NP** n=10	2h n= 5 24h n=5	confocal microscopy
	Code: F10 **C-NP** n=10	2h n= 5 24h n=5	confocal microscopy

3.4.4 Experimental design for *in vivo* protection experiments in 1-day old chicks

For protection studies against lethal *E. coli* infection, non-fluorescent formulations were administered to chicks on the day of hatch (n=40 per group). The chicks were challenged with *E. coli* at 2 days after immunization and another group at 5 days after immunization for each formulation. Chicks were monitored and evaluated for clinical signs of *E. coli* infection and survival after challenge and sections from euthanized birds were sectioned for histopathological analysis. A summary of the animal assignment to groups is provided below (Table 13).

Table 13 Experimental design of *in vivo* protection experiment against lethal *E. coli* challenge

	Treatment/ Number of animals	**Day of Challenge (post admin.)**	**Analysis**
Experiment 1	Code: PU-CpG12 (with PVP) **BG_{12}L-NP**	Day 2	Clinical Monitoring, Histopathology
	Code: PU-CpG16 (with PVP) **BG_{16}L-NP**		
	Code: PU-CpG18 (with PVP) **BG_{18}L-NP**		
Experiment 2	Code: PU-CpG12P (with PVP) **PVP BG_{12}L-NP**	Day 3	Clinical Monitoring, Histopathology
	Code: PU-CpG12M (with CMCNa) **CMCNa BG_{12}L-NP**		
Experiment 3	Code: 11 **G_{12}-NP**	Day 2	Clinical Monitoring, Histopathology
	Code: 11d-12 **1% CG_{12}-NP**		
	Code: 11d-16 **1% CG_{16}-NP**		
Experiment 4	Code: 11 **G_{12}-NP**	Day 4	Clinical Monitoring, Histopathology
	Code: 11-d-12 **1% CG_{12}-NP**		
	Code: PU-CpG12P (with PVP) **PVP 10,000 BG_{12}L-NP**		

Chapter 4 – Results

4.1 UPLC method development

A UPLC method suitable to analyze CpG-ODN in solution and in NP formulations was developed by modifying and optimizing a previous method [201]. The gradient developed (see Materials and Methods and Figure 13) provided a retention time of 3.4 minutes for CpG-ODN. A standard curve for detection of CpG-ODN by detection at 260 nm was generated for the concentration range of 0.125 – 4 µg CpG-ODN in triplicate with R^2= 0.99881. The limit of detection (LOD) and quantification (LOQ) were calculated based on the equations below:

$$LOD = \frac{3.3\sigma}{slope} \text{ and } LOQ = \frac{10\,\sigma}{slope}$$

where σ is the standard deviation of the residuals taken from the regression line, and slope is estimated from the curve.

The LOD was equivalent to 0.19 µg/µL and the LOQ was 0.57 µg/µL.

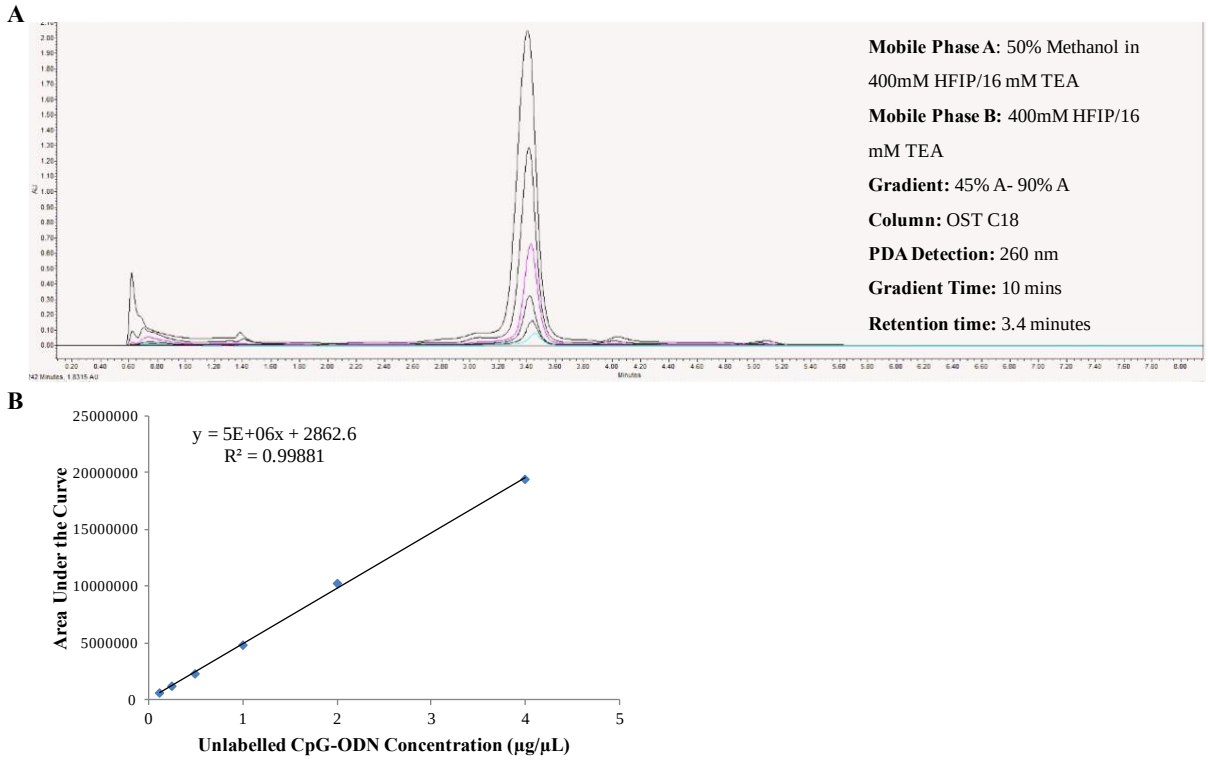

Figure 13 UPLC chromatogram of unlabelled naked CpG-ODN for standard curve generation from 0.125 µg – 4 µg CpG-ODN

A) UPLC Chromatogram of CpG-ODN separation and standard curve (B), n=3 for each concentration.

4.2 Nanoparticle characterization

4.2.1 Particle characterization by Zetasizer

Particle size for all formulations was measured and reported as Z-average diameter (n=3). The corresponding size distribution profile by intensity is shown in Appendix Figure 58 - Figure 68.

4.2.1.1 Effect of biopolymer and other excipients on the size and zeta potential of G_{12}L-NPs and BG_{12}L-NPs

The size range of all G_{12}L-NP particles, including biopolymer coated G_{12}L-NPs (BG_{12}L-NPs) complexed with CpG-ODN ranged from 160 – 250 nm. This represents a large increase in size from vesicles un-complexed with CpG-ODN that were under 20 nm in size (Table 14). The one exception is the BG_{12}L-NP formulated with CMCNa which decreased in size upon complexation with CpG-ODN in PEG 400 excipient. However, due to a high polydispersity index >0.5, the average diameter of the vesicles is not representative of the particle population. The effect of changing the excipient from PEG400 to PG to form gemini phospholipid vesicles decreases the size of G_{12}L-NPs and BG_{12}L-NPs blank particles. Although the change in size is limited to a maximum of 4 nm difference.

The addition of a biopolymer coating to G_{12}L-NPs did not have a significant effect on the size of the particles formulated in both PEG 400 and PG excipients. All formulations with the exception of those formulated with PVP Kollidon 25 and CMCNa polymers had a PDI of ~0.2, indicating that the size distribution of particles within the formulation was relatively uniform.

Table 14 Z-average hydrodynamic diameter and PDI measurements of gemini 12-3-12 phospholipid particles with and without CpG-ODN complexation*

Formulation	Measurement	PEG 400 blank particles	PEG400 Final Formulation	PG blank particles	PG Final Formulation
G_{12}L-NP n= 3	**Size (nm) ± S.D.**	11.2 ± 0.1	161.7 ± 15.8	9.9 ± 0.1	194.9 ± 8.4
	PDI ± S.D.	0.258 ± 0.003	0.211 ± 0.005	0.186 ± 0.022	0.185 ± 0.019
PVP 10,000 BG_{12}L-NP n= 3	**Size (nm) ± S.D.**	12.5 ± 0.1	173.0 ± 1.5	11.6 ± 0.3	177.1 ± 22.3
	PDI ± S.D.	0.171 ± 0.006	0.256 ± 0.013	0.150 ± 0.014	0.703 ± 0.035
PVP Kollidon25 BG_{12}L-NP n= 3	**Size (nm) ± S.D.**	17.5 ± 0.2	250.2 ± 85.3	13.4 ± 0.3	177.9 ± 8.8
	PDI ± S.D.	0.154 ± 0.006	0.620 ± 0.077	0.198 ± 0.003	0.236 ± 0.031
PVP40000 BG_{12}L-NP n= 3	**Size (nm) ± S.D.**	14.2 ± 0.2	172.5 ± 4.4	12.4 ± 0.2	213.2 ± 16.6
	PDI ± S.D.	0.183 ± 0.008	0.178 ± 0.01	0.202 ± 0.007	0.225 ± 0.031
CMCNa BG_{12}L-NP n= 3	**Size (nm) ± S.D.**	616.4 ± 170.8	174.7 ± 9.0	1.3 ± 1.5	139.8 ± 5.5
	PDI ± S.D.	0.705 ± 0.018	0.226 ± 0.020	0.775 ± 0.043	0.236 ± 0.024

* Note: size distribution curves shown in the appendix, Figure 58, Figure 59, Figure 60

Upon complexation with CpG-ODN, the zeta potential of the original particles decreases indicating complexation with negatively charged CpG-ODN DNA. The zeta potential of the G_{12}L-NP (+53.2 mV) is the highest in comparison to all other formulated BG_{12}L-NPs, and relatively similar to un-complexed G_{12}L-NP. Since a zeta potential above +30 mV indicates colloidal stability, this formulation is highly stable. Interestingly, the BG_{12}L-NP formulated with PVP Kollidon 25 polymer in both excipients has a zeta potential bordering +20 mV, which could indicate a less stable formulation. Overall, the zeta potential of final formulations in PEG400 excipient is higher than those formulated with PG. This effect is most evident for the G_{12}L-NP and PVP 10,000 BG_{12}L-NP.

Table 15 ζ potential measurements of empty gemini 12-3-12 phospholipid and CpG-ODN complexed with different biopolymers using PEG400 excipient or PG excipient

	Mean ζ potential (mV) ± S.D.			
	PEG 400		**PG**	
Formulation code	**Gemini-phospholipid vesicles**	**Final formulation (with CpG)**	**Gemini-phospholipid vesicles**	**Final formulation (with CpG)**
G_{12}L-NP	+ 48.1 ± 11.6	+ 53.2 ± 1.0	+ 32.8 ± 5.8	+ 35.7 ± 0.2
PVP 10,000 BG_{12}L-NP	+ 33.1 ± 15.7	+ 42.8 ± 0.4	+ 39.8 ± 1.6	+ 28.9 ± 0.9
PVP Kollidon 25 BG_{12}L-NP	+ 29.8 ± 6.0	+ 23.8 ± 1.6	+ 36.9 ± 3.4	+ 22.1 ± 2.7
PVP 40,000 BG_{12}L-NP	+ 63.2 ± 3.6	+ 34.4 ± 1.2	+ 39.4 ± 3.3	+ 31.8 ± 4.0
CMCNa BG_{12}L-NP	+ 41.0 ± 12.3	+ 36.4 ± 2.5	+ 38.8 ± 0.2	+ 33.7 ± 0.9

***pH** range of **6.6-7** corresponds to pH of formulation at the time of zeta potential measurement*

Values expressed as mean ± S.D.; n=3

4.2.1.2 Gemini nanoparticle characterization (G-NPs)

Since the positively charged quaternary ammonium groups of gemini surfactants can complex with DNA to form particles, CpG-ODN – gemini complexes were characterized. Characterization of gemini-CpG-ODN complexes was also important in order to compare hybrid NP formulations (CG-NPs) to gemini surfactant NPs.

The sizes of complexes formed with first generation gemini surfactant with three different tail lengths (12,16,18) are shown in Table 16. The average diameter of G-NPs increased proportionally from 175.2 nm, 290.5 nm, to 1429 nm corresponding with increasing tail length from 12, 16, 18 respectively. However, gemini 18-3-18 formed microparticles with a very polydisperse distribution (PDI > 0.5) unlike gemini 12-3-12 and 16-3-16 which had relatively uniform size populations.

As the spontaneous formation of micelles occurs above the CMC for each gemini surfactant, and the concentration of gemini was above this value in the final complex formulations, the particle distribution of gemini micelles alone was measured. The size

distribution of all gemini micelles are very polydisperse, therefore the average diameter is not representative of the population. It can be seen that upon complexation of CpG-ODN, the particle distribution becomes more uniform with the exception of gemini 18-3-18.

Table 16 Z-Average hydrodynamic diameter and PDI measurements of three different gemini-CpG-ODN complexes and gemini micelles

Sample	Formulation Code	Measurement	Gemini micelles	Final Formulation (with CpG-ODN)
gemini 12-3-12	**G_{12}-NP**	**Size (nm) ± S.D.**	298.4 ± 164.1	175.2 ± 2.6
		PDI ± S.D.	0.446 ± 0.087	0.249 ± 0.016
gemini 16-3-16	**G_{16}-NP**	**Size (nm) ± S.D.**	86.8 ± 4.1	290.5 ± 8.2
		PDI ± S.D.	0.555 ± 0.128	0.299 ± 0.021
gemini 18-3-18	**G_{18}-NP**	**Size (nm) ± S.D.**	292.2 ± 26.1	1429 ± 219.2
		PDI ± S.D.	0.560 ± 0.063	0.954 ± 0.056

** Note: size distribution curves shown in Appendix Figure 61*

Values expressed as mean ± S.D.; n=3

Complexation of CpG-ODN with gemini surfactant resulted in the formation of stable particles since all had a zeta potential above the +30mV threshold (Table 17). The zeta potential increased with longer gemini tail length with gemini 18-3-18 having the highest zeta potential corresponding to +54.9mV. Additionally, gemini surfactant micelles also exhibited > +30mV zeta potential indicating the colloidal stability of the gemini aggregates.

Table 17 ζ potential measurements of gemini micelles and G-NPs

Mean ζ potential (mV) ± S.D.

Sample	Formulation code	Gemini micelles	Final formulation (with CpG-ODN)
gemini 12-3-12	**G_{12}-NP**	+42.2 ± 4.6	+ 35.2 ± 1.1
gemini 16-3-16	**G_{16}-NP**	+ 48.4 ± 1.1	+ 41.8 ± 1.1
gemini 18-3-18	**G_{18}-NP**	+ 38.9 ± 1.7	+ 54.9 ± 6.1

** **pH** range of **6-6.5** corresponds to pH of formulation at the time of zeta potential measurement*

Values expressed as mean ± S.D.; n=3.

4.2.1.3 Chitosan Nanoparticles (C-NPs)

The ability of chitosan to spontaneously form NP with CpG-ODN DNA upon mixing was also tested in order to be able to compare against hybrid (CG-NPs) NPs. Since other investigators have found that low molecular weight chitosans can result in more stable chitosan NP formulations *in vitro*, two ranges of low molecular weight chitosans were applied to NP formulation in this project. Moreover, the chitosan concentration was tailored for NP formation with each size range to prevent aggregation during the preparation process.

The low MW C-NP and 1% ultra-low MW C-NP both formed relatively uniform NPs with sizes closer to the micron range (1566 nm and 965.1 nm, respectively). However, the 1.5% ultra-low MW C-NP formed much larger particles with higher polydispersity and inconsistent size distribution. As such, this formulation was not further investigated.

Table 18 Z-Average hydrodynamic diameter and PDI of chitosan-CpG-ODN complexes*

Sample	Formulation code	Measurement	Final formulation (with CpG-ODN)
0.1% Chitosan low M.W. (50-90 KDa)	**0.1% low MW C-NP**	**Size (nm) ± S.D.**	1566 ± 10.6
		PDI ± S.D.	0.227 ± 0.024
1% Ultra low M.W chitosan (2.5 KDa)	**1% ultra-low MW C-NP**	**Size (nm) ± S.D.**	965.1 ± 33.7
		PDI ± S.D.	0.239 ± 0.191
1.5 % Ultra low M.W chitosan (2.5 KDa)	**1.5% ultra low MW C-NP**	**Size (nm) ± S.D.**	3099.7 ± 162.2
		PDI ± S.D.	0.374 ± 0.137

* Note: size distribution curves shown in Appendix Figure 62

Values expressed as mean ± S.D.; n=3

Despite the larger particle size, both C-NP formulations maintained colloidal stability as both had zeta potential above +30mV. A higher zeta potential was seen when CpG-ODN was complexed with low MW chitosan versus ultra-low MW chitosan.

Table 19 Zeta Potential of chitosan-CpG-ODN complexes

Sample	Formulation code	ζ Potential (mV) ± S.D.
0.1% Chitosan low M.W. (50-90 KDa)	**0.1% low MW C-NP**	+ 52.5 ± 2.2
1% Ultra low M.W chitosan (2.5 KDa)	**1% ultra-low MW C-NP**	+ 44.3 ± 1.5

pH range of **3.5-4 corresponds to pH of formulation at the time of zeta potential measurement.*

Values expressed as mean ± S.D.; n=3

4.2.1.4 Characterization of chitosan-gemini-CpG-ODN complexes (CG-NPs)

In comparison to gemini-CpG-ODN (G-NPs) complexes, the addition of the chitosan biopolymer significantly increased the size of the final formulation. For gemini 12-3-12 the size of the CpG-ODN gemini complex is ~180 nm. However, upon addition of 0.1% chitosan the formulation size increased to ~900 nm (Table 20). The size increased proportionally with

increasing chitosan concentration in the formulation and the addition of 1% chitosan resulted in a microparticle formulation. The incorporation of 2% chitosan resulted in a PDI > 0.5 indicating a highly disperse population with sizes above the upper limit of the Zetasizer size range (6 micron). This may be due to the higher viscosity of the chitosan solution.

Due to the influence of pH on transfection efficiency by chitosan NPs *in vitro*, a buffering component was added to the formulation preparation to determine whether it would affect transfection in HD11 cells. Due to the nature of complexation resulting from ionic interactions in NPs formulated in this research, incorporating the salt buffer component into the formulation affected the size and polydispersity, as electrolytes affect the ionic charge on chitosan and the natural complexation of gemini with negatively charged CpG-ODN. Certainly, a higher size polydispersity due to lower colloidal stability is observed when formulating CG-NPs with DNA dissolved in TE buffer in comparison to DNA dissolved in water. In contrast, the addition of PBS buffer after gemini-CPG-ODN-chitosan complexation resulted in a more uniform size distribution, although still more polydisperse than the formulations without any buffer component (Appendix, Figure 64).

Size measurements of blank NPs were also obtained for comparison purposes (Table 20). However, the results were very inconsistent with variable size distributions as PDIs were also highly variable. These phenomena can be seen in the Appendix, Figure 63 and Figure 65.

Table 20 Z-Average hydrodynamic diameter and PDI measurements of Chitosan gemini 12-3-12 nanoparticles with different chitosan concentrations

Sample	Formulation code	Measurement	Particle	Final formulation (with CpG-ODN)
0.1% chitosan	**0.1% CG_{12}-NP**	**Size (nm) ± S.D.**	277.2 ± 20.4	897.7 ± 26.7
		PDI ± S.D.	0.928 ± 0.107	0.359 ± 0.037
1% chitosan	**1% CG_{12}-NP**	**Size (nm) ± S.D.**	3195.3 ± 387.8	2199.7 ± 126.2
		PDI ± S.D.	0.376 ± 0.104	0.225 ± 0.095
2% chitosan*	**2% CG_{12}-NP**	**Size (nm) ± S.D.**	11409.3 ± 2138.1	13700 ± 5392.6
		PDI ± S.D.	0.886 ± 0.198	0.704 ± 0.177
0.1% chitosan TE	**0.1% CG_{12}-NP TE**	**Size (nm) ± S.D.**	365.9 ± 31.9	884.5 ± 48.4
		PDI ± S.D.	0.905 ± 0.165	0.569 ± 0.06
0.1% chitosan PBS	**0.1% CG_{12}-NP PBS**	**Size (nm) ± S.D.**	233.3 ± 78.2	545.7 ± 7.6
		PDI ± S.D.	0.438 ± 0.171	0.399 ± 0.019

*Size exceeds upper size limit of Zetasizer.

Values expressed as mean ± S.D.; n=3. Size distribution curves are shown in the Appendix, Figure 63 and Figure ***64***.

The same pattern of increasing size with increasing chitosan concentration was seen for CG_{16}-NPs (Table 21). Once again addition of the 2% chitosan to gemini-CpG-ODN complexes resulted in large aggregates.

Table 21 Z-Average hydrodynamic diameter and PDI measurements of chitosan gemini 16-3-16 nanoparticles with different chitosan concentrations

Sample	Formulation code	Measurement	Particle	Final formulation (with CpG-ODN)
0.1% chitosan	**0.1% CG_{16}-NP**	**Size (nm) ± S.D.** **PDI ± S.D.**	355.4 ± 48.1 0.946 ± 0.009	820.3 ± 58.8 0.380 ± 0.157
1% chitosan	**1% CG_{16}-NP**	**Size (nm) ± S.D.** **PDI ± S.D.**	5919.7 ± 361.3 0.442 ± 0.174	3748.3 ± 269.5 0.138 ± 0.053
Sample	**Formulation code**	**Measurement**	**Particle**	**Final formulation (with CpG-ODN)**
2% chitosan*	**2% CG_{16}-NP**	**Size (nm) ± S.D.** **PDI ± S.D.± S.D.**	10071.7 ± 748.6 0.655 ± 0.187	17433.7 ± 7227.4 0.454 ± 0.113
0.1% chitosan PBS	**0.1% CG_{16}-NP PBS**	**Size (nm) ± S.D.** **PDI ± S.D.**	421 ± 27.1 0.912 ± 0.116	532.3 ± 17.6 0.382 ± 0.027

*Size exceeds upper size limit of Zetasizer.

Values expressed as mean ± S.D.; n=3. Size distribution curves shown in Appendix, Figure 64 and Figure ***66***

Unlike the CG_{12}-NPs and CG_{16}-NPs, incorporation of 0.1% chitosan into G_{18}-NP resulted in a smaller particle size (from 1429 nm to 750.6 nm) compared to G_{12}-NPs (Table 16, Table 22). Additionally, the size distribution became more uniform (PDI = 0.256).

Similar to CG_{12}-NPs and CG_{16}-NPs, increasing the chitosan concentration in CG-NPs also increased the size and polydispersity. Also, adding PBS buffer after complex formation again reduced the size of the NPs but increased the polydispersity like the CG_{12}-NPs and CG_{16}-NPs.

Table 22 Z-average hydrodynamic diameter and PDI measurements of chitosan gemini 18-3-18 nanoparticles with different chitosan concentrations

Sample	Formulation code	Measurement	Particles	Final formulation (with CpG-ODN)
0.1% chitosan	**0.1% CG_{18}-NP**	**Size (nm) ± S.D.**	1193.6 ± 266.6	750.6 ± 34.4
		PDI ± S.D.	0.966 ± 0.059	0.256 ± 0.037
1% chitosan	**1% CG_{18}-NP**	**Size (nm) ± S.D.**	7027.3 ± 1194.5	5406 ± 800.5
		PDI ± S.D.	0.879 ± 0.120	0.430 ± 0.112
2% chitosan	**2% CG_{18}-NP**	**Size (nm) ± S.D.**	5845.7 ± 920.6	9777.3 ± 907.3
		PDI ± S.D.	0.909 ± 0.158	0.311 ± 0.057
0.1% chitosan PBS	**0.1% CG_{18}-NP PBS**	**Size (nm) ± S.D.**	225 ± 19.2	543.5 ± 20.7
		PDI ± S.D.	0.881 ± 0.160	0.451 ± 0.026

*Size exceeds upper size limit of Zetasizer.

Values expressed as mean ± S.D.; n=3. Size distribution curves shown in Appendix Figure 64 and 66.

Overall, the chitosan concentration was the main factor affecting size distribution of CG-NPs. A proportional increase in size was seen with increasing chitosan concentration, with a more variable size distribution and size exceeding the upper size limit of the Zetasizer detector at 2% chitosan (Figure 14). The gemini tail length did not significantly affect the size at different chitosan concentrations except at 2% chitosan.

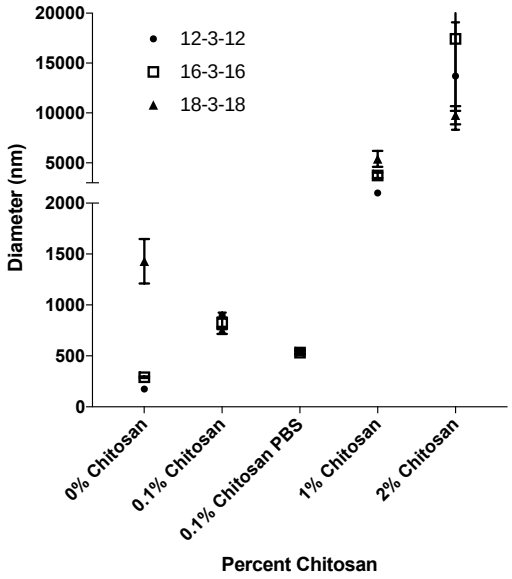

Figure 14 Effect of increasing chitosan concentration on size distribution of gemini-CpG-ODN complexes

Z-average of hydrodynamic diameter measured by DLS is presented for G-NPs and CG-NPs. Each group represents NP formulations with different gemini tail length: 12-3-12, 16-3-16, 18-3-18. Error bars represent S.D., n=3.

All CG-NPs had a zeta potential above +30mV. Increasing chitosan concentration by a factor of 10 resulted in an increase of zeta potential from +40mV to 61.3 mV, +54.1mV to +62.2 mV, +50mV to +58.8mV for gemini 12-3-12, gemini 16-3-16, and gemini 18-3-18 respectively. However, the increase from 1% to 2% chitosan did not increase zeta potential of final formulations significantly.

The addition of a buffer component to the formulation also affected the zeta potential of formulations with equivalent chitosan concentration. Addition of a buffer prior to complex formation decreased the final particle zeta potential from +40mV to +31.3 mV, which can be directly compared given the similar pH range. Adding the PBS buffer post complexation also decreased the zeta potential from +40mV to +38.6 mV. However, increase in the pH of the formulation after PBS addition could explain the slight decrease in zeta potential (Table 23).

Table 23 Average ζ potential of chitosan- gemini NPs formulated with three different gemini tail lengths at increasing chitosan concentrations

	Gemini 12-3-12		Gemini 16-3-16		Gemini 18-3-18	
	Mean ζ potential (mV) ± S.D.					
Percent Chitosan	**Final Formulation (with CpG-ODN)**	**pH Range**	**Final Formulation (with CpG-ODN)**	**pH Range**	**Final Formulation (with CpG-ODN)**	**pH Range**
0.1% chitosan (0.1% CG-NP)	+40.0 ± 0.2	3.31-3.38	+54.1 ± 0.7	3.28-3.37	+50.0 ± 0.6	3.29-3.38
1% chitosan (1% CG-NP)	+61.3 ± 0.5	4.24-4.4	+62.2 ± 2.2	4.17- 4.33	+58.8 ± 0.9	4.21-4.31
2% chitosan (2% CG-NP)	+60.0 ± 0.6	4.74-4.84	+59.0 ± 0.7	4.7-4.8	+60.5 ± 0.8	4.73
0.1% chitosan PBS (0.1% CG-NP PBS)	+38.6 ± 1.38	3.54-3.61	+41.4 ± 3.1	3.52-3.62	+48.3 ± 0.6	3.52-3.62
0.1% chitosan TE (0.1% CG-NP TE)	+31.3 ± 1.6	3.24-3.34				

*pH range corresponds to the pH of the formulation at the time of zeta potential measurement

Due to the self-assembly of gemini surfactant, it was interesting to determine the zeta potential of chitosan and gemini NPs. It is important to note that gemini 12-3-12 was below its CMC in the formulation which, could explain the difference in zeta potential in comparison to 16-3-16 and 18-3-18. Once again, it can be determined that the 1% and 2% chitosan have the most dramatic effect of increasing the zeta potential in comparison to 0% chitosan for the three different gemini tail lengths (Figure 15).

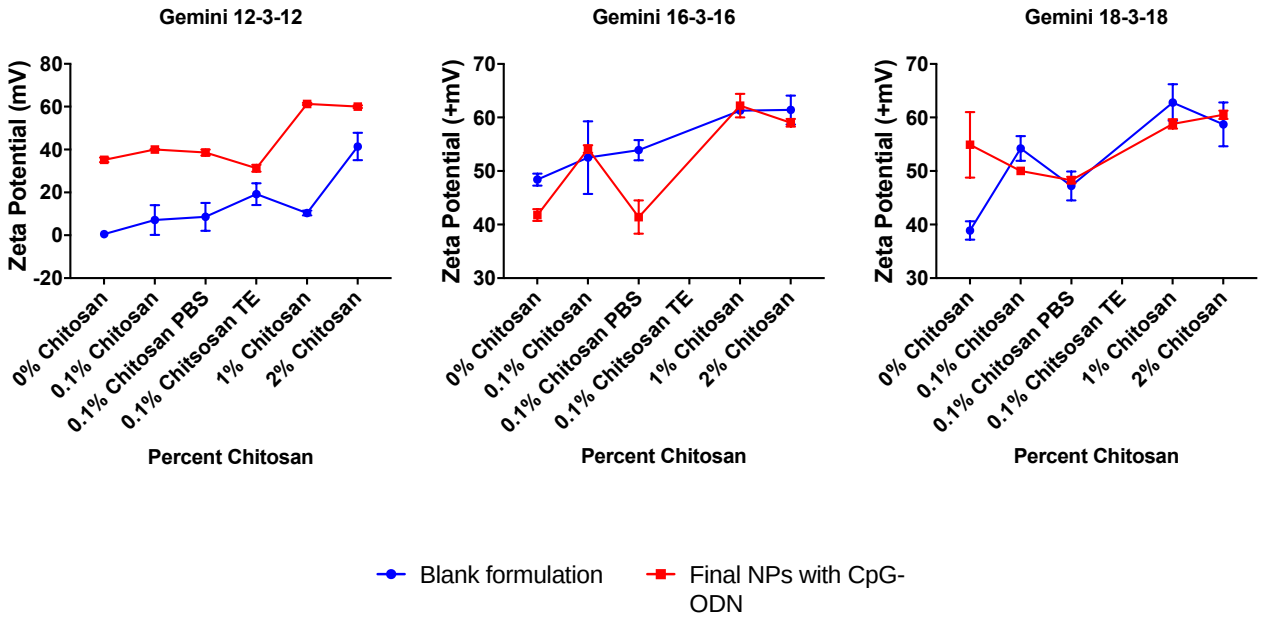

Figure 15 Change in zeta potential of CG-NPs with increasing chitosan concentration of blank particles and final CG-NP formulations complexed with CpG-ODN

Zeta potential measurements of blank NPs (A) and final NPs complexed with CpG-ODN (B). Formulation of blank particles was carried out by substituting CpG-ODN solution with sterile water. pH of formulation medium ranged from 6.28 to 6.35 for 0% chitosan, 3.16-3.48 for 0.1% chitosan, 3.43-3.68 for 0.1% chitosan PBS, 3.2-3.4 for 0.1% chitosan TE, 4.12-4.49 for 1% chitosan, 4.62-4.87 for 2% chitosan. Error bars represent mean ± S.D., n=3.

4.2.1.5 Characterization of CL-NP formulation

Substitution of the cationic gemini component from GL-NPs for cationic chitosan in CL-NPs resulted in an increase of particle size distribution from ~160 nm to 1060.9 nm (Table 24). Unlike the GL-NP, the zeta potential of the CL-NP was less than +30mV at +12.7mV, which could indicate an overall lower colloidal stability (Table 24).

Table 24 Z-average hydrodynamic diameter and average ζ potential of CL-NPs

Measurement	Final formulation (with CpG-ODN)
Size (nm) ± S.D.	1060.9 ± 54.3
PDI ± S.D.	0.244 ± 0.179
ζ potential (mV)*	+12.7 ± 0.8

Formulation had **pH 5.2 at the time of zeta potential measurement*

Values expressed as mean ± S.D.; n=3. Size distribution curves are shown in the Appendix, Figure 68

4.2.2 Effect of biological conditions on particle size and zeta potential

Due to the nature of the electrostatic forces involved in the complexation and release of CpG-ODN with chitosan and gemini components of the NPs formulated in this work, changes in size and zeta potential of selected formulations in different media that are more closely representative of the biological environment were also tested. Overall, the zeta potential decreased with increasing pH of biological media, corresponding to saline, basic media and complete media. All particles with the exception of the CL-NP formulation, decreased to zeta potential ~0mV in RPMI 1640 cell culture media supplemented with 10% FBS proteins (Figure 16).

The change in hydrodynamic diameter of NPs varied depending on the type of formulation (Figure 16). For G_{12}-NP, G_{12}L-NP, and BG_{12}L-NP formulated with PVP 10,000, size increased to the µM size range in saline, PBS, and basic media, which may indicate aggregation. It is notable that particle size of the G_{12}-NP formulation in 10% FBS RPMI 1640 media is similar to the size measured in water and its non-dilute state. For CG-NP formulations, particle size decreased upon dilution in all buffers including water, yet still in the µm size range. Unlike the other formulations, the CL-NP formulation maintained similar size range in all buffers except basic RPMI 1640 media, which may indicate aggregation (Figure 16).

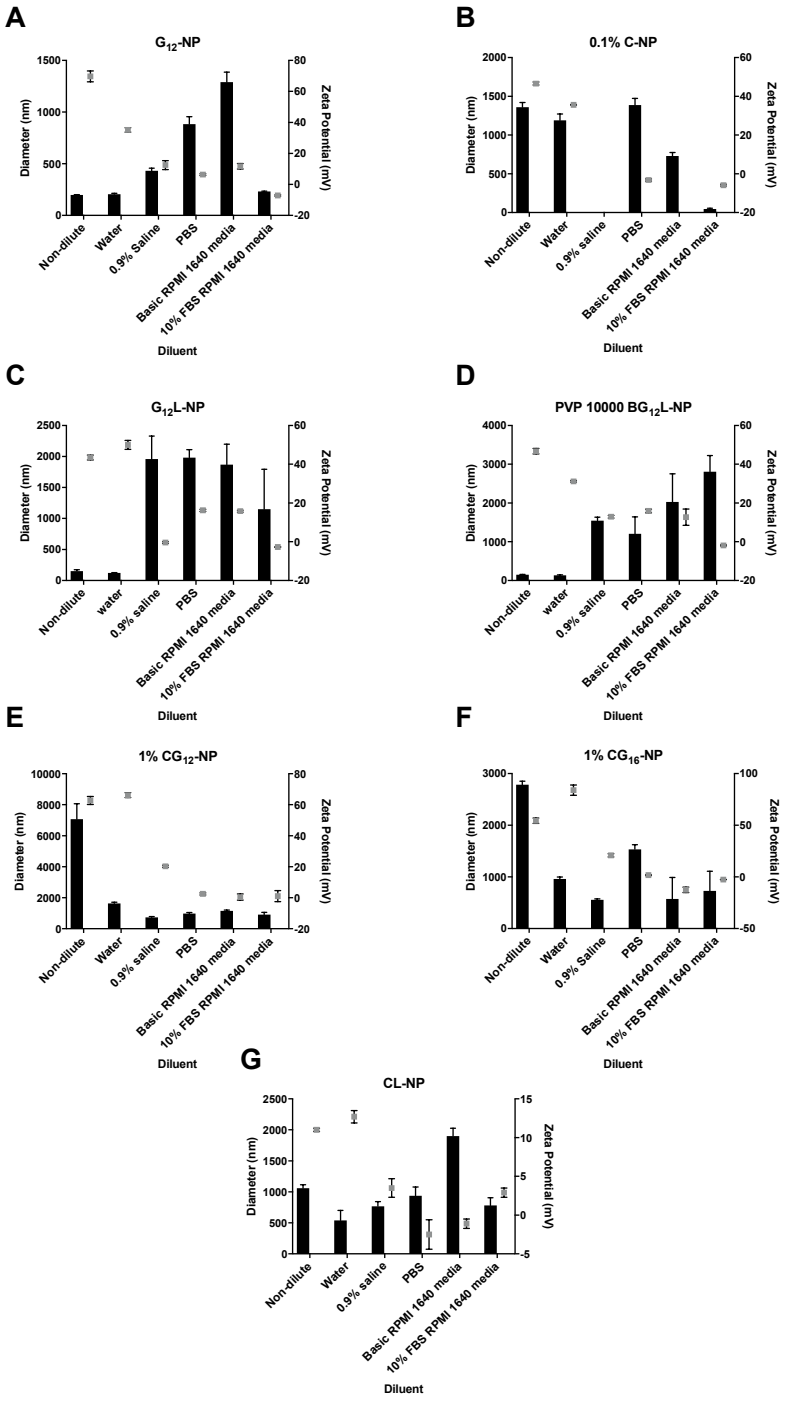

Figure 16 Changes in Z-average hydrodynamic diameter and zeta potential of NPs in different biological media

Formulations representative from each category were chosen for buffer characterization. Measurements were carried out in dilutions of CpG-ODN NP formulations in different biological media (1:20). Mean ± S.D. n=3. Bars represent Z-average hydrodynamic diameter and dot plots correspond to zeta potential values. pH of particle dilutions in PBS, basic RPMI 1640 media, and 10% FBS RPMI 1640 media ranges from 7-8.31. pH of G_{12}-NPs, G_{12}L-NPs, and BG_{12}L-NPs range from 6.0 – 7.7 in its non-dilute form, water, and 0.9% saline. pH of C-NPs and CG-NPs ranges from 4.1 – 5 in its non-dilute form, water, and 0.9% saline. pH of CL-NP ranges from 4.75 - 5.2 in its non-dilute form, water, and 0.9% saline.

4.2.3 Particle reproducibility

The preparation method for each particle was evaluated by determining batch to batch differences in NP hydrodynamic diameter. The preparation of blank G_{12}L-NP and BG_{12}L-NP vesicles in both PEG400 and PG excipients were very reproducible, giving similar sizes at each separate preparation (Figure 17 A,B). Only PVP Kollidon 25 and CMCNa BG_{12}L-NPs produced variable sizes for each preparation. Upon complexation with CpG-ODN, PEG400 excipient (Figure 17 C) resulted in more consistent NP formulation than PG (Figure 17 D). Variability of PVP Kollidon 25 and CMCNa BG_{12}L-NPs also translated into the final formulation and G_{12}L-NP and PVP10,000 BG_{12}L-NP generated the most consistent formulations.

G_{12}-NPs produced the most consistent particles from batch to batch (Figure 17 E) and was more consistent than the C-NP formulations (Figure 17 F). Unlike the other three types of formulations CG-NPs were more variable batch to batch (Figure 17 G, H, I) and 1% CG_{16}-NPs (Figure 17 H) were more reproducible than 1% CG_{12}-NPs (Figure 17 G).

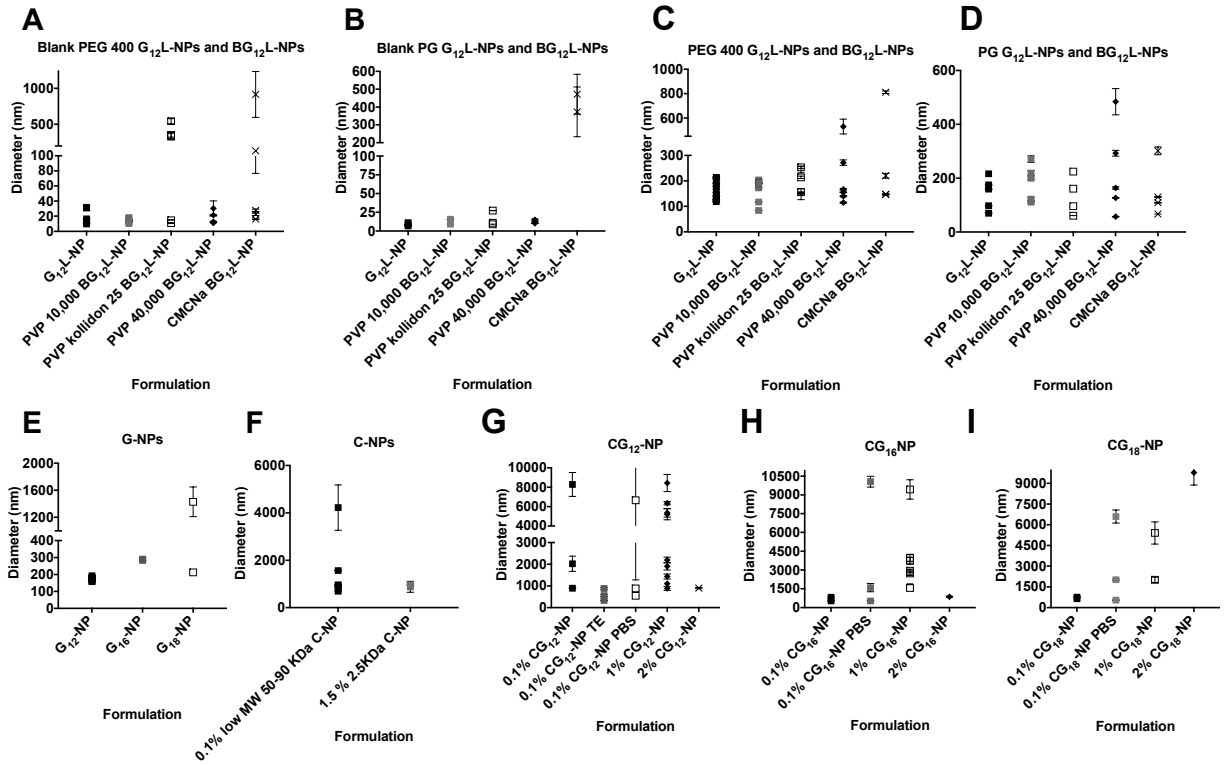

Figure 17 Batch to batch reproducibility of Z-average diameter of NPs in 8 categories of formulations
Compilation of Z-average hydrodynamic diameter measurements from repeat batches of NPs. Mean ± S.D., n= 3

4.2.4 Particle size stability of G_{12}L-NPs and BG_{12}L-NPs

In order to gain insight about the long-term stability of NPs, size distribution of blank GL-NPs was monitored over 30 days of storage at 4°C to identify changes in NP size, aggregation and sedimentation. Blank G_{12}L-NPs and BG_{12}L-NPs showed a similar size distribution throughout the 30-day period (Figure 18). The only exception was the blank BG_{12}L-NP formulated with biopolymer PVP Kollidon 25 and PEG 400 excipient, which showed variable particle size and aggregation by day 15 of storage at 4°C (Figure 18 A).

Upon complexation with CpG-ODN, the particle size over the 30-day period was more variable especially with the NPs formulated in PEG400 excipient. The change in size ranged from 200 nm to 350 nm by the end of the 30-day period. Of the PEG 400 formulations, PVP 10,000 BG_{12}L-NP aggregated the least ranging from 200 nm at day 1 to 280 nm by day 30. The NPs formulated with PG showed similar size over the 30-day period.

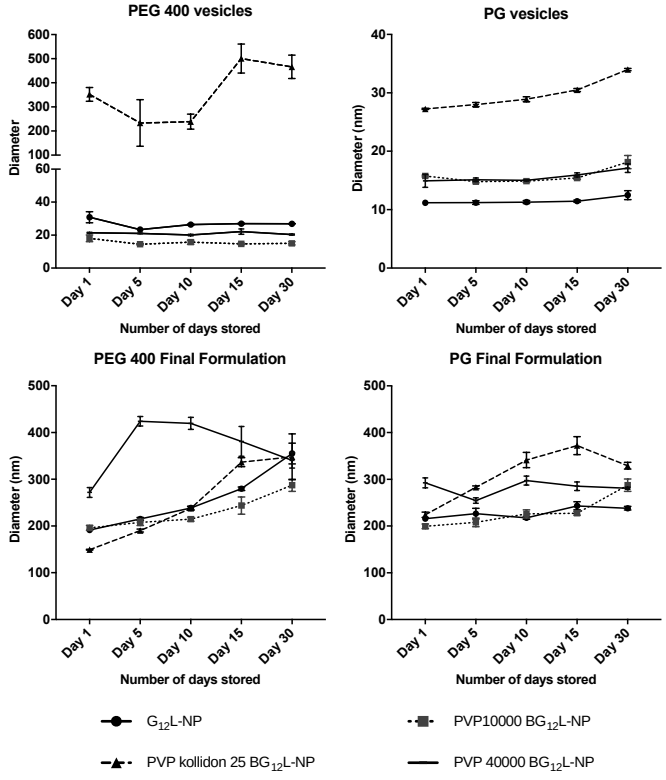

Figure 18 G_{12}L-NP and BG_{12}L-NP size stability at 4°C, over a 30-day period. Particle size of blank NPs and CpG-complexed NPs are shown

It is also important to note the PDI over the 30-day storage period since it gives insight into NP aggregation and formulation uniformity (Figure 19). The blank G_{12}-NPs and BG_{12}-NPs had more uniform PDIs and only PVP Kollidon 25 BG_{12}-NP in PEG 400 had variable polydispersity over the time period. Final formulations had much more variable polydispersity and were above the 0.5 threshold of the Zetasizer by day 15.

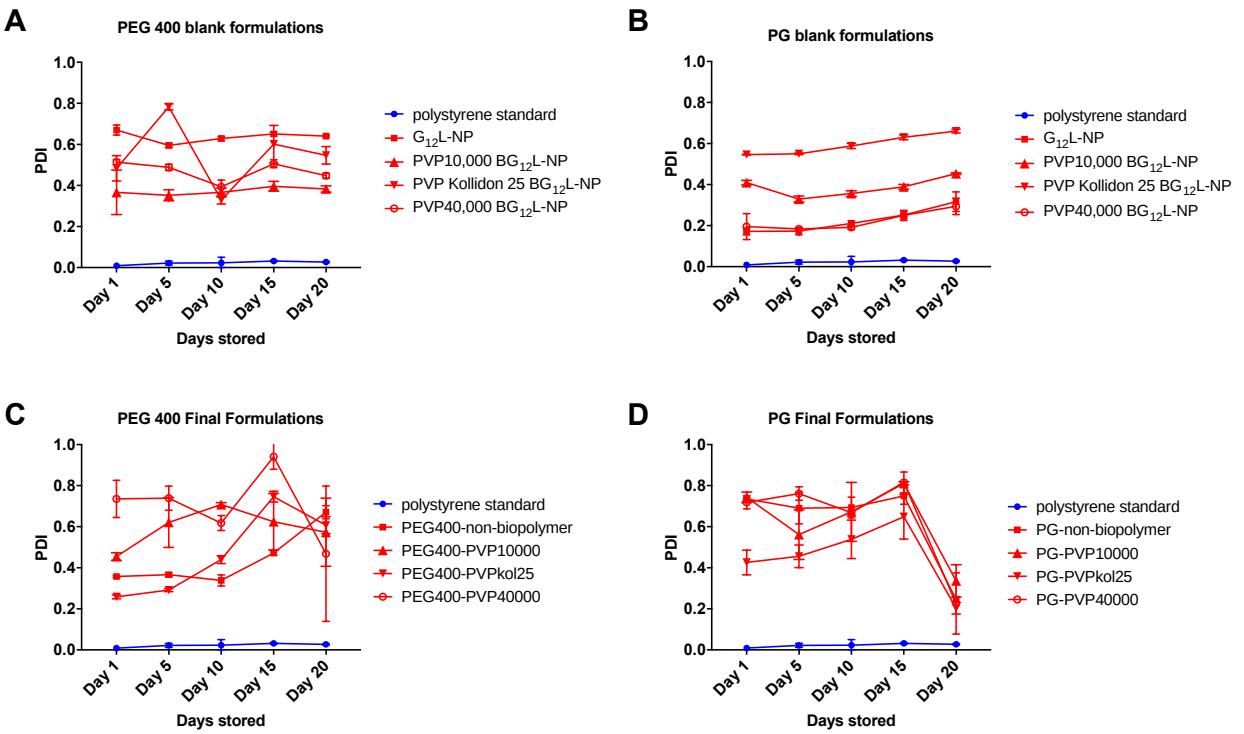

Figure 19 Change in the polydispersity index of G_{12}L-NP and BG_{12}L-NP formulations over a 30-day period at 4°C.

4.2.5 Particle Characterization by FCS

4.2.5.1 DNA – G_{12}L-NPs and B G_{12}L-NPs characterization: FCS

FCS can detect small fluctuations in fluorescence measured from fluorescence molecules molecular weights and molecular aggregations. This is useful in DNA NP size studies in attempt to correlate the number of DNA molecules per particle and also the characterization of particles that may not be spherical.

GL-NPs and BGL-NPs were formulated in a two-step process: the first step is the formation of gemini- neutral phospholipid (DPPC) – neutral polymer vesicles followed by the spontaneous complexation of CpG-ODN oligonucleotides. This assembly process was monitored by tracking the fluorescently labeled CpG-ODN. The diffusion coefficient of the CpG-ODN oligonucleotides was $1.61\pm0.07 \times 10^{-12}$ m^2/s. The autocorrelation curves for Alexa Fluor 647 CpG-ODN (Figure 20A) were fitted using a one-component free diffusion model. The concentration of CpG-ODN was normalized to 0.6 ng/µL so that any shifts in the FCS profiles of plasmid were due to interaction with other components during the assembly of NPs.

By looking at the raw photon stream from the avalanche photodiode detector (APD) for the naked CpG-ODN, one can see differences in comparison to the other formulations. Naked CpG-ODN count rates equilibrated at an average baseline around 100 kHz. Upon complexation with the gemini phospholipid vesicles, the count rate shows higher fluctuations with higher count rates in both excipients (Figure 20, Figure 21).

Complexation of CpG-ODN with GL-NPs shifted the autocorrelation curves in comparison to naked CpG-ODN. With the exception of PVP 40,000 BGL-NP, all polymers caused an upward translation in the autocorrelation curve (Figure 22 A). This upward shift indicates a decrease in the number of molecules and a decrease in the number of individual fluorophores passing through the fixed focal volume. This is most pronounced for PVP Kollidon 25 BGL-NP in PEG 400 (Figure 22 A) and PVP 10,000 BGL-NP in PG (Figure 22 C). The next change in the autocorrelation curve was a shift to the right which indicates a shift in diffusion time (Figure 22 B, D). The diffusion coefficients for each formulation are listed in Table 25. In the PEG 400 formulations, the diffusion coefficient increased with increasing polymer size, this effect was not seen in the PG formulations. The diffusion coefficients of each formulation were relatively similar and the calculated size range was in agreement with size measurements gathered from dynamic light scattering.

The number of CpG-ODN molecules per NP were also estimated by comparing the intensity histograms of free CpG-ODN to the NP formulations. The average number of CpG-ODN per particle was estimated based on average individual counts per particle (kHz) divided by average individual counts of CpG-ODN (Figure 23). As determined by DLS, PVP 40,000 and CMCNa resulted in non-uniform CpG-ODN complexation given the range of 0 - 129 and 0 -

429.6 CpG-ODN/NP as measured by FCS in PEG400 excipient. However, PVP 10,000 BG_{12}L-NP in PEG 400 excipient seemed to be able to complex a range of 1-11 CpG-ODN molecules per NP. The calculated median CpG-ODN numbers per particle were as follows: PEG400 excipient: G_{12}L-NP = 1.1; PVP 10,000 BG_{12}L-NP = 1.8; PVP Kollidon 25 BG_{12}L-NP = 2.0; PVP 40,000 BG_{12}L-NP = 0.8 and CMCNa BG_{12}L-NP = 1.3. PG excipient: G_{12}L-NP = 2.1; PVP 10,000 BG_{12}L-NP = 1.1; PVP Kollidon 25 BG_{12}L-NP = 1.0; PVP 40,000 BG_{12}L-NP = 0.81 and CMCNa BG_{12}L-NP = 0.7. All mean, median, and range values of number of CpG-ODN per NP are presented in Table 26.

Table 25 Diffusion coefficients of GL-NPs and BGL-NPs prepared with PEG 400 and PG 400 excipients. Particles size determined by FCS using the Stokes Einstein Equation

Polymer	PEG 400			PG		
	Mean diffusion coefficient (10^{-11} m^2/s)	Mean Diameter (nm)	CV%	Mean diffusion coefficient (10^{-11} m^2/s)	Mean Diameter (nm)	CV%
None	1.38	178.6	22.34	1.13	216.6	9.80
PVP 10,000	1.41	172.6	2.05	1.10	221.5	6.78
PVP Kollidon 25	1.80	136.5	13.09	1.15	211.8	9.69
PVP 40,000	2.04	119.9	4.39	1.62	171.0	78.22
CMCNa	2.14	116.1	19.25	1.52	163.0	21.33

Table 26 Mean, median, and range of number of CpG-ODN molecules per NP prepared with PEG 400 and PG excipients.

Polymer	PEG 400			PG		
	Mean #CpG-ODN per NP	Median #CpG-ODN per NP	Range of #CpG-ODN per NP	Mean #CpG-ODN per NP	Median #CpG-ODN per NP	Range of #CpG-ODN per NP
None	1.13	1.1	0.9-1.5	2.82	2.1	0.66-24.8
PVP 10,000	2.03	1.8	0.6-11	1.14	1.1	0.9-2
PVP Kollidon 25	2.33	2.0	0.8-17.76	1.00	1.0	0.75-1.58
PVP 40,000	4.31	0.8	0.3-129.1	3.50	0.81	0.33-133.8
CMCNa	7.34	1.3	0.2-429.6	0.81	0.7	0-6.19

The number of CpG-ODN molecules per NP was estimated by comparing the FCS intensity histograms of free CpG-ODN to the NP formulations. The average number of CpG-ODN per particle was estimated based on average individual counts per particle (kHz) divided by average individual counts of CpG-ODN.

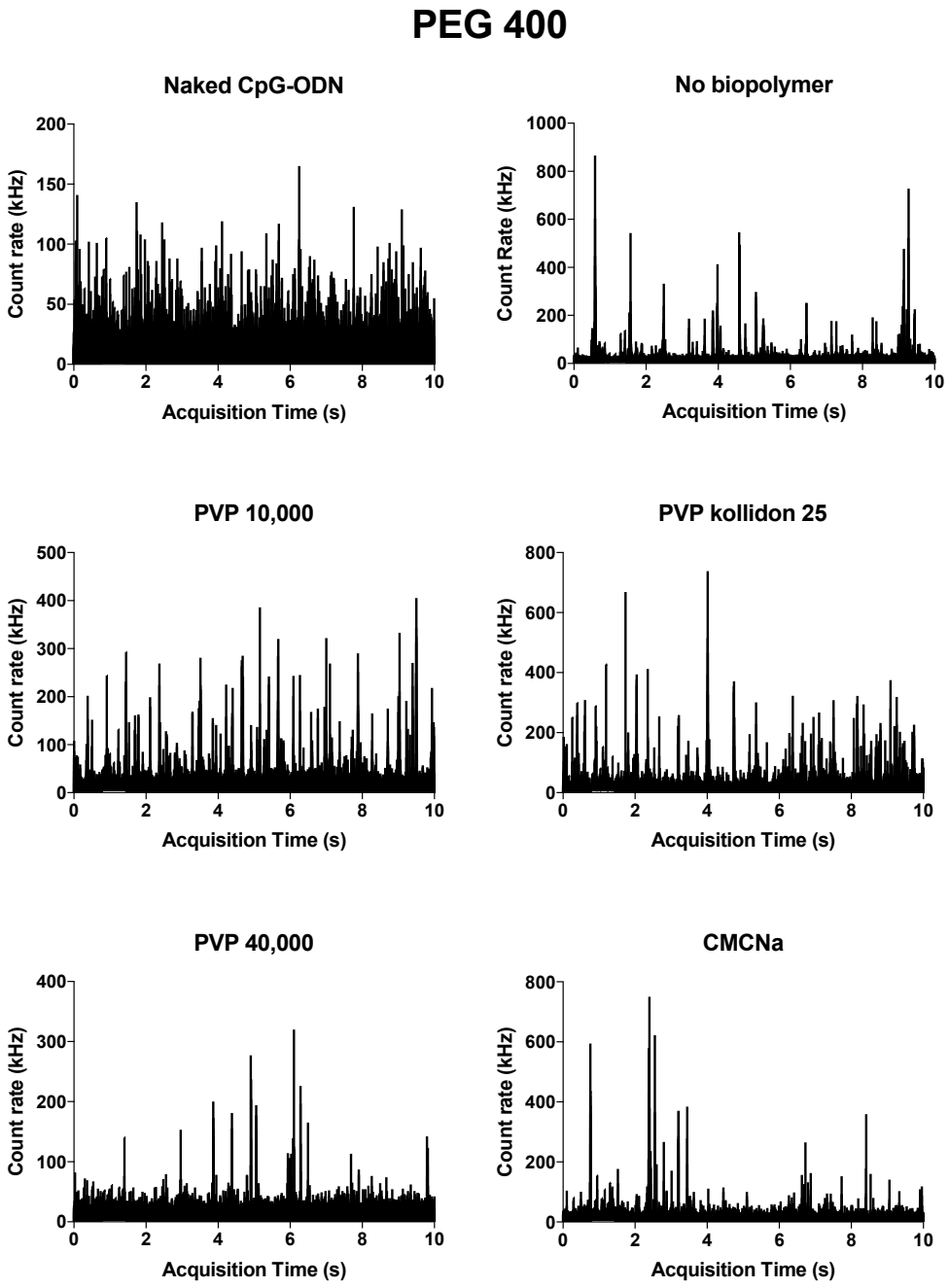

Figure 20 Raw intensity count rates for G_{12}L-NPs and BG_{12}L-NPs formulated in PEG 400 excipient

Count rate measurements for naked CpG-ODN, G_{12}L-NP (no biopolymer), and BG_{12}L-NPs with their corresponding polymer.

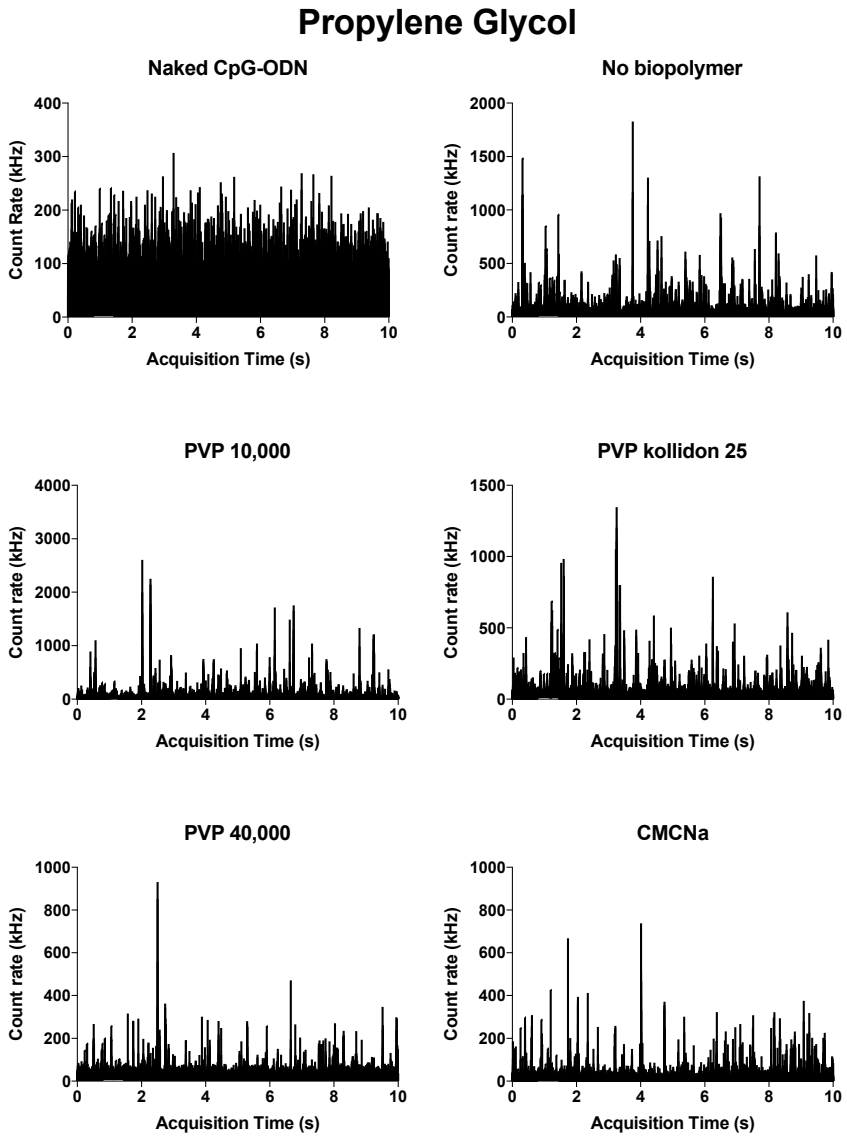

Figure 21 Raw intensity count rates for G_{12}L-NPs and BG_{12}L-NPs formulated in PG excipient

Count rate measurements for naked CpG-ODN, G_{12}L-NP (no biopolymer), and BG_{12}L-NPs with their corresponding polymer.

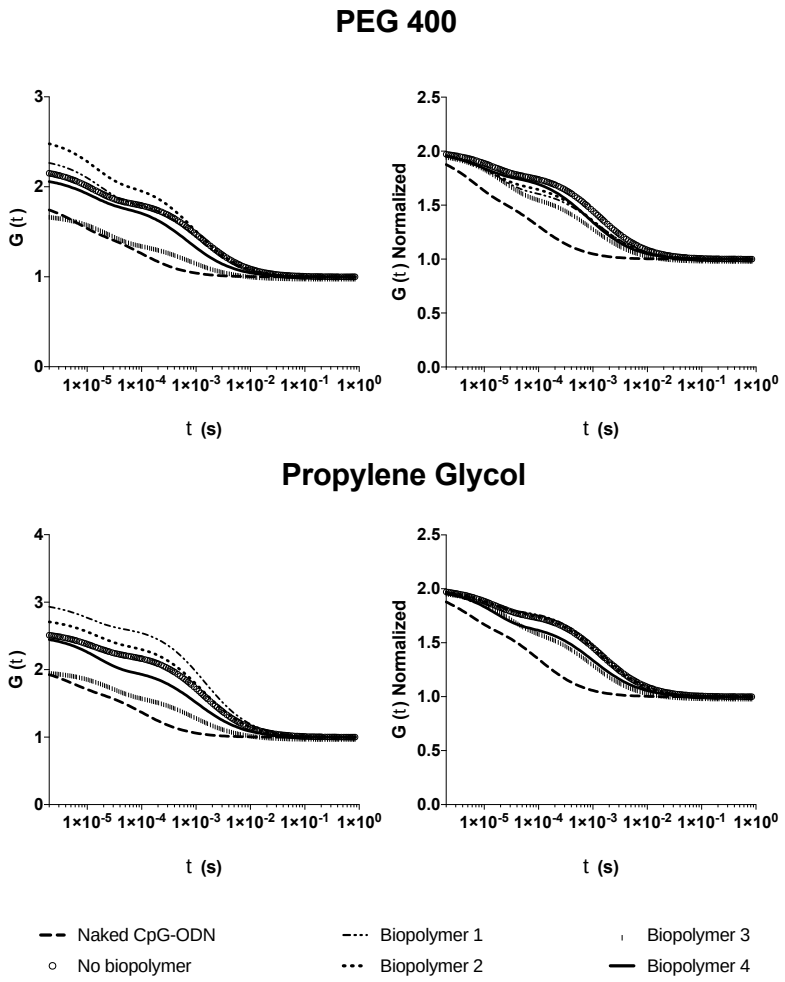

Figure 22 ACF of naked CpG-ODN and G_{12}L-NPs and BG_{12}L-NPs formulated inPEG 400 and PG excipient

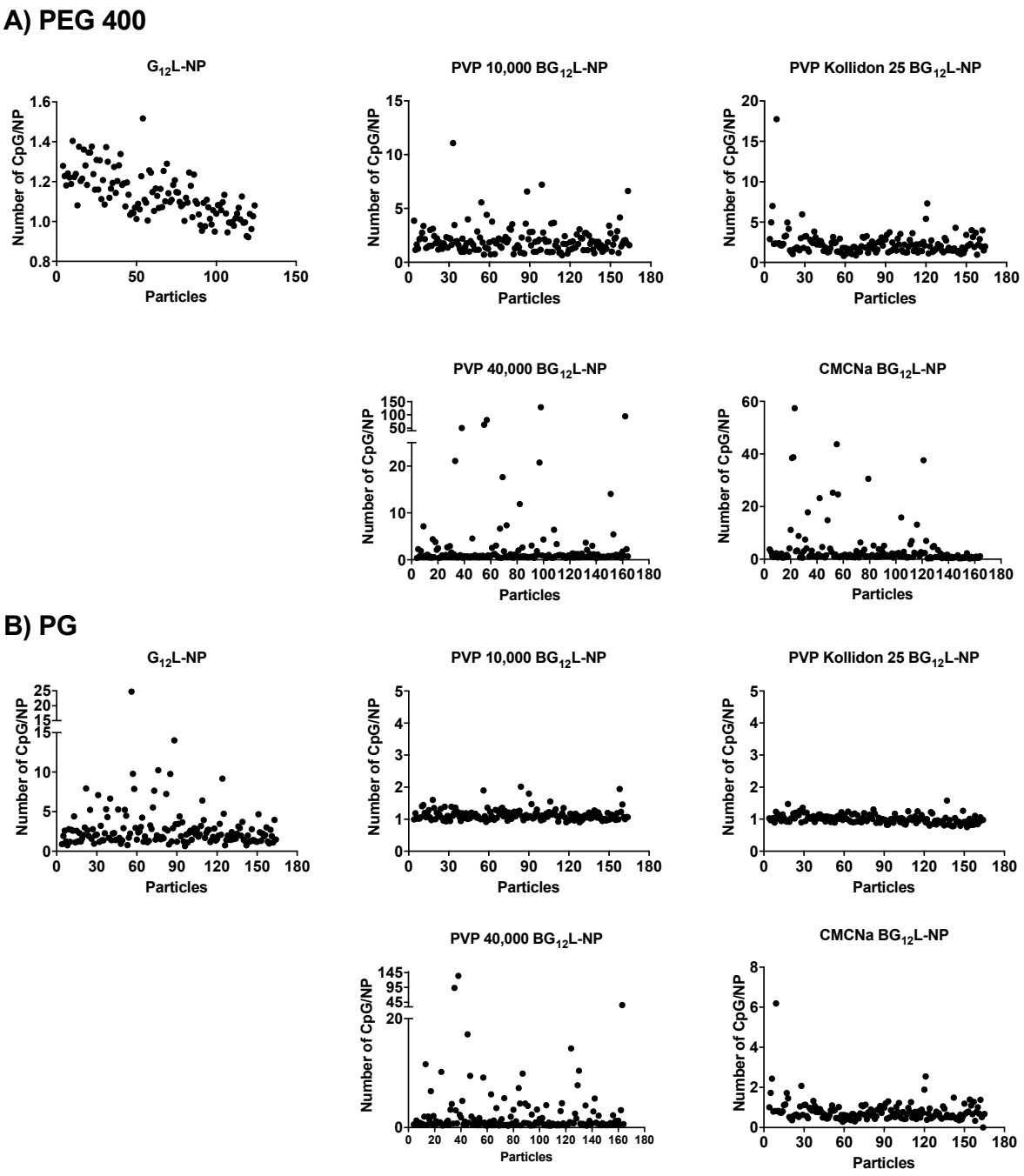

Figure 23 Estimation of number of CpG-ODN molecules per G_{12}L-NP and BG_{12}L-NP particles based on average individual counts per particle (kHz) divided by average individual counts of CpG-ODN (100 kHz and 200 kHz, for PEG400 (A) and PG (B) excipient formulations, respectively) n=40 runs. Median CpG-ODN number per particle: A) G_{12}L-NP = 1.1; PVP 10,000 BG_{12}L-NP = 1.8; PVP Kollidon 25 BG_{12}L-NP = 2.0; PVP 40,000 BG_{12}L-NP = 0.8 and CMCNa BG_{12}L-NP = 1.3. B) G_{12}L-NP = 2.1; PVP 10,000 BG_{12}L-NP = 1.1; PVP Kollidon 25 BG_{12}L-NP = 1.0; PVP 40,000 BG_{12}L-NP = 0.81 and CMCNa BG_{12}L-NP = 0.7. Range of CpG-ODN number per particle are presented in Table 26.

4.3 Assessing NPs as an effective CpG-ODN delivery vehicle in HD11 chicken macrophage cells

4.3.1 Uptake of naked CpG-ODN in HD11 macrophages

Since CpG-ODN uptake by avian immune cells is dependent on CpG-ODN sequence and cell type, HD11 cells were incubated with varying quantities of free or naked CpG-ODN for varying time points ranging from 1-4 hours. The percentage of cells with CpG-ODN uptake as detected by the Alexa Fluor 647 fluorescent label was determined at the end of each stimulation time point (Figure 24). Cellular uptake was dose and time dependent between 0.1-20 μg of CpG-ODN, reaching 50% uptake at 20 μg dose after 4 hours of stimulation. The percentage of cells containing CpG-ODN increased significantly from 2-4 hours of stimulation for higher quantities of CpG-ODN (1 - 20 μg) in comparison to stimulation from 1 to 2 hours. Since identifiable differences in CpG-ODN uptake at different quantities was evident after 4-hour incubation, dosing cells for 4 hours was chosen for preliminary NP uptake experiments.

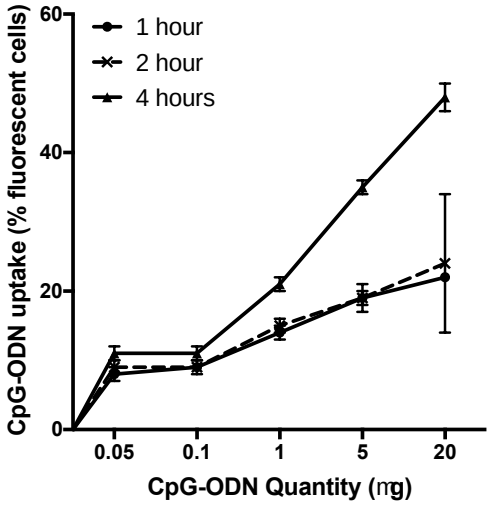

Figure 24 Dose and time dependent uptake of naked CpG-ODN in HD11 macrophages

HD11 macrophages were incubated with increasing quantities of naked CpG-ODN labeled with Alexa Fluor 647 at different stimulation times. CpG-ODN uptake was determined by the percentage of fluorescent cells at the end of each time point (n=3). Error bars represent mean ± S.D.

4.3.2 Evaluating the capacity of G_{12}L-NPs and BG_{12}L-NPs to improve uptake of CpG-ODN in HD11 chicken macrophages

To determine whether G_{12}L-NPs and BG_{12}L-NPs could enhance CpG-ODN uptake in comparison to naked CpG-ODN, HD11 macrophages were stimulated with increasing doses of CpG-ODN NPs and naked CpG-ODN for 4 hours. The first formulations tested for method development were two formulations previously tested *in vivo*: G_{12}L-NP (no biopolymer) and PVP 10,000 BG_{12}L-NP (PVP 10,000 polymer coating). After 4 hours of dosing, G_{12}L-NPs and PVP 10,000 BG_{12}L-NPs were able to significantly increase the number of HD11 macrophages containing CpG-ODN in comparison to naked CpG-ODN (Figure 25). In fact, it only took the equivalent of 0.5 μg of both CpG-ODN NPs to reach near 100% cell uptake. Conversely, it took 5 μg of naked CpG-ODN to reach 50% uptake and 10 μg of naked CpG-ODN to reach a comparable level of uptake associated with G_{12}L-NPs and BG_{12}L-NPs. The PVP 10,000 biopolymer component of the BG_{12}L-NP performed similar to the G_{12}L-NP without biopolymer also reaching near 100% cell uptake at 1 μg CpG-ODN dose. It was only at the lower CpG-ODN quantities of 0.1 and 0.5 μg, that the biopolymer seemed to slightly decrease the amount of CpG-ODN uptake in HD11 macrophages after 4-hour stimulation.

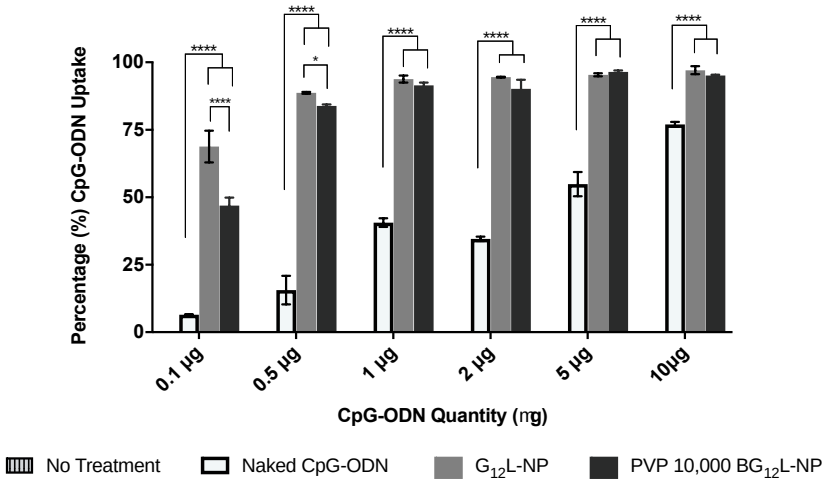

Figure 25 Assessment of CpG-ODN uptake after 4 hours dosing associated with G_{12}LP-NPs and BG_{12}LP-NPs in comparison to naked CpG-ODN

HD11 cells were incubated with CpG-ODN formulations in RPMI 1640 media for 4 hours and % CpG-ODN uptake was measured immediately after incubation, n=3. Error bars represent mean ± S.D. Statistically significant differences between experimental groups were determined by two-way ANOVA with Tukey's multiple comparison test. Statistics were performed between naked CpG-ODN and formulations at each dose where * $p < 0.05$, **** $p < 0.0001$.

Since there was a significant difference in CpG-ODN uptake observed after dosing with NP formulations for 4 hours in comparison to naked CpG-ODN, the extent of CpG-ODN uptake in cells dosed with NP formulations for different amounts of time over 4 hours was also tested.

One μg CpG-ODN was used for dosing cells at each time point and was evaluated. CpG-ODN uptake was detectable at all dosing times from 1-4 hours (Figure 26 A). Like the previous experiment, all formulations again significantly improved uptake of CpG-ODN in HD11 cells at all time points compared to stimulation with naked CpG-ODN (Figure 26 A). Additionally, the PVP 10,000 BG_{12}L-NP formulation in this experiment produced more uptake at all time points than the G_{12}L-NP formulation without biopolymer. It also performed better in comparison to CMCNa BG_{12}L-NP after 2 and 4 hours of dosing. Time of dosing had a minimal effect on uptake and was mainly evident comparing dosing of 1 and 4 hours (Figure 26B).

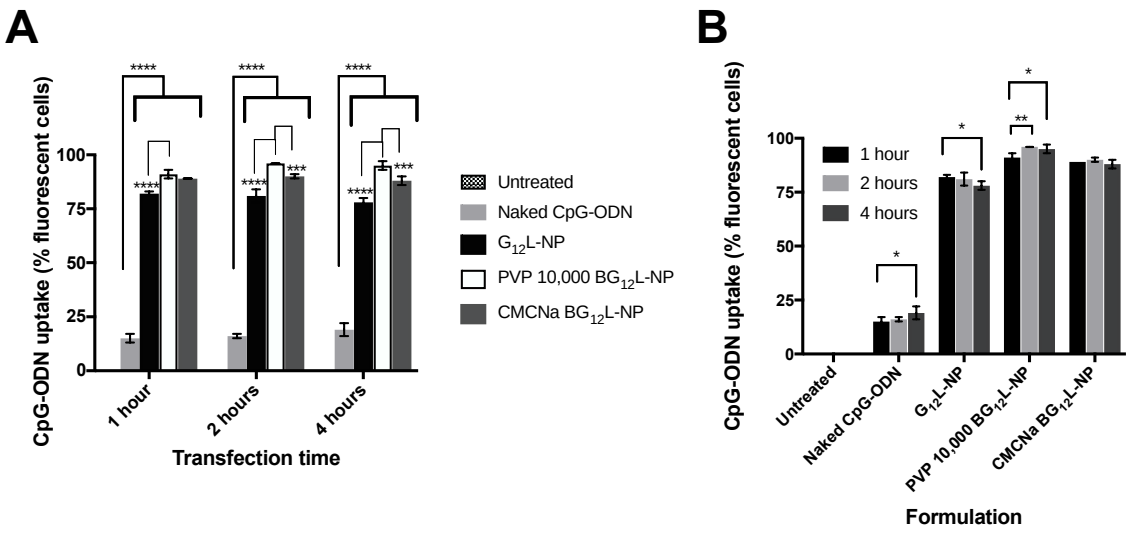

Figure 26 Time dependent uptake of CpG-ODN after dosing with G_{12}L-NPs and BG_{12}L-NPs in comparison to naked CpG-ODN DNA

HD11 cells were incubated with 1 μg CpG-ODN and dosed for 1, 2 and 4 hours. CpG-ODN uptake was measured immediately after dosing (n= 3) (A). The same data is transposed in B to outline changes in CpG-ODN uptake resulting from the increase of dosing time. Error bars represent mean ± S.D. Statistically significant differences between experimental groups were determined by two-way ANOVA with Tukey's multiple comparison test. Statistics were performed between naked CpG-ODN and formulations at each dose where * $p < 0.05$, **$p<0.001$, ***$p=0.001$ **** $p < 0.0001$.

4.3.3 Evaluating the capacity of G_{12}L-NPs and BG_{12}L-NPs to improve CpG-ODN retention in HD11 macrophages

As one of the goals of formulating CpG-ODN is to extend effects of immune stimulation, the retention of CpG-ODN 24 hours post dosing with G_{12}L-NPs and BG_{12}L-NPs was also evaluated in HD11 cells. Retention, refers to whether CpG-ODN can still be detected 24 hours later in cells after the initial dosing for 2 hours. An incubation time of 2 hours was chosen since time had minimal effect on CpG-ODN uptake over a 4-hour time period and had near 100% cellular uptake as previously stated (Figure 26).

New G_{12}L-NP and BG_{12}L-NP formulations using 4 different biopolymers of different molecular weights (PVP 10,000; PVP Kollidon 25; PVP 40,000, CMCNa), formulated in 2 different excipients (PEG 400, PG) were tested for their ability to retain CpG-ODN within cells. All G_{12}L-NPs and BG_{12}L-NPs resulted in significantly higher retention of CpG-ODN uptake 24 hours after initial dosing for 2 hours in comparison to naked CpG-ODN, $\geqq$30% versus 10%, respectively (Figure 27). Moreover, the PVP 10,000 BG_{12}L-NP formulation which has the lowest MW of the polymers, resulted in the highest retention of CpG-ODN uptake in comparison to the other formulations. PVP 10,000 BG_{12}L-NP formulated in PEG 400 did perform significantly better than PVP Kollidon 25 BG_{12}L-NP in PEG 400 and the G_{12}L-NP in PG. However, PVP 10,000 BG_{12}L-NP resulted in similar CpG-ODN uptake in comparison to G_{12}L-NP without biopolymer (Figure 27). Using PEG400 versus PG excipient did not significantly affect the retention of CpG-ODN in the different formulations.

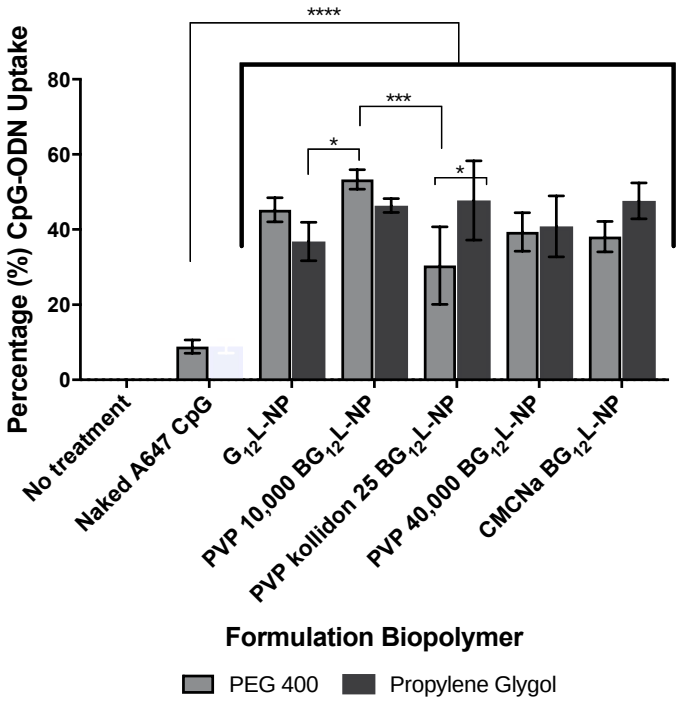

Figure 27 Retention of CpG-ODN in HD11 macrophages 24 hours after initial cell dosing with G_{12}L-NPs and BG_{12}L-NPs in different excipients

HD11 cells were incubated with 1 µg CpG-ODN and dosed for 2 hours followed by removal of media, and CpG-ODN uptake was measured 24 hours later, after media removal. Error bars represent mean ± S.D. (n=3). Statistically significant differences between experimental groups were determined by two-way ANOVA with Tukey's multiple comparison test. Statistics were performed between naked CpG-ODN and formulations, where * $p < 0.05$, **$p=0.0013$, ***$p=0.001$ **** $p < 0.0001$.

4.3.4 Evaluating the capacity of G-NPs and CG-NPs to improve retention of CpG-ODN in HD11 macrophages

G-NPs (CpG-ODN-gemini complexes) were used as the intermediate for CG-NPs. The addition of chitosan (low MW, 55-90 KDa) to G-NPs resulted in the formation of CG-NPs and was directly compared to G-NPs. Once again, all formulations improved the retention of CpG-ODN compared to naked CpG-ODN 24 hours after dosing (Figure 28). However, unlike the G_{12}L-NPs and BG_{12}L-NPs it was more evident that some formulations performed better than others.

Interestingly, cells treated with G-NPs retained higher CpG-ODN uptake than GC-NPs regardless of the chitosan concentration. More cells retained CpG-ODN when dosed with G_{12}-NP and G_{16}-NP formulations (Figure 28 A,B) than G_{18}-NP (Figure 28 C) 24 hours after dosing (90%, versus 70%, respectively). Although G-NPs performed better than CG-NPs, increasing

chitosan concentration significantly improved retention proportionally in comparison to naked CpG-ODN.

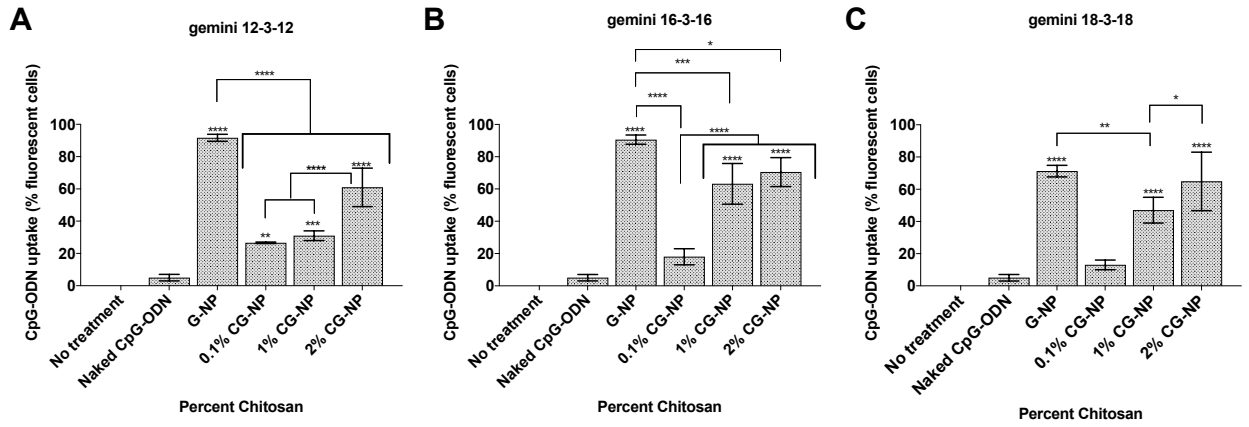

Figure 28 Evaluation of the effect of increasing chitosan concentration in CG-NPs on the retention of CpG-ODN-gemini complexes 24 hours post initial dosing

HD11 cells were incubated with 1 µg CpG-ODN and dosed for 2 hours followed by removal of media, and CpG-ODN uptake was measured 24 hours later, after media removal. CG-NPs formulated with gemini 12-3-12 (A), gemini 16-3-16 (B), and gemini 18-3-18 (C) are compared to their G-NP equivalent. Error bars represent mean ± S.D., (n=3). Statistically significant differences between experimental groups were determined by two-way ANOVA with Tukey's multiple comparison test. Statistics were performed between naked CpG-ODN and formulations, where * $p < 0.05$, **$p < 0.01$, ***$p < 0.001$ **** $p < 0.0001$. Statistics present directly above error bars show significance in comparison to naked CpG-ODN.

4.3.5 Evaluating the retention of CpG-ODN in HD11 cells transfected with C-NPs

Ultra-low MW chitosan (2.5kDa) and low MW chitosan (55-90 kDa) were also formulated to form C-NP complexes given that positively charged amine groups of chitosan in acidic media complexes simultaneously with DNA to form NPs. Neither C-NPs significantly improved CpG-ODN retention 24 hours post dosing in comparison to naked CpG-ODN and there was high variability in the percentage of cells still containing CpG-ODN (Figure 29). However, the 2.5k C-NP performed marginally better compared to the 0.1% 55-90 kDa C-NP.

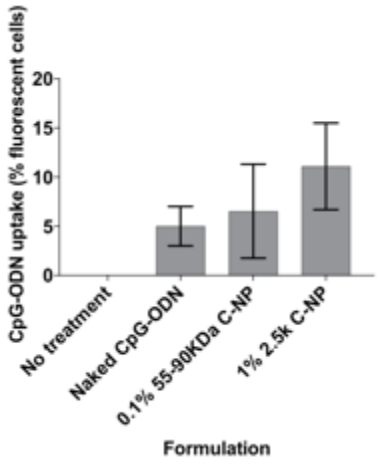

Figure 29 Evaluation of the effect of chitosan molecular weight on the retention of C-NPs 24 hours post initial dosing

HD11 cells were incubated with 1 µg CpG-ODN and dosed for 2 hours followed by removal of media. CpG-ODN uptake was measured 24 hours later, after media removal. Error bars represent mean ± S.D., (n= 3).

4.3.6 Evaluation of the capacity of CL-NPs to improve uptake and retention of CpG-ODN in HD11 macrophages

Unlike other formulations CL-NP did not improve CpG-ODN uptake in HD11 macrophage cells. The relative uptake was under 10% at 2 and 24 hours post dosing (Figure 30). In contrast, ~40% of cells were transfected with naked CpG-ODN after 2 hours of dosing.

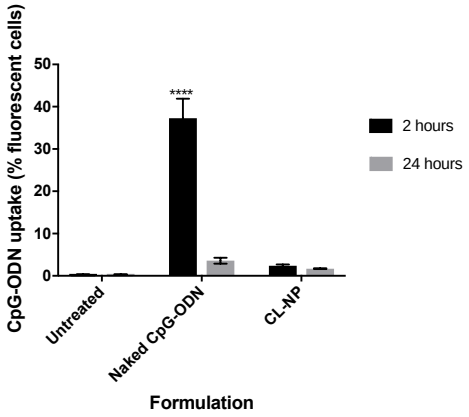

Figure 30 Effect of CL-NP on CpG-ODN uptake after 2 hours of dosing and retention 24 hours post dosing

HD11 cells were incubated with 1 µg CpG-ODN for 2 hours followed by removal of media, and CpG-ODN uptake was measured after 2 hours of dosing and 24 hours later, after dosing. Error bars represent mean ± S.D., (n= 3). Statistically significant differences between experimental groups were determined by two-way ANOVA with Tukey's multiple comparison test. Statistics were performed between naked CpG-ODN and formulations, where **** $p < 0.0001$. Statistics present directly above error bars show significance in comparison to CL-NPs and untreated cells at 2 hours post dosing.

4.4 Effect of CpG-ODN and NP complexation on immune stimulation in HD11 macrophages

4.4.1 Effect of Naked CpG-ODN dose on the extent of immune stimulation

To investigate the correlation between cellular CpG-ODN uptake and innate immune activation in HD11 macrophages, the concentration of nitrite produced in macrophages was measured. Nitrite production is a standard result from CpG-ODN stimulation in the avian innate immune system and indirectly measures nitric oxide production, which results in bactericidal activity. Since there was evidence of CpG-ODN uptake up to 4 hours of CpG-ODN dosing, nitrite levels were measured after stimulation (incubation) of HD11 macrophages for 1, 2, and 4 hours with naked CpG-ODN (Figure 31). No significant levels of nitrite production were detectable with 0.05-1 μg CpG-ODN over the four hours. However, the concentration of nitrite produced with 5 and 20 μg CpG-ODN was significantly higher than untreated cells after 4 hours of stimulation (Figure 31).

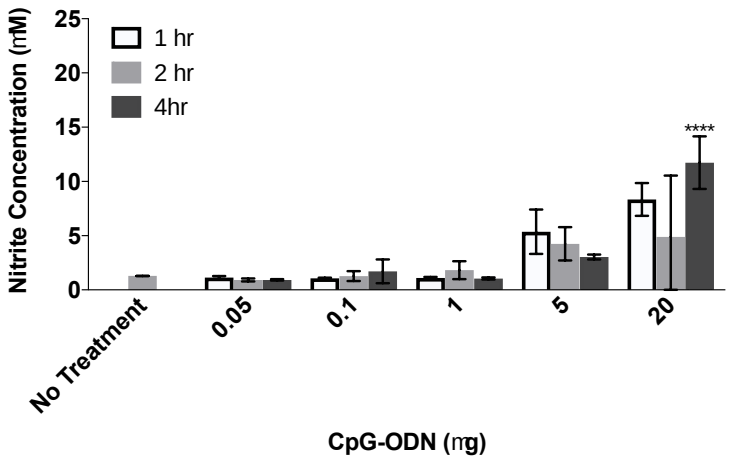

Figure 31 Comparison of nitrite production in HD11 macrophages after stimulation with increasing quantities of CpG-ODN for 1, 2, and 4 hours.

Nitrite concentration in HD11 macrophage cell supernatants were measured using the standard Greiss Assay as an indication of macrophage activation. HD11 cells were stimulated with 5 different concentrations of naked CpG-ODN for 3 different time points: 1, 2, 4 hours. Error bars represent mean ± S.D., (n=3). Statistically significant differences between experimental groups were determined by two-way ANOVA with Tukey's multiple comparison test. Statistics were performed between untreated cells and naked CpG-ODN, as well as between quantities and time where **** $p < 0.0001$. Statistical values present directly above error bars represent significant differences in comparison to untreated cells.

Due to the relatively low concentration of nitrite produced after 4 hours of stimulation with reasonable quantities of naked CpG-ODN (up to 20 μg), the extent of immune stimulation 24 hours after dosing with increasing quantities of naked CpG-ODN was also determined. The extent of immune stimulation was low for the first 4 hours post incubation (Figure 32), similar to the previous data. However, at 24 hours post incubation, all CpG-ODN doses ranging from 0.05 - 20 μg produced nitrite levels higher than unstimulated cells (Figure 32A). The amount of nitrite produced at 24 hours was similar within the range of 0.05-20 μg (Figure 32B).

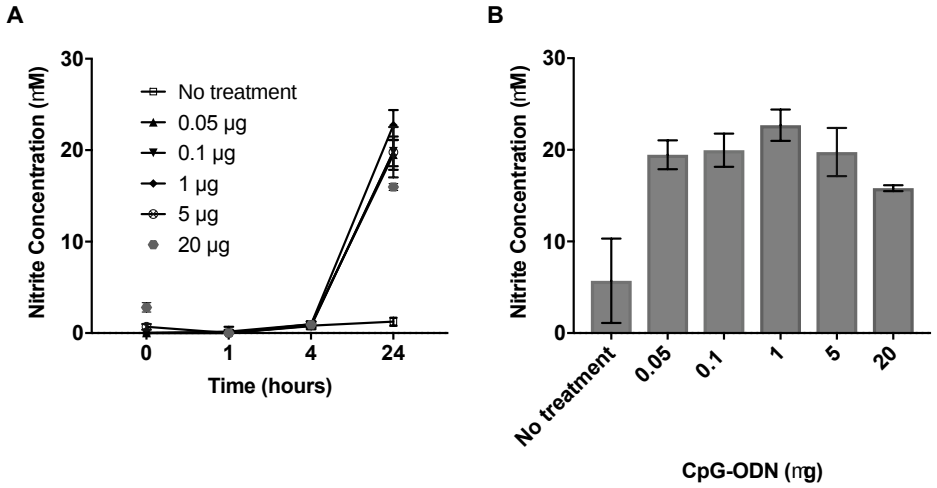

Figure 32 Comparison of nitrite production in HD11 macrophages after stimulation with increasing concentration of CpG-ODN for 2 hours.

The nitrite concentration produced after two hours of cell incubation with CpG-ODN concentrations ranging from 0.05 - 20 μg was measured over 24 hours using the standard Greiss Assay (A). Nitrite produced at 24 hours with different concentrations is also shown (B). Cell supernatant was collected at each time point. Values expressed represent mean ± S.D. (n=3).

4.4.2 Comparison of innate immune stimulation from G_{12}L-NPs and BG_{12}L-NPs to naked CpG-ODN

In order to determine whether G_{12}L-NPs and BG_{12}L-NPs had an effect on macrophage activation, the extent of immune stimulation produced by G_{12}L-NPs and BG_{12}L-NPs were compared to immune stimulation with naked CpG-ODN only. The equivalent of 0.1 μg CpG ODN formulated with NPs was incubated with HD11 cells for 2 hours and nitrite was measured at 1, 4 and 24 hours. Once again, no significant nitrite production occurred before 24 hours. G_{12}L-NPs (containing no biopolymer) produced nitrite concentration comparable to naked CpG-

ODN whereas the formulations containing biopolymers showed a significant lower effect (Figure 33 A,B). The delivery of NPs without CpG-ODN (blank NPs), were also tested to determine whether they had stimulatory effects on their own. However, no significant stimulatory effect on HD11 macrophages occurred from NP formulations compared to naked CpG-ODN even after 24 hours (Figure 33 C,D).

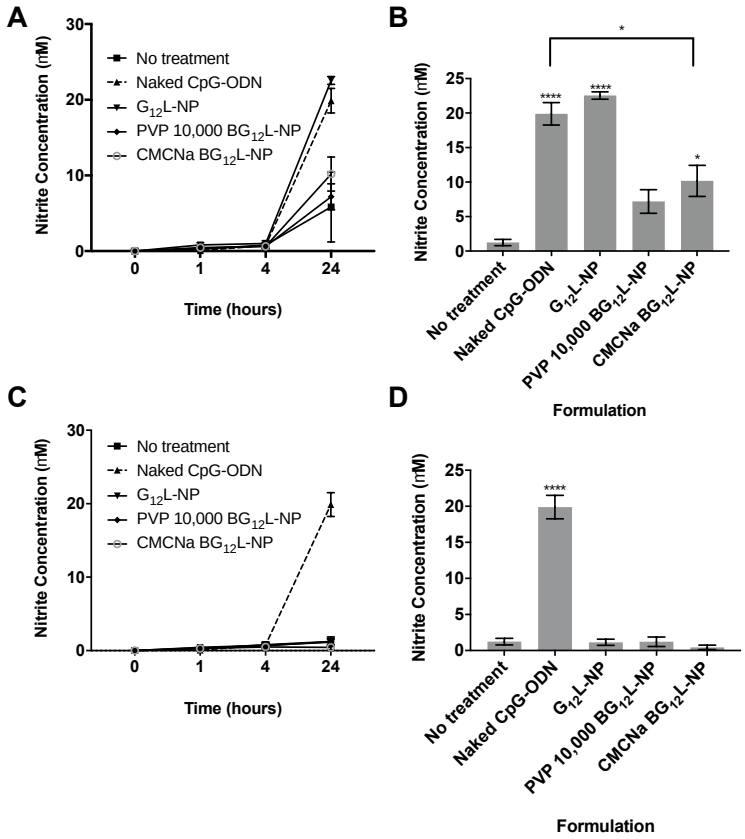

Figure 33 Comparison of immune stimulation between naked CpG-ODN, G_{12}L-NPs, and BG_{12}L-NPs formulations

Extent of nitrite production in HD11 macrophages after 2-hour stimulation with 0.1 μg naked CpG-ODN and complexed with G_{12}L-NPs, PVP 10,000 BG_{12}L-NPs, and CMCNa BG_{12}L-NPs. Particles were formulated as previously described. Nitrite production over 24 hours was monitored in HD11 cells after incubation with CpG-ODN complexed with NPs (A) and blank NPs (C). The extent of production at 24 hours for both instances was compared (B,D). Values expressed represent mean ± S.D., (n=3). Statistically significant differences between experimental groups were determined by one-way ANOVA with Tukey's multiple comparison test. Statistics were performed between untreated cells and cells dosed with CpG-ODN NP formulations, where **** $p < 0.0001$, *$p < 0.05$. Statistical values present directly above error bars represent significant differences in comparison to untreated cells.

4.4.3 Effect of dispersion excipient on immune stimulation

After 2-hour incubation with formulations containing the equivalent of 1 μg CpG-ODN, the absolute nitrite concentration produced in HD11 macrophages was measured after 24 hours and compared to nitrite produced by naked CpG-ODN. After 24 hours, PVP 10,000 and PVP Kollidon 25 BG_{12}L-NP formulations in PEG 400 excipient produced increased nitrite levels in comparison to naked CpG-ODN and G_{12}L-NP (Figure 34A). For G_{12}L-NP and BG_{12}L-NP formulations in PG excipient, none performed better than formulations with PEG400 and only PVP Kollidon 25 and CMCNa BG_{12}L-NP produced nitrite levels comparable to naked CpG-ODN (Figure 34B). Stimulation with G_{12}L-NPs and BG_{12}L-NPs not complexed with CpG-ODN (blank controls) once again did not produce any significant nitrite after 24 hours (Figure 34 C,D).

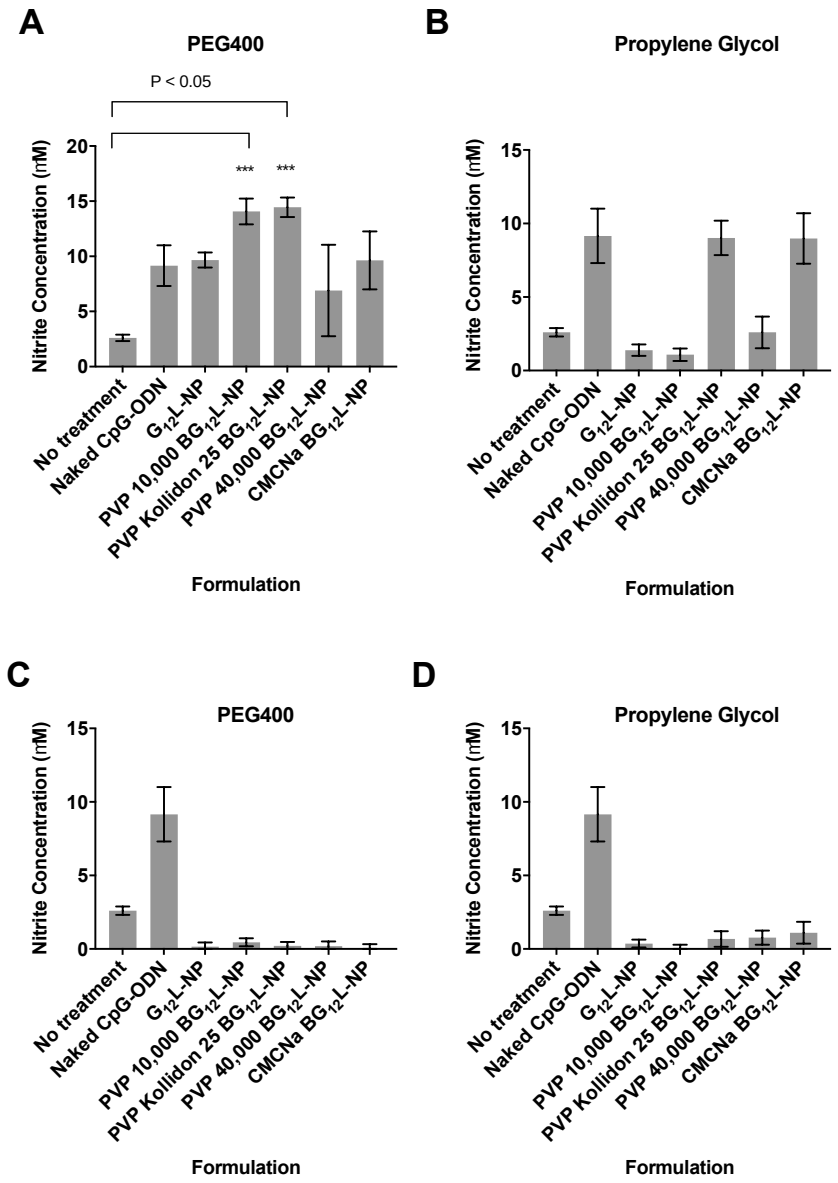

Figure 34 Comparison of nitrite production 24 hours post stimulation with G_{12}L-NP and BG_{12}L-NP formulations in PEG400 or PG excipients and naked CpG-ODN

Nitrite production in HD11 macrophage cells 24 hours post stimulation with 1 μg CpG-ODN in all formulations was measured using the standard Greiss assay. NP formulations were prepared as described for gemini phospholipid formulations. Nitrite production by G_{12}L-NPs, BG_{12}L-NPs formulated with PEG400 excipient (A) and formulated with PG excipient (B). Blank G_{12}L-NPs, BG_{12}L-NPs formulated with PEG400 excipient (C) and formulated with PG excipient (D) were used as blank controls. Values are expressed as mean ± S.D. (n = 4). Statistically significant differences between experimental groups were determined by two-way ANOVA with Tukey's multiple comparison test. Statistics were performed between untreated cells and cells dosed with CpG-ODN NP formulations, where **** $p < 0.0001$, ***$p < 0.001$, *$p < 0.05$.

4.4.4 Effect of G-NPs on macrophage activation and nitrite production

The influence of G-NPs on the ability of HD11 macrophages to produce nitrite was investigated in comparison to naked CpG-ODN. The nitrite production after 2 hours of stimulation with 1 μg CpG-ODN was measured 12 and 24 hours post stimulation. Nitrite levels produced 24 hours post stimulation were higher in comparison to nitrite concentration at 12 hours (Figure 35). However, nitrite levels produced from cells stimulated with formulations changed in relation to naked CpG-ODN from 12 to 24 hours post dosing. At 12 hours, all the formulations induced greater nitrite than unstimulated cells, with the G_{18}-NP producing more nitrite than naked CpG-ODN (Figure 35A). At 24 hours, nitrite levels produced by formulations were lower in comparison to naked CpG-ODN (Figure 35B). In particular, G_{12}-NP formulation produced the least nitrite in comparison to G_{16}-NP and G_{18}-NP. Blank G-NPs did not induce nitrite production in comparison to unstimulated cells at 12 and 24 hours (Figure 35 A,B).

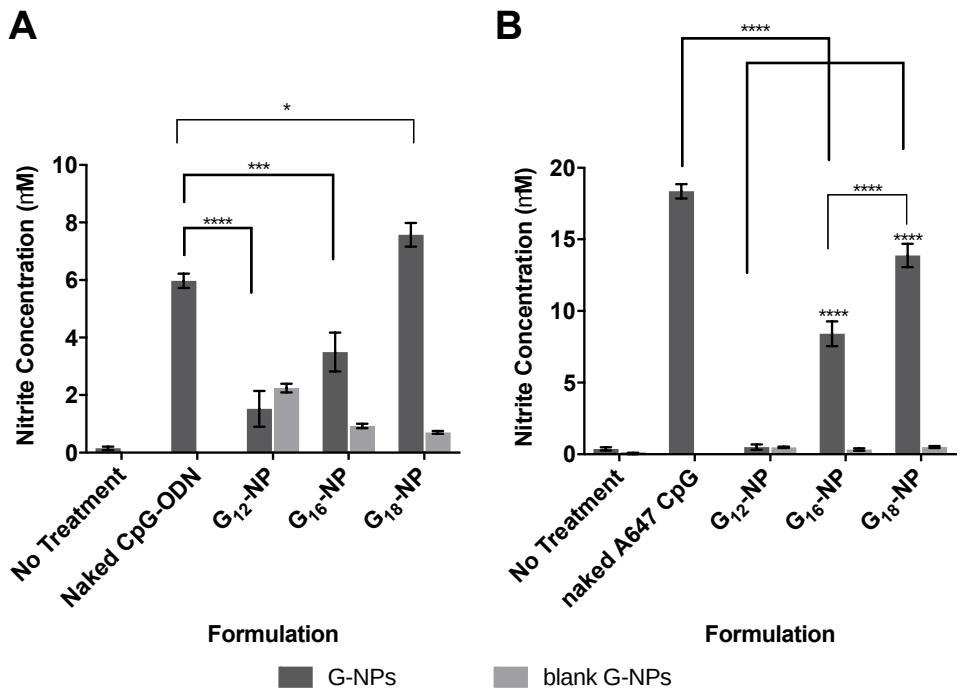

Figure 35 Comparison of nitrite production at 12 and 24 hours post stimulation with G-NPs complexed with CpG-ODN and blank gemini micelles

Nitrite production in HD11 macrophages was measured at 12 and 24 hours post stimulation with G-NPs and blank gemini micelles using the standard Greiss assay. Blank gemini micelles were added equivalent to the quantity that would be contained with 1 μg G-NPs. NP formulations were prepared as described previously. Nitrite production at 12 hours (A) and 24 hours (B). Values expressed represent mean ± S.D., (n=3). Statistically significant differences between experimental groups were determined by two-way ANOVA with Tukey's multiple comparison test. Statistics were performed between untreated cells and cells dosed with CpG-ODN NP formulations, where **** $p < 0.0001$, ***$p < 0.001$, *$p < 0.05$. Statistical values present directly above error bars represent significant differences in comparison to untreated cells.

4.4.5 Effect of C-NPs on macrophage activation and nitrite production

The influence of C-NPs on the ability of HD11 macrophages to produce nitrite was investigated in comparison to naked CpG-ODN. First, the effect of chitosan excipient on nitrite production was evaluated after 2 hours of stimulation at 12 and 24 post stimulation. Both chitosan solutions stimulated nitrite production in HD11 cells to some degree 12 hours later (Figure 36A). Nitrite production by C-NPs both at 12 and 24-hour time points was similar to naked CpG-ODN (Figure 36 A,B).

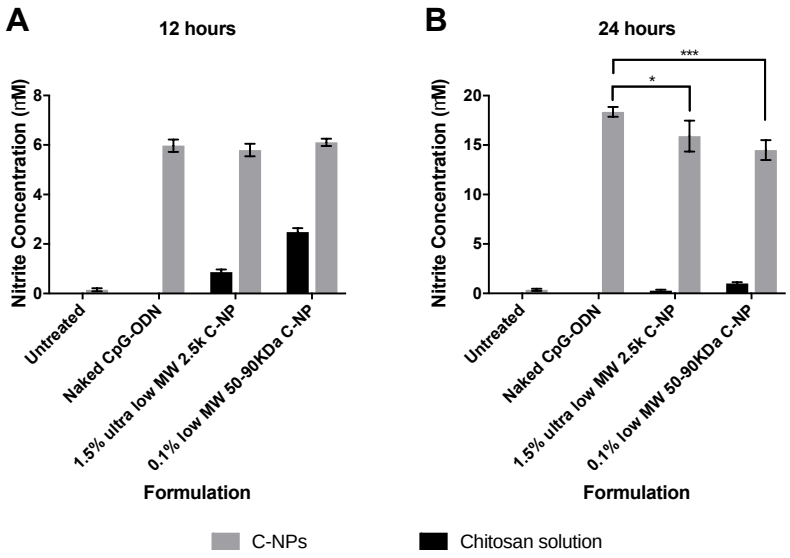

Figure 36 Stimulation of HD11 chicken macrophages with C-NPs in comparison to naked CpG-ODN

Nitrite production in HD11 macrophages was measured at 12 and 24 hours post stimulation with C-NPs and chitosan solution using the standard Greiss assay. Chitosan solution was added equivalent to the chitosan quantity that would be contained in the C-NPs 1 µg dose. NP formulations were prepared as described previously. Nitrite production is shown at 12 hours (A) and 24 hours (B). Values expressed represent mean ± S.D., (n=3). Statistically significant differences between experimental groups were determined by two-way ANOVA with Tukey's multiple comparison test. Statistics were performed between untreated cells and cells dosed with CpG-ODN NP formulations, where ***$p < 0.001$, *$p < 0.05$.

4.4.6 Effect of CG-NPs on macrophage activation and nitrite production

Next, the incorporation of chitosan into G-NPs with three different gemini surfactants (m=12,16,18) was also investigated. Similarly to G-NPs, the nitrite production rate doubled from 12 to 24 hours for all formulations (Figure 37 A,B,C). Additionally, the nitrite production induced by formulations was comparable to naked CpG-ODN at 12 hours and showed a decreasing trend with increasing chitosan concentration at 24 hours for all gemini surfactants.

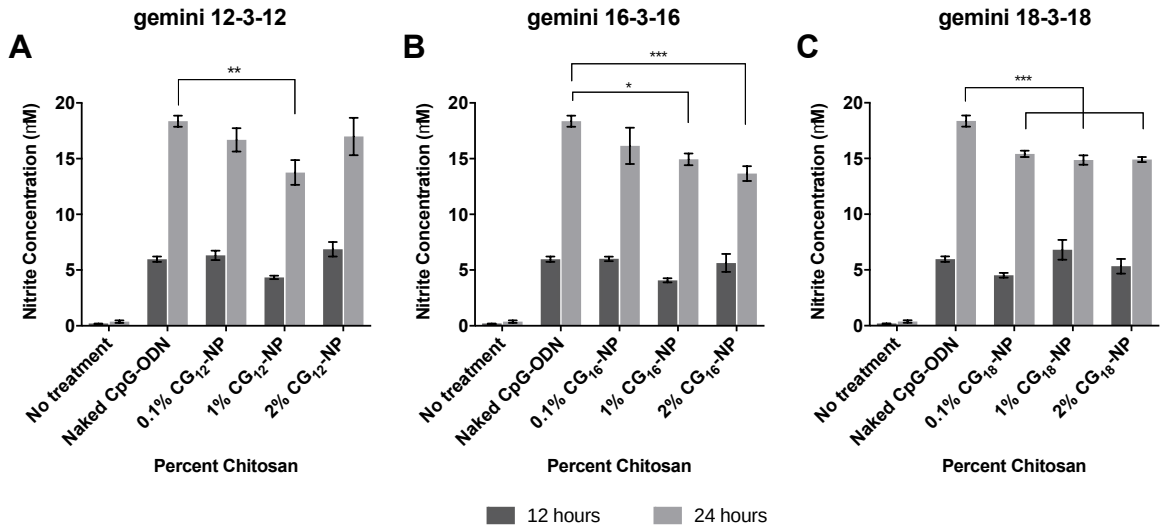

Figure 37 Stimulation of HD11 chicken macrophages with CG-NPs in comparison to naked CpG-ODN at 12 and 24 hours post dosing

Nitrite production in HD11 macrophages was measured at 12 and 24 hours post stimulation with CG-NPs using the standard Greiss assay. NP formulations were prepared as described previously. Cells were dosed with 1 µg CpG-ODN. Nitrite production at 12 hours and 24 hours resulting from CG_{12}-NPs (A), CG_{16}-NPs (B), and CG_{18}-NPs (C). Values expressed represent mean ± S.D., (n=3). Statistically significant differences between experimental groups were determined by two-way ANOVA with Tukey's multiple comparison test. Statistics were performed between untreated cells and cells dosed with CpG-ODN NP formulations, where ***$p < 0.001$, **$p < 0.01$, *$p < 0.05$.

4.4.7 Effect of CL-NPs on macrophage activation and nitrite production

Despite the low level of CpG-ODN uptake, transfection with CL-NPs still resulted in an increase in nitrite production in comparison to untreated cells (Figure 38). Nitrite production resulting from CL-NP transfection was similar to nitrite production resulting from naked CpG-ODN.

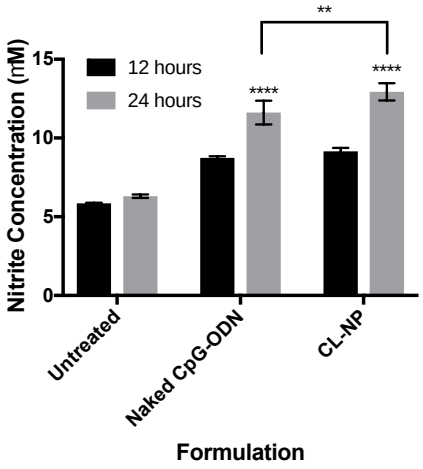

Figure 38 Stimulation of HD11 chicken macrophages with CL-NPs in comparison to naked CpG-ODN at 12 and 24 hours post dosing.

Nitrite production in HD11 macrophages was measured at 12 and 24 hours post stimulation with CL-NPs using the standard Greiss assay. NP formulations were prepared as described previously. Cells were dosed with 1 µg CpG-ODN. Values expressed represent mean ± S.D. (n=3). Statistically significant differences between experimental groups were determined by two-way ANOVA with Tukey's multiple comparison test. Statistics were performed between untreated cells and cells dosed with CpG-ODN NP formulations, where ****$p < 0.0001$, **$p < 0.01$. Statistical values present directly above error bars represent significant differences in comparison to untreated cells.

4.5 Assessment of HD11 cell toxicity after CpG-ODN NP stimulation

4.5.1 Viability in HD11 cells after naked CpG-ODN stimulation

CpG-ODN has been deemed as a safe adjuvant and is being tested in human clinical trials [135, 202]. In order to determine the viability of HD11 cells after naked CpG-ODN stimulation and compare it to HD11 cells stimulated with CpG-ODN NPs, the viability of cells was measured with Calcein AM. The viability of HD11 cells remained above 90% after 1, 2, and 4 hours of stimulation across all CpG-ODN quantities (Figure 39).

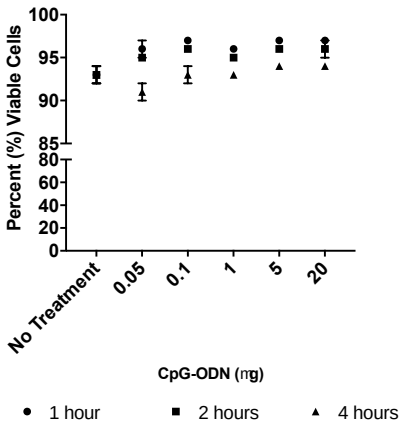

Figure 39 Viability of HD11 chicken macrophages after stimulation with naked CpG-ODN. Values expressed as mean ± S.D. (n=3).

Cell viability after stimulation with 1 μg CpG-ODN for 4 hours was measured using Calcein AM.

4.5.2 Cell Viability and Mitochondrial Activity after NP transfection

4.5.2.1 Gemini 12-3-12 phospholipid formulations maintain high mitochondrial activity

Considering previous evidence of changes in membrane permeability after gemini NP transfection [203], NP toxicity was also investigated using the viability dye MitoTracker Green FM that measures active mitochondrial activity in cells versus Calcein AM, which is dependent on membrane integrity. The effect of NP formulations on viability of HD11 macrophages was investigated. The viability was first investigated after stimulation with the G_{12}L-NPs formulated in PEG 400, including the addition of PVP 10,000 and CMCNa to the BG_{12}L-NPs (Figure 40). All formulations decreased the viability of HD11 cells at all time points significantly in comparison to untreated cells and cells stimulated with naked CpG-ODN when stained with Calcein AM cell permeability dye. The overall trend was that cell viability decreased over the period of 4 hours for all formulations, with the G_{12}L-NPs formulation having better viability than both BG_{12}L-NPs. The PVP 10,000 BG_{12}L-NPs however, produced variable results at 2 hours of stimulation.

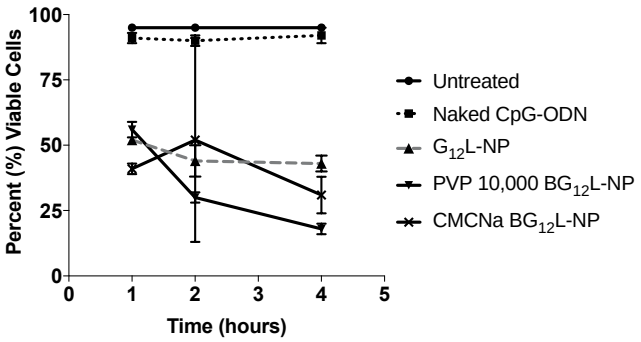

Figure 40 Viability of HD11 macrophages after stimulation with different G_{12}L-NP and BG_{12}L-NP formulations in comparison to naked CpG-ODN.

Cell viability after stimulation with 1 μg CpG-ODN NPs from 1-4 hours was measured using Calcein AM viability dye. Values expressed as mean ± S.D, n=3.

In contrast, MitoTracker Green FM viability dye produced significantly different viability results. After 4 hours of stimulation, all formulations maintained high mitochondrial activity and had near 100% viability similar to untreated cells and cells stimulated with naked CpG-ODN (Figure 41). At 4 hours, the viability measured using Calcein AM showed that cells treated with G_{12}L-NPs appear to have higher viability in comparison to both BG_{12}L-NPs, although the overall viability was low for all formulations.

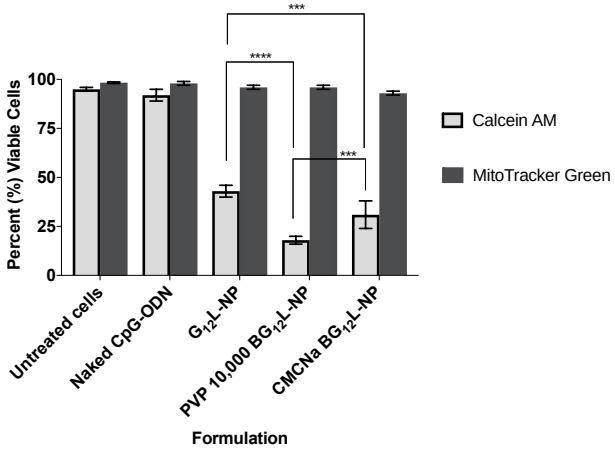

Figure 41 Comparison of cell viability measured by Calcein AM and MitoTracker Green FM viability dyes after 4 hours stimulation with G_{12}L-NP and BG_{12}L-NP formulations

Viability of HD11 chicken macrophages after 4 hours of stimulation with G_{12}L-NPs and BG_{12}L-NPs complexed with 1 μg CpG-ODN was measured using two different viability dyes: MitoTracker Green FM and Calcein AM. Viability was measured immediately after stimulation. Values expressed represent mean ± S.D. (n=3). Statistically significant differences between experimental groups were determined by two-way ANOVA with Tukey's multiple comparison test. Statistics were performed between untreated cells and cells dosed with NP formulations, where ****$p < 0.0001$, ***$p < 0.001$.

The viability of HD11 chicken macrophages was also measured 24 hours after initial dosing, to determine whether cells maintained overall health while processing CpG-ODN. Additionally, the viability of cells transfected with blank NP formulations without CpG-ODN was measured after 24 hours after initial dosing.

Once again G_{12}L-NPs and BG_{12}L-NPs in both excipients (PEG400 and PG) maintained high mitochondrial activity comparable to cells stimulated with naked CpG-ODN and untreated cells. They all maintained a viability above 95% (Figure 42 A,B). The same viability was also maintained when cells were stimulated with blank G_{12}L-NPs and BG_{12}L-NPs.

However, when measuring cell viability as a function of cell permeability and activity using calcein AM, the viability of the cells stimulated with naked CpG-ODN, G_{12}L-NPs, and BG_{12}L-NPs was around 50% after 24 hours unlike untreated cells which maintained near 100% viability (Figure 42 C,D). In contrast, cells transfected with blank NPs had lower viability (<20%) than CpG-ODN NP formulations and naked CpG-ODN for all formulations (Figure 42 C,D).

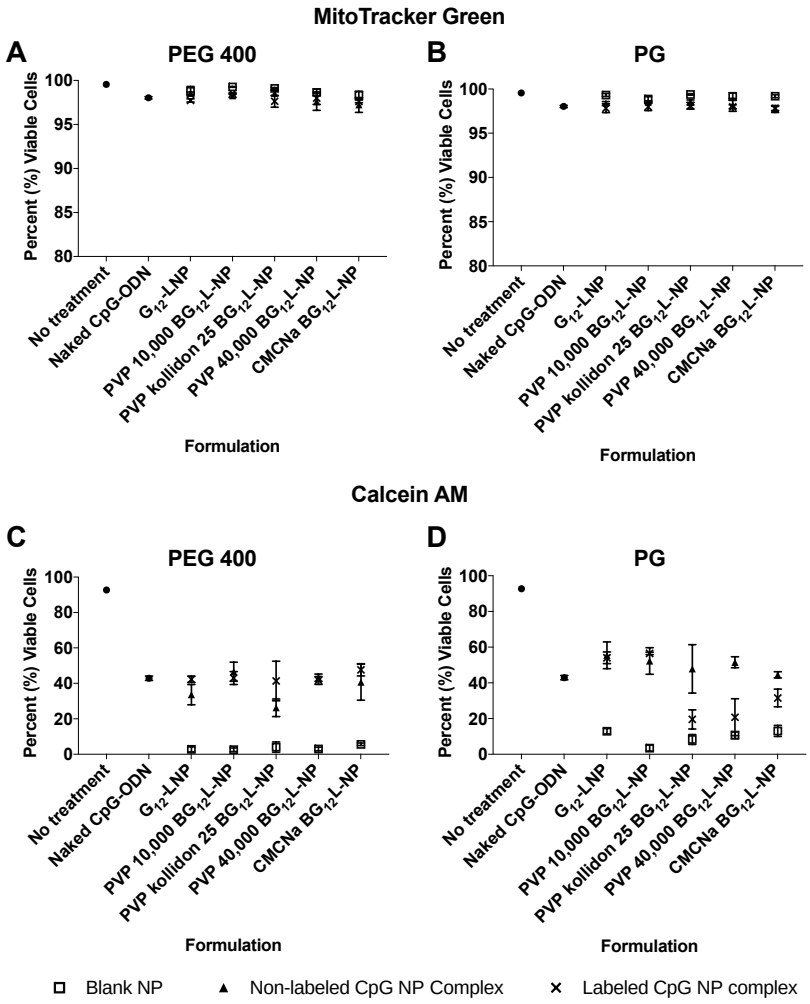

Figure 42 Comparison of viability in HD11 macrophages stimulated with G_{12}L-NPs, BG_{12}L-NPs, and blank NP formulations measured by two mechanistically different viability dyes 24 hours post stimulation.

Viability of HD11 cells measured by MitoTracker green (A, B) was compared to HD11 cell viability measured by calcein AM (C, D). 1 μg CpG-ODN was used to stimulated all samples for 2 hours. Viability was measured 24 hours post stimulation. Values expressed represent mean ± S.D. (n=3).

4.5.2.2 HD11 cell viability after transfection with G-NPs

Due to possible transient membrane changes resulting from NP transfection, mitochondrial activity was used to monitor cell viability for subsequent formulations. After transfection with G-NPs and gemini micelles (blank NP), cells showed near 100% viability 24 hours after initial cell dosing (Figure 43).

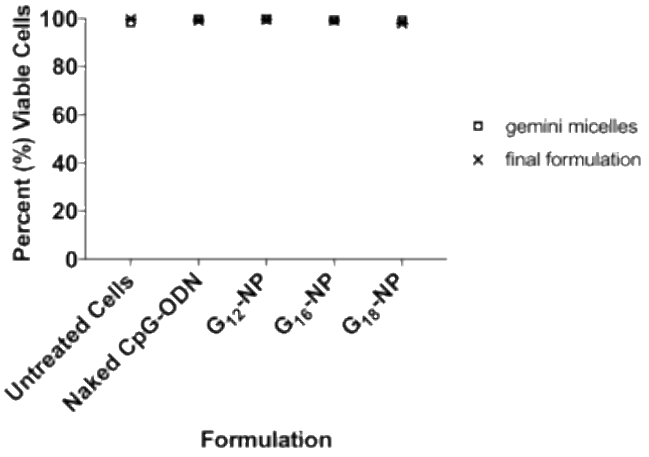

Figure 43 Evaluation of HD11 cell viability 24 hours after transfection with G-NPs and blank gemini NPs by mitochondrial activity.

Cells were dosed with NP formulations complexed with 1µg CpG-ODN for 2 hours. Cell viability was measured 24 hours post dosing using MitoTracker Green FM viability stain. Values are expressed as mean ± S.D. (n=3).

4.5.2.3 HD11 cell viability after transfection with C-NPs

After transfection with C-NPs no difference in viability was observed in comparison to untreated cells and naked CpG-ODN (Figure 44). Neither MW of chitosan were harmful to cells.

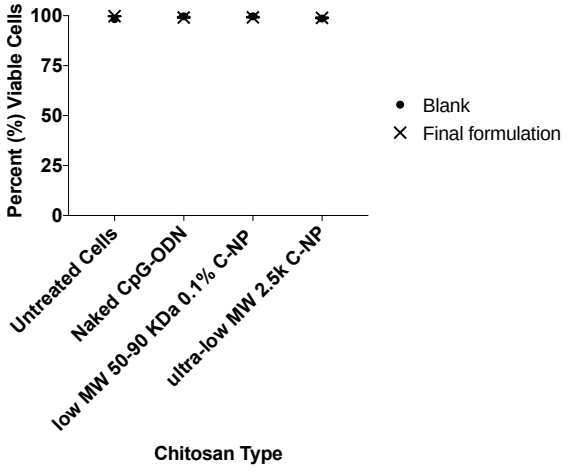

Figure 44 Evaluation of HD11 cell viability 24 hours after transfection with C-NPs and blank chitosan solution by mitochondrial activity.

Cells were dosed with NP formulations complexed with 1µg CpG-ODN for 2 hours. Cell viability was measured 24 hours post dosing using MitoTracker Green FM viability stain. Values are expressed as mean ± S.D. (n=3).

4.5.2.4 HD11 cell viability after transfection with CG-NPs

Similar to the other NPs, all CG-NPs were compatible with HD11 macrophages with approximately 100% viability 24 hours post stimulation similar to naked CpG-ODN and untreated cells (Figure 45 A-C). Chitosan concentration or gemini tail length did not significantly alter the percentage of viable cells. Cells dosed with blank NP formulations also maintained near 100% viability.

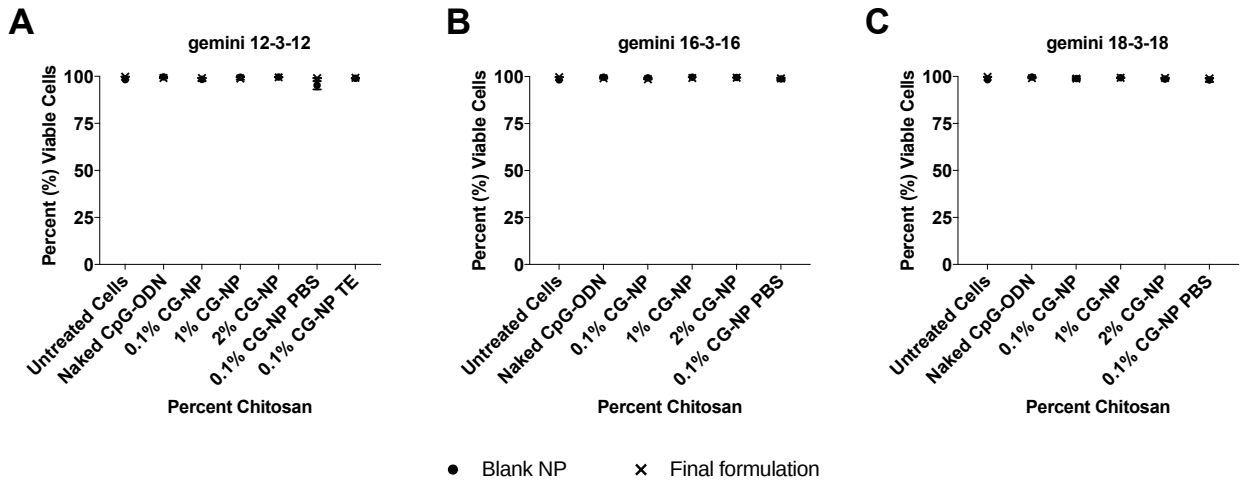

Figure 45 HD11 cell viability 24 hours after transfection with CG-NPs and blank CG-NP formulations

Cells were dosed with NP formulations complexed with 1µg CpG-ODN for 2 hours. Cell viability was measured 24 hours post dosing using MitoTracker Green FM viability stain. Values are expressed as mean ± S.D. (n=3).

4.5.2.5 HD11 cell viability after transfection with CL-NPs

Unlike other formulations, CL-NPs were very toxic to HD11 cells. A low percentage of the cell population had mitochondrial activity at 2 and 24 hours post dosing in comparison to untreated cells and cells transfected with naked CpG-ODN (Figure 46A). In fact, the flow cytometry scatter data revealed a high density of cells having lower cell forward and side scatter, as well as a dramatic increase in the number of events indicative of a high presence of cellular debris (Figure 46B).

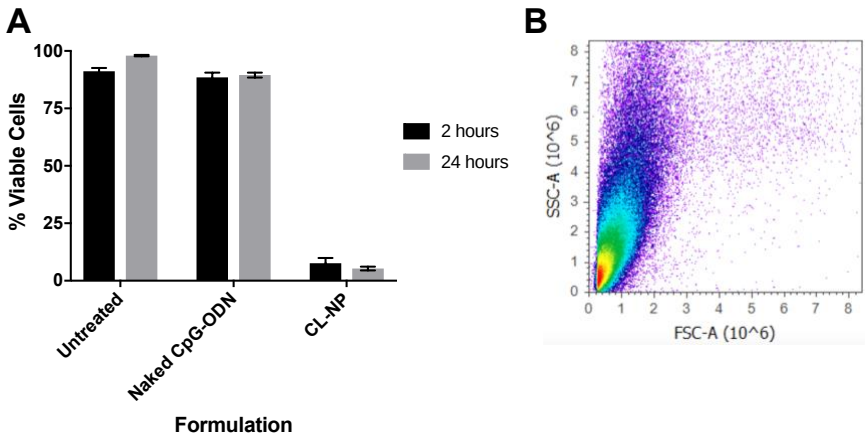

Figure 46 HD11 cell viability 2 and 24 hours after transfection with CpG-ODN CL-NPs

Cells were dosed with NP formulations complexed with 1µg CpG-ODN for 2 hours. Cell viability was measured directly after dosing (2 hours) and 24 hours post dosing using MitoTracker Green FM viability stain. Values are expressed as mean ± S.D. (n=3).

4.5.3 Particle uptake assessment using flow cytometry light scatter

Transfection of HD11 cells with NP formulations directly changed cellular complexity and size when measured for scatter. Forward scatter (FSC) is a measure of overall cell size while side scatter (SSC) can provide information on internal cellular structures and cell complexity (granularity) [204]. Cell populations with decreased FSC and SSC (closer to the bottom left corner of a scatter plot) often comprise debris and dead necrotic cells.

Since SSC can give an insight into cellular toxicity following particle uptake, changes in SSC between different formulations were compared. After cellular uptake of all formulations including naked CpG-ODN, there was an increase in SSC in comparison to untreated cells (Figure 47). An increase in SSC has been shown to enhance light reflection and refraction correlated with protein crosslinking and nuclear/cytoplasmic, which could indicate cellular apoptosis [205]. However, increase in SSC has also been associated with changes in light reflection caused by particle uptake [204]. Unlike G-NPs, G_{12}L-NPs, and BG_{12}L-NPs, CG-NP formulations resulted in more similar FSC to naked CpG-ODN, but an increase in SSC, which could reflect this particle uptake phenomenon in a more viable cell population.

Most formulations also resulted in a decrease in FSC of the HD11 cell population, prominently seen after G-NP transfection (Figure 47 D, E). The increase in chitosan

concentration of CG_{12}-NPs, CG_{16}-NPs, and CG_{18}-NPs from 0.1 – 2 % also appears to shift an increasing percentage of the cell population to the left as a result of lower FSC (Figure 47 I, L, O).

Transfection of cells with G_{12}L-NPs and BG_{12}L-NPs also resulted in a dramatic change in cell scatter. Cells transfected with G_{12}L-NPs had decreased FSC similar to G-NPs, and CG-NPs (Figure 47P). However, the addition of the biopolymer coating corresponding to PVP 10,000 BG_{12}L-NPs and CMCNa BG_{12}L-NPs appeared to result in a larger proportion of the cell population with increased SSC without the decrease in FSC in comparison to cells transfected with G_{12}L-NPs (Figure 47 Q, R).

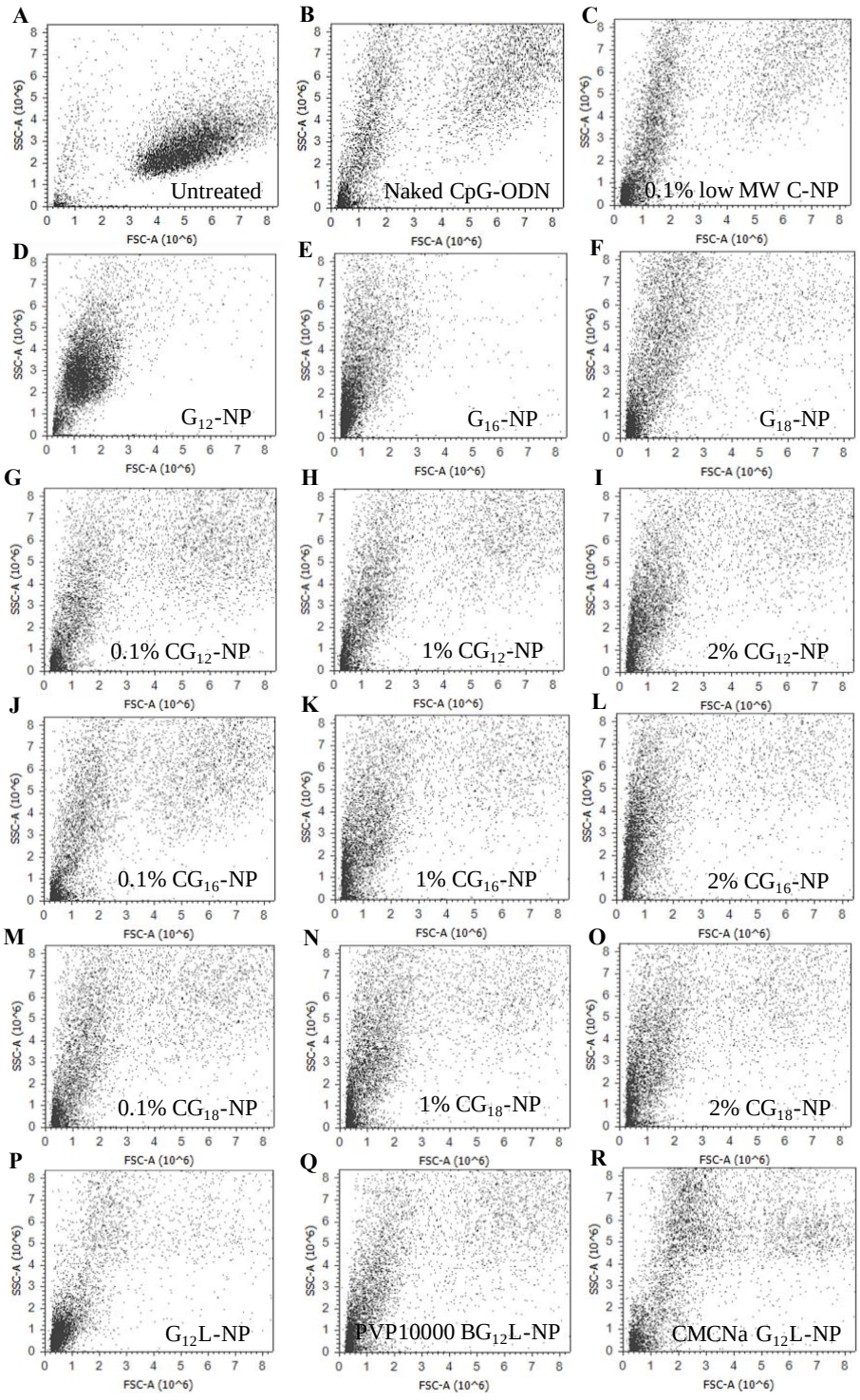

Figure 47 Flow cytometry scatter plots of HD11 chicken macrophages 24 hours post stimulation with C-NPs, G-NPs, CG-NPs, G_{12}L-NPs, and BG_{12}L-NPs.

Comparison of the change in cell scattering following naked CpG-ODN and NP uptake 24 hours post stimulation in HD11 chicken macrophages. Figures A-F show scattering of untreated, naked CpG-ODN, G-NPs, and C-NPs. Figures G-O show the scattering of CG-NPs with increasing chitosan concentration, and P-R represent scattering after G_{12}L-NP and BG_{12}L-NP uptake. 15,000 events are shown in each plot.

Interestingly, there were differences between some of the cell populations treated with blank NP formulations (without CpG-ODN). After transfection with blank 0.1% C-NP, cells looked very similar to untreated cells (Figure 48 C). For G-NP formulations, G_{12}-NP and G_{16}-NP treatment decreased SSC (Figure 48 D, E) while G_{18}-NP had no effect on SSC (Figure 48 F).

Chitosan concentration of blank CG-NP particle formulations did not affect FSC and SSC in comparison to untreated cells. However, blank gemini 12-3-12 formulations (G_{12}-NPs), generated a cell population highly concentrated towards the lower left corner of the grid (Figure 48 G, H, I).

The FSC and SSC profile in cells transfected with blank G_{12}L-NPs and BG_{12}L-NPs resulted in changed in scatter depending on the biopolymer used. Both G_{12}L-NPs and CMCNa BG_{12}L-NPs resulted in a cell population with decreased FSC. At the same time, the presence of a cell population having higher SSC while maintaining similar FSC corresponding to C-NPS, and CG-NPs was lost (Figure 48 P, R). However, cells transfected with PVP 10,000 BG_{12}L-NPs provided a similar scatter profile to untreated cells and CG-NPs (Figure 48 Q).

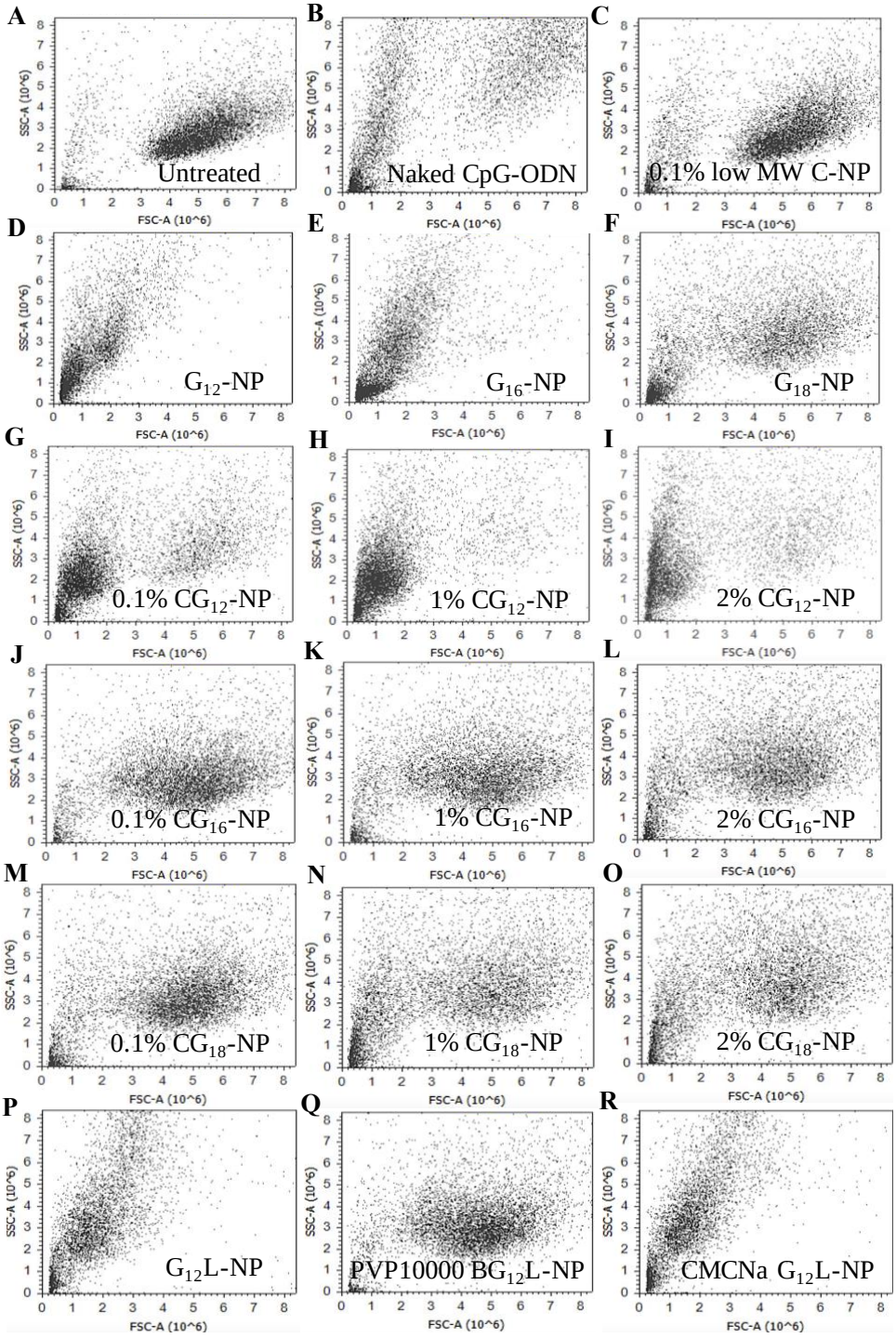

Figure 48 Flow cytometry scatter plots of HD11 chicken macrophages 24 hours post stimulation with blank C-NPs, G-NPs, CG-NPs, G_{12}L-NPs, and BG_{12}L-NPs.

Comparison of the change in cell scattering following naked CpG-ODN and blank NP uptake 24 hours post stimulation in HD11 chicken macrophages. Figures A-F show scattering of untreated, naked CpG-ODN, G-NPs, and C-NPs. Figures G-O show the scattering of CG-NPs with increasing chitosan concentration, and P-R represent scattering after G_{12}L-NP and BG_{12}L-NP uptake. 15,000 events are shown in each plot.

4.6 Effect of nebulization on particle characteristics and *in vitro* performance

Selected formulations based on CpG-ODN uptake, ease and reproducibility of formulation, were tested *in vitro* after nebulization and compared to non-nebulized formulations. Nebulization had no effect on particle characteristics as the average hydrodynamic diameter and zeta potential were very similar before and after nebulization for all formulations (Figure 49 A, B). The *in vitro* performance of nebulized formulations was also similar with respect to CpG-ODN uptake, nitrite production, and viability at 2 and 24 hours in comparison to non-nebulized formulations (Figure 49 C-H).

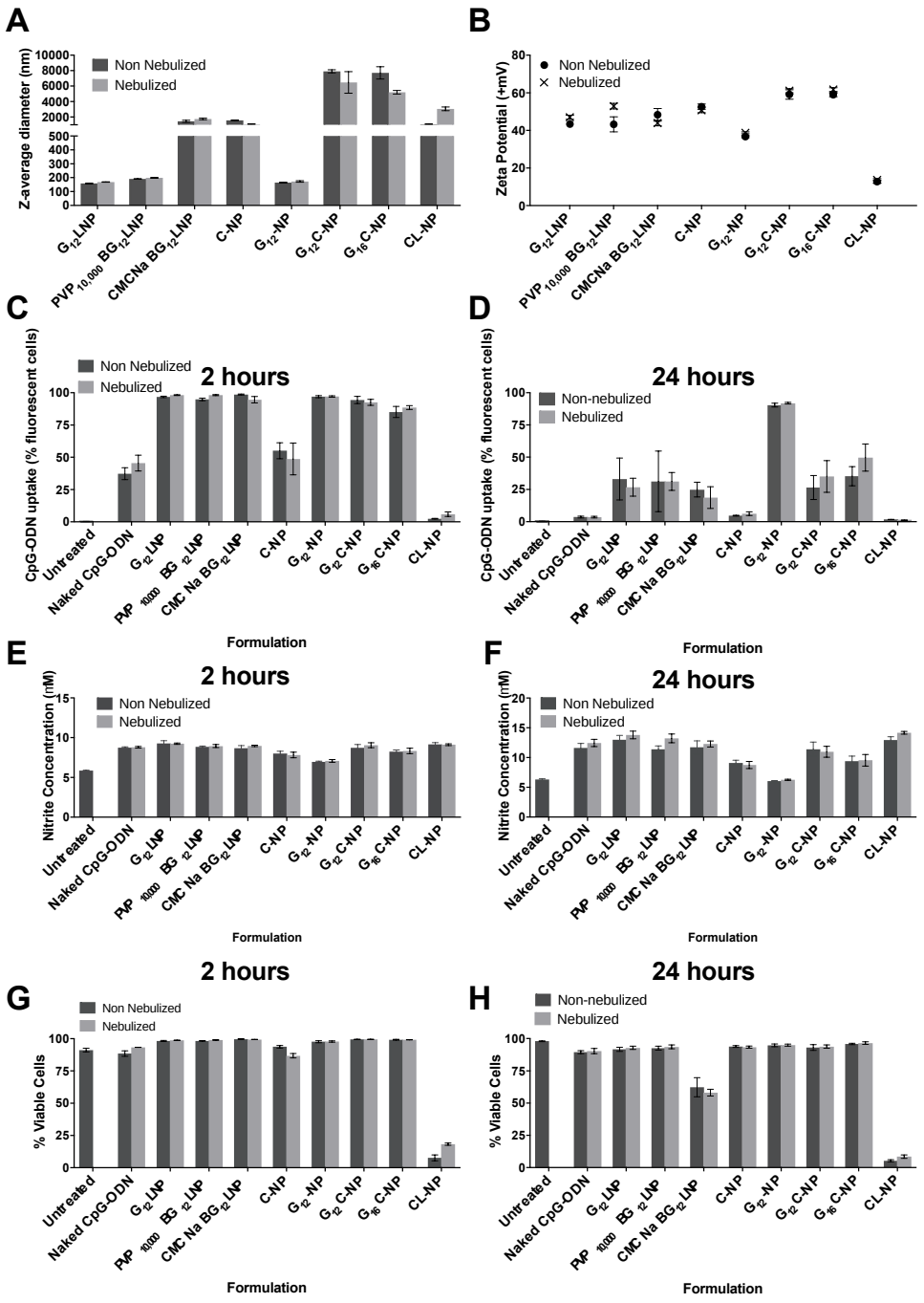

Figure 49 Effect of nebulization on physicochemical characteristics and performance of NP formulations.

NP formulations were nebulized with a compressor nebulizer and subsequently collected for characterization and testing *in vitro* in HD11 cells. Differences in Z-average hydrodynamic diameter size (A), zeta potential (B) and effect on CpG-ODN uptake (C, D), nitrite production (E, F), and viability (G, H) in HD11 cells were compared to non-nebulized formulations. Effects nebulization on CpG-ODN uptake, nitrite production, and viability were measured 2 hours post dosing and 24 hours post dosing. Values expressed represent mean ± S.D., n=3.

4.7 Cellular CpG-ODN localization post transfection

The localization of Alexa Fluor 647 labeled CpG-ODN during transfection of HD11 cells was tracked by confocal microscopy immediately after dosing for 2 hours (Figure 50), and 24 hours after dosing (Figure 51). Cells were labeled with Vybrant™ green Dil cell membrane dye (green) in order to determine whether CpG-ODN was membrane bound or intracellular.

Two hours after transfection with naked CpG-ODN (pink) it was evident that the CpG-ODN was surrounding the cell membrane. However, cells transfected with G_{12}L-NPs and BG_{12}L-NPs showed CpG-ODN bound to the cell membrane and inside the cells. G_{12}-NPs and CG_{12}-NPs show CpG-ODN also interacting with the cell membrane, but no CpG-ODN was visible within the cytoplasm of the cells, as opposed to G_{12}L-NP and BG_{12}L-NP treated cells, which showed intracellular CpG-ODN. After treatment with each of these NPs, cell morphology noticeably changed. Transfection with the CL-NP formulation was the most toxic to cells, as a significant amount of cellular debris was present after 2 hours of dosing. These morphological observations were consistent with the results of flow cytometry which detected an increase in cellular debris and changes in cell size and granularity.

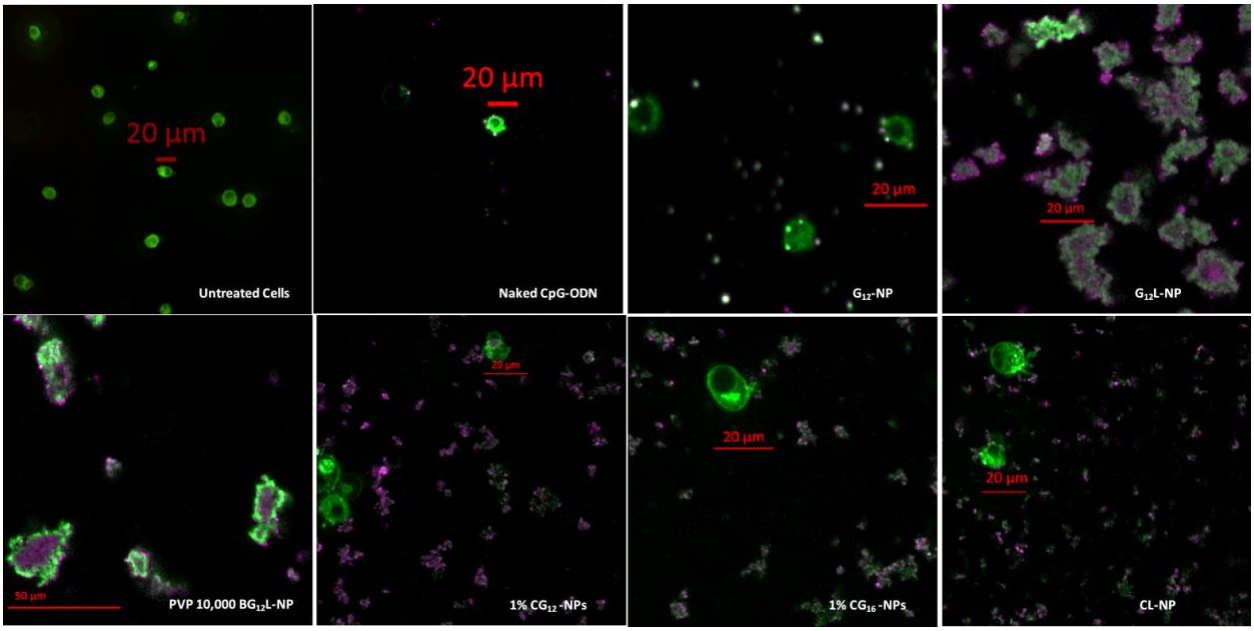

Figure 50 Localization of CpG-ODN uptake in HD11 cells transfected with naked CpG-ODN and NP formulations 2 hours post dosing

HD11 cells were transfected with NPs containing Alexa Fluor 647 labelled CpG-ODN for 2 hours. Cell membrane was stained with Vybrant™ green Dil for localization (green). Images were taken immediately after 2-hour dosing and evaluated for presence of red fluorescence resulting from CpG-ODN (pink).

Twenty-four hours after initial dosing, CpG-ODN was intracellularly located with all NP formulations (Figure 51). The confocal microscopic images confirm intracellular CpG-ODN uptake and reveal that the cells recovered from the initial toxic effects at the 2-hour time point (see Figure 50, versus Figure 51). Additionally, the G_{12}-NP formulation appears to result in the most significant amount of CpG-ODN retention. In G_{12}-NP treated cells, CpG-ODN is present throughout the cellular cytoplasm in comparison to other formulations and naked CpG-ODN, which had only concentrated areas of CpG-ODN within the cytoplasm.

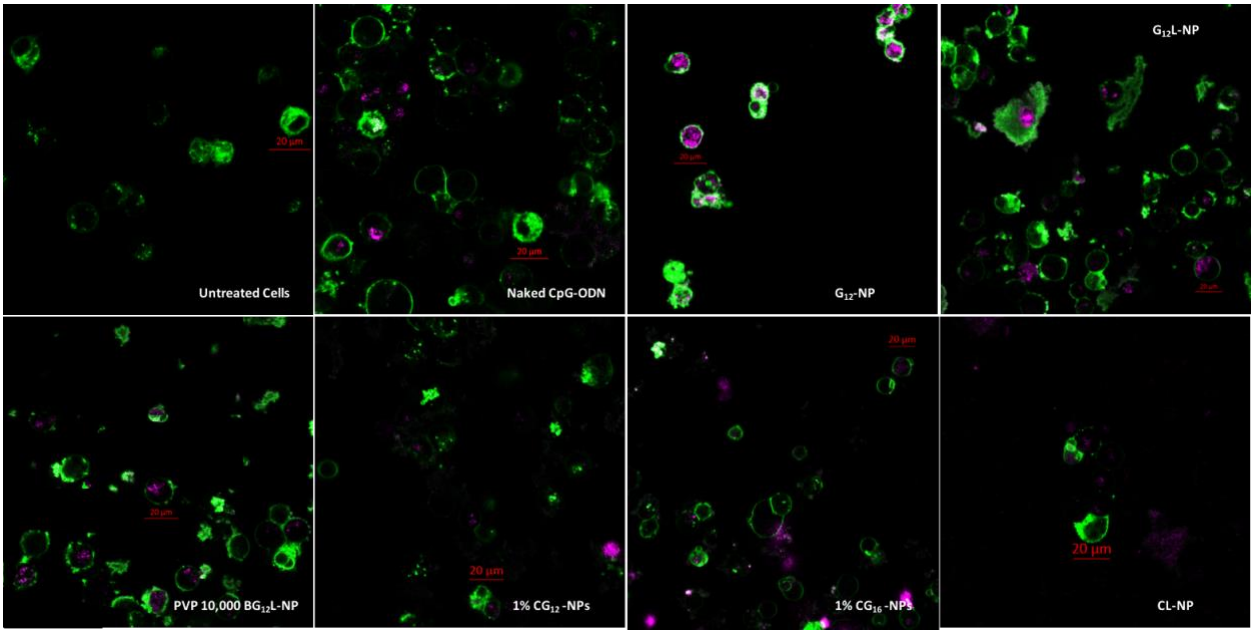

Figure 51 Localization of CpG-ODN uptake in HD11 cells transfected with naked CpG-ODN and NP formulations 24 hours post dosing.

HD11 cells were transfected with NPs containing Alexa Fluor 647 labelled CpG-ODN for 2 hours. Cell media was replaced and cell membrane was stained with Vybrant™ green Dil for localization 24 hours later (green). Images were taken 24 hours post dosing and evaluated for presence of red fluorescence resulting from CpG-ODN (pink).

4.8 *In vivo* biodistribution of CpG-ODN NP formulations versus naked CpG-ODN solution

NPs were selected for *in vivo* evaluation based on physicochemical properties and *in vitro* data. One formulation from each different type of NP was evaluated with the exception of C-NPs, since they were inferior to G-NPs, G_{12}L-NPs, BG_{12}L-NPs, and CG-NPs based on CpG-ODN uptake and retention *in vitro* studies. The formulation from each group was chosen based on colloidal stability, ease of formulation, and highest retention, and uptake.

Two separate biodistribution experiments were performed over the course of this work. In the first set of experiments the biodistribution of G_{12}L-NP and BG_{12}L-NP formulations after 2 hours of NP administration in the chick respiratory tract were compared. Since G_{12}L-NPs and PVP 10,000 BG_{12}L-NPs in PEG 400 excipient were the most uniform, had > +40mV zeta potential, were stable over a 20-day period, reproducible, and increased uptake and retention of CpG-ODN, they were chosen for biodistribution in chick lungs. The objective of the first experiment was to determine the extent of short term biodistribution (2 hours post nebulization)

in different areas of the chick respiratory tract. Formulations were tagged with NBD-PC lipid for detecting NP distribution. Serial cross sections along the chick respiratory tract were cut and examined for evidence of NP deposition. After two hours of dosing, particles (green) could be identified in the tracheal epithelium near the lumen (Figure 52). Particles were also present in the top of the lung cranially located near the lumen primary bronchi in the cranial lung (Figure 52). Here, distinct cluster areas of fluorescence were present. Towards the middle of the lung, distinct areas of fluorescence were seen among the bronchi. Sections caudally located in the lung were also examined for evidence of particle deposition, although minimal particle deposition was observed. A summary of areas of the lung were particles were located is shown in Table 27.

Section	Nanoparticle Type	Time Point (minutes)	Area of particle deposition	Total Number of Images	# of times present	# of birds it occurred in/ total # birds analyzed
Tracheal bifurcation	Saline Control	120	no immediate signs	10	5	2/2
	Saline Control	120	some signs of autofluorescence, some chondrocyte cell structures (stained images)		2	1 (bird control 2)
	PVP 10,000 BG_{12}L-NP	15	chondrocytes within trachea	20	16	5/5
	PVP 10,000 BG_{12}L-NP	15	mucosal lining of trachea near lumen		1	2/5
	PVP 10,000 BG_{12}L-NP	120	chondrocytes within trachea	27	15	4/5
	PVP 10,000 BG_{12}L-NP	120	mucosal lining of trachea near lumen		6	2/5
	G_{12}L-NP	15	chondrocytes within trachea	18	13	4/5
	G_{12}L-NP	15	mucosal lining of trachea near lumen		2	3/5
	G_{12}L-NP	120	chondrocytes within trachea	16	8	4/5
	G_{12}L-NP	120	mucosal lining of trachea near lumen		3	3/5
Top Lung	Saline Control	120	no immediate signs	17	12	2/2
	Saline Control	120	some signs of autofluorescence (diffuse)		5	2/2 (only in bird control 2 top lung section 1)
	PVP 10,000 BG_{12}L-NP	15	within primary bronchus tissue	17	12	3/5
	PVP 10,000 BG_{12}L-NP	15	within lung tissue		3	
	PVP 10,000 BG_{12}L-NP	120	within primary bronchus mucosal tissue	24	22	3/5
	G_{12}L-NP	15	Primary bronchus (diffuse fluorescence)	11	9	3/5
	G_{12}L-NP	120		13	12	1/4
Mid lung	Saline Control	120	no immediate sign, faint autofluorescence	7	7	2/2
	PVP 10,000 BG_{12}L-NP	15	tissue between bronchi (scattered)	7	5	4/5
	PVP 10,000 BG_{12}L-NP	120	fluorescent areas near bronchi lumen	21	20	3/5
	G_{12}L-NP	15	lung tissue near bronchi/parabronchi? (scattered/diffuse)	23	12	2/5
	G_{12}L-NP	15	lung tissue near bronchi/parabronchi? (localized)		10	3/5
	G_{12}L-NP	120	lung tissue near bronchi/parabronchi? (scattered/diffuse)	14	9	2/5
	G_{12}L-NP	120	lung tissue near bronchi/parabronchi? (localized)		7	3/5
Lower Lung	Saline Control	120	no immediate signs	22	18	1/1
	PVP 10,000 BG_{12}L-NP	15	fluorescent areas near bronchi lumen (very faint, rare)	13	4	1/2
	G_{12}L-NP	15	autofluorescence?	1	1	1/1
	G_{12}L-NP	120	lung tissue near bronchi/parabronchi? (scattered/diffuse)	1	1	1/1

Table 27 Summary of evidence of particle distribution in the respiratory tract of day old chicks post nebulization with G_{12}L-NPs and PVP 10,000 BG_{12}L-NPs

Lung sections of birds were imaged using CLSM. Particles were labelled with fluorescent NBD-PC lipid tag for detection in the respiratory tract. Description of observations are outlined.

After evidence of NP deposition within different areas of the chick respiratory tract, the main objective of the second biodistribution experiment was to better identify interactions between NP and CpG-ODN association once in the biological lung environment. Formulations with dual labelling of CpG-ODN and the polymer/lipid component of the NP were formulated: G_{12}-NPs of which only CpG-ODN was labelled (red); 1% CG_{12}-NP and 1% CG_{16}-NP formulations that contained labelled chitosan to tag the NP (green) and labelled CpG-ODN (red); and labelled naked CpG-ODN (red). Tissues were screened for NP and CpG-ODN co-localization at 2 hours post administration. Sections were cut longitudinally along the chick lung so that the top face of the section represented the cranial lung and the bottom the caudal lung. All images are representative of sections toward the longitudinal middle of the lung near the primary bronchi (Figure 53). Alexa Fluor 647 labelled CpG-ODN (red) could be detected in distinct patterns along the airspaces of the lung. Naked CpG-ODN appeared to have an even distribution throughout the longitudinal face of the lung with accumulation of CpG-ODN near the lumen of the air spaces. Birds nebulized with 1% CG_{16}-NPs also displayed a similar distribution pattern to naked CpG-ODN with signs of CpG-ODN nearer to the cranial face of the lung.

Birds nebulized with 1% CG_{12}-NPs had NPs present nearer to the caudal region of the lung, but less accumulation was found in comparison to 1% CG_{16}-NPs. Furthermore, evidence of particle and CpG-ODN co-localization existed in 1% CG_{12}-NPs whereas free CpG-ODN seemed to have been released in sections of birds nebulized with 1% CG_{16}-NPs. As the gemini component of G_{12}-NPs cannot be labelled, only CpG-ODN was labelled in this formulation. Limited CpG-ODN deposited in the sections observed, and there was a high degree of green auto-fluorescence present in these sections, which resulted in appearance of yellow particles.

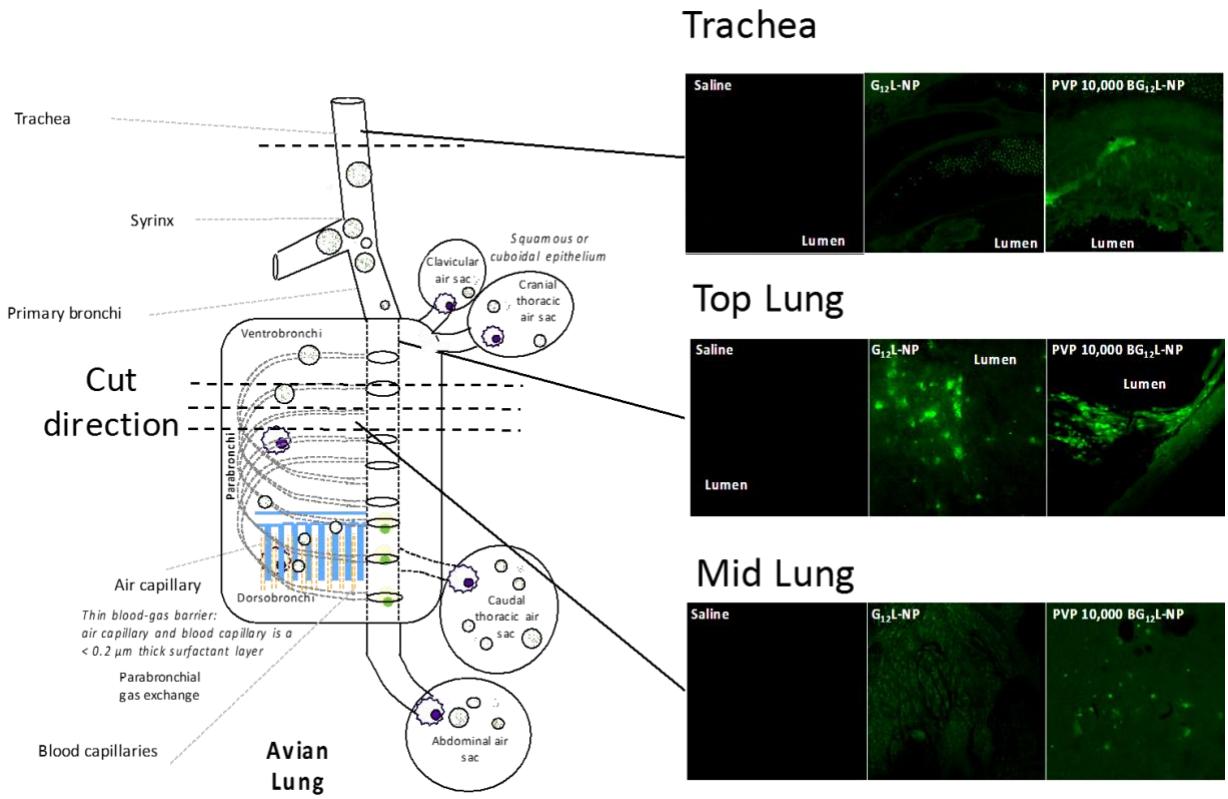

Figure 52 Biodistribution of G_{12}L-NPs and PVP 10,000 BG_{12}L-NPs in the respiratory tract of 1-day old chicks 2 hours post nebulization

1-day old chicks were nebulized in a chamber for 15 minutes with selected NP formulation. Respiratory tract tissues including the trachea and lung were isolated 2 hours post nebulization. NP formulations were labeled with NBD-PC lipid (green).

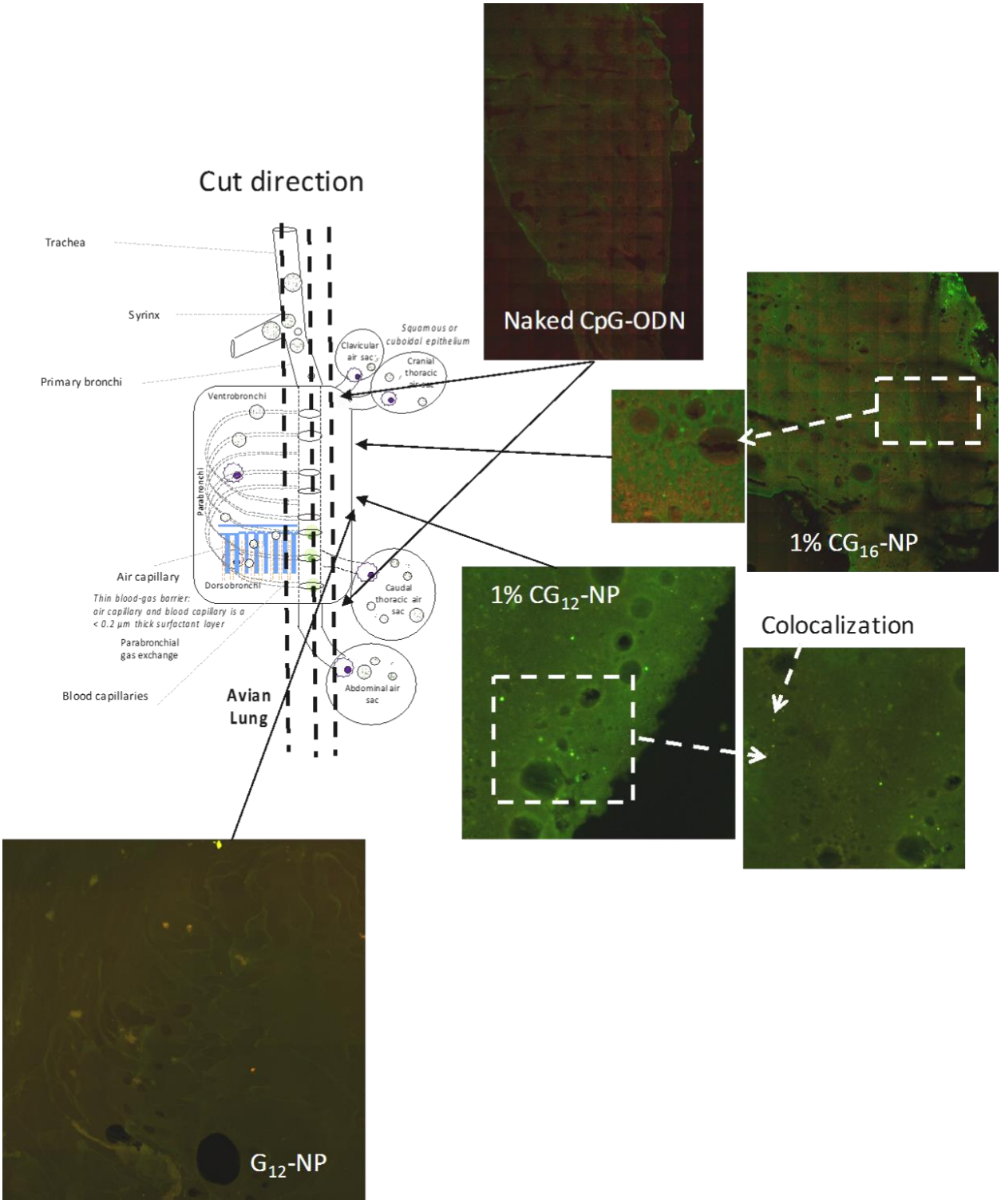

Figure 53 Biodistribution of naked CpG-ODN, G_{12}-NPs, 1% CG_{12}-NPs and PVP 10,000 $BG_{12}L$-NPs in the respiratory tract of 1-day old chicks 2 hours post nebulization

1-day old chicks were nebulized in a chamber for 15 minutes with corresponding NP formulation. The chick lung was isolated 2 hours post nebulization. NP formulations were labeled with FITC-chitosan (green) and Alexa Fluor 647 CpG-ODN (red).

4.9 Evaluation of protection against *E. coli* challenge

NP formulations that were able to elicit innate immune activation, i.e. retain the highest *in vitro* uptake after 24 hours of dosing, and maintain reproducible formulation characteristics were chosen to evaluate the extent of protection in 1-day old chicks. Over the course of this work, several *in vivo* experiments were conducted to evaluate formulations in a step by step manner (Figure 54). Data shown is the result of combined challenge with high and low *E. coli* dose for clarity.

In the first experiment, the effect of gemini-tail length on BGL-NPs efficacy was evaluated. BGL-NPs constructed with gemini 12-3-12 and 16-3-16 resulted in 90% survival and reduced combined clinical score, whereas naked CpG-ODN and gemini 18-3-18 BGL-NPs produced about 75% survival rate. The saline control was at a 40% survival rate using a 2-day post-treatment challenge protocol (Figure 54 A).

In the next experiment, the biopolymer of BGL-NPs was evaluated. Both PVP and CMCNa polymers had similar effects in improving survival and clinical score compared to naked CpG-ODN and saline control (60% survival for each polymer group vs. 40% for naked CpG-ODN and saline, respectively) (Figure 54 B). These survival scores are lower compared to the first experiment, which is attributed to the timing of the challenge (3 days vs 2 days post-treatment in the previous experiment).

Given enhanced retention, G_{12}-NPs, 1% CG_{12}-NPs, and 1% CG_{16}-NPs were also tested for their ability to improve bird survival after infection. All three NP formulations were able to enhance bird survival in comparison to the saline control (Figure 54 C). The effect of gemini tail length of 1% CG-NPs on percent survival was not significant (both about 65% survival rate). In comparison, G_{12}-NPs provided about 80% survival rate. However, this was similar to naked CpG-ODN using a 2-day post-treatment challenge protocol. The saline control was at a 40% survival rate.

The final protection experiment had two objectives. The first, was to test whether NP formulations would increase the length of time that CpG-ODN was effective. The second, was to evaluate which NP formulation (G_{12}-NPs, 1% CG_{12}-NP, PVP 10,000 $BG_{12}L$-NP) would result in higher bird survival rates. Birds treated with G_{12}-NPs had somewhat higher percent survival and lowest cumulative clinical score in comparison to other formulations (Figure 54 D). However,

this was not significantly different from the PVP 10,000 BG_{12}L-NP or naked CpG-ODN. Interestingly, the distilled water control also showed high survival similar to birds treated with G_{12}-NPs and higher than birds treated with naked CpG-ODN, therefore this experiment is inconclusive.

A

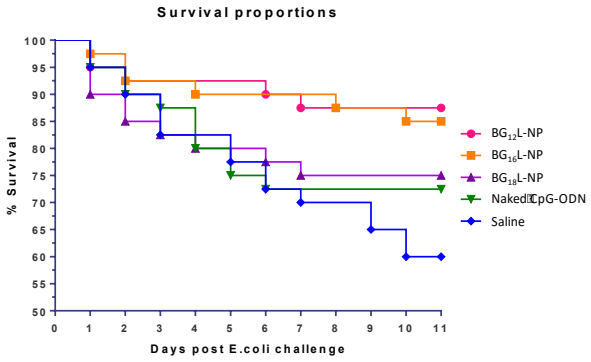
Survival proportions
% Survival
Days post E.coli challenge
BG12L-NP
BG16L-NP
BG18L-NP
Naked CpG-ODN
Saline

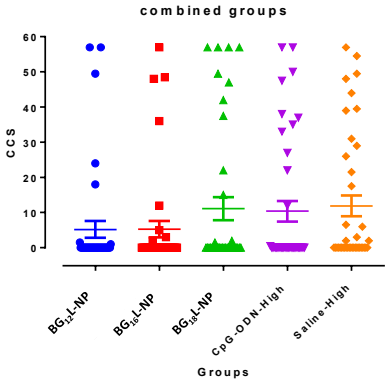
combined groups
CCS
BG12L-NP
BG16L-NP
BG18L-NP
CpG-ODN-High
Saline-High
Groups

B

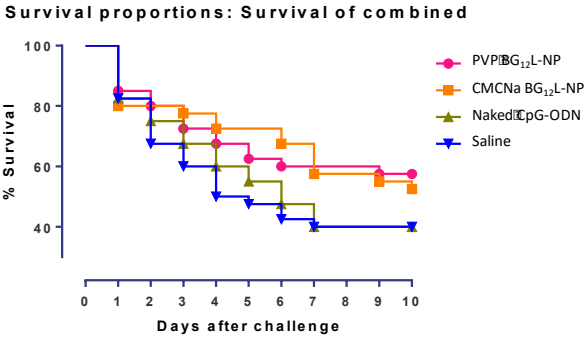
Survival proportions: Survival of combined
% Survival
Days after challenge
PVP BG12L-NP
CMCNa BG12L-NP
Naked CpG-ODN
Saline

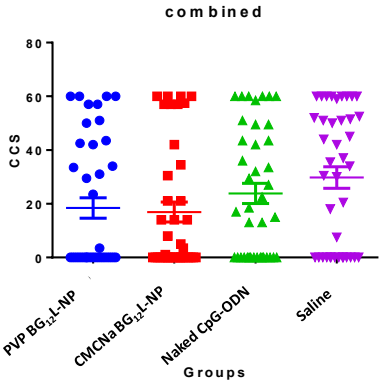
combined
CCS
PVP BG12L-NP
CMCNa BG12L-NP
Naked CpG-ODN
Saline
Groups

C

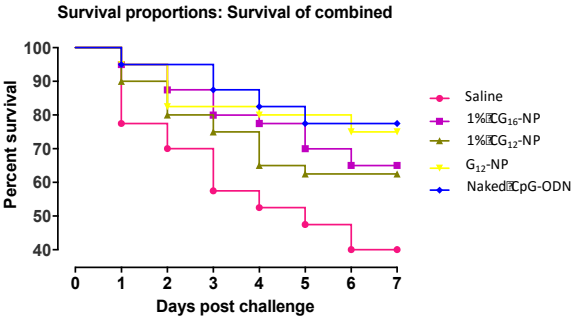
Survival proportions: Survival of combined
Percent survival
Days post challenge
Saline
1% CG16-NP
1% CG12-NP
G12-NP
Naked CpG-ODN

D

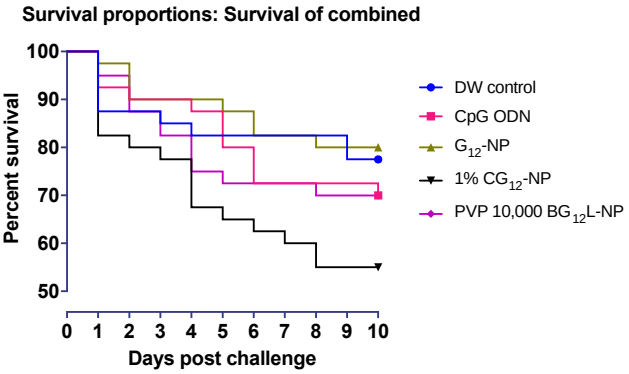
Survival proportions: Survival of combined
Percent survival
Days post challenge
DW control
CpG ODN
G12-NP
1% CG12-NP
PVP 10,000 BG12L-NP

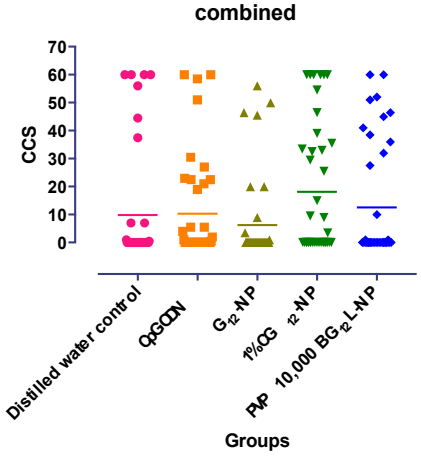
combined
CCS
Distilled water control
CpG ODN
G12-NP
1% CG12-NP
PVP 10,000 BG12L-NP
Groups

Figure 54 *In vivo* protection of neonatal chicks from E. coli challenge after intrapulmonary treatment with CpG-ODN in various NP delivery systems. Protection was evaluated by measuring chick survival and monitoring clinical signs (combined clinical score, CCS). The in vivo screening selected delivery systems are shown. NP formulations were nebulized with Medpro compressor nebulizer to groups of 1-day old chicks followed by challenge with E. coli. Over time the protocol underwent some modifications to reflect the knowledge learned from previous experiments. These improvements are indicated within each experimental description below.

A) Screening of BGL-NPs to compare the effect of gemini structure on efficacy. Gemini surfactants 12-3-12, 16-3-16 and 18-3-18 were evaluated with PVP Kollidon 25 as the biopolymer. Neonatal broiler chicks were given CpG-ODN solution or NP formulations by nebulization at the age of day 1. Chicks were challenged with two lethal doses of *E. coli* 2 days post CpG-ODN administration. Data were collected on daily mortality, bacteriological scoring and daily clinical scoring. CpG-ODN dose was 100µg/ 100µL/bird; n=40; challenge was performed with *E. coli* $1X10^5$CFU/ bird on Day 2 after treatment.

B) Screening of BGL-NPs to compare the effect of two different biopolymers on efficacy. Gemini surfactants 12-3-12 with two different biopolymers (PVP and CMCNa) were evaluated. Neonatal broiler chicks were given CpG-ODN solution or NP formulations by nebulization at the age of day 1. Data were collected on daily mortality, bacteriological scoring and daily clinical scoring. CpG-ODN dose was 100µg/ 100µL/bird; n=40; challenge was performed with *E. coli* $1X10^5$CFU/ bird on Day 3 after treatment.

C) Evaluation of G-NPs (12-3-12) and 1% CG NPs prepared with gemini surfactant 12-3-12 or 16-3-16. Neonatal broiler chicks were given CpG-ODN solution or NP formulations by nebulization at the age of day 1. Data were collected on daily mortality, bacteriological scoring and daily clinical scoring. CpG-ODN dose was 100µg/ 100µL/bird; n=40; challenge was performed with *E. coli* $1X10^5$CFU/ bird on Day 2 after treatment.

D) Evaluation of G-NPs (12-3-12) and CG_{12}-NPs prepared with gemini surfactant 12-3-12 and $BG_{12}L$-NPs (12-3-12). The effect of time of challenge after administration was evaluated: *E. coli* challenge 4 days post CpG-ODN administration. Neonatal broiler chicks were given CpG-ODN solution or NP formulations by nebulization at the age of day 1. Data were collected on daily mortality, bacteriological scoring and daily clinical scoring. CpG-ODN dose was 100µg/ 100µL/bird; n=40; challenge was performed with *E. coli* $1X10^5$CFU/ bird on Day 4 after treatment.

Chapter 5: Discussion

In the fields of drug, DNA, and protein delivery, NPs have continually shown to improve cellular uptake, improve the biological stability of their cargo, and improve delivery to the therapeutic target site [24]. Based on previous work in this laboratory, gemini NP delivery systems have improved DNA delivery *in vitro* and *in vivo* in comparison to naked DNA for skin, ocular, and mucosal applications [45, 182, 184, 187, 206]. As such, a gemini NP delivery system was employed for a CpG-ODN vaccine in attempt to improve the stimulation of innate immunity and protective properties of CpG-ODN in broiler chicks against bacterial infection such as *E. coli*. Previous studies have proven that CpG-ODN is a protective vaccine against *E. coli* infection and other bacterial infections common in broilers [7, 27, 82, 96]. Moreover, the incorporation of CpG-ODN in NPs has improved the protective effects of CpG-ODN in broiler chicks *in vivo* through subcutaneous and *in ovo* routes of vaccination [14, 27]. By developing a novel gemini-biopolymer NP delivery system, it was expected that improved delivery and immune stimulation will occur in broiler chicks via the pulmonary route, a cost-effective immunization method in poultry. In fact, previous studies conducted by our group have solidified this theory and the gemini NP formulation previously tested (G_{12}L-NPs, PVP BG_{12}L-NPs) was used as a starting point of characterizing physicochemical aspects of CpG-ODN nanoparticles, and their effectiveness *in vitro* and *in vivo.* Since macrophages migrate into the chicken respiratory system upon recognition of foreign pathogens and act as antigen presenting cells to induce an innate immune response, the chicken macrophage cell line HD11 was chosen to investigate immune-stimulatory properties of the CpG-ODN NP vaccines formulated in this project.

NP modification is a popular method to improve gene delivery by lipid and polymer based NPs that have shown limited gene transfection *in vivo.* Techniques to achieve superior multifunctional NPs include chemical modification of materials, antibody/aptamer conjugation, peptide functionalization, and multi-material incorporation. This project pioneered several hybrid NP formulations made up of different classes of biocompatible materials, a much simpler method than chemical modification. Hybrid NPs in this project were tested in a chicken cellular model and evaluated for their ability to improve transfection (uptake) and innate immune stimulation of the oligonucleotide CpG-ODN in comparison to naked CpG-ODN and non-hybrid NP counterparts. For each of the 6 types of NP groups investigated (G_{12}L-NPs, BG_{12}L-NPs, G-NPs,

C-NPs, CG-NPs, CL-NPs), characterization was undertaken based on reproducibility, colloidal stability, and manufacturing capacity. In this study, PVP 10,000 BG_{12}L-NPs and G_{12}-NPs were able to successfully improve uptake of CpG-ODN in comparison to naked CpG-ODN by HD11 macrophages and improve the length of time cells were associated with CpG-ODN (retained). Moreover, the different NP groups were characterized and compared in their ability to improve transfection *in vivo*.

5.1 Characterization of nanoparticle formulations

First generation gemini surfactants (general structure *m*-*s*-*m*) with a spacer length of *s*=3 (12-3-12 and 16-3-16), have been shown previously to be effective transfection agents *in vitro* in comparison to first generation surfactants with longer spacers (n= 4-16) [206]. Since one of the goals of this project was to develop a formulation that could be easily scalable to large-batch manufacturing, gemini 12-3-12 was chosen over gemini 16-3-16 and 18-3-18 for formulation of G_{12}L-NPs and BG_{12}L-NPs due to its solubility at room temperature. The first parameter monitored was the effect of PVP biopolymer MW on the size and zeta potential of the BG_{12}L-NPs formulated in PEG400, of which a derivative had been previously tested *in vivo*. The MW of the polymer did not affect the size of the particles, and gave a relatively uniform size distribution around 200 nm. Since formulation preparation for the G_{12}L-NPs/BG_{12}L-NPs particles involved formation of blank NP vesicles prior to CpG-ODN addition, the diameter of the blank NPs was also measured prior to complexing with CpG-ODN. Once again, the polymer did not influence particle size with any of the blank NPs, all were about15-20 nm.

The most problematic formulations were the PVP Kollidon 25 BG_{12}L-NPs and CMCNa BG_{12}L-NPs. Use of these two polymers resulted in high batch to batch particle size distribution variability. Problems with formulation uniformity were most likely due to the fact that Kollidon 25 is a mixture of soluble and insoluble PVP molecules of different grades. Furthermore, CMCNa requires high shear for proper dispersion (FMC Biopolymer), which is undesirable for large scale manufacturing in comparison to the PVP 10,000 and 40,000 polymers which easily mix into solution.

Of the ten formulations tested, the G_{12}L-NP and PVP 10,000 BG_{12}L-NP formulations in PEG 400 excipient were subjected to further testing owing to reproducibility of particle size from

bath to batch. They also had a positive zeta potential (+53.2 and +42.8 mV, respectively), well above the +30 mV threshold for colloidal stability [207].

G-NPs were also tested to compare the basic micellar NP with the lipid and polymeric hybrid components (G_{12}L-NPs/BG_{12}L-NPs and CG-NPs, respectively). Interestingly, gemini 12-3-12 complexed with CpG-ODN (G_{12}-NP) resulted in NPs with similar size distribution to G_{12}L-NPs and BG_{12}L-NPs (175.2, 161.7, 173.0 nm, respectively). Increasing tail length of the gemini surfactant affected the size and zeta potential of G-NPs which has also been previously observed in plasmid-gemini complexation with a charge ratio (+/-) 10:1 [208]. Similar to plasmid-gemini complexes, an increase in zeta potential with increasing tail length of G-NPs was observed. The change was not as dramatic and all were above the +30 mV threshold. Unlike the plasmid-gemini complexation, an increase in size with increasing gemini tail length was observed with CpG-ODN oligonucleotides. However, the difference may be attributed to the 5:1 charge ratio used in this project, which is half of the charge ratio used for plasmid-gemini complexation (10:1). Once again, the gemini 12-3-12 molecule was chosen for further study due to its easy incorporation into formulations and for comparative purposes to G_{12}L-NPs and BG_{12}L-NPs.

Of the C-NPs tested, two types of low molecular weight chitosan were used with a relatively high DD since these characteristics have been reported as factors that improve gene transfection [188, 190, 194, 200]. The ultra-low molecular weight chitosan (2.5k) produced smaller NPs in comparison to the low molecular weight chitosan (50-90k), similar to previous observations in [41, 200]. However, unlike other investigations, the size of C-NPs in this project were in the micron size range, not in the NP size range of <1000 nm. This is not likely due to incomplete formation of complexes and low stability, as has been previously reported when a low charge ratio is used for complexation of DNA-chitosan particles [41, 191], as the high zeta potential of C-NPs in this project indicated colloidal stability. Instead, perhaps particle aggregation occurred which resulted in the sedimentation of the formulation over time.

Although chitosan is very biocompatible promising gene delivery vector, its low solubility in neutral environments affects its stability of NP delivery upon entering biological systems. Its incorporation into gemini delivery systems was tested as a means to improve stability in biological media and improve transfection. Increasing chitosan concentration was the main factor influencing the final size and zeta potential of the CG-NPs to increase, but gave very

polydisperse populations and micron sized particles. All CG-NPs were stable colloids in acidic conditions (pH 3.3-4.8). However, 1% CG_{12}-NP and 1% CG_{16}-NP were chosen for further characterization due to lower PDI indexes (<0.3) indicating more uniform formulations.

The final type of formulation investigated was the CL-NP formulation. Similar to C-NPs and CG-NPs, CG-NPs had a size of ~1 µm. However, in contrast to C-NPs and CG-NPs, it had a low zeta potential (+12.7 mV) which indicated a formulation with low stability. Nevertheless, it was still tested *in vitro* in order to compare its performance with G_{12}L-NPs.

In this work, particle characterization was done by DLS for determination of the hydrodynamic radius of NPs. Hydrodynamic radius assumes a spherical shape. However, previous studies with gemini NPs and ODNs have shown that complexation of gemini 12-3-12 with ODNs results in a particle that is loosely packed and organizes into an ellipsoid shape that resembles a multi-layered sandwich [209]. NPs made of chitosan polymer have also shown to vary in shape depending on the chitosan MW and N/P ratio [194]. Given the hybrid nanoparticles presented in this work using combinations of gemini surfactant and chitosan with ODNs, the NPs may not be structurally spherical. Therefore, the hydrodynamic radius may not be the best indicator of NP size. Perhaps other methods such as TEM may give insight into more conclusive NP structures and sizes that could explain transfection efficiencies.

5.1.1 NP Characterization in biological buffers

An important aspect of NP delivery systems is the ability to maintain stability within the biological environment in order to provide protection against enzymatic degradation prior to reaching the target site. Upon entering the biological environment, proteins have been found to easily adsorb to NPs and form a protein corona which in turn affects clearance, biodistribution, and toxicity [210]. In terms of vaccine development, the protein-NP interactions could also affect antigen presentation. Yet, most analyses characterize size and zeta potential of NP formulations in its prepared state. Characterization of NPs in biological media could give insight into their behavior upon entering biological environments. As such, the selected NP formulations were measured for size and zeta potential in four different buffers resembling the biological environment.

The zeta potential for all groups of formulations (G-NPs, G_{12}L-NPs/BG_{12}L-NPs, C-NPs, CG-NPs, CL-NPs) in all biological media decreased below +20 mV. This indicated a decrease in stability of formulations upon entering the biological environment. For C-NPs and CG-NPs, low zeta potential could coincide with decreased solubility of chitosan in the neutral medium as has been previously discovered [188, 211]. All chitosan based formulations were essentially neutral in basic media and 10% FBS supplemented RPMI 1640 complete media which is in agreement with previous studies and could affect particle stability and their efficacy *in vivo* [41, 188]. Unlike the chitosan formulations, the G_{12}L-NPs and PVP 10,000 BG_{12}L-NPs maintained a positive charge around +10 mV which could help improve transfection and retention, which will be later discussed.

Dilution of NP formulations in biological buffer also affected size distribution in comparison to their as-prepared state. The G_{12}L-NPs and PVP 10,000 BG_{12}L-NPs increased in size in saline, PBS, basic RPMI 1640 media and 10% FBS supplemented RPMI 1640. This could be explained by aggregation and protein adsorption in complete media due to their low positive charge (lower repulsive forces). In contrast, the CG-NPs decreased in size. This phenomenon has been previously observed in chitosan NPs and was attributed to the decreased solubility of chitosan in neutral environments that increases condensation of chitosan chains and results in a decrease of particle size [211]. Despite the incorporation of gemini surfactant into the hybrid CG-NPs, the same phenomenon was observed. Whether gemini surfactant improved the solubility of chitosan based NP formulations remains to be determined.

5.1.2 Particle size stability after long term storage at 4°C

In this work, the design of a NP delivery system for CpG-ODN aimed to produce a commercially viable pharmaceutical product. Long term stability is an important factor for manufacturing, inventory and consumer use of a successful pharmaceutical product. Preliminary investigations of long-term stability of formulations were monitored for insight into product shelf-life. In this project, PEG400 and PG were used as excipients to provide a proper medium for G_{12}L-NP/BG_{12}L-NP formation but also because both are used in a variety of pharmaceutical formulations as stabilizing agents [212]. The size of nanoparticles during storage for one month at 4ºC was investigated for G_{12}L-NPs and BG_{12}L-NPs. During the storage period, the vesicles without CpG-ODN complexation maintained similar size in PEG400 and PG excipients with the

exception of PVP 10,000 BG_{12}L-NPs. PVP 10,000 BG_{12}L-NPs fluctuated in size but stayed relatively the same over the first 10 days, then increased in size slightly at 15 days. Final CpG-ODN complexed formulations had a slight increase in size over the thirty-day period as well. An increase in size could correspond to aggregation and dissociation of lipoplexes which in turn could affect and decrease biological activity and transfection efficiency as has been previously reported [213-215]. The variable polydispersity could also be a result of this factor.

Monitoring the chitosan formulations over long term storage would also be important, especially as they are prepared in acidic media which could affect degradation of the CpG-ODN DNA. Although CpG-ODN stability was not greatly explored in this work, a UPLC method was developed and can be used in the future for monitoring long term stability.

5.1.3 Investigation of NP complexation FCS

Gemini complexation with plasmid DNA has been studied in our group in the past and in such formulations, a phospholipid plays a key role in compaction of plasmid-gemini complexes into more uniform and smaller structures [208]. Given the difference in DNA type used for formulations in this project (oligonucleotide DNA vs plasmid DNA), and the order of manufacturing the GL-NPs, and BGL-NPs, the dynamics of complexation were studied using FCS.

In this project CpG-ODN DNA was complexed with pre-formed gemini-phospholipid vesicles hydrated with water (GL-NPs) or polymer solution in water (BGL-NPs). Additionally, both PEG 400 and PG excipients were tested during formulation development. The focus of this analysis was on PEG 400 NPs, as these were the formulations carried out through further study. In comparison to naked CpG-ODN, the GL-NPs had a relatively heterogeneous population. The PVP 10,000 component of the BGL-NP formulation however appeared more uniform. Other polymers did not result in such uniform particle populations.

The advantage of FCS characterization is that it can estimate the number of CpG-ODN molecules per particle with which other NP characterization techniques cannot. Overall, the GL-NP and BGL-NP vesicles were able to complex a range of 1-20 CpG-ODN molecules per particle. When compared to plasmid complexes, fewer number of CpG-ODN molecules were

complexed per gemini-phospholipid particle around the same size [208]. This may be related to the +/- ratio used, e.g. 2:1 for CpG vs.10:1 for plasmid complexes.

5.2 Correlation of particle characteristics with cellular uptake

One mechanism of immune activation by CpG-ODN in chickens, is through the recognition of TLR 21 in chicken macrophages. Similar to its mammalian functional homolog TLR 9, TLR 21 receptors are located intracellularly in the endoplasmic reticulum and active in the endo-lysosome [143]. Delivery of CpG-ODN into immune cells is an important factor for generating a protective innate immune response against infection. As such, the uptake of CpG-ODN in HD11 chicken macrophages was studied. Previous investigations have established that cell type mitigates the amount of DNA transfection (uptake). An optimal NP delivery system that is able to transfect one cell line may not exhibit the same transfection results in another [41, 188]. The transfection ability of naked CpG-ODN in HD11 cells prior to testing NP formulations was monitored to establish proper transfection parameters for future experiments.

CpG-ODN uptake over 4 hours was monitored in HD11 cells at different quantities of naked CpG-ODN. G_{12}L-NPs and BG_{12}L-NPs consistently and significantly improved the percentage of cells transfected with CpG-ODN in comparison to naked CpG-ODN over the 4 hours. Moreover, G_{12}L-NPs and BG_{12}L-NPs were able to increase the percentage of cells with CpG-ODN uptake within the same time period despite incubation with a lower amount of CpG-ODN. Additionally, uptake was observed only 1 hour after incubation. Because of this, subsequent experiments were executed with a dosing/incubation time of 2 hours with naked CpG-ODN and formulations.

Of the six groups of formulations (G_{12}-L-NPs, BG_{12}-L-NPs, G-NPs, C-NPs, CG-NPs, CL-NPs), all were able to improve transfection efficiency with CpG-ODN uptake after 2 hours when compared to naked CpG-ODN with the exception of CL-NPs (see Figure 55A). Comparatively, all formulations that contained gemini surfactant performed better than C-NP and CL-NP formulations without gemini. C-NP was only able to transfect half the cell population in comparison to gemini containing formulations. This is not unexpected as previous studies have indicated that the low buffering capacity of chitosan can result in low solubility in biological media and can limit the success of chitosan NP delivery systems [43]. It is also important to note that in this work, transfection refers directly to cellular CpG-ODN uptake,

while most other investigations refer to transfection as a function of gene expression—an umbrella term that combines uptake of the NP, endosomal escape, and translation. Many investigations have attributed low transfection efficiency to inability to escape the endosomal compartment. Our study suggests that a major factor of lower transfection by C-NPs is also due to its inability to interact with the cell membrane and improve cellular uptake. This work further supports theories that chitosan NP delivery systems would perform better with additional components that improve stability, solubility, and membrane interaction given that hybrid CG-NPs were able to improve transfection despite use of a low MW chitosan with sufficient deacetylation (>80%).

Another aspect of this project was also to explore slow or sustained release of CpG-ODN for lasting immune activation. As such, the retention of CpG-ODN was also observed 24 hours after the removal of transfection media following the initial uptake after 2 hours of treatment (Figure 55 B, C). Distinctions between formulations were more easily obtainable when analyzing retention of CpG-ODN following transfection. In fact, several formulation groups (HA-NP, A-NP, DGL-NP) not discussed here were not further investigated since they performed inferior to the formulations highlighted in Figure 55 A, B.

The formulation groups: G_{12}-L-NPs, BG_{12}-L-NPs, G-NPs, and CG-NPs were all able to sustain CpG-ODN within the cellular environment up to 24 hours post dosing. G-NPs were best at retaining CpG-ODN within HD11 macrophages and had similar percentage of cells with CpG-ODN at 2 hours and 24 hours. This indicated a high stability of G-NP formulations. Hybrid NP groups G_{12}L-NPs, BG_{12}L-NPs, and CG-NPs performed similarly but had a more dramatic decrease in percentage of cells retaining CpG-ODN. Given the greater detection of CpG-ODN in cells treated with NP formulations, this could indicate a sustained release property from the NPs. This sustained release effect could prolong an active innate immune response *in vivo*. C-NPs and CL-NPs were not able to retain a significant amount of CpG-ODN in comparison to naked CpG-ODN, which is not surprising considering the low uptake efficiency.

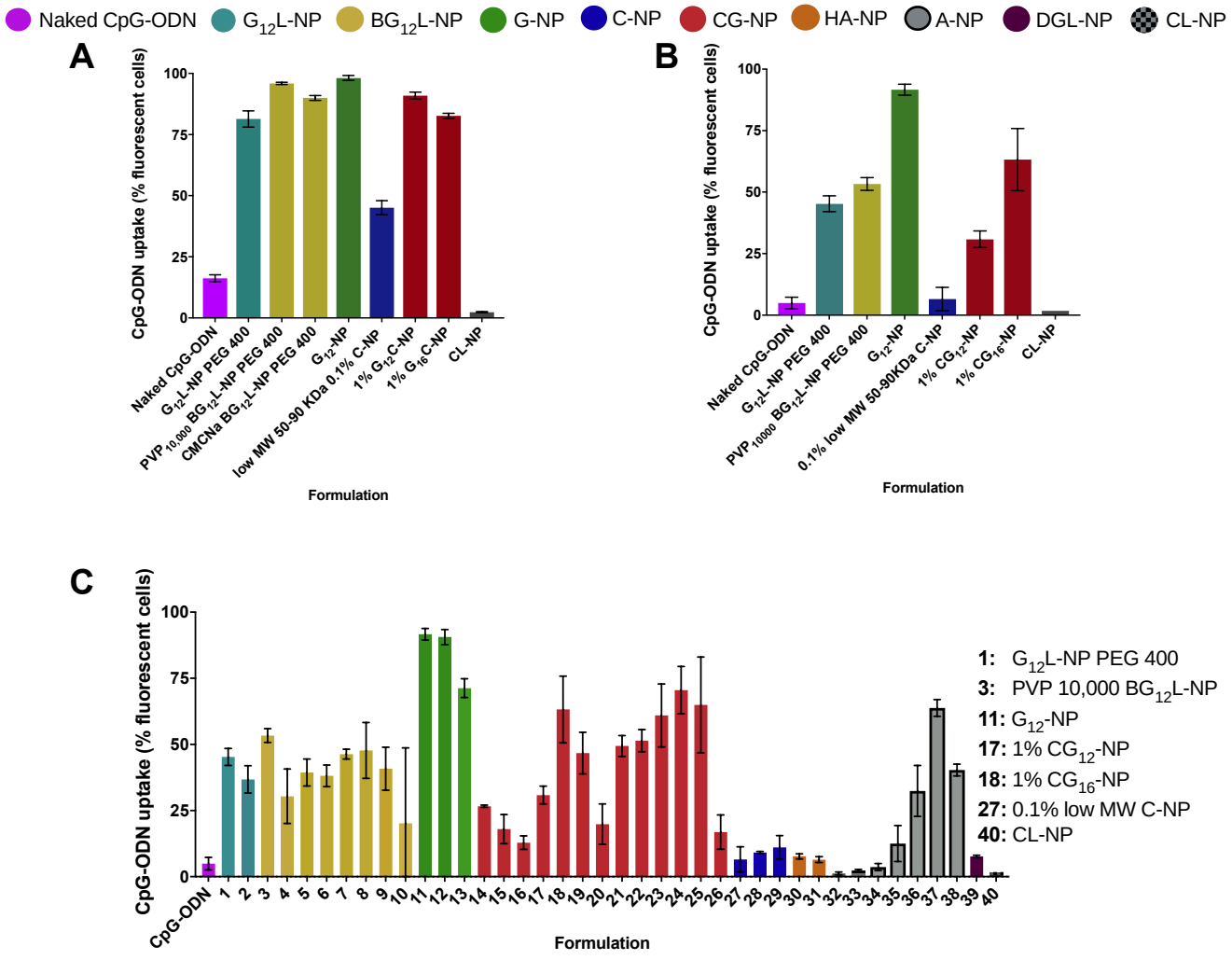

Figure 55 Overall comparison of CpG-ODN uptake and retention in HD11 cells resulting from transfection with different types of NPs

All formulations were compared in their ability to enhance CpG-ODN uptake in comparison to naked CpG-ODN. Best formulations based on method preparation and CpG-ODN uptake were compared at 2 hours post dosing (A) and 24 hours post dosing (B). Retained level of CpG-ODN uptake 24 hours post dosing of all formulations generated in this project categorized by group are also compared (C). Values expressed represent mean ± S.D., n=3.

Whether or not gene transfection by NPs is successful at the cellular level, has been attributed to size and zeta potential. Certain investigations have shown that zeta potential can influence cellular association and trafficking. As investigated by Fromen et. al, NPs preferentially associate with pulmonary macrophages and dendritic cells dependent on anionic versus cationic zeta potential. Anionic NPs associated more with alveolar macrophages, yet cationic NPs preferentially associated with dendritic cells and generated chemoattractant

production and increased antibody production [74]. Effects of zeta potential on HD11 macrophage uptake was also explored in this study using NP characterization data in its prepared state and in RPMI 1640 basic transfection media (Figure 56). Generally, preparation of formulations with ζ potential above +40 mV resulted in higher CpG-ODN uptake (Figure 56A). However, characterization of ζ potential in biological buffers mimic the environment of the lung more closely. From the data collected in this work, both negative and positively charged NPs resulted in high NP uptake corresponding to the G_{12}-NP, G_{12}L-NP, and BG_{12}L-NPs (Figure 56B). NPs with greater negative charge (1% CG_{16}-NP) in basic media also achieved relatively high uptake while near neutral formulations (C-NPs) did not which can be attributed to decreased solubility of chitosan at basic pH. It would be interesting to investigate whether the ζ potential would influence immune responses with other APCs in the chicken immune system as it develops over its relatively short lifespan.

A relationship between uptake and size distribution was not present. The cells were able to take up particles from 150 nm – 4 μM in size with no obvious preference (Figure 56 C, D). Similarly, other investigators have found no size dependent uptake in NP vaccine applications [216]. Conversely, size of vaccine formulations in mammals has been found to affect trafficking through the lymphatic system and sizes greater than 500 nm do not enter initial lymphatic vessels [216, 217]. The effect of NP size on CpG-ODN uptake was not seen in an *in vitro* avian cell model, but may have effects related to immune stimulation *in vivo.*

Transfection of HD11 cells with blank CG_{16}-NPs, CG_{18}-NPs, PVP 10,000 BG_{12}L-NPs suggested that these particles also associate with HD11 cells without uptake because of the increase in cell FSC profile, which indicates a larger cell size. Although SSC also increased, the effect was not as great as one would expect if there was a large level of uptake and consequently, changes in cell granularity. This was not seen in cells transfected with naked CpG-ODN. Therefore, the CpG-ODN molecule could play a role in initiating further NP uptake, as CpG-ODN class B has been associated with activation of cell surface TLR 15 in addition to TLR 21. For G_{18}-NP, CG_{16}-NPs, CG_{18}-NPs, PVP 10,000 BG_{12}L-NP the main cell population also showed increased SSC, which could indicate uptake of blank NPs.

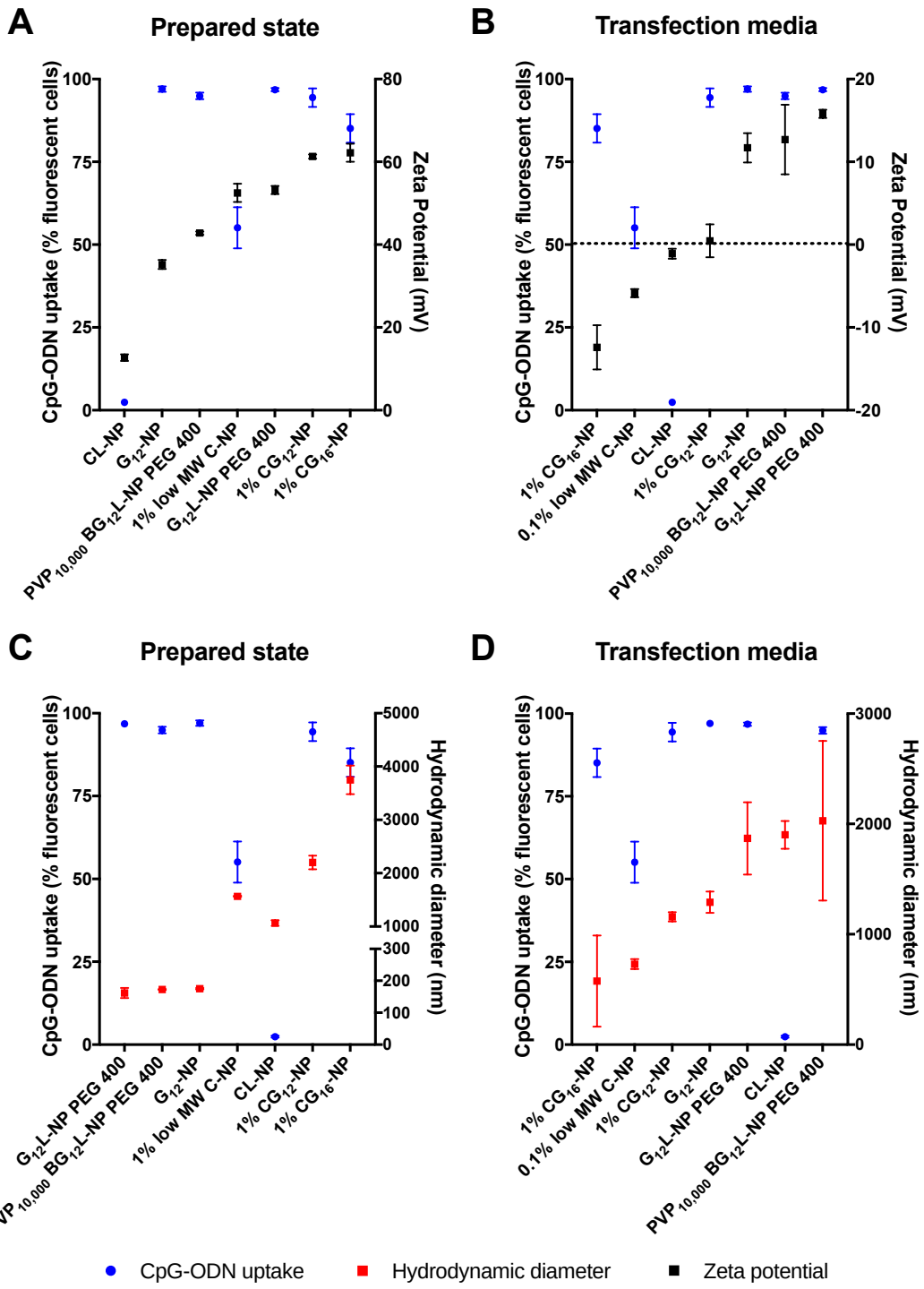

Figure 56 Relationship between size and zeta potential of particles and CpG-ODN uptake

Comparison of the relationship between NP uptake and zeta potential and NP uptake and hydrodynamic diameter. Size and ζ potential of particles was measured in its prepared state (A,C) and in transfection media (RPMI 1640 basic media) (B,D). Values expressed as mean ± S.D., n=3.

This work has established that G-NPs, C-NPs, G_{12}L-NPs, BG_{12}L-NPs, and CG-NPs are able to overcome barriers to cellular internalization improve CpG-ODN uptake. Furthermore, with the exception of C-NPs, these formulations are able to retain more CpG-ODN intracellularly 24 hours post dosing. A high uptake in HD11 cells could translate into an improvement in antigen presentation and increased phagocytic activity in antigen presenting cells in the chicken immune system. The capacity to retain CpG-ODN could translate into extended release vaccine formulations that could promote formation of long-term immunity in chickens. From an economic standpoint, increased uptake and retention of CpG-ODN by NPs could reduce the amount of CpG-ODN needed in a single vaccine dose and reduce costs.

5.3 Comparing immune stimulation effects from different nanoparticle formulations

The relationship between CpG-ODN uptake and NP delivery may not directly translate into activation of innate immune stimulation in HD11 cells. Investigations of gene transfection by NP delivery systems in mammalian cells have found that barriers to nucleic acid delivery include intracellular mechanisms such as endosomal escape and cellular trafficking [218]. Unlike other applications of gene delivery systems that require gene translation in the cytoplasm, in chickens a CpG-ODN molecule interacts intracellularly with its receptor TLR 21 within the endo-lysosome [139, 140]. However, CpG-ODN NP delivery could change intracellular trafficking of CpG-ODN within the cell and possibly mask innate immune activation. On the other hand, BGL-NPs, G-NPs, and CG-NPs could result in extended release of the CpG-ODN antigen and prolong effects of immunity against infection given their high retention capacity. To ensure that improved CpG-ODN uptake and retention by NP formulations in this project correlated with improved stimulation, activation of HD11 macrophages was also investigated post dosing.

This work provided evidence of enhanced CpG-ODN uptake through flow cytometric evaluation and confocal imaging after 2 hours of incubation. However, the level of nitrite (NO) production was most evident at 24 hours post stimulation and no significant stimulation was measured after four hours of incubation. Similarly, other investigations of CpG-ODN activation in HD11 cells have found that NO is not detectable until 24 hours after stimulation and that 4 hours of stimulation is an optimum time that results in maximum achievable NO production when measured 24 hours post dosing [144, 146]. Preliminary CpG-ODN trafficking studies by

CLSM in this project suggest that the reason NO isn't detectable within the first hours of CpG-ODN incubation is because CpG-ODN is still interacting with the cell membrane at this stage. Additionally, endosomal processing is still beginning at this stage since G_{12}L-NPs and PVP 10,000 BG_{12}L-NPs have some CpG-ODN internalization at this stage, but no NO production.

There are many examples where NPs in combination with vaccine antigens have increased immune stimulation *in vivo* in a variety of species [14, 35, 42, 58, 83, 85, 119, 121]. Of the formulations tested in this project, a significant amount of nitrite production *in vitro* was observed 12 and 24 hours post dosing in relation to untreated cells (Figure 57). In general, nitrite concentration doubled from 12 to 24 hours post dosing. Of the 6 formulation groups, PVP 10,000 BG_{12}L-NPs, C-NPs, and CG-NPs resulted in cells producing the greatest amount of nitrite in comparison to untreated cells (Figure 57B). Despite no further nitrite production compared to naked CpG-ODN, it is important to note that the phosphorothioate backbone and specific sequence of CpG-ODN already enhances innate immune stimulation in comparison to a phosphodiester backbone and CpG-ODN sequence with decreased immune stimulating properties [145, 147]. Therefore, further enhancement may be limited by the *in vitro* cellular model.

What is interesting to note is that high 24-hour retention by G_{12}-NPs did not correlate with higher nitrite production in comparison to the other formulations. This could be due to inhibited or slow release of CpG-ODN formulated with gemini surfactant in cells [139, 219]. The slower release could slow interaction with TLR 21. Given the evidence that PVP 10,000 BG_{12}L-NP and CG-NP result in greater CpG-ODN retention *in vitro* by CLSM and flow cytometry compared to naked CpG-ODN, intracellular processing of CpG-ODN may last longer than the 24-hour period monitored in this project. In fact, Huang et al. have found that chitosan NPs release DNA at a slow rate up to 10 days *in vitro* depending on MW and DD of chitosan [220]. A similar phenomenon could explain limited nitrite production by PVP 10,000 BG_{12}L-NP, CG-NP, and G-NPs given that CpG-ODN is still detectable in cells after 24 hours in comparison to naked CpG-ODN.

Corresponding to other investigations that have measured whether NP delivery systems without antigen result in immune stimulation, blank G_{12}L-NPs and BG_{12}L-NPs vesicles formulated in this work, also did not result in nitrite production in comparison to untreated cells.

Since chitosan has been reported to have adjuvant properties in mammals and chickens [221, 222], it was surprising that blank chitosan formulations without CpG-ODN formulated in this project did not have significant immune enhancing effects in HD11 macrophages at the 24-hour time period, although this may be due to dose-dependent effects.

Although the Greiss assay is the inexpensive standard, and fairly robust method for detecting macrophage activation, it is an indirect endpoint measure of nitric oxide. It has been found to easily react with free radical species and give inaccurate results [223]. In this project, the toxic CL-NP formulation produced similar nitrite levels to viable cells transfected with NP formulations. An antibody detection assay for NF-kB or IFN-Ɣ may be a more accurate determination of activated chicken macrophages and hint at specific differences in immune activation by different formulations.

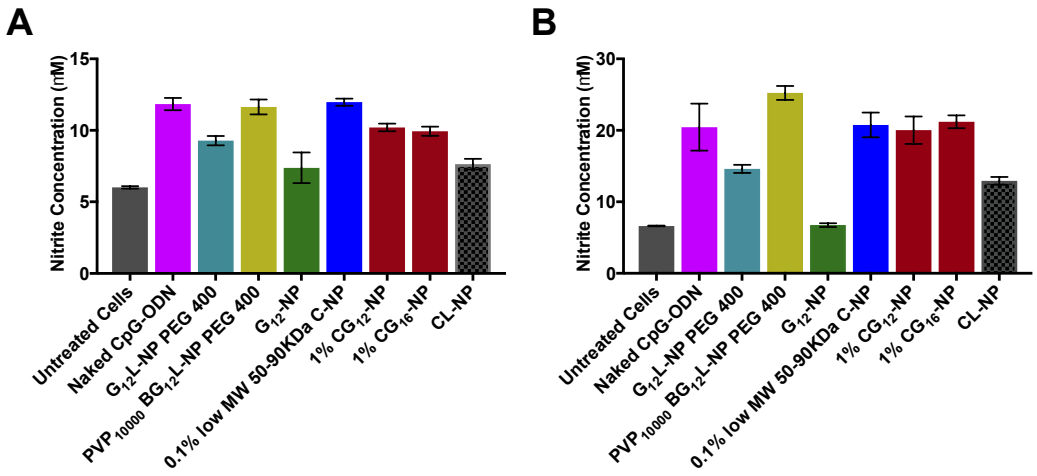

Figure 57 Nitrite production in HD11 cells after transfection with CpG-ODN formulations at 12 and 24 hours post dosing.

Nitrite production in HD11 macrophages was measured at 12 (A) and 24 (B) hours post stimulation with CL-NPs using the standard Greiss assay. NP formulations were prepared as described previously. Cells were dosed with 1 µg CpG-ODN. Values expressed represent mean ± S.D. (n=3).

5.4 Assessment of cellular toxicity after nanoparticle uptake

The use of non-viral gene delivery systems for DNA delivery is advantageous over viral delivery systems because there is no concern of integration into the cellular genome. Liposomal and polymer formulations are also regarded as safer than viral delivery systems. In fact, liposomal formulations are approved and available for human use in the market. However, cationic liposomes are also known to induce cellular toxicity such as cellular shrinking and

vacuolation [224]. Considering gemini's cationic nature, its low CMC is advantageous in this manner as it can form vesicles at a relatively low molar concentration and decrease toxicity. Neutral lipids such as DPPC, have also shown to decrease toxicity of gemini surfactant gene delivery systems [182].

Similar to other investigations which show minimal cellular toxicity from gemini-lipid formulations and chitosan NP formulations, G_{12}L-NPs, BG_{12}L-NPs, C-NPs, and CG-NP formulations developed in this project were also well tolerated. This is not surprising as components of G_{12}L-NPs and BG_{12}L-NPs include PEG excipient, a biocompatible polymer [225] and DPPC, found in the lung environment. Chitosan was also chosen as a component of CpG-ODN NP delivery systems formulated in this project, as it is also a highly biocompatible and biodegradable polymer.

Differences in viability measurements by Calcein AM and MitoTracker Green FM were likely due to changes in membrane porosity as has been previously observed in PAM212 keratinocytes transfected with gemini surfactant formulations [203]. In this study, it was concluded that viable mitochondrially active cells also exhibited high membrane porosity as membrane changes were evident after CpG-ODN and NP incubation from microscopic assessment 2 hours post dosing, and SSC analysis by flow cytometry. Yet, CLSM revealed cellular membranes returned to normal after successfully internalizing CpG-ODN. The dramatic increase in SSC, indicative of high cell granularity resulting from uptake of CpG-ODN G_{12}L-NPs, BG_{12}L-NPs, G-NPs, CG-NPs may be the consequence of a high number of endosomes within cells containing NPs. A similar phenomenon has been observed in HeLa cells following uptake of polymeric nanoparticles [226]. In contrast, naked CpG-ODN and C-NP transfected cells did not have as dramatic a shift due to lower levels of CpG-ODN uptake.

Lipid NP formulations are known to aid gene delivery through membrane adhesion and endocytosis. Since macrophages are highly phagocytic cells, it is not unreasonable that there is a high degree of trafficking occurring upon NP interaction that could contribute to membrane porosity. This may contribute to Calcein AM leaking out of the cellular environment and could explain the low level of viability seen in this experiment. It is also important to note that cells transfected with blank G_{12}L-NPs and BG_{12}L-NPs also had low viability when measured by Calcein AM. In this project, cellular toxicity caused by NP formulations must be further

evaluated, given that the mitochondria is known to play an essential role in apoptosis. An important factor involved in apoptosis is the loss of mitochondrial membrane potential [205]. There is conflicting evidence regarding the sensitivity of MitoTracker Green dye to mitochondrial membrane potential and integrity. A study in 2000 determined that it was membrane potential sensitive, yet a more recent study has observed an opposite effect after treatment of cells with hydrogen peroxide [227]. Given the role of macrophages in production of ROS during innate immune stimulation, further work needs to be done to determine the actual viability and apoptotic status of the cellular population transfected with NP formulations, perhaps with other more sensitive apoptotic cellular markers.

5.5 Local lung biodistribution of NPs

Few investigators have studied the biodistribution of particles within the avian respiratory tract after spray vaccination. Of the few studies that exist, spray vaccine particles can provide local and topical treatment in air sacs [102]. Additionally, particle deposition in the avian respiratory tract is age dependent [102, 131]. In order to establish local drug levels in the lung and air sacs, it has been found that particles less than 3 µm are able to bypass the mucociliary transport [103]. The nebulizer used in this study theoretically generates 1-5 µM sized aerosol droplets as per the manufacturer and therefore should bypass mucociliary transport to a certain extent. Evidence of G_{12}L-NP and BG_{12}L-NP deposition was observed in the chick respiratory tract 2 hours after nebulization and can confirm that the delivery method effectively administers the vaccine to the lung. G_{12}L-NPs and BG_{12}L-NPs deposited in the trachea, the tracheal bifurcation, and appeared to diffuse through the connective lung tissue. This is similar to other investigations of particle deposition in the avian lung where larger particles deposit in the upper airways, particularly the tracheal bifurcation [103, 104].

In general, extensive *in vivo* mammalian studies of NP distribution in the lung enviroment are performed with more controlled dose administration by intra-tracheal instillation or inhaler administration to individual animals. However, not many groups have attempted to investigate whether NPs and DNA dissociate within the lung environment. In this project evidence of intact CpG-ODN NPs within the lung environment were found using 1%CG_{12}-NPs along the mid lung region. However, 1%CG_{12}-NPs and 1%CG_{16}-NPs mainly appeared to dissociate from CpG-ODN within the first 2 hours of being in the lung environment.

Infection by *E. coli* in broiler chickens is commonly associated with pathogenic bacteria within the environment that can be inhaled by chicks. Therefore, confirmation of the presence of G_{12}L-NP, BG_{12}L-NP, G_{12}-NP, and 1%CG-NP biodistribution in the chick lung confirms delivery of the vaccine to the chick respiratory system, and initiation of an immune response at the site of infection. A limitation of this project is the relatively uncontrolled dosing in individual chick respiratory tracts that prevents direct quantitative comparison of biodistribution by the different NP groups. Several birds are nebulized all at once, and therefore it cannot be determined how much dose is entering the respiratory tract in each bird. Additionally, particles could deposit on other external areas such as the eyes, nasal cavity and body. Although, deposits of vaccine in these areas are also thought to contribute to immunity [228].

Compatibility between the nebulizer and formulations is a key component of efficient output and delivery by inhalation. The formulations administered to chicks were chosen based on low viscosity. Deposits of naked CpG-ODN in the lungs appeared more even than NP formulations. This may be due to the higher viscosity of NP formulations in general. For example, it was noted that the nebulizer had difficulty generating an aerosol of the 1%CG_{12}-NP formulations, which had comparatively the highest viscosity among the selected formulations, and larger particles that settled over time. Since vibrating mesh or plate nebulizers that physically break up the liquid into smaller droplets work very efficiently for suspensions or liposomes [25], switching from a compressed air nebulization mechanism to the latter may improve delivery to chicks for more viscous formulations.

Since only short-term particle deposition was observed, further examination of the particle deposition at 24 hours post nebulization in the lung and perhaps other organs must be carried out to see if the particles are retained within the respiratory tract, and whether they get trafficked to other organs.

5.6 Evaluation of protection in 1-day old chicks against *E. coli* challenge

Applications of NP drugs/vaccines could theoretically reduce dosing frequency due to the increased accumulation of drug per particle at specific sites [70]. Evidence of this phenomenon was seen in HD11 cellular CpG-ODN uptake studies. Based on CpG-ODN uptake and retention data, viability, nebulization compatibility, and cellular toxicity, G_{12}-NPs and BG_{12}L-NPs appear the most compatible and effective for the intrapulmonary delivery of CpG-ODN.

Previous investigations of CpG-ODN administration to broiler chicks against *E. coli* challenge have reported that encapsulation with NPs have improved chick survival, decreased clinical scores, and lower bacterial colony counts after *in ovo* administration in comparison to naked CpG-ODN [14, 27].

Using intrapulmonary administration in this project, PVP BGL-NPs were also able to enhance protection in chicks against *E. coli* challenge in comparison to naked CpG-ODN. This is advantageous as spray vaccination does not require needle administration and targets mucosal immunity which can produce local and systemic effects. In the first NP group tested, gemini tail length affected vaccine effectiveness in the following order of effectiveness in protecting chicks: 12-3-12 ≥ 16-3-16 > 18-3-18. Subsequently, $BG_{12}L$-NPs with either PVP or CMCNa showed that both biopolymers were equally effective in enhancing survival rates. This may be explained by similarities in NP uptake, NO production and particle characteristics. For example, the number of CpG-ODN molecules per NP was similar in both types of NP formulations. However, the variability in formulation uniformity at the molecular level from manual mixing of CMCNa suggests that PVP is a better candidate for our application that must be easily manufactured on a large scale. Quantitative measures of antibody and cytokine responses in chicks treated with CpG-ODN NPs was not carried out in this work. However, given that other studies in broilers have found that encapsulation of vaccines enhances antibody titres [19, 229], it is expected that a similar phenomenon may occur from PVP $BG_{12}L$-NP CpG-ODN delivery.

The hybrid 1%CG-NPs group of CpG-NPs did not enhance survival in comparison to the BGL-NPs. While chitosan has been highly investigated for its antibacterial properties against gram negative and positive bacteria [230-232], and it could be assumed that not only would the hybrid formulation initiate innate immune stimulation but aid in bacterial cell killing, this was not the case in this project. The lower efficacy of these formulations, however, may be attributed to nebulizer incompatibility. As previously mentioned, delivery of $1\%CG_{12}$-NPs was difficult and produced variable results in bird survival in the protection studies.

One of the main goals of NP vaccine delivery is to prolong immune activation so that immune memory is generated without the need of repeated vaccine administration. As such, in the last protection experiment we aimed to compare the top 3 groups of formulations (G_{12}-NPs, PVP10,000 $BG_{12}L$-NPs, and $1\%CG_{12}$-NPs) in prolonging innate immune stimulation effects of

CpG-ODN that have normally last 3-6 days [7, 82, 96]. Challenge was performed on Day four post vaccine administration. From the data in this experiment it is not possible to determine whether there are any differences between NP formulations and naked CpG as this trial showed no protection based on the saline control. Additional trials and specific studies CpG-ODN release from NPs may give more insight into the mechanisms of PVP10,000 $BG_{12}L$-NP interactions with immune cells in the lung environment.

As an overall assessment, the survival experimental settings were designed to gain some information about the optimum timing of the challenge and duration of protective effect of the naked CpG-ODN and NP formulations in order to help rank formulations and develop an understanding of the effect of NP composition on protection. We previously found that naked CpG-ODN solution can protect chicks up to 5 days. However the extent of protection decreased significantly by Day 4-5 [99], indicating that the later the chicks are challenged with *E. coli* after the vaccination, the lower the rate of survival.

In the NP screening experiments, we have used Day 2, 3, or 4 post vaccination for administering the *E. coli* challenge. This experimental variable indicated that PVP BGL-NPs improved protection of chicks compared to naked CpG-ODN when challenged on Day 2 or 3, and appeared similarly low in protecting (although inconclusive) on Day 4 (Fig 54 A, B and D).

5.7 Future Work

Future experiments could enlighten certain aspects of NP delivery that have yet to be confirmed. Firstly, cell toxicity resulting from NP transfection must be further characterized with apoptotic cell markers to confirm safety of NP formulations. Additionally, since one of the goals is to enhance long term immunity against bacterial infection in chicks, other cellular markers of immune stimulation should be identified in order to better correlate CpG-ODN uptake with increased innate immune stimulation. Other NP internalization characteristics could also be explored such as identification of specific phagocytic mechanisms involved in chicken macrophage cellular NP uptake so that perhaps NP formulations that are able to enter through several mechanisms would be able to better CpG-ODN antigen presentation and receptor interaction.

Another major future endeavour that should be monitored is specific stability of NP formulations by UPLC. Although a method was developed for detection of CpG-ODN in NPs,

specific stability studies were not performed. Additionally, correlation between degradation and transfection effectiveness should be investigated.

Conclusion

CpG-ODN DNA is a promising approach to vaccinate vulnerable broiler chicks against bacterial infections common to birds such as *E.* coli infection. Past investigations have shown that NP delivery systems can improve protection of chicks *in vivo* via *in ovo* routes of vaccination [14, 27]. In this project, gemini surfactants, phospholipids and bio adhesive polymers, were tested as the foundation for formulation of six types of hybrid NPs for delivering CpG-ODN DNA to the respiratory tract of neonatal chicks via nebulization. Optimization of polymer concentration and type allowed the determination of promising formulations that improved CpG-ODN uptake and retention compared to the naked CpG-ODN in HD11 cells *in vitro*. Additionally, the formulations were able to activate NO production in macrophages, an internal mechanism for intracellular bacterial killing. Of the six formulation groups, gemini containing formulations G_{12}-NPs, G_{12}L-NPs, PVP 10,000 BG_{12}L-NPs, and 1% C$G_{12,16}$-NPs were the most promising candidates for delivering CpG-ODN vaccine to broiler chicks. All four NP types were detected in the chick respiratory tract. This confirms the delivery method, although PVP 10,000 BG_{12}L-NPs were able to improve protection against *E. coli* in chicks with minimal toxicity with respect to naked CpG-ODN, while G_{12}-NPs and other hybrid NPs made with chitosan polymer did not. In this project, PVP 10,000 BG_{12}L-NPs show potential as vaccine candidates for further development into the first inhalable CpG-ODN NP vaccine on the market for poultry.

Copyright permissions

SPRINGER LICENSE
TERMS AND CONDITIONS

Aug 08, 2017

This Agreement between University of Waterloo -- Daniella Calderon-nieva ("You") and Springer ("Springer") consists of your license details and the terms and conditions provided by Springer and Copyright Clearance Center.

License Number	4164390237211
License date	Aug 08, 2017
Licensed Content Publisher	Springer
Licensed Content Publication	Drug Delivery and Translational Research
Licensed Content Title	Veterinary vaccine nanotechnology: pulmonary and nasal delivery in livestock animals
Licensed Content Author	Daniella Calderon-Nieva
Licensed Content Date	Jan 1, 2017
Licensed Content Volume	7
Licensed Content Issue	4
Type of Use	Thesis/Dissertation
Portion	Full text
Number of copies	1
Author of this Springer article	Yes and you are the sole author of the new work
Order reference number	
Title of your thesis / dissertation	Improving the delivery and immunogenicity of an inhalable CpG-ODN DNA vaccine by bio-adhesive gemini nanoparticles in broiler chickens
Expected completion date	Sep 2017
Estimated size(pages)	150
Requestor Location	University of Waterloo 10a Victoria Street South Kitchener, ON N2G1C5 Canada Attn: University of Waterloo
Billing Type	Invoice
Billing Address	University of Waterloo 10a Victoria Street South Kitchener, ON N2G1C5 Canada Attn: University of Waterloo
Total	0.00 CAD
Terms and Conditions	

References

[1] H. Shirota, D.M. Klinman, Recent progress concerning CpG DNA and its use as a vaccine adjuvant, Expert review of vaccines, 13 (2014) 299-312.

[2] C. Bode, G. Zhao, F. Steinhagen, T. Kinjo, D.M. Klinman, CpG DNA as a vaccine adjuvant, Expert review of vaccines, 10 (2011) 499-511.

[3] A.D. Bins, J.H. van den Berg, K. Oosterhuis, J.B. Haanen, Recent advances towards the clinical application of DNA vaccines, The Netherlands journal of medicine, 71 (2013) 109-117.

[4] U.S.D.o.H.a.H. Services, Phasing Out Certain Antibiotic Use in Farm Animals, in: Consumer Updates, U.S. Food and Drug Administration, U.S.A., 2013.

[5] L. Hughes, P. Hermans, K. Morgan, Risk factors for the use of prescription antibiotics on UK broiler farms, Journal of Antimicrobial Chemotherapy, 61 (2008) 947-952.

[6] R. Bywater, M. McConville, I. Phillips, T. Shryock, The susceptibility to growth-promoting antibiotics of Enterococcus faecium isolates from pigs and chickens in Europe, Journal of Antimicrobial Chemotherapy, 56 (2005) 538-543.

[7] S. Gomis, L. Babiuk, B. Allan, P. Willson, E. Waters, N. Ambrose, R. Hecker, A. Potter, Protection of neonatal chicks against a lethal challenge of Escherichia coli using DNA containing cytosine-phosphodiester-guanine motifs, Avian diseases, 48 (2004) 813-822.

[8] J.T. van Oirschot, Present and future of veterinary viral vaccinology: a review, The Veterinary quarterly, 23 (2001) 100-108.

[9] J.A. Roth, Veterinary Vaccines and Their Importance to Animal Health and Public Health, Procedia in Vaccinology, 5 (2011) 127-136.

[10] C. Bitter, K. Suter-Zimmermann, C. Surber, Nasal drug delivery in humans, Current problems in dermatology, 40 (2011) 20-35.

[11] K. Song, D.L. Bolton, C.J. Wei, R.L. Wilson, J.V. Camp, S. Bao, J.J. Mattapallil, L.A. Herzenberg, L.A. Herzenberg, C.A. Andrews, J.C. Sadoff, J. Goudsmit, M.G. Pau, R.A. Seder, P.A. Kozlowski, G.J. Nabel, M. Roederer, S.S. Rao, Genetic immunization in the lung induces potent local and systemic immune responses, Proceedings of the National Academy of Sciences of the U S A, 107 (2010) 22213-22218.

[12] N. Lycke, Recent progress in mucosal vaccine development: potential and limitations, Nature Reviews Immunology, 12 (2012) 592-605.

[13] V. Gerdts, G.K. Mutwiri, S.K. Tikoo, L.A. Babiuk, Mucosal delivery of vaccines in domestic animals, Veterinary research, 37 (2006) 487-510.

[14] A. Taghavi, B. Allan, G. Mutwiri, M. Foldvari, A. Van Kessel, P. Willson, L. Babiuk, A. Potter, S. Gomis, Enhancement of immunoprotective effect of CpG-ODN by formulation with polyphosphazenes against E. coli septicemia in neonatal chickens, Current drug delivery, 6 (2009) 76-82.

[15] V.L. Alcón, M. Baca-Estrada, M.A. Vega-López, P. Willson, L.A. Babiuk, P. Kumar, M. Foldvari, Intranasal immunization using biphasic lipid vesicles as delivery systems for OmlA bacterial protein antigen and CpG oligonucleotides adjuvant in a mouse model, Journal of Pharmacy and Pharmacology, 57 (2005) 955-961.

[16] F. Mansoor, B. Earley, J.P. Cassidy, B. Markey, S. Doherty, M.D. Welsh, Comparing the immune response to a novel intranasal nanoparticle PLGA vaccine and a commercial BPI3V vaccine in dairy calves, BMC Veterinary Research, 11 (2015) 220.

[17] A.K. Panda, Nanotechnology in vaccine development, Proceedings of the National Academy of Sciences, India Section B: Biological Sciences, 82 (2012) 13-27.

[18] H. Shams, Recent developments in veterinary vaccinology, The Veterinary Journal, 170 (2005) 289-299.

[19] N. Csaba, M. Garcia-Fuentes, M.J. Alonso, Nanoparticles for nasal vaccination, Advanced Drug Delivery Reviews, 61 (2009) 140-157.

[20] M.-G. Kim, J.Y. Park, Y. Shon, G. Kim, G. Shim, Y.-K. Oh, Nanotechnology and vaccine development, Asian Journal of Pharmaceutical Sciences, 9 (2014) 227-235.

[21] A. Nasir, Nanotechnology in vaccine development: a step forward, Journal of Investigative Dermatology, 129 (2009) 1055-1059.

[22] P. Couvreur, Nanoparticles in drug delivery: Past, present and future, Advanced Drug Delivery Reviews, 65 (2013) 21-23.

[23] X. Guo, L. Huang, Recent advances in nonviral vectors for gene delivery, Accounts of Chemical Research, 45 (2012) 971-979.

[24] V. Weissig, T.K. Pettinger, N. Murdock, Nanopharmaceuticals (part 1): products on the market, International Journal of Nanomedicine, 9 (2014) 4357-4373.

[25] M.B. Dolovich, R. Dhand, Aerosol drug delivery: developments in device design and clinical use, The Lancet, 377 1032-1045.

[26] A. Gautam, J. Clifford Waldrep, C.L. Densmore, Aerosol gene therapy, Molecular Biotechnology, 23 (2003) 51-60.

[27] T. Gunawardana, M. Foldvari, T. Zachar, S. Popowich, B. Chow-Lockerbie, M.V. Ivanova, S. Tikoo, S. Kurukulasuriya, P. Willson, S. Gomis, Protection of neonatal broiler chickens following in ovo delivery of oligodeoxynucleotides containing CpG motifs (CpG-ODN) formulated with carbon nanotubes or liposomes, Avian diseases, 59 (2015) 31-37.

[28] Y. Jia, L. Krishnan, A. Omri, Nasal and pulmonary vaccine delivery using particulate carriers, Expert Opinion on Drug Delivery, 12 (2015) 993-1008.

[29] L.A. Babiuk, S.L. Babiuk, B.I. Loehr, S. van Drunnen Littel-van den Hurk, Nucleic acid vaccines: research tool or commercial reality, Veterinary Immunology and Immunopathology, 76 (2000) 1-23.

[30] Z. Cheng, A. Al Zaki, J.Z. Hui, V.R. Muzykantov, A. Tsourkas, Multifunctional Nanoparticles: Cost versus benefit of adding targeting and imaging capabilities, Science, 338 (2012) 903-910.

[31] F. Andrade, D. Rafael, M. Videira, D. Ferreira, A. Sosnik, B. Sarmento, Nanotechnology and pulmonary delivery to overcome resistance in infectious diseases, Advanced Drug Delivery Reviews, 65 (2013) 1816-1827.

[32] M.D.I. Manunta, R.J. McAnulty, A. McDowell, J. Jin, D. Ridout, J. Fleming, S.E-*---. Bottoms, L. Tossici-Bolt, G.J. Laurent, L. Biassoni, C. O'Callaghan, S.L. Hart, Airway deposition of nebulized gene delivery nanocomplexes monitored by radioimaging agents, American Journal of Respiratory Cell and Molecular Biology, 49 (2013) 471-480.

[33] J. McCaskill, R. Singhania, M. Burgess, R. Allavena, S. Wu, A. Blumenthal, N.A.J. McMillan, Efficient biodistribution and gene silencing in the lung epithelium via intravenous liposomal delivery of siRNA, Molecular Therapy Nucleic Acids, 2 (2013) e96.

[34] G. Shim, H.-w. Choi, S. Lee, J. Choi, Y.H. Yu, D.-E. Park, Y. Choi, C.-W. Kim, Y.-K. Oh, Enhanced Intrapulmonary Delivery of Anticancer siRNA for Lung Cancer Therapy Using Cationic Ethylphosphocholine-based Nanolipoplexes, Molecular Therapy, 21 (2013) 816-824.

[35] C. Sawaengsak, Y. Mori, K. Yamanishi, P. Srimanote, W. Chaicumpa, A. Mitrevej, N. Sinchaipanid, Intranasal chitosan-DNA vaccines that protect across influenza virus subtypes, International Journal of Pharmaceutics, 473 (2014) 113-125.

[36] J.S. Suk, A.J. Kim, K. Trehan, C.S. Schneider, L. Cebotaru, O.M. Woodward, N.J. Boylan, M.P. Boyle, S.K. Lai, W.B. Guggino, J. Hanes, Lung gene therapy with highly compacted DNA nanoparticles that overcome the mucus barrier, Journal of Controlled Release, 178 (2014) 8-17.

[37] M. Bivas-Benita, K.E. van Meijgaarden, K.L.M.C. Franken, H.E. Junginger, G. Borchard, T.H.M. Ottenhoff, A. Geluk, Pulmonary delivery of chitosan-DNA nanoparticles enhances the immunogenicity of a DNA vaccine encoding HLA-A*0201-restricted T-cell epitopes of Mycobacterium tuberculosis, Vaccine, 22 (2004) 1609-1615.

[38] J.F.S. Mann, P.F. McKay, S. Arokiasamy, R.K. Patel, K. Klein, R.J. Shattock, Pulmonary delivery of DNA vaccine constructs using deacylated PEI elicits immune responses and protects against viral challenge infection, Journal of Controlled Release, 170 (2013) 452-459.

[39] G.P. Andrews, T.P. Laverty, D.S. Jones, Mucoadhesive polymeric platforms for controlled drug delivery, European Journal of Pharmaceutics and Biopharmaceutics, 71 (2009) 505-518.

[40] D. Calderon-Nieva, K.B. Goonewardene, S. Gomis, M. Foldvari, Veterinary vaccine nanotechnology: pulmonary and nasal delivery in livestock animals, Drug Delivery and Translational Research, 7 (2017) 558-570.

[41] S. Mao, W. Sun, T. Kissel, Chitosan-based formulations for delivery of DNA and siRNA, Advanced Drug Delivery Reviews, 62 (2010) 12-27.

[42] T. Negash, M. Liman, S. Rautenschlein, Mucosal application of cationic poly(D,L-lactide-co-glycolide) microparticles as carriers of DNA vaccine and adjuvants to protect chickens against infectious bursal disease, Vaccine, 31 (2013) 3656-3662.

[43] H. Ragelle, G. Vandermeulen, V. Preat, Chitosan-based siRNA delivery systems, Journal of Controlled Release, 172 (2013) 207-218.

[44] H. Yin, R.L. Kanasty, A.A. Eltoukhy, A.J. Vegas, J.R. Dorkin, D.G. Anderson, Non-viral vectors for gene-based therapy, Nature Reviews Genetics, 15 (2014) 541-555.

[45] J. Singh, D. Michel, H.M. Getson, J.M. Chitanda, R.E. Verrall, I. Badea, Development of amino acid substituted gemini surfactant-based mucoadhesive gene delivery systems for potential use as noninvasive vaginal genetic vaccination, Nanomedicine (Lond), 10 (2015) 405-417.

[46] K.E. Jones, N.G. Patel, M.A. Levy, A. Storeygard, D. Balk, J.L. Gittleman, P. Daszak, Global trends in emerging infectious diseases, Nature, 451 (2008) 990-993.

[47] T.P. Monath, Vaccines against diseases transmitted from animals to humans: A one health paradigm, Vaccine, 31 (2013) 5321-5338.

[48] V. Gerdts, G. Mutwiri, J. Richards, S.v.D.L.-v.d. Hurk, A.A. Potter, Carrier molecules for use in veterinary vaccines, Vaccine, 31 (2013) 596-602.

[49] M. Look, A. Bandyopadhyay, J.S. Blum, T.M. Fahmy, Application of nanotechnologies for improved immune response against infectious diseases in the developing world, Advanced Drug Delivery Reviews, 62 (2010) 378-393.

[50] P. Villegas, S.H. Kleven, Aerosol vaccination against newcastle disease I. studies on particle size, Avian diseases, 20 (1976) 179-190.

[51] S. Gallorini, D.T. O'Hagan, B.C. Baudner, Concepts in mucosal immunity and mucosal vaccines, in: J. das Neves, B. Sarmento (Eds.) Mucosal Delivery of Biopharmaceuticals: Biology, Challenges and Strategies, Springer US, Boston, MA, 2014, pp. 3-33.

[52] A.D. White, L. Sibley, M.J. Dennis, K. Gooch, G. Betts, N. Edwards, A. Reyes-Sandoval, M.W. Carroll, A. Williams, P.D. Marsh, H. McShane, S.A. Sharpe, Evaluation of the Safety and Immunogenicity of a Candidate Tuberculosis Vaccine, MVA85A, Delivered by Aerosol to the Lungs of Macaques, Clinical and Vaccine Immunology, 20 (2013) 663-672.

[53] Terrence_E_Greenway, Induction of protective immune responses against Venezuelen equine encephalitis (VEE) virus aerosol challenge with microencapsulated VEE virus vaccine, Vaccine, 15 (1998) 1314-1323.

[54] L. Illum, Nasal drug delivery—possibilities, problems and solutions, Journal of Controlled Release, 87 (2003) 187-198.

[55] L.A. Tell, K. Stephens, S.V. Teague, K.E. Pinkerton, O.G. Raabe, Study of nebulization delivery of aerosolized fluorescent microspheres to the avian respiratory tract, Avian diseases, 56 (2012) 381-386.

[56] B. Morein, K.F. Hu, I. Abusugra, Current status and potential application of ISCOMs in veterinary medicine, Advanced Drug Delivery Reviews, 56 (2004) 1367-1382.

[57] R. Muzzarelli, Chitins and chitosans as immunoadjuvants and non-allergenic drug carriers, Marine Drugs, 8 (2010) 292.

[58] M. Günbeyaz, A. Faraji, A. Özkul, N. Puralı, S. Şenel, Chitosan based delivery systems for mucosal immunization against bovine herpesvirus 1 (BHV-1), European Journal of Pharmaceutical Sciences, 41 (2010) 531-545.

[59] E.N.T. Meeusen, J. Walker, A. Peters, P.-P. Pastoret, G. Jungersen, Current status of veterinary vaccines, Clinical Microbiology Reviews, 20 (2007) 489-510.

[60] C.-J. Chiou, L.-P. Tseng, M.-C. Deng, P.-R. Jiang, S.-L. Tasi, T.-W. Chung, Y.-Y. Huang, D.-Z. Liu, Mucoadhesive liposomes for intranasal immunization with an avian influenza virus vaccine in chickens, Biomaterials, 30 (2009) 5862-5868.

[61] E.L. Giudice, J.D. Campbell, Needle-free vaccine delivery, Advanced Drug Delivery Reviews, 58 (2006) 68-89.

[62] P.M. Dowling, Inhalation Therapy for Airway Disease, in, Merck Sharp & Dohme Corporation, 2014.

[63] M.J. Rathbone, M.N. Martinez, Modified release drug delivery in veterinary medicine, Drug Discovery Today, 7 (2002) 823-829.

[64] T.F. Vandamme, K.J. Ellis, Issues and challenges in developing ruminal drug delivery systems, Advanced Drug Delivery Reviews, 56 (2004) 1415-1436.

[65] A. Rothen-Weinhold, R. Gurny, M. Dahn, Formulation and technology aspects of conrolled drug delivery in animals, Pharmaceutical Science and Technology Today, 3 (2000) 222-231.

[66] G.d. Lange, Spray vaccination of day-old-chicks at the hatchery, in, Pas Reform Integrated hatchery solutions, Pas Reform Integrated hatchery solutions.

[67] B. Peeters, W.F. Tonnis, S. Murugappan, P. Rottier, G. Koch, H.W. Frijlink, A. Huckriede, W.L.J. Hinrichs, Pulmonary immunization of chickens using non-adjuvanted spray-freeze dried whole inactivated virus vaccine completely protects against highly pathogenic H5N1 avian influenza virus, Vaccine, 32 (2014) 6445-6450.

[68] R. Siekmeier, G. Scheuch, Treatment of systemic diseases by inhalation of biomolecule aerosols, Journal of Physiology and Pharmacology, 60 Suppl 5 (2009) 15-26.

[69] J.S. Patton, P.R. Byron, Inhaling medicines: delivering drugs to the body through the lungs, Nature Reviews Drug Discovery, 6 (2007) 67-74.

[70] S. Azarmi, W.H. Roa, R. Löbenberg, Targeted delivery of nanoparticles for the treatment of lung diseases, Advanced Drug Delivery Reviews, 60 (2008) 863-875.

[71] W.G. Kreyling, S. Hirn, C. Schleh, Nanoparticles in the lung, Nature Biotechnology, 28 (2010) 1275-1276.

[72] T. Nagamoto, Y. Hattori, K. Takayama, Y. Maitani, Novel chitosan particles and chitosan-coated emulsions inducing immune response via intranasal vaccine delivery, Pharmaceutical Research, 21 (2004) 671-674.

[73] S. Yan, W. Gu, Z.P. Xu, Re-considering how particle size and other properties of antigen–adjuvant complexes impact on the immune responses, Journal of Colloid and Interface Science, 395 (2013) 1-10.

[74] C.A. Fromen, T.B. Rahhal, G.R. Robbins, M.P. Kai, T.W. Shen, J.C. Luft, J.M. DeSimone, Nanoparticle surface charge impacts distribution, uptake and lymph node trafficking by pulmonary antigen-presenting cells, Nanomedicine: Nanotechnology, Biology and Medicine, 12 (2016) 677-687.

[75] C.L. Hardy, J.S. Lemasurier, R. Mohamud, J. Yao, S.D. Xiang, J.M. Rolland, R.E. O'Hehir, M. Plebanski, Differential uptake of nanoparticles and microparticles by pulmonary APC subsets induces discrete immunological imprints, Journal of Immunology 191 (2013) 5278-5290.

[76] C. Thomas, V. Gupta, F. Ahsan, Particle size influences the immune response produced by Hepatitis B vaccine formulated in inhalable particles, Pharmaceutical Research, 27 (2010) 905-919.

[77] R.A. Rosalia, L.J. Cruz, S. van Duikeren, A.T. Tromp, A.L. Silva, W. Jiskoot, T. de Gruijl, C. Löwik, J. Oostendorp, S.H. van der Burg, F. Ossendorp, CD40-targeted dendritic cell delivery of PLGA-nanoparticle vaccines induce potent anti-tumor responses, Biomaterials, 40 (2015) 88-97.

[78] T.E. Rajapaksa, M. Stover-Hamer, X. Fernandez, H.A. Eckelhoefer, D.D. Lo, Claudin 4-targeted protein incorporated into PLGA nanoparticles can mediate M cell targeted delivery, Journal of Controlled Release, 142 (2010) 196-205.

[79] L.J. Cruz, P.J. Tacken, R. Fokkink, C.G. Figdor, The influence of PEG chain length and targeting moiety on antibody-mediated delivery of nanoparticle vaccines to human dendritic cells, Biomaterials, 32 (2011) 6791-6803.

[80] B. Carrillo-Conde, E.-H. Song, A. Chavez-Santoscoy, Y. Phanse, A.E. Ramer-Tait, N.L.B. Pohl, M.J. Wannemuehler, B.H. Bellaire, B. Narasimhan, Mannose-functionalized "pathogen-like" polyanhydride nanoparticles target C-Type lectin receptors on dendritic cells, Molecular Pharmaceutics, 8 (2011) 1877-1886.

[81] L.J. Cruz, P.J. Tacken, R. Fokkink, B. Joosten, M.C. Stuart, F. Albericio, R. Torensma, C.G. Figdor, Targeted PLGA nano- but not microparticles specifically deliver antigen to human dendritic cells via DC-SIGN in vitro, Journal of Controlled Release, 144 (2010) 118-126.

[82] A. Taghavi, B. Allan, G. Mutwiri, A. Van Kessel, P. Willson, L. Babiuk, A. Potter, S. Gomis, Protection of neonatal broiler chicks against Salmonella Typhimurium septicemia by DNA containing CpG motifs, Avian diseases, 52 (2008) 398-406.

[83] M.A. Volkova, A.V. Irza, I.A. Chvala, S.F. Frolov, V.V. Drygin, D.R. Kapczynski, Adjuvant effects of chitosan and calcium phosphate particles in an inactivated Newcastle disease vaccine, Avian diseases, 58 (2014) 46-52.

[84] L.-P. Tseng, C.-J. Chiou, C.-C. Chen, M.-C. Deng, T.-W. Chung, Y.-Y. Huang, D.-Z. Liu, Effect of lipopolysaccharide on intranasal administration of liposomal Newcastle disease virus vaccine to SPF chickens, Veterinary Immunology and Immunopathology, 131 (2009) 285-289.

[85] D.A. Zaharoff, C.J. Rogers, K.W. Hance, J. Schlom, J.W. Greiner, Chitosan solution enhances both humoral and cell-mediated immune responses to subcutaneous vaccination, Vaccine, 25 (2007) 2085-2094.

[86] V. Saluja, J.P. Amorij, J.C. Kapteyn, A.H. de Boer, H.W. Frijlink, W.L.J. Hinrichs, A comparison between spray drying and spray freeze drying to produce an influenza subunit vaccine powder for inhalation, Journal of Controlled Release, 144 (2010) 127-133.

[87] T. Sou, E.N. Meeusen, M. de Veer, D.A.V. Morton, L.M. Kaminskas, M.P. McIntosh, New developments in dry powder pulmonary vaccine delivery, Trends in Biotechnology, 29 (2011) 191-198.

[88] J.P. Amorij, V. Saluja, A.H. Petersen, W.L.J. Hinrichs, A. Huckriede, H.W. Frijlink, Pulmonary delivery of an inulin-stabilized influenza subunit vaccine prepared by spray-freeze drying induces systemic, mucosal humoral as well as cell-mediated immune responses in BALB/c mice, Vaccine, 25 (2007) 8707-8717.

[89] L. Garcia-Contreras, Y.-L. Wong, P. Muttil, D. Padilla, J. Sadoff, J. DeRousse, W.A. Germishuizen, S. Goonesekera, K. Elbert, B.R. Bloom, R. Miller, P.B. Fourie, A. Hickey, D. Edwards, Immunization by a bacterial aerosol, Proceedings of the National Academy of Sciences of the United States of America, 105 (2008) 4656-4660.

[90] S. Agarkhedkar, P.S. Kulkarni, S. Winston, R. Sievers, R.M. Dhere, B. Gunale, K. Powell, P.A. Rota, M. Papania, Safety and immunogenicity of dry powder measles vaccine administered by inhalation: A randomized controlled Phase I clinical trial, Vaccine, 32 (2014) 6791-6797.

[91] W. De Cort, F. Haesebrouck, R. Ducatelle, F. van Immerseel, Administration of a Salmonella Enteritidis DeltahilAssrAfliG strain by coarse spray to newly hatched broilers reduces colonization and shedding of a Salmonella Enteritidis challenge strain, Poultry science, 94 (2015) 131-135.

[92] K. Yaguchi, T. Ohgitani, T. Noro, T. Kaneshige, Y. Shimizu, Vaccination of chickens with liposomal inactivated avian pathogenic Escherichia coli (APEC) vaccine by eye drop or coarse spray administration, Avian diseases, 53 (2009) 245-249.

[93] J. Scheiermann, D.M. Klinman, Clinical evaluation of CpG oligonucleotides as adjuvants for vaccines targeting infectious diseases and cancer, Vaccine, 32 (2014) 6377-6389.

[94] S. Garlapati, R. Garg, R. Brownlie, L. Latimer, E. Simko, R.E.W. Hancock, L.A. Babiuk, V. Gerdts, A. Potter, S. van Drunen Littel-van den Hurk, Enhanced immune responses and protection by vaccination with respiratory syncytial virus fusion protein formulated with CpG oligodeoxynucleotide and innate defense regulator peptide in polyphosphazene microparticles, Vaccine, 30 (2012) 5206-5214.

[95] K.M. Mackinnon, H. He, C.L. Swaggerty, J.L. McReynolds, K.J. Genovese, S.E. Duke, J.R. Nerren, M.H. Kogut, In ovo treatment with CpG oligodeoxynucleotides decreases colonization of Salmonella enteriditis in broiler chickens, Veterinary Immunology and Immunopathology, 127 (2009) 371-375.

[96] S. Gomis, L. Babiuk, D.L. Godson, B. Allan, T. Thrush, H. Townsend, P. Willson, E. Waters, R. Hecker, A. Potter, Protection of chickens against Escherichia coli infections by DNA containing CpG motifs, Infection and Immunity, 71 (2003) 857-863.

[97] S.P. Kalhari Bandara Goonewardene, Thushari Gunwardana, Suresh Tikoo, Marianna Foldvari, Philip Willson, and Susantha Gomis, Immunoprotective effects against Escherichia coli septicemia in neonatal broiler chickens following intrapulmonary delivery of oligodeoxynucleotides containing CpG motifs (CpG-ODN) as micro-droplets (in preparation).

[98] K.B.G. Daniella Calderon, Susantha Gomis, Shelly Popowich, Thushari Gunawardana, Suresh Tikoo, Marianna Foldvari, Poultry vaccine nanoparticle design for inhalation: intrapulmonary delivery of oligodeoxynucleotides containing CpG motifs (CpG-ODN) in lipid-based and polymeric nanoparticles (in preparation).

[99] K. Goonewardene, S. Popowich, T. Gunwardana, A. Gupta, S. Kurukulasuriya, R. Karunarathna, B. Chow-Lockerbie, K.A. AHMED, S.K. Tikoo, M. Foldvari, P. Willson, S. Gomis, Intrapulmonary Delivery of CPG-ODN Micro-Droplets Provides Protection against Escherichia Coli Septicemia in Neonatal Broiler Chickens, Avian diseases, In Press.

[100] E.A. Corbanie, C. Vervaet, J.H.H. van Eck, J.P. Remon, W.J.M. Landman, Vaccination of broiler chickens with dispersed dry powder vaccines as an alternative for liquid spray and aerosol vaccination, Vaccine, 26 (2008) 4469-4476.

[101] J. Steitz, R.A. Wagner, T. Bristol, W. Gao, R.O. Donis, A. Gambotto, Assessment of route of administration and dose escalation for an adenovirus-based Influenza A Virus (H5N1) vaccine in chickens, Clinical and Vaccine Immunology, 17 (2010) 1467-1472.

[102] E.V.H. Katherine E. Quesenberg, Supportive care and Emergency Therapy, in: Avian Medicine, Iowa State University Press, 1994, pp. 9.

[103] R.B. Hayter, E.L. Besch, Airborne-particle deposition in the respiratory tract of chickens, Poultry science, 53 (1974) 1507-1511.

[104] E.A. Corbanie, M.G. Matthijs, J.H. van Eck, J.P. Remon, W.J. Landman, C. Vervaet, Deposition of differently sized airborne microspheres in the respiratory tract of chickens, Avian Pathol, 35 (2006) 475-485.

[105] S. Deville, J.B. Arous, F. Bertrand, V. Borisov, L. Dupuis, Efficacy of intranasal and spray delivery of adjuvanted live vaccine against infectious bronchitis virus in experimentally infected poultry, Procedia in Vaccinology, 6 (2012) 85-92.

[106] A. Sharma, A. Krause, Y. Xu, B. Sung, W. Wu, S. Worgall, Adenovirus-based vaccine with epitopes incorporated in novel fiber sites to induce protective immunity against Pseudomonas aeruginosa, PloS one, 8 (2013) e56996.

[107] M. Jeyanathan, Z. Shao, X. Yu, R. Harkness, R. Jiang, J. Li, Z. Xing, T. Zhu, AdHu5Ag85A respiratory mucosal boost immunization enhances protection against pulmonary tuberculosis in BCG-Primed Non-Human Primates, PloS one, 10 (2015) e0135009.

[108] M.W. Auten, W. Huang, G. Dai, A.J. Ramsay, CD40 ligand enhances immunogenicity of vector-based vaccines in immunocompetent and CD4+ T cell deficient individuals, Vaccine, 30 (2012) 2768-2777.

[109] Z. Xing, C.T. McFarland, J.M. Sallenave, A. Izzo, J. Wang, D.N. McMurray, Intranasal mucosal boosting with an adenovirus-vectored vaccine markedly enhances the protection of BCG-primed guinea pigs against pulmonary tuberculosis, PloS one, 4 (2009) e5856.

[110] M. Santosuosso, X. Zhang, S. McCormick, J. Wang, M. Hitt, Z. Xing, Mechanisms of mucosal and parenteral tuberculosis vaccinations: adenoviral-based mucosal immunization preferentially elicits sustained accumulation of immune protective CD4 and CD8 T cells within the airway lumen, Journal of Immunology, 174 (2005) 7986-7994.

[111] J. Mu, M. Jeyanathan, C.R. Shaler, C. Horvath, D. Damjanovic, A. Zganiacz, K. Kugathasan, S. McCormick, Z. Xing, Respiratory mucosal immunization with adenovirus gene transfer vector induces helper CD4 T cell-independent protective immunity, Journal of Gene Medicine, 12 (2010) 693-704.

[112] L.E. Ayalew, P. Kumar, A. Gaba, N. Makadiya, S.K. Tikoo, Bovine adenovirus-3 as a vaccine delivery vehicle, Vaccine, 33 (2015) 493-499.

[113] S. Gogev, N. Vanderheijden, M. Lemaire, F. Schynts, J. D'Offay, I. Deprez, M. Adam, M. Eloit, E. Thiry, Induction of protective immunity to bovine herpesvirus type 1 in cattle by intranasal administration of replication-defective human adenovirus type 5 expressing glycoprotein gC or gD, Vaccine, 20 (2002) 1451-1465.

[114] L.A. Babiuk, S.K. Tikoo, Adenoviruses as vectors for delivering vaccines to mucosal surfaces, Journal of Biotechnology, 83 (2000) 105-113.

[115] R. Brownlie, P. Kumar, L.A. Babiuk, S.K. Tikoo, Recombinant bovine adenovirus-3 co-expressing bovine respiratory syncytial virus glycoprotein G and truncated glycoprotein gD of bovine herpesvirus-1 induce immune responses in cotton rats, Molecular Biotechnology, 57 (2015) 58-64.

[116] P. Kumar, L.E. Ayalew, D.L. Godson, A. Gaba, L.A. Babiuk, S.K. Tikoo, Mucosal immunization of calves with recombinant bovine adenovirus-3 coexpressing truncated form of bovine herpesvirus-1 gD and bovine IL-6, Vaccine, 32 (2014) 3300-3306.

[117] A.N. Zakhartchouk, C. Pyne, G.K. Mutwiri, Z. Papp, M.E. Baca-Estrada, P. Griebel, L.A. Babiuk, S.K. Tikoo, Mucosal immunization of calves with recombinant bovine adenovirus-3: induction of protective immunity to bovine herpesvirus-1, Journal of General Virology, 80 (1999) 1263-1269.

[118] M. Trudel, G. Boulay, C. Seguin, F. Nadon, G. Lussier, Control of infectious bovine rhinotracheitis in calves with a BHV-1 subunit-ISCOM vaccine, Vaccine, 6 (1988) 525-529.

[119] S. Sjolander, D. Drane, R. Davis, L. Beezum, M. Pearse, J. Cox, Intranasal immunisation with influenza-ISCOM induces strong mucosal as well as systemic antibody and cytotoxic T-lymphocyte responses, Vaccine, 19 (2001) 4072-4080.

[120] A. Coulter, R. Harris, R. Davis, D. Drane, J. Cox, D. Ryan, P. Sutton, S. Rockman, M. Pearse, Intranasal vaccination with ISCOMATRIX adjuvanted influenza vaccine, Vaccine, 21 (2003) 946-949.

[121] A.G. Díaz, D.A. Quinteros, J.M. Llabot, S.D. Palma, D.A. Allemandi, G. Ghersi, V. Zylberman, F.A. Goldbaum, S.M. Estein, Spray dried microspheres based on chitosan: A promising new carrier for intranasal administration of polymeric antigen BLSOmp31 for prevention of ovine brucellosis, Materials Science and Engineering: C, 62 (2016) 489-496.

[122] F. Tajdini, M.A. Amini, A.R. Mokarram, M. Taghizadeh, S.M. Azimi, Foot and Mouth Disease virus-loaded fungal chitosan nanoparticles for intranasal administration: impact of formulation on physicochemical and immunological characteristics, Pharmaceutical Development and Technology, 19 (2014) 333-341.

[123] M.J. Santander-Ortega, J.M. Peula-García, F.M. Goycoolea, J.L. Ortega-Vinuesa, Chitosan nanocapsules: Effect of chitosan molecular weight and acetylation degree on electrokinetic behaviour and colloidal stability, Colloids and Surfaces B: Biointerfaces, 82 (2011) 571-580.

[124] C. Çokçalışkan, F. Özyörük, R.N. Gürsoy, M. Alkan, M. Günbeyaz, H.Ç. Arca, E. Uzunlu, S. Şenel, Chitosan-based systems for intranasal immunization against foot-and-mouth disease, Pharmaceutical Development and Technology, 19 (2014) 181-188.

[125] M.C. Rebelatto, P. Guimond, T.L. Bowersock, H. HogenEsch, Induction of systemic and mucosal immune response in cattle by intranasal administration of pig serum albumin in alginate microparticles, Veterinary Immunology and Immunopathology, 83 (2001) 93-105.

[126] A.C. Stanley, D. Buxton, E.A. Innes, J.F. Huntley, Intranasal immunisation with Toxoplasma gondii tachyzoite antigen encapsulated into PLG microspheres induces humoral and cell-mediated immunity in sheep, Vaccine, 22 (2004) 3929-3941.

[127] H.S. Choi, Y. Ashitate, J.H. Lee, S.H. Kim, A. Matsui, N. Insin, M.G. Bawendi, M. Semmler-Behnke, J.V. Frangioni, A. Tsuda, Rapid translocation of nanoparticles from the lung airspaces to the body, Nature Biotechnology, 28 (2010) 1300-1303.

[128] J.N. Maina, Structural and Biomechanical Properties of the Exchange Tissue of the Avian Lung, Anatomical Record (Hoboken), 298 (2015) 1673-1688.

[129] W. Bernhard, A. Gebert, G. Vieten, G.A. Rau, J.M. Hohlfeld, A.D. Postle, J. Freihorst, Pulmonary surfactant in birds: coping with surface tension in a tubular lung, American Journal of Physiology - Regulatory, Integrative and Comparative Physiology, 281 (2001) R327-R337.

[130] L.A. Tell, S. Smiley-Jewell, D. Hinds, K.E. Stephens, S.V. Teague, C.G. Plopper, K.E. Pinkerton, An aerosolized fluorescent microsphere technique for evaluating particle deposition in the avian respiratory tract, Avian diseases, 50 (2006) 238-244.

[131] E.A. Corbanie, M.G.R. Matthijs, J.H.H. van Eck, J.P. Remon, W.J.M. Landman, C. Vervaet, Deposition of differently sized airborne microspheres in the respiratory tract of chickens, Avian Pathology, 35 (2006) 475-485.

[132] S.S.A.A. Hasson, J.K.Z. Al-Busaidi, T.A. Sallam, The past, current and future trends in DNA vaccine immunisations, Asian Pacific Journal of Tropical Biomedicine, 5 (2015) 344-353.

[133] J.B. Ulmer, U. Valley, R. Rappuoli, Vaccine manufacturing: challenges and solutions, Nature Biotechnology, 24 (2006) 1377-1383.

[134] L. Zhao, A. Seth, N. Wibowo, C.-X. Zhao, N. Mitter, C. Yu, A.P.J. Middelberg, Nanoparticle vaccines, Vaccine, 32 (2014) 327-337.

[135] J. Scheiermann, D.M. Klinman, Clinical evaluation of CpG oligonucleotides as adjuvants for vaccines targeting infectious diseases and cancer, Vaccine, 32 (2014) 6377-6389.

[136] A. Bhat, S. Gomis, A. Potter, S.K. Tikoo, Role of Hsp90 in CpG ODN mediated immunostimulation in avian macrophages, Molecular Immunology, 47 (2010) 1337-1346.

[137] B.A. Patel, S. Gomis, A. Dar, P.J. Willson, L.A. Babiuk, A. Potter, G. Mutwiri, S.K. Tikoo, Oligodeoxynucleotides containing CpG motifs (CpG-ODN) predominantly induce Th1-type immune response in neonatal chicks, Developmental and comparative immunology, 32 (2008) 1041-1049.

[138] J. Fu, J. Liang, H. Kang, J. Lin, Q. Yu, Q. Yang, Effects of different CpG oligodeoxynucleotides with inactivated avian H5N1 influenza virus on mucosal immunity of chickens, Poultry science, 92 (2013) 2866-2875.

[139] S. Chen, A. Cheng, M. Wang, Innate sensing of viruses by pattern recognition receptors in birds, Veterinary research, 44 (2013) 82-82.

[140] R. Brownlie, J. Zhu, B. Allan, G.K. Mutwiri, L.A. Babiuk, A. Potter, P. Griebel, Chicken TLR21 acts as a functional homologue to mammalian TLR9 in the recognition of CpG oligodeoxynucleotides, Molecular Immunology, 46 (2009) 3163-3170.

[141] C. Ciraci, S.J. Lamont, Avian-specific TLRs and downstream effector responses to CpG-induction in chicken macrophages, Developmental and comparative immunology, 35 (2011) 392-398.

[142] C. Ciraci, S.J. Lamont, The Regulatory Mechanism of Response to CpG-ODN, a Pathogen-derived Molecule, in Chicken Macrophages, Animal Industry Report, (2011) AS 657, ASL R2617. .

[143] A.M. Keestra, M.R. de Zoete, L.I. Bouwman, J.P. van Putten, Chicken TLR21 is an innate CpG DNA receptor distinct from mammalian TLR9, Journal of Immunology, 185 (2010) 460-467.

[144] H. He, M.H. Kogut, CpG-ODN-induced nitric oxide production is mediated through clathrin-dependent endocytosis, endosomal maturation, and activation of PKC, MEK1/2 and p38 MAPK, and NF-kappaB pathways in avian macrophage cells (HD11), Cellular signalling, 15 (2003) 911-917.

[145] H. He, K.M. MacKinnon, K.J. Genovese, M.H. Kogut, CpG oligodeoxynucleotide and double-stranded RNA synergize to enhance nitric oxide production and mRNA expression of inducible nitric oxide synthase, pro-inflammatory cytokines and chemokines in chicken monocytes, Innate Immunity, 17 (2011) 137-144.

[146] H. Xie, R.B. Raybourne, U.S. Babu, H.S. Lillehoj, R.A. Heckert, CpG-induced immunomodulation and intracellular bacterial killing in a chicken macrophage cell line, Developmental & Comparative Immunology, 27 (2003) 823-834.

[147] H. He, T.L. Crippen, M.B. Farnell, M.H. Kogut, Identification of CpG oligodeoxynucleotide motifs that stimulate nitric oxide and cytokine production in avian macrophage and peripheral blood mononuclear cells, Developmental & Comparative Immunology, 27 (2003) 621-627.

[148] A. Dar, A. Potter, S. Tikoo, V. Gerdts, K. Lai, L.A. Babiuk, G. Mutwiri, CpG oligodeoxynucleotides activate innate immune response that suppresses infectious bronchitis virus replication in chicken embryos, Avian diseases, 53 (2009) 261-267.

[149] C.A. Ruge, J. Kirch, C.M. Lehr, Pulmonary drug delivery: from generating aerosols to overcoming biological barriers-therapeutic possibilities and technological challenges, Lancet Respiratory Medicine, 1 (2013) 402-413.

[150] M. Dho-Moulin, J.M. Fairbrother, Avian pathogenic Escherichia coli (APEC), Veterinary research, 30 (1999) 299-316.

[151] N.R. Labiris, M.B. Dolovich, Pulmonary drug delivery. Part I: Physiological factors affecting therapeutic effectiveness of aerosolized medications, British Journal of Clinical Pharmacology, 56 (2003) 588-599.

[152] M.B. Dolovich, R. Dhand, Aerosol drug delivery: developments in device design and clinical use, The Lancet, 377 (2011) 1032-1045.

[153] W.H. Finlay, 8 - Jet nebulizers, in: W.H. Finlay (Ed.) The Mechanics of Inhaled Pharmaceutical Aerosols, Academic Press, London, 2001, pp. 175-220.

[154] C.F. MacNeish, D. Meisner, R. Thibert, S. Kelemen, E.B. Vadas, A.L. Coates, A comparison of pulmonary availability between Ventolin (albuterol) nebules and Ventolin (albuterol) Respirator Solution, Chest, 111 (1997) 204-208.

[155] S. Akapo, J. Gupta, E. Martinez, C. McCrea, L. Ye, M. Roach, Compatibility and aerosol characteristics of formoterol fumarate mixed with other nebulizing solutions, Annals of Pharmacotherapy, 42 (2008) 1416-1424.

[156] W. Kamin, A. Schwabe, I. Kramer, Inhalation solutions: which one are allowed to be mixed? Physico-chemical compatibility of drug solutions in nebulizers, J Cyst Fibros, 5 (2006) 205-213.

[157] W. Kamin, F. Erdnüss, I. Krämer, Inhalation solutions — Which ones may be mixed? Physico-chemical compatibility of drug solutions in nebulizers — Update 2013, Journal of Cystic Fibrosis, 13 (2014) 243-250.

[158] W. Kamin, A. Schwabe, I. Krämer, Inhalation solutions: which one are allowed to be mixed? Physico-chemical compatibility of drug solutions in nebulizers, Journal of Cystic Fibrosis, 5 (2006) 205-213.

[159] M.R. Fedde, Relationship of structure and function of the avian respiratory system to disease susceptibility, Poultry science, 77 (1998) 1130-1138.

[160] R.E. Brown, J.D. Brain, N. Wang, The avian respiratory system: a unique model for studies of respiratory toxicosis and for monitoring air quality, Environmental Health Perspectives, 105 (1997) 188-200.

[161] H.R. Duncker, Structure of the avian respiratory tract, Respiration Physiology, 22 (1974) 1-19.

[162] E.D. de Geus, C.A. Jansen, L. Vervelde, Uptake of Particulate Antigens in a Nonmammalian Lung: Phenotypic and Functional Characterization of Avian Respiratory Phagocytes Using Bacterial or Viral Antigens, The Journal of Immunology, 188 (2012) 4516-4526.

[163] J. Kirch, A. Schneider, B. Abou, A. Hopf, U.F. Schaefer, M. Schneider, C. Schall, C. Wagner, C.M. Lehr, Optical tweezers reveal relationship between microstructure and nanoparticle penetration of pulmonary mucus, Proceedings of the Natural Academy of Sciences U S A, 109 (2012) 18355-18360.

[164] C.A. Ruge, U.F. Schaefer, J. Herrmann, J. Kirch, O. Canadas, M. Echaide, J. Perez-Gil, C. Casals, R. Muller, C.M. Lehr, The interplay of lung surfactant proteins and lipids assimilates the macrophage clearance of nanoparticles, PloS one, 7 (2012) e40775.

[165] W. Liang, P.C. Kwok, M.Y. Chow, P. Tang, A.J. Mason, H.K. Chan, J.K. Lam, Formulation of pH responsive peptides as inhalable dry powders for pulmonary delivery of nucleic acids, European Journal of Pharmaceutics and Biopharmaceutics, 86 (2014) 64-73.

[166] C. de Souza Carvalho, N. Daum, C.M. Lehr, Carrier interactions with the biological barriers of the lung: advanced in vitro models and challenges for pulmonary drug delivery, Advanced Drug Delivery Reviews, 75 (2014) 129-140.

[167] S. Härtle, B. Kaspers, Chapter 14 - The Avian Respiratory Immune System, in: Avian Immunology (Second Edition), Academic Press, Boston, 2014, pp. 251-263.

[168] A.Z. Wilczewska, K. Niemirowicz, K.H. Markiewicz, H. Car, Nanoparticles as drug delivery systems, Pharmacological Reports, 64 (2012) 1020-1037.

[169] D. Mishra, J.R. Hubenak, A.B. Mathur, Nanoparticle systems as tools to improve drug delivery and therapeutic efficacy, Journal of Biomedical Materials Research A, 101 (2013) 3646-3660.

[170] S. Roy, K. Pal, A. Anis, K. Pramanik, B. Prabhakar, Polymers in Mucoadhesive Drug-Delivery Systems: A Brief Note, Designed Monomers and Polymers, 12 (2009) 483-495.

[171] H.O. Alpar, S. Somavarapu, K.N. Atuah, V.W. Bramwell, Biodegradable mucoadhesive particulates for nasal and pulmonary antigen and DNA delivery, Advanced Drug Delivery Reviews, 57 (2005) 411-430.

[172] S.K. Lai, D.E. O'Hanlon, S. Harrold, S.T. Man, Y.Y. Wang, R. Cone, J. Hanes, Rapid transport of large polymeric nanoparticles in fresh undiluted human mucus, Proceedings of the National Academy of Sciences of the U S A, 104 (2007) 1482-1487.

[173] H. Yamamoto, Y. Kuno, S. Sugimoto, H. Takeuchi, Y. Kawashima, Surface-modified PLGA nanosphere with chitosan improved pulmonary delivery of calcitonin by mucoadhesion and opening of the intercellular tight junctions, Journal of Controlled Release, 102 (2005) 373-381.

[174] U. Griesenbach, C. Meng, R. Farley, M.Y. Wasowicz, F.M. Munkonge, M. Chan, C. Stoneham, S.G. Sumner-Jones, I.A. Pringle, D.R. Gill, S.C. Hyde, B. Stevenson, E. Holder, H. Ban, M. Hasegawa, S.H. Cheng, R.K. Scheule, P.L. Sinn, P.B. McCray, Jr., E.W. Alton, The use of carboxymethylcellulose gel to increase non-viral gene transfer in mouse airways, Biomaterials, 31 (2010) 2665-2672.

[175] C. Kelly, A.B. Yadav, C. Lawlor, K. Nolan, J. O'Dwyer, C.M. Greene, N.G. McElvaney, N. Sivadas, J.M. Ramsey, S.A. Cryan, Therapeutic aerosol bioengineering of siRNA for the treatment of inflammatory lung disease by TNFalpha gene silencing in macrophages, Molecular Pharmaceutics, 11 (2014) 4270-4279.

[176] E.H. Lin, H.Y. Chang, S.D. Yeh, K.Y. Yang, H.S. Hu, C.W. Wu, Polyethyleneimine and DNA nanoparticles-based gene therapy for acute lung injury, Nanomedicine : nanotechnology, biology, and medicine, 9 (2013) 1293-1303.

[177] A. Dube, J.L. Reynolds, W.C. Law, C.C. Maponga, P.N. Prasad, G.D. Morse, Multimodal nanoparticles that provide immunomodulation and intracellular drug delivery for infectious diseases, Nanomedicine : nanotechnology, biology, and medicine, 10 (2014) 831-838.

[178] J.F. Mann, P.F. McKay, S. Arokiasamy, R.K. Patel, K. Klein, R.J. Shattock, Pulmonary delivery of DNA vaccine constructs using deacylated PEI elicits immune responses and protects against viral challenge infection, Journal of Controlled Release, 170 (2013) 452-459.

[179] M. Bivas-Benita, M.Y. Lin, S.M. Bal, K.E. van Meijgaarden, K.L. Franken, A.H. Friggen, H.E. Junginger, G. Borchard, M.R. Klein, T.H. Ottenhoff, Pulmonary delivery of DNA encoding Mycobacterium tuberculosis latency antigen Rv1733c associated to PLGA-PEI nanoparticles enhances T cell responses in a DNA prime/protein boost vaccination regimen in mice, Vaccine, 27 (2009) 4010-4017.

[180] L. Wasungu, D. Hoekstra, Cationic lipids, lipoplexes and intracellular delivery of genes, Journal of Controlled Release, 116 (2006) 255-264.

[181] A.J. Kirby, P. Camilleri, J.B.F.N. Engberts, M.C. Feiters, R.J.M. Nolte, O. Söderman, M. Bergsma, P.C. Bell, M.L. Fielden, C.L. García Rodríguez, P. Guédat, A. Kremer, C. McGregor, C. Perrin, G. Ronsin, M.C.P. van Eijk, Gemini surfactants: new synthetic vectors for gene transfection, Angewandte Chemie International Edition, 42 (2003) 1448-1457.

[182] S. Alqawlaq, J.M. Sivak, J.T. Huzil, M.V. Ivanova, J.G. Flanagan, M.A. Beazely, M. Foldvari, Preclinical development and ocular biodistribution of gemini-DNA nanoparticles after intravitreal and topical administration: Towards non-invasive glaucoma gene therapy, Nanomedicine: Nanotechnology, Biology and Medicine, 10 (2014) 1637-1647.

[183] M. Rajesh, J. Sen, M. Srujan, K. Mukherjee, B. Sreedhar, A. Chaudhuri, Dramatic influence of the orientation of linker between hydrophilic and hydrophobic lipid moiety in liposomal gene gelivery, Journal of the American Chemical Society, 129 (2007) 11408-11420.

[184] P. Yang, J. Singh, S. Wettig, M. Foldvari, R.E. Verrall, I. Badea, Enhanced gene expression in epithelial cells transfected with amino acid-substituted gemini nanoparticles, European Journal of Pharmaceutics and Biopharmaceutics, 75 (2010) 311-320.

[185] C. Bombelli, L. Giansanti, P. Luciani, G. Mancini, Gemini surfactant based carriers in gene and drug delivery, Current Medicinal Chemistry, 16 (2009) 171-183.

[186] I. Badea, R. Verrall, M. Baca-Estrada, S. Tikoo, A. Rosenberg, P. Kumar, M. Foldvari, In vivo cutaneous interferon-γ gene delivery using novel dicationic (gemini) surfactant–plasmid complexes, The journal of gene medicine, 7 (2005) 1200-1214.

[187] I. Badea, S. Wettig, R. Verrall, M. Foldvari, Topical non-invasive gene delivery using gemini nanoparticles in interferon-gamma-deficient mice, European Journal of Pharmaceutics and Biopharmaceutics, 65 (2007) 414-422.

[188] H.-Q. Mao, K. Roy, V.L. Troung-Le, K.A. Janes, K.Y. Lin, Y. Wang, J.T. August, K.W. Leong, Chitosan-DNA nanoparticles as gene carriers: synthesis, characterization and transfection efficiency, Journal of Controlled Release, 70 (2001) 399-421.

[189] M. Huang, C.W. Fong, E. Khor, L.Y. Lim, Transfection efficiency of chitosan vectors: effect of polymer molecular weight and degree of deacetylation, Journal of Controlled Release, 106 (2005) 391-406.

[190] T. Sato, T. Ishii, Y. Okahata, In vitro gene delivery mediated by chitosan. effect of pH, serum, and molecular mass of chitosan on the transfection efficiency, Biomaterials, 22 (2001) 2075-2080.

[191] M. Koping-Hoggard, I. Tubulekas, H. Guan, K. Edwards, M. Nilsson, K.M. Varum, P. Artursson, Chitosan as a nonviral gene delivery system. Structure-property relationships and characteristics compared with polyethylenimine in vitro and after lung administration in vivo, The Journal of Gene Therapy, 8 (2001) 1108-1121.

[192] X. Liu, K.A. Howard, M. Dong, M.O. Andersen, U.L. Rahbek, M.G. Johnsen, O.C. Hansen, F. Besenbacher, J. Kjems, The influence of polymeric properties on chitosan/siRNA nanoparticle formulation and gene silencing, Biomaterials, 28 (2007) 1280-1288.

[193] S. Danielsen, S. Strand, C. de Lange Davies, B.T. Stokke, Glycosaminoglycan destabilization of DNA–chitosan polyplexes for gene delivery depends on chitosan chain length and GAG properties, Biochimica et Biophysica Acta (BBA) - General Subjects, 1721 (2005) 44-54.

[194] P. Erbacher, S. Zou, T. Bettinger, A.M. Steffan, J.S. Remy, Chitosan-based vector/DNA complexes for gene delivery: biophysical characteristics and transfection ability, Pharmaceutical Research, 15 (1998) 1332-1339.

[195] M. Koping-Hoggard, Y.S. Mel'nikova, K.M. Varum, B. Lindman, P. Artursson, Relationship between the physical shape and the efficiency of oligomeric chitosan as a gene delivery system in vitro and in vivo, The journal of gene medicine, 5 (2003) 130-141.

[196] W. Liu, S. Sun, Z. Cao, X. Zhang, K. Yao, W.W. Lu, K.D.K. Luk, An investigation on the physicochemical properties of chitosan/DNA polyelectrolyte complexes, Biomaterials, 26 (2005) 2705-2711.

[197] P. Schwille, Fluorescence correlation spectroscopy and its potential for intracellular applications, Cell Biochemistry and Biophysics, 34 (2001) 383-408.

[198] H. Beug, A. von Kirchbach, G. Doderlein, J.F. Conscience, T. Graf, Chicken hematopoietic cells transformed by seven strains of defective avian leukemia viruses display three distinct phenotypes of differentiation, Cell, 18 (1979) 375-390.

[199] K.C. Klasing, Avian macrophages: regulators of local and systemic immune responses, Poultry science, 77 (1998) 983-989.

[200] M. Huang, E. Khor, L.-Y. Lim, Uptake and cytotoxicity of chitosan molecules and nanoparticles: effects of molecular weight and degree of deacetylation, Pharmaceutical Research, 21 (2004) 344-353.

[201] M. Gilar, UPLC Analysis of Phosphorothioate Oligonucleotides: Method Development, in: W. Corporation (Ed.) Oligonucleotide Analysis Solutions, Milford, MA, U.S., 2017.

[202] D.M. Klinman, Immunotherapeutic uses of CpG oligodeoxynucleotides, Nature Reviews Immunology, 4 (2004) 249-259.

[203] M. Gharagozloo, A. Rafiee, D.W. Chen, M. Foldvari, A flow cytometric approach to study the mechanism of gene delivery to cells by gemini-lipid nanoparticles: an implication for cell membrane nanoporation, Journal of Nanobiotechnology, 13 (2015) 62.

[204] R.M. Zucker, E.J. Massaro, K.M. Sanders, L.L. Degn, W.K. Boyes, Detection of TiO2 nanoparticles in cells by flow cytometry, Cytometry Part A, 77A (2010) 677-685.

[205] D. Wlodkowic, W. Telford, J. Skommer, Z. Darzynkiewicz, Apoptosis and beyond: cytometry in studies of programmed cell death, Methods in Cell Biology, 103 (2011) 55-98.

[206] I. Badea, R. Verrall, M. Baca-Estrada, S. Tikoo, A. Rosenberg, P. Kumar, M. Foldvari, In vivo cutaneous interferon-gamma gene delivery using novel dicationic (gemini) surfactant-plasmid complexes, The journal of gene medicine, 7 (2005) 1200-1214.

[207] T.S. and, L.D. Shea, Materials for non-viral gene delivery, Annual Review of Materials Research, 31 (2001) 25-46.

[208] C. Dong, I. Badea, M. Poorghorban, R. Verrall, M. Foldvari, Impact of phospholipids on plasmid packaging and toxicity of gemini nanoparticles, Journal of materials chemistry. B, Materials for biology and medicine, 3 (2015) 8806-8822.

[209] S. Falsini, E. Di Cola, M. In, M. Giordani, S. Borocci, S. Ristori, Complexation of short ds RNA/DNA oligonucleotides with Gemini micelles: a time resolved SAXS and computational study, Physical Chemistry Chemical Physics, 19 (2017) 3046-3055.

[210] K. Giri, K. Shameer, M.T. Zimmermann, S. Saha, P.K. Chakraborty, A. Sharma, R.R. Arvizo, B.J. Madden, D.J. McCormick, J.-P.A. Kocher, R. Bhattacharya, P. Mukherjee, Understanding Protein–Nanoparticle Interaction: A New Gateway to Disease Therapeutics, Bioconjugate Chemistry, 25 (2014) 1078-1090.

[211] M. Gaumet, A. Vargas, R. Gurny, F. Delie, Nanoparticles for drug delivery: The need for precision in reporting particle size parameters, European Journal of Pharmaceutics and Biopharmaceutics, 69 (2008) 1-9.

[212] R.C. Rowe, P.J. Sheskey, S.n.C. Owen, A. American Pharmacists, Handbook of pharmaceutical excipients, APhA/Pharmaceutical Press, London; Chicago, 2009.

[213] W. Walther, U. Stein, C. Voss, T. Schmidt, M. Schleef, P.M. Schlag, Stability analysis for long-term storage of naked DNA: impact on nonviral in vivo gene transfer, Analytical biochemistry, 318 (2003) 230-235.

[214] E. Lai, J.H. van Zanten, Evidence of lipoplex dissociation in liquid formulations, Journal of pharmaceutical sciences, 91 (2002) 1225-1232.

[215] W. Mohammed-Saeid, D. Michel, A. El-Aneed, R.E. Verrall, N.H. Low, I. Badea, Development of lyophilized gemini surfactant-based gene delivery systems: influence of lyophilization on the structure, activity and stability of the lipoplexes, Journal of Pharmacy and Pharmaceutical Sciences, 15 (2012) 548-567.

[216] M.F. Bachmann, G.T. Jennings, Vaccine delivery: a matter of size, geometry, kinetics and molecular patterns, Nature Reviews Immunology, 10 (2010) 787-796.

[217] V. Manolova, Nanoparticles target distinct dendritic cell populations according to their size, European Journal of Immunology, 38 (2008) 1404-1413.

[218] D. Vercauteren, J. Rejman, T.F. Martens, J. Demeester, S.C. De Smedt, K. Braeckmans, On the cellular processing of non-viral nanomedicines for nucleic acid delivery: mechanisms and methods, Journal of Controlled Release, 161 (2012) 566-581.

[219] Z. Du, M.M. Munye, A.D. Tagalakis, M.D.I. Manunta, S.L. Hart, The role of the helper lipid on the DNA transfection efficiency of lipopolyplex formulations, Scientific Reports, 4 (2014) 7107.

[220] M. Huang, C.-W. Fong, E. Khor, L.-Y. Lim, Transfection efficiency of chitosan vectors: Effect of polymer molecular weight and degree of deacetylation, Journal of Controlled Release, 106 (2005) 391-406.

[221] F. Rauw, Y. Gardin, V. Palya, S. Anbari, M. Gonze, S. Lemaire, T. van den Berg, B. Lambrecht, The positive adjuvant effect of chitosan on antigen-specific cell-mediated immunity after chickens vaccination with live Newcastle disease vaccine, Veterinary Immunology and Immunopathology, 134 (2010) 249-258.

[222] G. Gafvelin, H. Grönlund, Chitosan-based adjuvants, in: M. Giese (Ed.) Molecular Vaccines: From Prophylaxis to Therapy - Volume 2, Springer International Publishing, Cham, 2014, pp. 623-631.

[223] R.A. Hunter, W.L. Storm, P.N. Coneski, M.H. Schoenfisch, Inaccuracies of Nitric Oxide measurement methods in biological media, Analytical Chemistry, 85 (2013) 1957-1963.

[224] H. Lv, S. Zhang, B. Wang, S. Cui, J. Yan, Toxicity of cationic lipids and cationic polymers in gene delivery, Journal of Controlled Release, 114 (2006) 100-109.

[225] J.S. Suk, Q. Xu, N. Kim, J. Hanes, L.M. Ensign, PEGylation as a strategy for improving nanoparticle-based drug and gene delivery, Advanced Drug Delivery Reviews, 99 (2016) 28-51.

[226] M.R. Lorenz, V. Holzapfel, A. Musyanovych, K. Nothelfer, P. Walther, H. Frank, K. Landfester, H. Schrezenmeier, V. Mailänder, Uptake of functionalized, fluorescent-labeled polymeric particles in different cell lines and stem cells, Biomaterials, 27 (2006) 2820-2828.

[227] W. Pendergrass, N. Wolf, M. Poot, Efficacy of MitoTracker Green and CMXrosamine to measure changes in mitochondrial membrane potentials in living cells and tissues, Cytometry. Part A : the journal of the International Society for Analytical Cytology, 61 (2004) 162-169.

[228] J.D. Evans, S.A. Leigh, J.L. Purswell, S.D. Collier, E.J. Kim, D.L. Boykin, S.L. Branton, The impact of deposition site on vaccination efficiency of a live bacterial poultry vaccine1, Poultry science, 94 (2015) 1849-1852.

[229] S.M. Singh, T.N. Alkie, É. Nagy, R.R. Kulkarni, D.C. Hodgins, S. Sharif, Delivery of an inactivated avian influenza virus vaccine adjuvanted with poly(D,L-lactic-co-glycolic acid) encapsulated CpG ODN induces protective immune responses in chickens, Vaccine, 34 (2016) 4807-4813.

[230] M.C. Cruz-Romero, T. Murphy, M. Morris, E. Cummins, J.P. Kerry, Antimicrobial activity of chitosan, organic acids and nano-sized solubilisates for potential use in smart antimicrobially-active packaging for potential food applications, Food Control, 34 (2013) 393-397.

[231] N. Liu, X.-G. Chen, H.-J. Park, C.-G. Liu, C.-S. Liu, X.-H. Meng, L.-J. Yu, Effect of MW and concentration of chitosan on antibacterial activity of Escherichia coli, Carbohydrate Polymers, 64 (2006) 60-65.

[232] K.W. Kim, B.J. Min, Y.-T. Kim, R.M. Kimmel, K. Cooksey, S.I. Park, Antimicrobial activity against foodborne pathogens of chitosan biopolymer films of different molecular weights, LWT - Food Science and Technology, 44 (2011) 565-569.

Appendix

A.1 Particle size distribution graphs

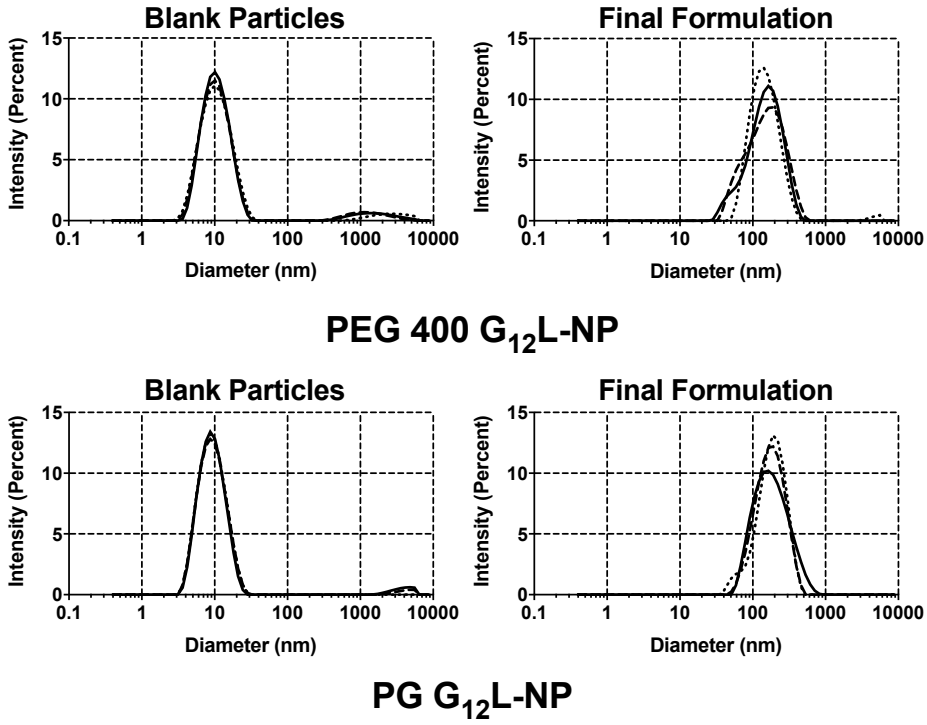

Figure 58 Size distribution by intensity for GL-NP blank particles and final CpG-ODN formulations formulated in PEG400 (top) and PG (bottom) excipients

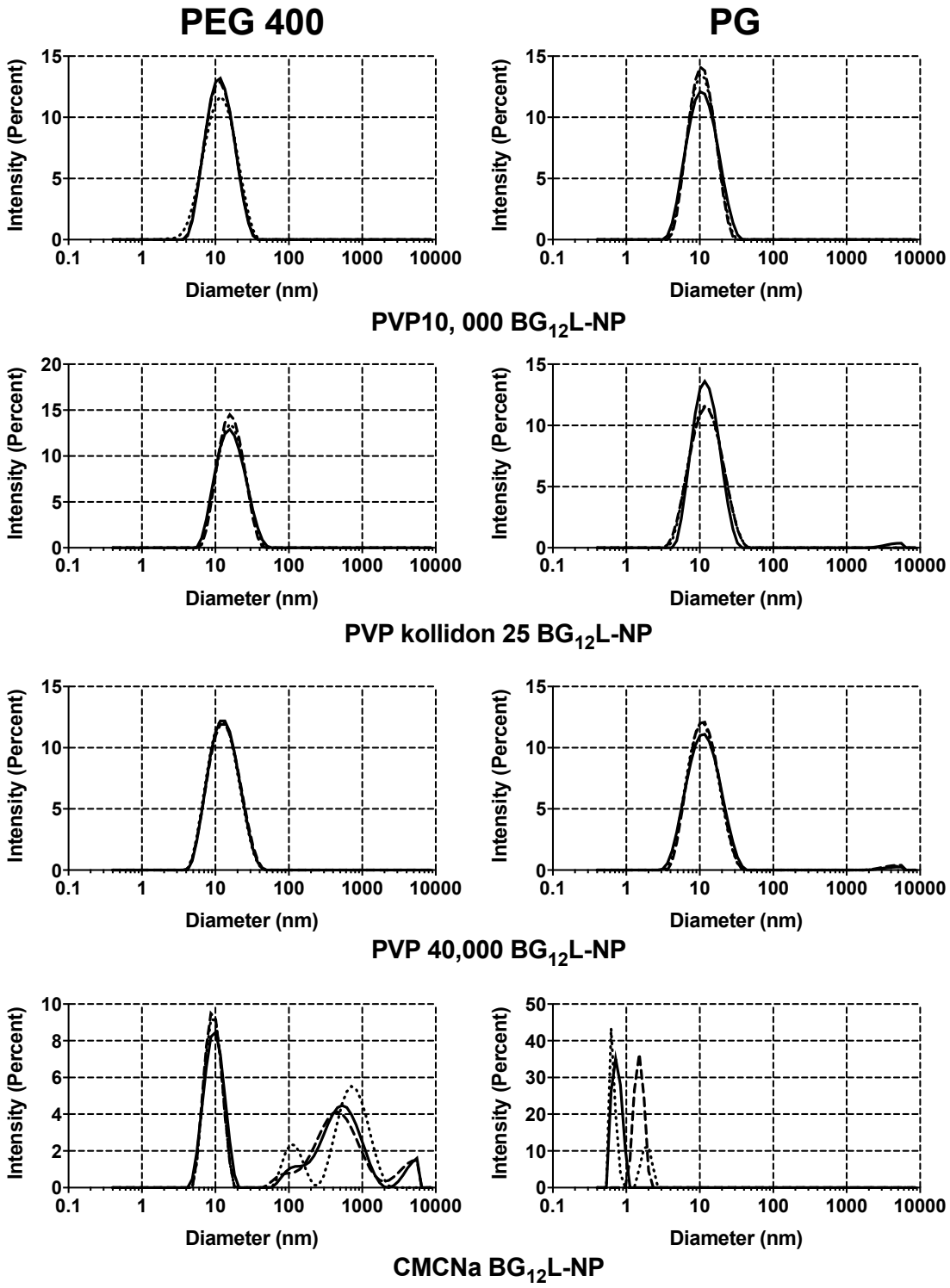

Figure 59 Size distribution by intensity for BG_{12}L-NP blank particles in PEG400 (left column) and PG (right column) excipients

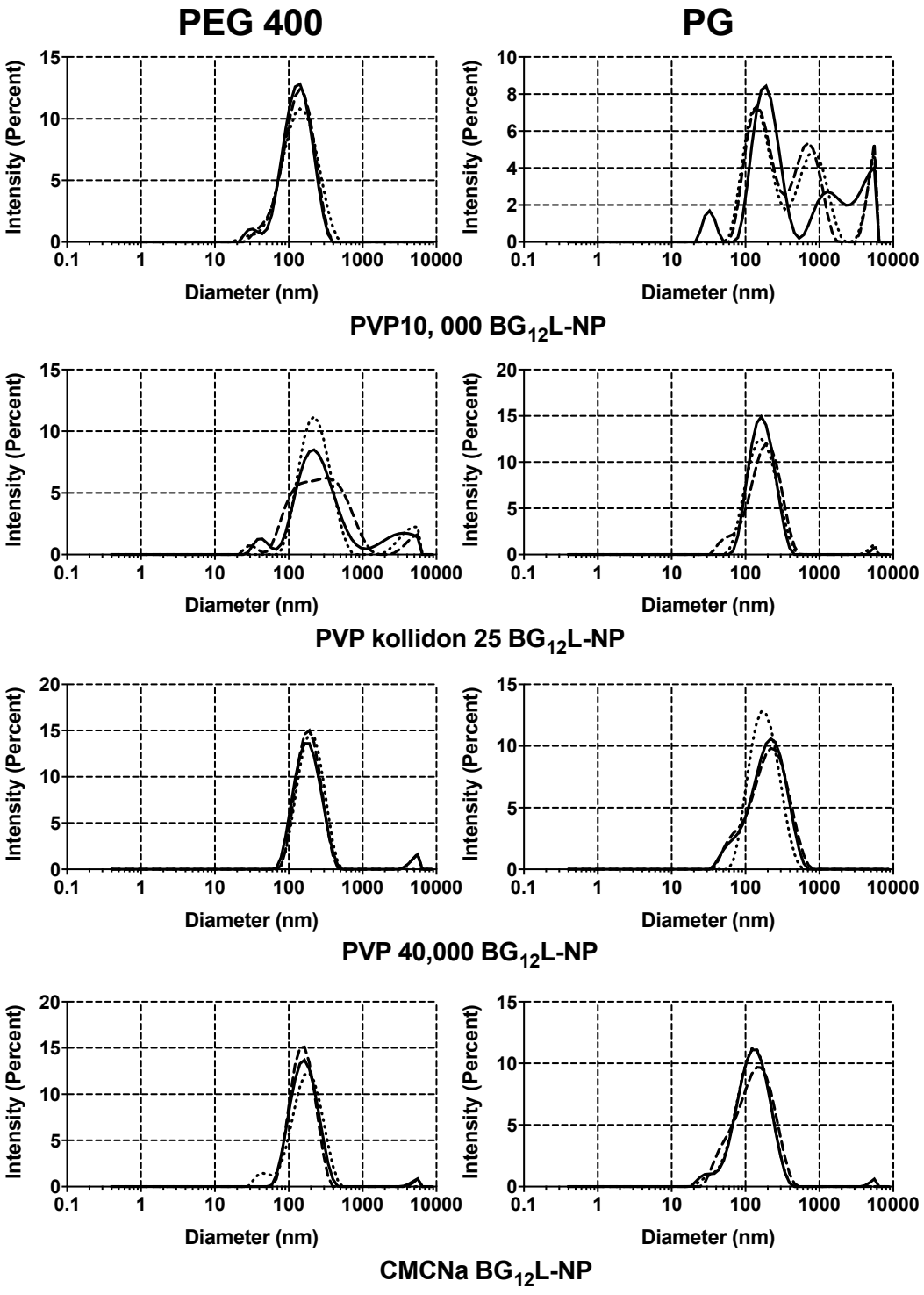

Figure 60 Size distribution by intensity for BG_{12}L-NP final formulations in PEG400 (left column) and PG (right column) excipients

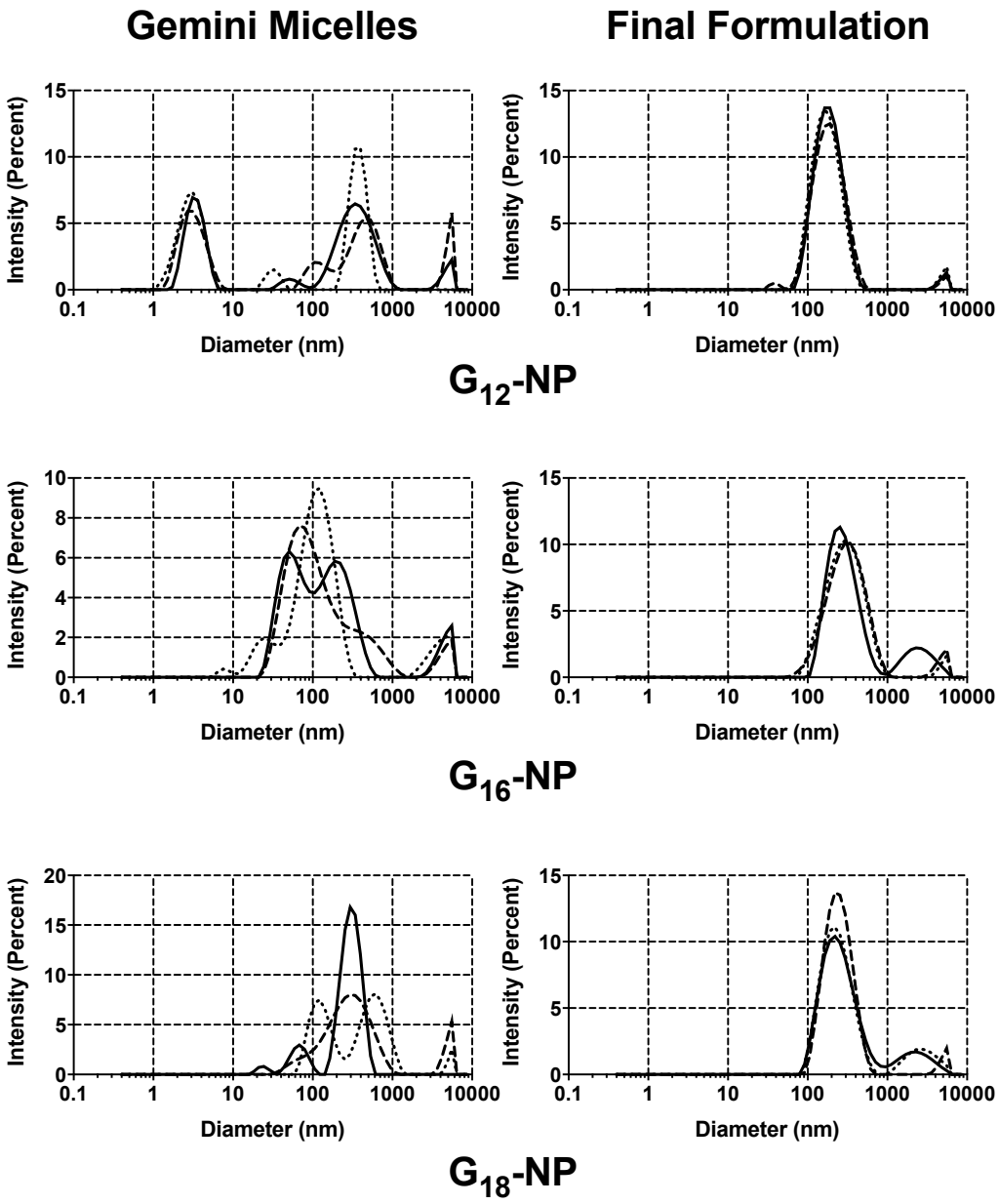

Figure 61 Size distribution by intensity for gemini micelles (left column) and final gemini CpG-ODN complexes (right column)

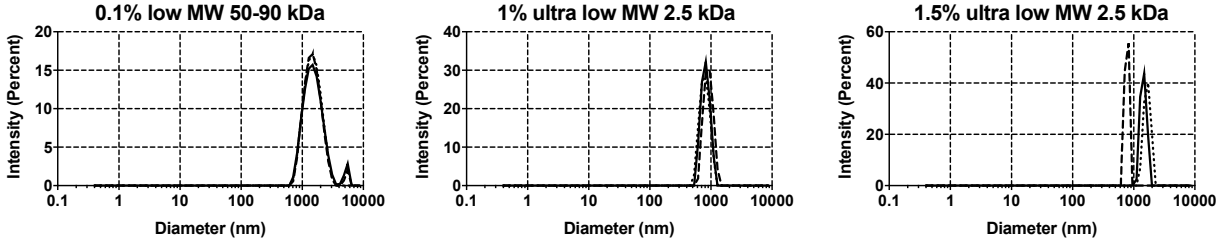

Figure 62 Size distribution by intensity for C-NPs

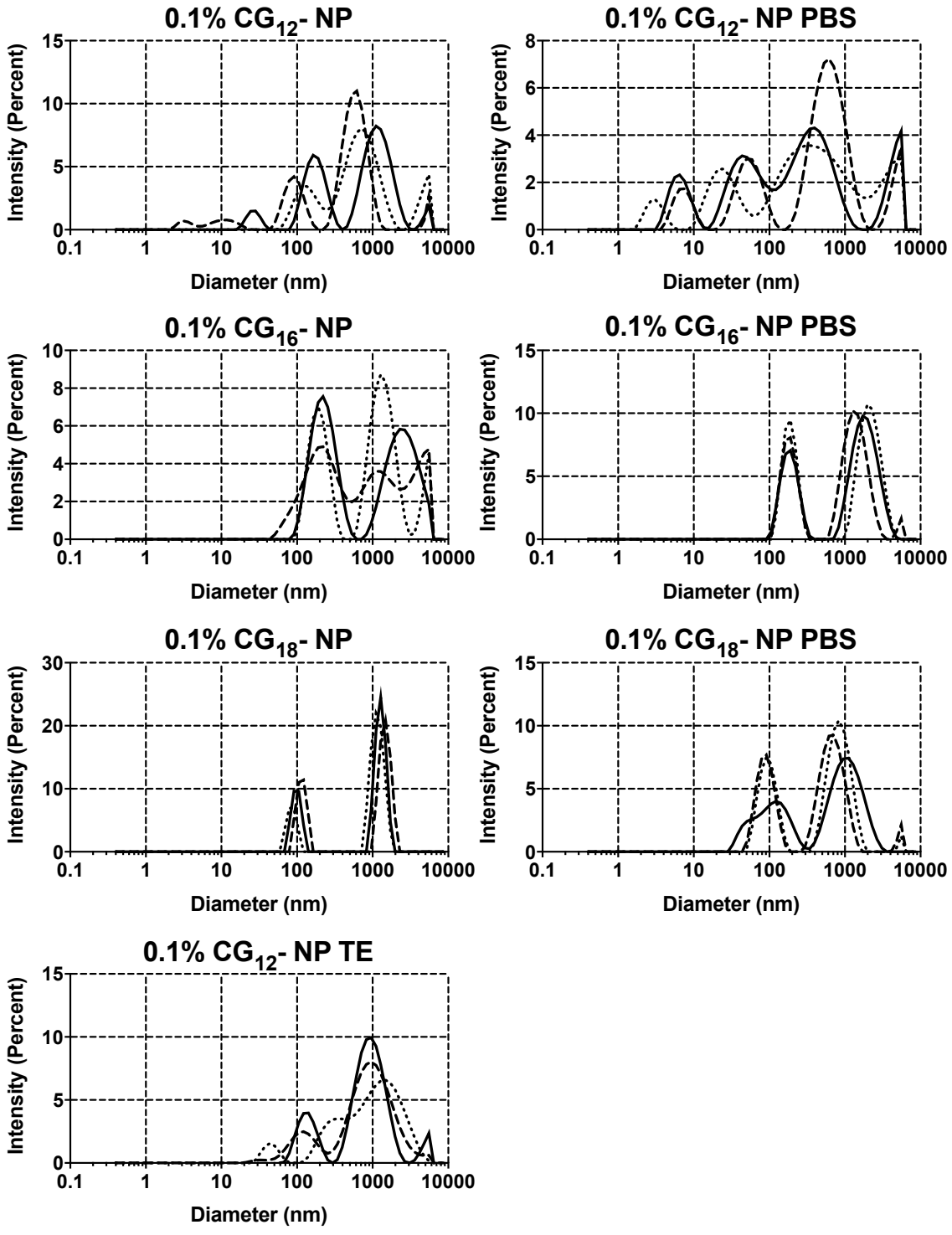

Figure 63 Size distribution by intensity for 0.1% CG-NP blank particles formulated with and without PBS and TE buffers

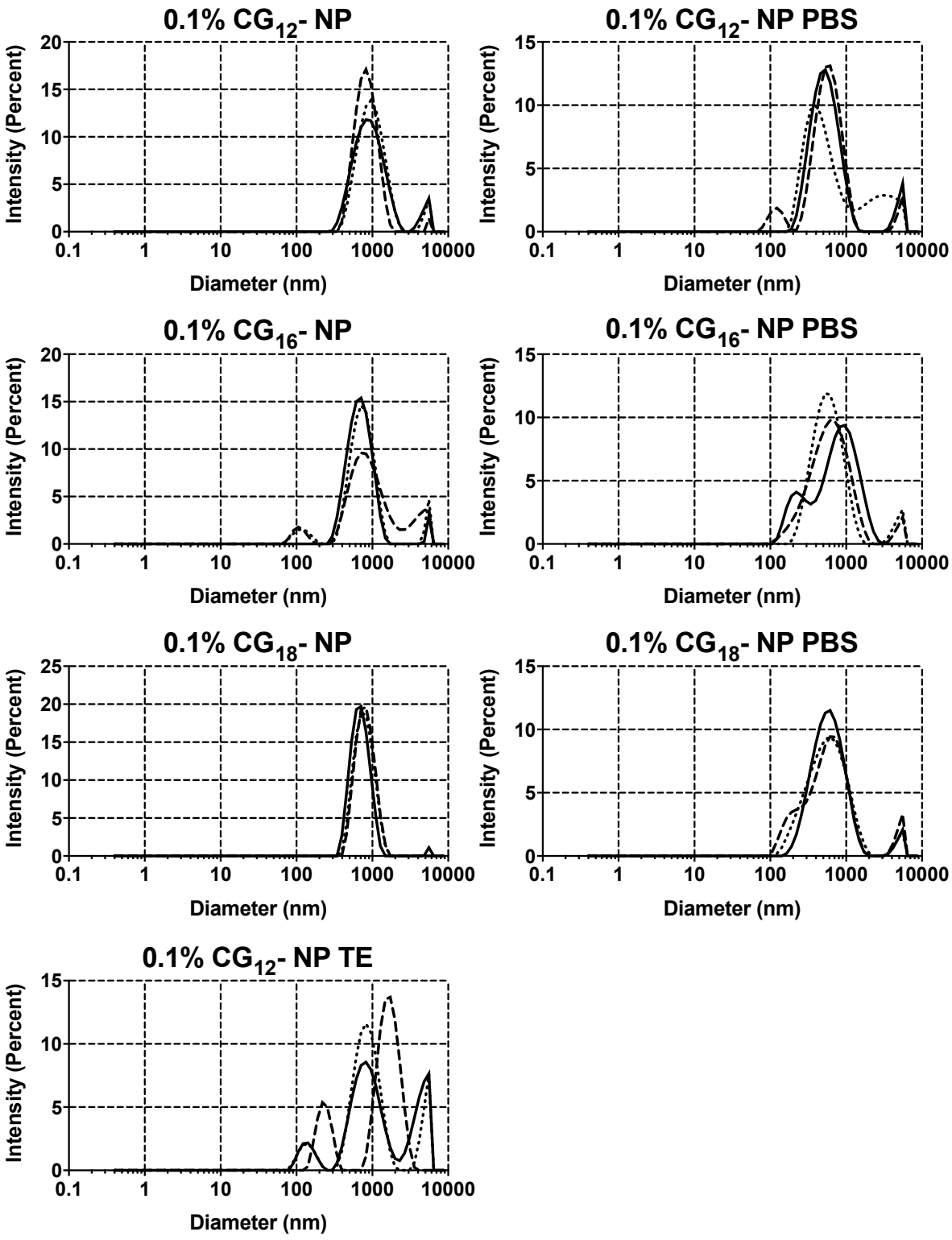

Figure 64 Size distribution by intensity for 0.1% CG-NPs formulated with and without PBS and TE buffers

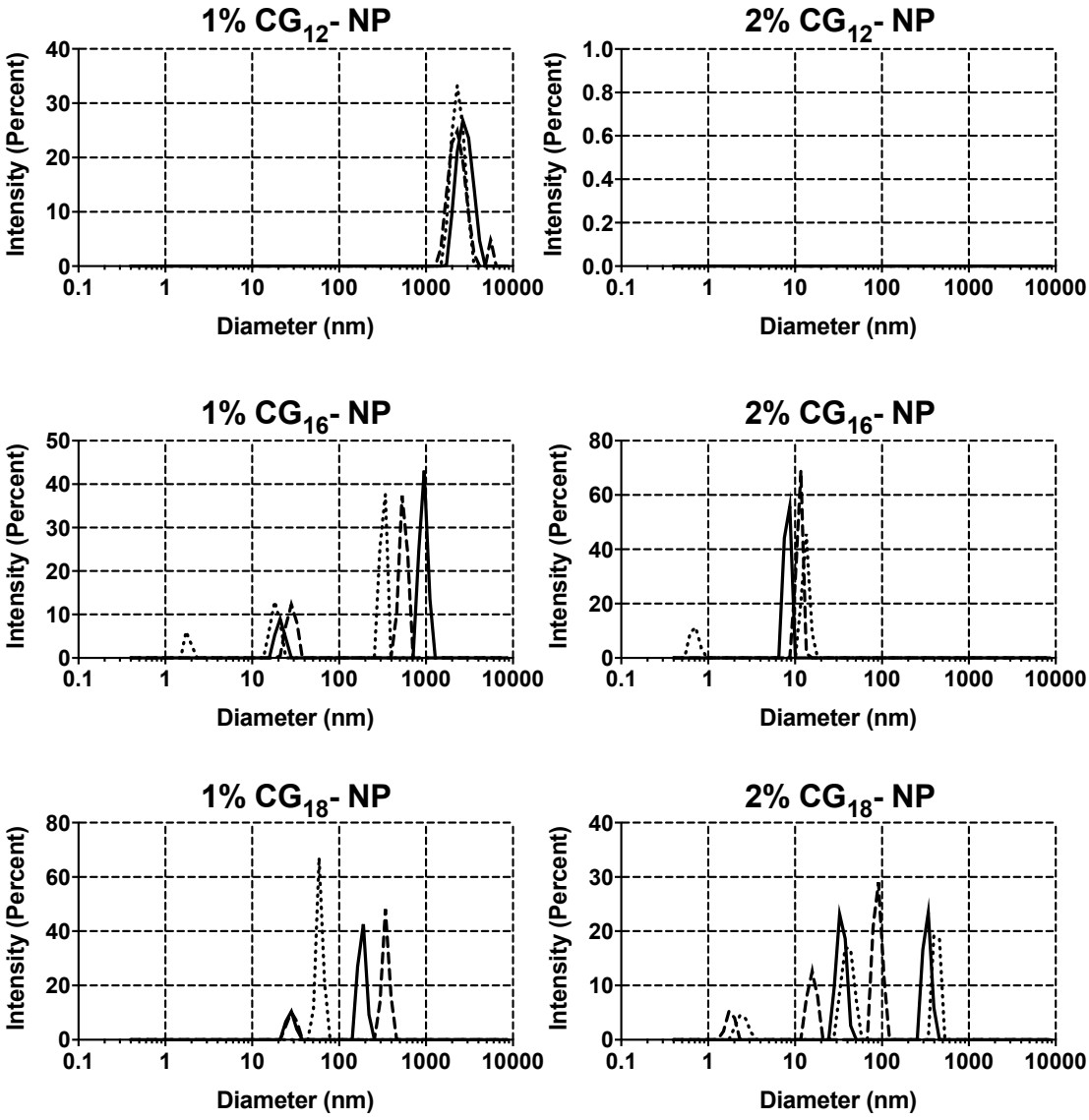

Figure 65 Size distribution by intensity for 1% and 2% CG-NP blank particles

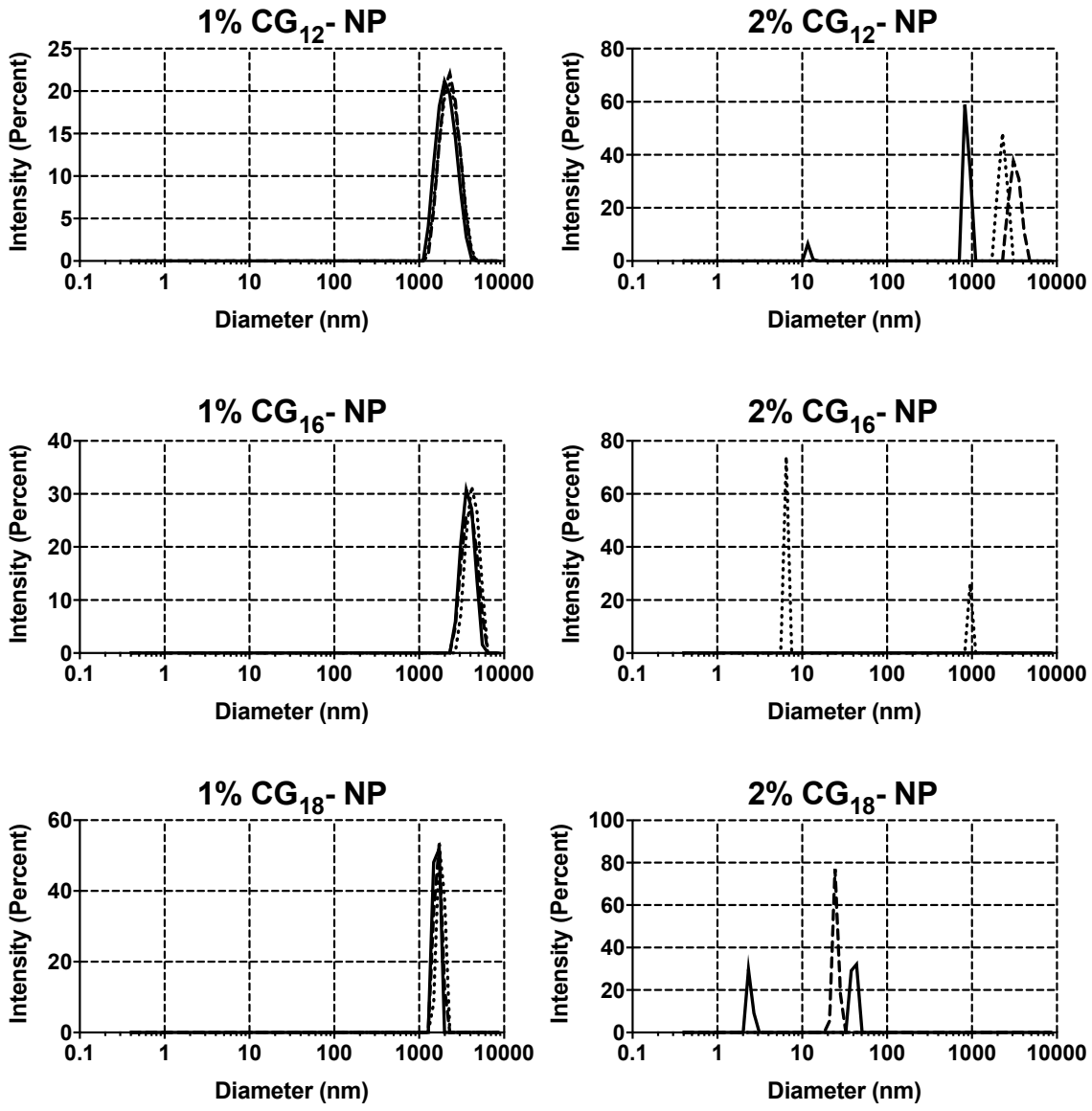

Figure 66 Size distribution by intensity for 1% and 2% CG-NPs

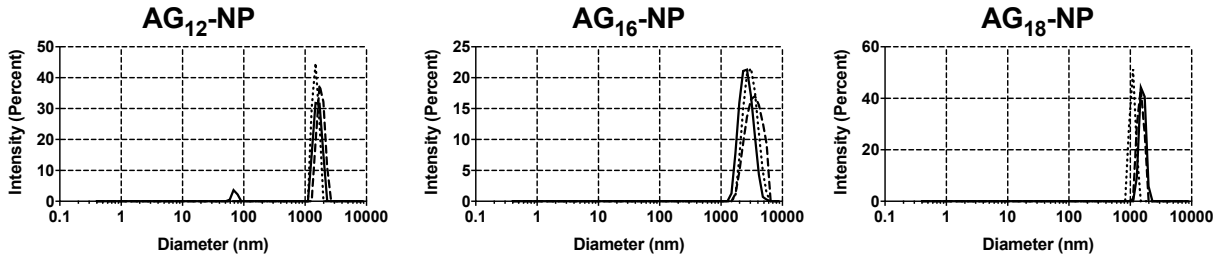

Figure 67 Size distribution by intensity for AG-NPs of blank particles

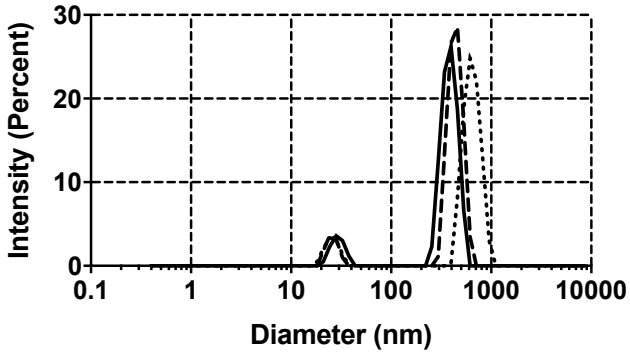

Figure 68 Size distribution by intensity for CL-NP formulation

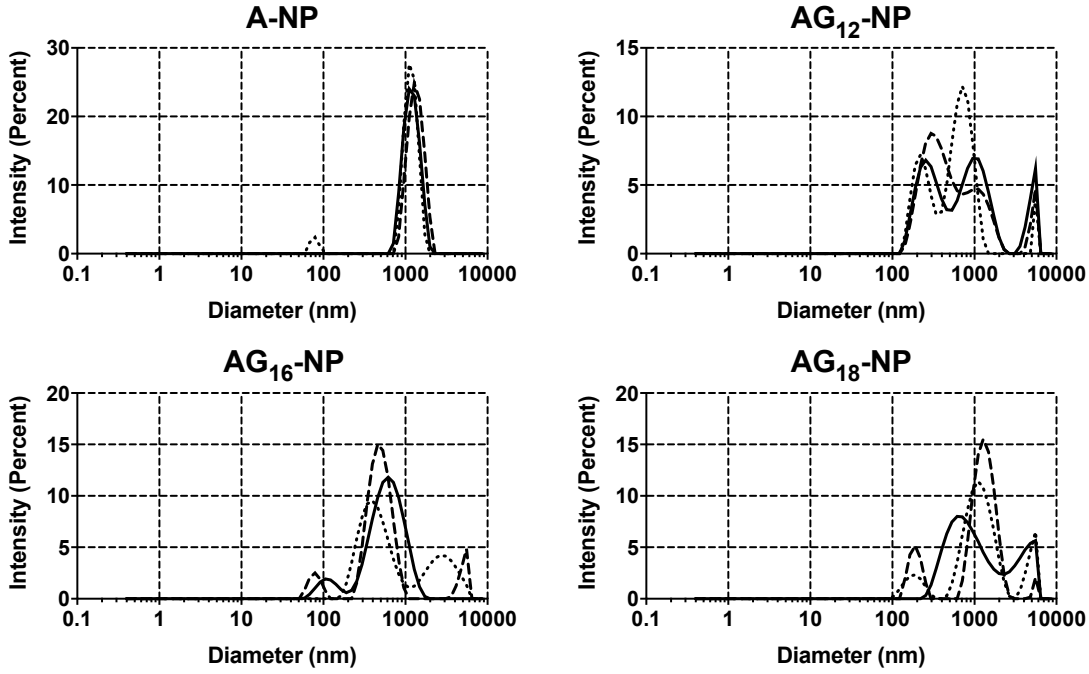

Figure 69 Size distribution by intensity for A-NPs and AG-NPs

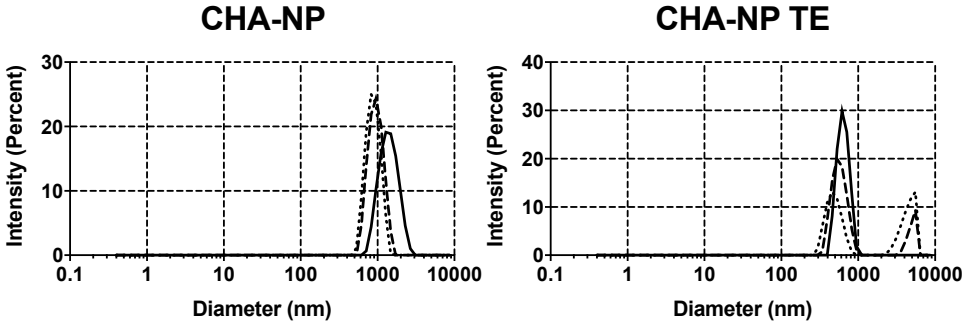

Figure 70 Size distribution by intensity for CHA-NP blank particles

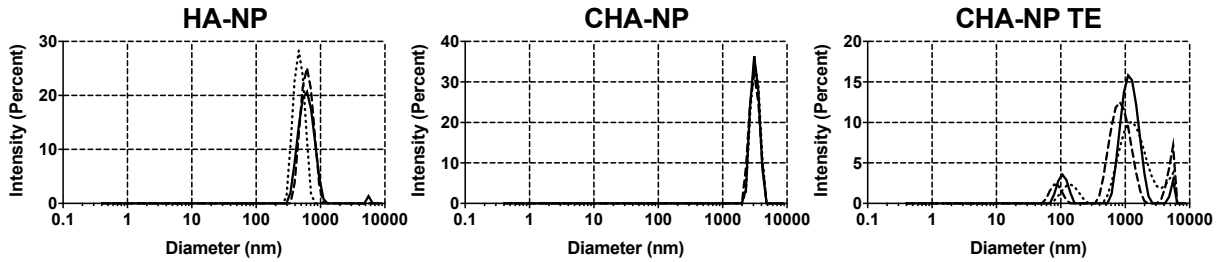

Figure 71 Size distribution by intensity for HA-NPs and CHA-NPs

A.2 Retention and viability results from discontinued particles

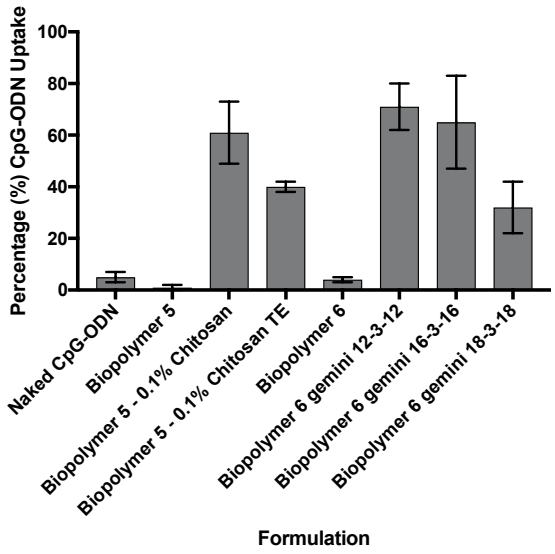

Figure 72 Retention of CpG-ODN uptake 24 hours post stimulation in HD11 macrophages with A-NPs, HA-NPs, AG-NPs

HD11 cells were dosed with 1 µg of CpG-ODN Hyaluronic acid (Biopolymer 5) and Sodium Alginate (Biopolymer 6) hybrid NP formulations and were compared in their ability to enhance CpG-ODN uptake in comparison to naked CpG-ODN. Chitosan used for formulation development was low MW chitosan of 50-190 kDa dissolved in 1% acetic acid. Retention of CpG-ODN uptake at 24 hours post dosing is shown. Values expressed represent mean ± S.D. , n=3.

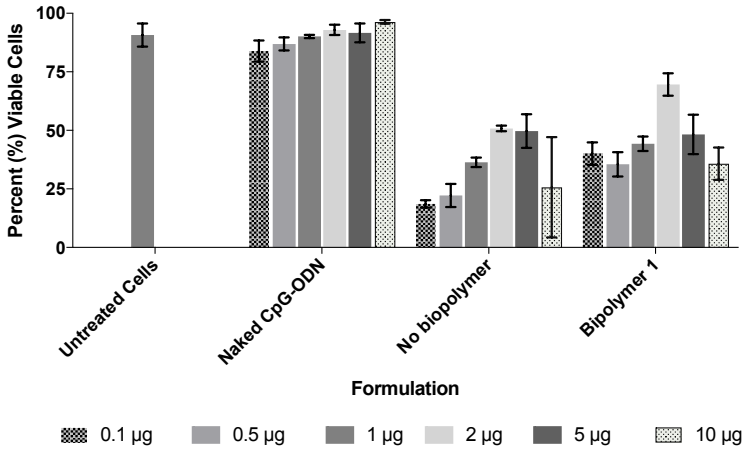

Figure 73 Dose dependent toxicity of G_{12}L-NPs (no biopolymer) and PVP 10,000 (biopolymer 1) BG_{12}L-NPs in HD11 chicken macrophages in comparison to naked CpG-ODN stimulation and untreated cells

HD11 chicken macrophage cells were stimulated with increasing quantities of CpG-ODN G_{12}L-NP and BG_{12}L-NP formulations. Cell viability was measured after 4 hours of stimulation using Calcein AM cell permeant dye and analyzed using flow cytometry. Fluorescent threshold was determined with untreated unstained cells. Values expressed represent mean ± S.D. , n=3.

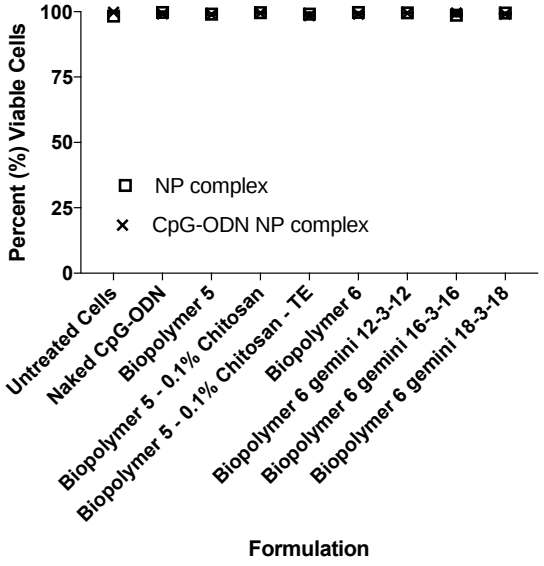

Figure 74 Cellular toxicity resulting from transfection with HA-NPs, A-NPs and AG-NPs in HD11 chicken macrophages 24 hours post stimulation with CpG-ODN NPs

HD11 cells were dosed with 1 µg of CpG-ODN Hyaluronic acid (Biopolymer 5) and Sodium Alginate (Biopolymer 6) hybrid NP formulations Chitosan used for formulation development was low MW chitosan of 50-190 kDa dissolved in 1% acetic acid. Cell toxicity based on percent viability by MitoTracker Green FM after transfection with CpG-ODN NPs 24 hours post dosing is shown. Values expressed represent mean ± S.D. , n=3.